Development of Ferrate(Fe(VI))-Coated Sand Composites for Stabilized Reactivity and Remediation of (In)Organic Contaminants in Synthetic Wastewater Effluent

Fanny Etonam Kekeli Okaikue-Woodi

A Dissertation

submitted in partial fulfillment of the

requirements for the degree of

Doctor of Philosophy

University of Washington

2024

Reading Committee:

Jessica Ray, Chair

Michael Dodd

Edward Kolodziej

Miqin Zhang

Program Authorized to Offer Degree:

Civil and Environmental Engineering

University of Washington

Abstract

Development of Ferrate (Fe(VI))-Coated Sand Composites for Stabilized Reactivity and Remediation of (In)Organic Contaminants in Synthetic Wastewater Effluent

Fanny Etonam Kekeli Okaikue-Woodi

Chair of the Supervisory Committee
Jessica Ray
Civil and Environmental Engineering

Efficient treatment technologies are needed to address the increased presence of contaminants in wastewater effluents and to protect ecosystems in receiving water bodies. Ferrate (Fe(VI)) iron oxide is a high valence (+6), environmentally friendly chemical widely investigated for water treatment applications because of its demonstrated capacity for simultaneous oxidation, disinfection and coagulation. Furthermore, reduction of Fe(VI) produces non-toxic Fe(III) hydroxide phases that are commonly used as coagulants in water treatment. However, Fe(VI) redox potential, speciation and reactivity are pH dependent. Under alkaline pH conditions, Fe(VI) is chemically stable but possesses a lower redox potential (E^0 = 0.72 V) which impedes Fe(VI) reactivity under environmentally relevant pH conditions. Previous studies have demonstrated that silica (SiO_2) gels can stabilize Fe(VI) and catalyze oxidation of organic compounds by Fe(VI). However, the use of SiO_2 gels during water treatment can result in additional solids that will need to be disposed of after Fe(VI) treatment. Additionally, in treatment systems with infiltration processes, the use of SiO_2 gels can lead to frequent clogging. Therefore, to stabilize Fe(VI) reactivity and facilitate its deployment for wastewater effluent treatment application, this research seeks to develop, characterize and apply Fe(VI) coatings onto sand—a commonly used water filtration media with primary constituent (>80%) SiO_2. Coating

Fe(VI) onto sand substrates can facilitate multiple contaminant treatment pathways: (1) removal in the aqueous phase by aqueous Fe^{3+} ions; (2) sorption/coagulation with precipitated Fe(III) solids formed form Fe(VI) reduction; and (3) removal on the sand surface via sorption or oxidation by Fe(VI). To generate the composite, sand was first mixed with a silica precursor, tetraethyl orthosilicate, to improve binding affinity to Fe(VI). Then, the modified sand was added to a slurry of potassium ferrate to synthesize a stable Fe(VI)-coated sand composite media. Surface analyses techniques coupled with colorimetric methods confirmed the coating of Fe(VI) onto the sand surface. The aqueous stability of the media was driven by water chemistries (e.g., pH, buffering ions). Batch studies conducted to assess the Fe(VI)-coated sand reactivity revealed removal of phenol—a representative and commonly occurring trace organic compound and moiety in wastewater—was achieved at a faster rate by the composite than by application of aqueous K_2FeO_4 powder (51% removed after 5 min compared to 37%). Batch studies to evaluate the effects of pH and wastewater effluent ions on the media capacity for treatment of multiple contaminants (i.e., trace metals and trace organics) demonstrated that organic compound oxidation is favored at lower pH whereas metals sorption was enhanced at higher pH. Furthermore, the presence of divalent cations improved metals sorption due to the rapid production of Fe(III). The presence of effluent organic matter promoted formation of the more reactive Fe(V) and Fe(IV) species which led to an increased removal of organic compounds in a synthetic wastewater effluent matrix. This research highlights a novel media for advanced treatment of wastewater treatment and presents an opportunity for more effective deployment of Fe(VI) in water treatment applications, especially for filtration processes.

Acknowledgments

I express my deepest appreciation and gratitude to my advisor, Dr. Jessica Ray, for the opportunity to conduct this research and to be part of such an inclusive and collaborative research group. I am immensely grateful for her support and mentorship. Thank you to my committee members, Drs. Michael C. Dodd, Edward Kolodziej, Miqin Wang, and Joel Baker for their feedback on this work. I would like to acknowledge Dr. Dodd for the use of the VWR recirculating chiller needed in the synthesis of the Fe(VI)-coated sand and Dr. Kolodziej for the use of the QTOF-HRMS at UW Tacoma Center for Urban Waters.

I thank the students who have greatly assisted me with this project: Gina Dickson, Joseph Severin, Michelle Kane, Megan Vance, Yiran Wan, Kiana Gholamy and Reyna Morales Lumagui. I would like to also thank other AIMS group lab members for their camaraderie, support, feedback and collaboration over the years: Dr. Jessica Steigerwald (thank you for the adventures and brainstorming discussions), Dr. Katya Cherukumilli, Dr. Yuemei Ye, Jen Hooper, Alanna Hildebrant, Amy Quintanilla, Kovas Zygas, and Reagan Beers (who has helped with XRD data collection and analysis). Thank you especially to Jen, Alanna and Reagan for their help with the column studies.

Thank you to Dr. Martin Sadilek at the University of Washington (UW) Department of Chemistry Mass Spectrometry Facility for assistance and training during the initial stages of this project, to Dr. Adrienne Roehrich at the UW Department of Chemistry Spectroscopic and Analytical Instrumentation Facility for assistance with ICP-OES analyses, to Dr. Michael Sienna and Dr. Scott Braswell at the UW Molecular Analysis Facility for assistance with SEM-EDS and ICP-MS analyses.

I would like to extend my gratitude to the communities and organizations that have supported me professionally and personally during my time at UW. I am grateful to the Office of Graduate Student Equity and Excellence, to the Black Graduate Students Association, to the inaugural cohort of CEE Graduate Student Advisory Board, to the “In Between Cultures” group at the UW Counseling Center. I am honored to have met amazing and inspiring people here.

Special thank you to my friends, close and far, for your words of encouragement. Alex and Azi, thank you for always checking on me and being a phone call away. Azi, thank you for always reminding me to rest. Anne-Marie, thank you for opening your home to me, the adventures and for all the food you brought me during busy times. To my Togolese community in

Seattle and elsewhere—Amen, Aubin, Esi, Elliot, Sepnos, Laté, Marlène and many more—thank you for your cheers and support.

Finally, I would like to sincerely thank my family for grounding me these past five years. Thank you to my parents for their support in my educational journey and for the opportunities you have provided that have led me to this point. Most importantly, I would like to express my deepest gratitude to my sister, Sandra, for your unwavering support, care and advice. Thank you to you, Nowa, Louis, Zuri and Leif for always opening your home to me, making me laugh, and taking care of me when I come home. Thank you especially for getting me through these last moments of my graduate school journey.

Part of this work was conducted at the Molecular Analysis Facility, which is supported in part by funds from the Molecular Engineering & Sciences Institute, the Clean Energy Institute, the National Science Foundation, and the National Institutes of Health. Part of this work was conducted at the Washington Clean Energy Testbeds, a facility operated by the University of Washington Clean Energy Institute. This material is based upon work supported by funds from the Washington Research Foundation, the University of Washington, and the National Science Foundation (Grant CBET 2242483). I would like to also acknowledge the NSF MRI Program for Grant No. 2117239. Any opinions, findings, and conclusions or recommendations expressed in this material are those of the authors and do not necessarily reflect the views of the National Science Foundation.

Contents

List of Figures

phenol to maximum aqueous Fe(VI) concentrations ratio (right axis) with time; Fe(VI) concentration at 5 min was taken as the maximum aqueous Fe(VI) concentration, (bottom) changes in aqueous Fe.

Figure 2.6. **(A)** Degradation of 219±12 µg/L phenol by 2 g/L Fe(VI)-coated sand in 10 mM borate buffer pH 9 and **(B)** subsequent formation of the oxidation product with maximum absorbance at 307 nm.

Figure 2.7. (A) Removal of 283±2.1 µg/L phenol and 865±15 µg/L PMSO by 2 g/L Fe(VI)-coated sand. (**B**) Changes in aqueous Fe concentration.

Figure 3.1. SEM images of (**A**) non-coated sand Ottawa sand and (**B**) Fe(VI)-coated sand. The insets are SEM images at lower magnification. The adjoining tables report elemental composition by weight percent on the media surface.

Figure 3.2. Removal of nominally 500 µg/L Cu, Pb, Zn (each) by 2 g/L Fe(VI)-coated sand (**A**) in the **M9 system**; and in the presence of nominally 500 µg/L ACM, BZT, and SMX (each) (**B**) in the **MO9** and (**C**) **MO7.5 systems.**

Figure 3.3. (**A**) Normalized degradation of nominally 500 µg/L ACM, BZT, SMX (each) by 2 g/L Fe(VI)-coated sand in the **O9 system**; and (**B** and **C**) the formation of the most abundant transformation products as a function of time.

Figure 3.4. (**A**) Normalized degradation of nominally 500 µg/L ACM, BZT, SMX (each) by 2 g/L Fe(VI)-coated sand in the M**O9 system** in the presence of nominally 500 µg/L Cu, Pb, Zn (each); and (**B** and **C**) the formation of the most abundant transformation products as a function of time.

Figure 3.5. (**A**) Normalized degradation of nominally 500 µg/L ACM, BZT, SMX (each) by 2 g/L Fe(VI)-coated sand in the M**O7.5 system** in the presence of nominally 500 µg/L Cu, Pb, Zn (each); and (**B** and **C**) the formation of the most abundant transformation products as a function of time.

Figure 3.6. Removal of nominally 500 µg/L (each) of (**A**) ACM, BZT, SMX and (**B**) Cu, Pb, Zn by 2 g/L Fe(VI)-coated sand in synthetic wastewater solution as a function of time.

Figure 4.1. Degradation of nominally 250 µg/L phenol in 10 mM borate buffer pH 9 in the presence of synthetic effluent organic matter by (**A**) 12.6 mg/L Fe(VI) powder and (**B**) 2 g/L Fe(VI)-coated sand. (Top) Normalized degradation of phenol and total organic carbon, (**bottom**) changes in aqueous Fe(VI).

Figure 4.2. Normalized removal of nominally 50 µg/L of (**left panel**) Cu, Pb, and Zn each and (**right panel**) 50 µg/L of ACM, PHE, SMX each in the synthetic wastewater effluent containing synthetic effluent organic matter in (**A**) the absence and (**B**) the presence of 2 g/L of Fe(VI)-coated sand.

Figure 4.3. Changes in total organic carbon concentration in the synthetic wastewater effluent with (**A**) effluent organic matter in the presence of Fe(VI)-coated sand, (**B**) effluent organic matter and trace metals and trace organics in the absence of Fe(VI)-coated sand and (**C**) effluent organic matter and trace organics and trace metals in the presence of Fe(VI)-coated sand.

Figure A1. Spectroscopic characterization of the Fe(VI)-coated sand. (A) UV-vis absorbance spectra of Fe(VI) leached from the Fe(VI)-coated sand (dashed line) and reacted with ABTS (solid line). (B) UV-vis absorbance of Fe(VI) leached from the media (solid line) and reacted with ferrozine (dashed line). (C) UV-vis absorbance of Fe-ferrozine complex formed with Fe(II) chloride (straight line) and with reduction of Fe(VI) (dashed line).

Figure A2. Total aqueous Fe concentration after 1 g/L Fe(VI)-coated sand was stirred in 1% HNO_3 for 1 min, 1 hr, 12 hrs and 24 hrs. The Fe(VI)-coated sand was prepared with virgin sand (no TeOS), 3hr-TeOS sand, and 24hr-TeOS sand.

Figure A3. Spectroscopic analysis of TeOS stability on TeOS-coated sand. The UV-Vis spectrum of the supernatant of 1 g/L TeOS-coated sand (dashed line) placed in 10 mM borate buffer and sonicated was compared to the UV-Vis spectrum of TeOS (4 mL solution). The absence of a peak at 292 nm in the spectrum of the TeOS-sand indicates that TeOS did not leach from the TeOS-coated sand surface.

Figure A4. Kinetics of Fe(VI), Fe(III) and total Fe leached from 1 g/L Fe(VI)-coated sand into a 10 mM $Na_2B_4O_7$ solution at pH 7 as a function of time. Total Fe refers to the total Fe leached into solution at a given time.

Figure A5. Kinetics of Fe(VI), Fe(III) and total Fe leached from 1 g/L Fe(VI)-coated sand with 3hr-TeOS sand modification into a 10 mM Na_2HPO_4/NaH_2PO_4 solution at pH 7, 8, 9 as a function of time. Max total Fe refers to the maximum mass of Fe that would leach of the surface of Fe(VI)-coated sand. This was determined by mixing 1 g/L Fe(VI)-coated sand into 1% HNO_3 and measuring total Fe in solution. Total Fe refers to the total Fe leached into solution at a given time.

Figure A6. Decay kinetics of aqueous Fe(VI) from 1 g/L Fe(VI)-coated sand in a 10 mM 10 mM $Na_2B_4O_7$ at pH 7, 8, and 9. r^2 denotes the correlation coefficient of the fitted linear regression curve.

Figure A7. Aqueous Fe(VI) concentration leached from 1 g/L Fe(VI)-coated sand in a 10 mM Na_2HPO_4/NaH_2PO_4 and 10 mM $Na_2B_4O_7$ solution at pH 8.

Figure A8. Decay of Fe(VI) in (A) 0.21 g/L K_2FeO_4 powder and (B) 1 g/L Fe(VI)-coated sand. The 0.21 g/L initial concentration of K_2FeO_4 was chosen to obtain a concentration of Fe(VI) that will be equivalent to the concentration of total Fe in the Fe(VI)-coated sand system.

Figure A9. Total Fe and Fe(VI) coating mass leached from Fe(VI)-coated sand surface as a function of time. 3 g/L Fe(VI)-coated sand was mixed with 1% HNO_3 for the total Fe

measurement. For the Fe(VI) coating mass determination, 3 g/L Fe(VI)-coated sand was mixed with 5 mM Na_2HPO_4/1mM NaB_4O_7 buffer.

Figure A10. Oxidation of PMSO to $PMSO_2$ by 2 g/L Fe(VI)-coated sand in (A) 10 mM phosphate buffer and (B) 10 mM borate buffer at pH 9. The initial PMSO concentration was 705±20 µg/L PMSO in the phosphate buffer and 738±14 µg/L PMSO in the borate buffer.

Figure A11. Linear fitting of the reaction kinetics of 219±12 µg/L phenol and (A) 12.6 mg/L Fe(VI) powder and (B) 2 g/L Fe(VI)-coated sand in 10 mM borate buffer pH 9.

Figure A12. UV-Vis scans of 219±12 µg/L phenol reacted with 2 g/L Fe(VI)-coated sand in 10 mM borate buffer pH 9 measured at various time intervals within the 120-min and a hydroquinone blank solution.

Figure A13. (**Row 1**) Degradation of phenol and oxidation of PMSO at different concentrations (**A**. 520±8.1 µg/L phenol and 739±148 µg/L PMSO; **B**. 245±3.0 µg/L phenol and 394±4.7 µg/L PMSO) by 2 g/L Fe(VI)-coated sand and (**row 2**) the corresponding changes in aqueous Fe concentrations.

Figure B1. **(A)** Speciation of Fe(VI) (left axis, black lines) and aqueous Fe(VI) self-decay rate (right axis, blue line) as a function of pH. (**B**) Distribution of the standard potential of iron species including Fe(VI) species. The pKa values: $H_3FeO_4^+$ (pKa = 1.6); H_2FeO_4 (pKa = 3.5); $HFeO_4^-$ (pKa = 7.3) were obtained from Rush et al.,1996 and decay rate constants from Lee et al., 2014. Data for the standard potentials was obtained from Pogliani et al., 2021 and Wulfsberg, 2000

Figure B2. XRD measurements of (**A**) non-coated Ottawa sand, (**B**) TeOS-sand, (**C**) Fe(VI) powder and (**D**) Fe(VI)-coated sand.

Figure B3. Normalized removal of nominally 500 µg/L trace organics (top) and trace metals (bottom) by 26±1.8 mg/L $Fe(NO_3)_3$ in the (**A**) **MO9 system** and (**B**) **MO7.5 system.**

Figure B4. Changes in aqueous Fe(VI) concentrations during reaction in the (**A**) **M9 system**; (**B**) **O9 system**; (**C**) **MO9 system**; and the (**D**) **MO7.5 system**. The nominal concentration for each contaminant is 500 µg/L.

Figure B5. Results showing normalized loss of Cu, Pb, and Zn (i.e., control experiments with no media present) with (**A**) nominally 500 µg/L Cu, Pb, and Zn in 10 mM sodium borate buffer at pH 9; (**B**) nominally 500 µg/L Cu, Pb, and Zn in 10 mM sodium borate buffer at pH 9 in the presence of select trace organics (**C**) nominally 500 µg/L Cu, Pb, and Zn in 10 mM sodium borate buffer at pH 7.5 in the presence of select trace organics and (**D**) nominally 500 µg/L Cu, Pb, and Zn in the synthetic wastewater effluent solution in the presence of select trace organics.

Figure B6. Results showing normalized loss ACM, BZT and SMX (i.e., control experiments with no media present) with (**A**) nominally 500 µg/L ACM, BZT, and SMX in 10 mM sodium

borate buffer at pH 9; (**B**) nominally 500 μg/L ACM, BZT, and SMX in 10 mM sodium borate buffer at pH 9 in the presence of select trace metals (**C**) nominally 500 μg/L ACM, BZT, and SMX in 10 mM sodium borate buffer at pH 7.5 in the presence of select trace metals and (**D**) nominally 500 μg/L ACM, BZT, and SMX in the synthetic wastewater effluent solution in the presence of select trace metals.

Figure B7. Control experiments (no media) with BZT and Cu under different experimental conditions. BZT initial concentrations were 427±21.4 μg/L in 10 mM $Na_2B_4O_7$ pH 9, 365±35.9 μg/L in 10 mM $Na_2B_4O_7$ pH 7.5, and 371±39.9 μg/L in the synthetic wastewater effluent (SWW) solution.

Figure B8. Possible oxidation pathways of ACM by the Fe(VI)-coated sand.

Figure B9. Possible oxidation pathways of SMX by the Fe(VI)-coated sand.

Figure B10. Changes in aqueous Fe(VI) concentrations during reaction with trace metals and trace organics at a nominal concentration of 500 μg/L in the synthetic wastewater effluent solution.

Figure C1. Results of control experiments with no media showing normalized loss of nominally 50 μg/L of (**A**) Cu, Pb, and Zn each and (**B**) ACM, PHE, and SMX each in the synthetic wastewater effluent containing synthetic effluent organic matter.

Figure C2. Changes in aqueous concentration of Fe(VI) in the synthetic wastewater effluent solution containing effluent organic matter with (open squares) and without (shaded squares) trace metals and trace organics.

Figure D1. A proposed secondary wastewater effluent treatment train that employs Fe(VI)-coated sand.

Figure D2. Column test set up

Figure D3. Image of the Fe(VI) leaching off the sand surface and exiting the column

Figure D4. Image showing gradual decrease in Fe exiting the column with (**A**) 100 wt % Fe(VI)-coated sand and (**B**) 25 wt% Fe(VI)-coated sand

Figure D5. Regenerated Fe(VI)-coated sand via (**A**) method 1 and (**B**) method 2.

Figure E1. Synthesized data from the International Stormwater Best Management Practices (BMPs) Database showing **(A)** number of sites reporting measurements and **(B)** the average removal efficiency of select, representative urban stormwater contaminants in grass swales, detention basins, retention ponds, and wetland basins. The boxplots in panel B were created by calculating the average removal efficiency for each unique BMP site reporting paired influent and effluent parameter concentration measurements during multiple storm events. COD = chemical oxygen demand; TSS = total suspended solids.

Figure E2. Boxplots show the range of reported or calculated removal efficiencies of conventional organic and inorganic media for different stormwater contaminant categories tested

in 18 different studies (indicated by individual points for each specific media/contaminant pair). General media categories refer to grouped materials as follows: compost-based media (compost only and compost mixed with either sand, biochar, or activated carbon); woodchips-based (woodchips only and woodchips mixed with straw mulch or biochar); and iron-based (iron filings and iron filings mixed with sand, and iron hydroxides). General contaminant categories refer to grouped contaminants as follows: solids (total suspended and volatile suspended solids); pesticides (diuron, atrazine, fipronil, 2,4-dichlorophenoxyacetic acid, simazine, oryzalin and prometon); pathogens (*E. coli*, *Enterococcus faecalis*, total coliforms and fecal coliforms); other organics (tris(3-chloro-2propyl)phosphate, tris(2-chloroethyl)phosphate, perfluorooctanoic acid, perfluorooctanesulfonic acid, benzotriazole, 1H-benzotriazole, 5-methyl-1H-benzotriazole, and total organic carbon); nutrients (total P, orthophosphates, total P, total Kjeldahl nitrogen, NH_4^+, and NO_3^-); metals (As, Cd, Cu, Cr, Ni, Pb and Zn); and hydrocarbons (total petroleum hydrocarbons, motor oil, naphthalene, phenanthrene and benzo(a)pyrene).

Figure E3. Column breakthrough results for removal of select metals and organic contaminants in columns amended with (A) 3 wt% biochar-97 wt% sand columns and columns with (B) virgin sand. The feed solutions contained 10 µg/L of each contaminant in (1) a synthetic stormwater matrix and in (2) the same synthetic stormwater matrix with 5 mg-C/L DOC. 24D = 2,4-dichlorophenoxyacetic acid. DIU = diuron, PFOA = perfluorooctanoic acid. The figure was created with permission from the authors (Ray et al., 2019)

Figure E4. Schematic illustrating how Phoslock®, a lanthanum (La^{3+})-modified bentonite clay can complex free phosphate (PO_4^{3-}) in solution

Figure E5. Schematic describing the synthesis of (A) polymer-clay composites and (B) surfactant modified zeolites. Polymer-clay composites are typically synthesized by (A1) mixing polycations and negatively charged phyllosilicate clays. Mono- and di-valent cations within the clay layers are exchanged with the positively charged monomers to create an (A2) organoclay, reversing the negative surface charge of the clay. Further addition of polycation will generate a (A3) composite of positively charged organoclays functionalized with hydrophobic domains to adsorb negatively charged species (e.g., CrO_4^{2-}) as well as organic compounds (e.g., benzene). (B1) Surfactant-modified zeolite synthesis undergoes a similar exchange of mono- and di-valent cations with a positively charged surfactant, such as hexadecyltrimethylammonium bromide. (B2a) The positively charged polar head groups will adsorb to the negatively charged zeolite surface exposing the hydrophobic surfactant tail, which can bind organic compounds. (B2b) If enough surfactant is added to induce micelle formation (e.g., critical micelle concentration (CMC) is reached), additional adsorption of negatively charged species can occur on the modified zeolite composite.

List of Tables

collective average from six main urban land uses: 49% residential, 20% commercial, 13% industrial, 6% freeways, 6% institutional, and 6% open space.

Table E2. Summary of studies on media performance to remove various stormwater pollutants, physicochemical properties and removal mechanisms of media. It is important to consider that the specific physicochemical properties of media may vary depending on how the media is prepared or synthesized.

Table E3. Media properties and column performance for trace metal removal in synthetic stormwater (Liu et al., 2005)

Table E4. Techniques recommended for characterization of organic and inorganic media.

Table E5. Summary of studies on conventional media performance to remove various stormwater pollutants. This table is contained in the associated Microsoft Excel® spreadsheet.

Chapter 1. Ferrate (Fe(VI)) Iron Oxide for Multifunctional Water Treatment

1.1. Motivation

Increased population growth coupled with the overuse of anthropogenic chemicals has led to the increased presence of chemical contaminants in wastewater.[1, 2] Chemicals such as micropollutants and metals enter wastewater treatment plants from households, workplaces, surface runoff and many other sources.[2-4] This multitude of contaminants from varied origins lead to complex wastewater matrices which places a performance and operational burden on existing wastewater treatment systems that are not well equipped for treatment of these contaminants.[5] If not treated well, these contaminants will enter natural water sources (e.g., groundwater, surface water) through wastewater discharges. In fact, wastewater effluents are considered a major point source of pollution.[2, 6]

Conventional wastewater treatment systems are primarily designed to achieve the removal of solid wastes and suspended solids via coagulation and sedimentation processes (i.e., primary treatment) and the removal of nutrients (i.e., phosphorus and nitrogen) and biodegradable organic matter via biological treatment (i.e., secondary treatment).[2, 7]Additionally, microorganisms are treated via disinfection.[7] Metals and organic compounds can be removed via sorption to particles and microbial biomass that are removed during the coagulation and separation processes. Organic compounds can also be transformed and/or mineralized during biological treatment. However, complete degradation of these contaminants is not achieved. In particular, conventional wastewater treatment systems only achieve about 50% removal of their micropollutant loads, and the removal is contaminant specific.[2, 8] For example, the presence of these contaminant types in secondary wastewater effluents are still reported at trace level

concentrations (i.e., nanograms per liter to micrograms per liter).[3, 4, 9, 10] The compounding effects of multiple trace contaminants can lead to chronic effects in receiving streams.[11] For example, the discharge of untreated antibiotics from wastewater treatment plants into aquatic environments can lead to an increase in antibiotic-resistant genes in bacteria[12, 13] in surface waters that may be used as drinking water sources. Studies have reported reproductive[14, 15] and histopathological[14] effects in fishes from effluent-dominated streams. For example, Kidd et al. observed the feminization of male fishes exposed to wastewater discharges.[16] The seven-year study done in northwestern Ontario, Canada reported the presence of endocrine disrupting compounds (e.g., 17β-estradiol, 17α-ethynylestradiol, nonyphenol) in lakes receiving wastewater effluent.[16] Fathead minnow chronically exposed to these compounds experienced reproductive effects such as the production of vitellogenin mRNA (a protein normally synthesized by females during oocyte maturation) and impacts on gonadal development.[16] Vajda et al. also reported reproductive effects in fishes exposed to wastewater effluents.[15] They investigated white suckers upstream and downstream of wastewater treatment plant in Boulder, CO. They noticed the presence of intersex fish in the downstream location, but not upstream of the plant.[15] They also observed disrupted ovarian and testicular histopathology and vitellogenin production in male white suckers.[15] Analyses of the wastewater effluent revealed the presence of 17β-estradiol, 17α-ethynylestradiol, alkylphenols and bisphenol A at a total estrogen equivalence of 31 ng/L.[15] This highlights the potential toxicity of low concentrations of wastewater effluent contaminants.

Process optimization and additional treatment processes (i.e., tertiary treatment) have been added to wastewater treatment trains to enhance the removal of trace metals and trace organics during wastewater treatment. For example, activated carbon can be used as a polishing step to achieve sorption of trace metals and trace organics after biological treatment.[7] Additionally,

ozone and chlorine have been conventionally used as oxidants for organic compounds remediation in tertiary treatment.[2, 17] They can also be added after conventional secondary treatment for disinfection purposes,[7] which promotes to the abiotic degradation of organic compounds during secondary treatment. However, their application can lead to formation of harmful inorganic (e.g., chlorate and bromate)[18] and organic (e.g., trihalomethanes and haloacetic acids)[18, 19] byproducts.[5, 20] For example, N-nitrosodimethylamine (NDMA), a potent human carcinogen generated from the oxidation of amino-containing compounds such as dimethylamine and 1,1-dimethylhydrazine, has been detected after ozonation of secondary wastewater effluents.[21, 22] Various advanced oxidation processes (AOPs) have been explored to enhance degradation of organic compounds in water. While effective, other AOPs such as ultraviolet (UV)-AOPs (e.g., combination of UV and chlorine,[23, 24] combination of UV and hydrogen peroxide[25]), electrochemical AOPs,[26] Fenton processes[27] sometimes exhibit complications and other limitations that reduce their effectiveness and safety for water treatment.[5] For example, during Fenton reactions, reactive hydroxy radicals (OH·) are formed from the reaction of ferrous ions and hydrogen peroxide.[5, 28] However, this process requires acidic pH conditions and contributes to precipitation of Fe(III) solid waste,[5, 29] which necessitates further steps (i.e., pH neutralization, solids disposal) after treatment.

Highly efficient treatment technologies are needed to address the continuing degradation of water quality and water shortages challenges. Increasing population growth has led to increased water demands. Some cities and communities facing water shortage crises are increasingly considering treated wastewater for augmentation of water sources.[7, 21, 30] The potential for direct potable reuse has especially gained momentum in arid regions.[30] Thus, treatment technologies

with very minimal negative consequences will be needed to ensure a high quality for the wastewater effluent that will be reclaimed for potable use.

1.2. Ferrate Application in Water Treatment

Ferrate (FeO_4^{2-}; Fe(VI)) is a high-valent iron oxide with a tetrahedral structure composed of an iron atom centered by four oxygen atoms (**Figure 1.1**). Over the last few decades, Fe(VI) has emerged as a promising water treatment technology investigated for diverse applications in green organic synthesis,[31] waste remediation,[32] and iron batteries synthesis.[33, 34]

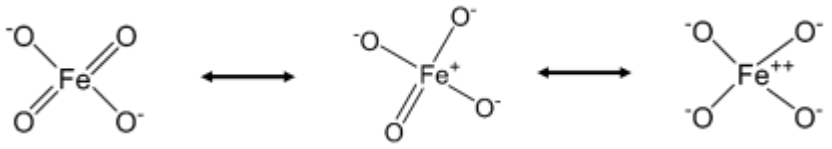

Figure 1.1. Resonance hybrid structures of ferrate. [35]

The advantage of Fe(VI) application in water treatment is its ability to participate in multiple modes of contaminant remediation. Fe(VI) has been investigated in numerous studies with a demonstrated ability to treat a wide range of organic compounds (e.g., pharmaceuticals,[36-42] herbicides,[43] and other micropollutants[31, 44, 45]), inorganic pollutants (e.g., Cu,[46-48] As,[48-50] Mn,[47, 51] Zn[47, 48]) and microorganisms.[48, 52-54] Its multifunctional properties as an oxidant, coagulant and disinfectant make it an attractive technology for water treatment. Furthermore, the degradation product of Fe(VI) is nontoxic Fe(III) species via chemical or biological reduction of the +6 valence state, which has been leveraged in applications as coagulants[54, 55] and adsorbents.[56, 57] Thus the utilization of Fe(VI) can enable multiple types of treatment processes (i.e., oxidation, disinfection and coagulation) in a single unit, which presents economical and spatial benefits for water treatment systems.

Table 1.1 shows that Fe(VI) possesses a high redox potential compared to other commonly used oxidants, indicating that Fe(VI) has a greater capacity for organic compounds

oxidation. Furthermore, compared to ozone and chlorine, Fe(VI) is less reactive towards bromide[58, 59] and has been shown to reduce the formation of brominated transformation byproducts compared to ozone.[59-61] Han et al. reported that ozonation of 100 µg/L bromide in ultrapure water with an initial ozone concentration of 2.5 mg/L led to the formation of 20 µg/L bromate which is above the EPA bromate maximum contaminant level of 10 µg/L. However, a pretreatment with 1 mg/L of Fe(VI) completed inhibited bromate formation under identical conditions.[62] In contrast, while Fe(VI) can react with iodide,[58] studies have shown that drinking water pretreatment with Fe(VI) led to decreased formation of iodinated disinfection byproducts in chlorinated waters which ultimately results in lower overall cytotoxicity of the treated water.[61] Gombos et al. also reported reduced formation of disinfection byproducts during Fe(VI) treatment compared to chlorine treatment.[63] Municipal wastewater secondary effluents were collected at a wastewater treatment plant and treated with chlorine and Fe(VI) separately in laboratory scale jar tests.[63] For an initial adsorbable organic haloids (AOX) concentration 106 µg Cl^- L^{-1}, they measured 264 µg Cl^- L^{-1} and 182 µg Cl^- L^{-1} of AOX after treatment with chlorine (dose = 15 mg/L) and Fe(VI) (dose = 3 mg/L) respectively.[63]

Table 1.1 Standard redox potential for different oxidants and disinfectants.

Disinfectant/Oxidant	**Reactions**	**E^0 (V)**
Chlorine dioxide	$ClO_2(aq) + e^- \rightarrow ClO_2^-$	0.954
Dissolved oxygen	$O_2(aq) + 4H^+ + 4e^- \rightarrow 2H_2O$	1.229
Chlorine	$Cl_2(g) + 2e^- \rightarrow 2Cl^-$	1.358
Perchlorate	$ClO_4^- + 8H^+ + 8e^- \rightarrow Cl^- + 4H_2O$	1.389
Hypochlorite	$HOCl + H^+ + 2e^- \rightarrow Cl^- + H_2O$	1.482
Permanganate	$MnO_4^- + 4H^+ + 3e^- \rightarrow MnO_2 + 2H_2O$	1.679
	$MnO_4^- + 8H^+ + 5e^- \rightarrow Mn^{2+} + 4H_2O$	1.507
Hydrogen peroxide	$H_2O_2 + 2H^+ 2e^- \rightarrow 2H_2O$	1.776
Ozone	$O_3 + 2H^+ + 2e^- \rightarrow O_2 + H_2O$	2.076
Ferrate	$FeO_4^{2-} + 8H^+ + 3e^- \rightarrow Fe^{3+} + 4H_2O$	2.20

1.2.1. Organics

Fe(VI) demonstrates high selectivity toward electron-donating organic compounds (e.g., phenols, amines, olefins, and anilines).[44] The reactions of Fe(VI) with organic compounds follow second-order kinetics with values between 0.1-10^5 M^{-1} s^{-1} reported for reaction rate constants.[45, 64] For example, Karlesa et al. identified transformation products following oxidation of penicillin G and cephalexin by Fe(VI), and concluded that Fe(VI) attacks the electron rich thioether and amine moieties within these compounds.[65] Furthermore, they reported a high reactivity (apparent second-order rate constants of 110-770 M^{-1} s^{-1}) of Fe(VI) towards β-lactam antibiotics (penicillin G, cephalexin, cloxacillin, and amoxicillin) and observed more than 98% degradation in real wastewater effluent solutions spiked with 2 μM of the β-lactams.[65] For compounds with olefinic functional groups (e.g., carbamazepine,[66] tetracycline[67]), oxidation occurs through Fe(VI) electrophilic attack of the olefinic bond. In a study investigating the potential of Fe(VI) for the treatment of secondary wastewater effluent spiked with 68 selected endocrine disrupting chemicals and pharmaceuticals and personal care products (initial concentrations of 100 μg/L each), Yang et al. reported complete removal (>98%) of estrogenic compounds with electron-rich phenolic moieties (i.e., estrone, 17-beta-estradiol, 17-alpha-ehinylestradiol, diethylstilbestrol, bisphenol A, 4-tert-octylphenol and 4-nonlyphenol) when these compounds were exposed to a dose of 10 mg/L of Fe(VI) for 1 min.[42] However, Fe(VI) did not react with electron withdrawing compounds such as triclocarban or cycloalkane compounds such as epi-androsterone and 5-alpha-dihydrotesterone despite longer exposure time up to 3 hours.[42] Nevertheless, at lower concentrations (0.2±0.1 to 1156±192 ng/L) as detected in the secondary effluents of two wastewater effluents of two wastewater treatment plants, the oxidation of the recalcitrant compounds (i.e., triclocarban, 2,4-dichlorophenoxyacetic acid, 2-methyl-4-chlorophenoxyacetic acid, clofibric acid, gemfibrozil, and erythromycicn-H_2O) ranged from 10-100% when exposed

to 10 mg/L Fe(VI) for 3 hours.[42] This demonstrates that Fe(VI) is an effective technology in the treatment of trace organics in polluted waters.

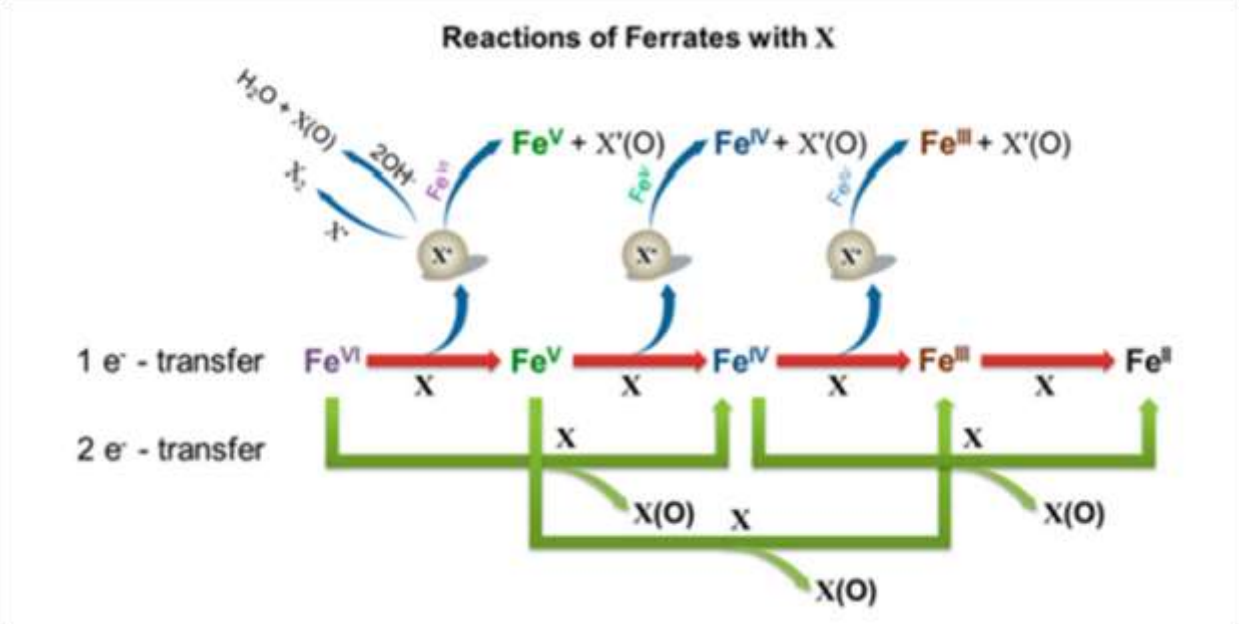

Figure 1.2. Scheme of the oxidation mechanisms of organic compounds (X) by Fe(VI). Image taken from Sharma et al.[32]

The oxidation of organic compounds by Fe(VI) reportedly occurs through the following reactions: (i) a 1 e^- transfer to form Fe(V) followed by a 2 e^- transfer to form Fe(III); (ii) a 2e^- transfer to form Fe(II) through a Fe(IV) intermediate; (iii) reaction of Fe(V) and/or Fe(IV) intermediates with the organic compound; (iv) oxygen atom transfer to the organic compound (**Figure 1.2**).[32, 68] These mechanisms present multiple opportunities for oxidation of organic compounds by Fe(VI) during treatment. In particular, Fe(V) and Fe(IV) are four and two order of magnitude more reactive than Fe(VI) and can achieve greater oxidation of organic compounds.[64, 69-71] For example, Yates et al. observed that Fe(VI) achieved less than 5% removal of perfluorooctanesulfonate (initial concentration 0.779-1.252 mg/L) at pH 7 whereas Fe(V) and Fe(IV) achieved removal efficiencies of 17 and 34 % respectively.[72]

1.2.2. Inorganics

Although the majority of past studies have focused on the oxidation capacity of Fe(VI), in recent years researchers have also evaluated the ability of Fe(VI) to remove inorganic pollutants such as phosphates,[45, 73] heavy metals,[46, 49-51, 74, 75] and metal complexes[70, 74, 76, 77] via coagulation. The reduction of Fe(VI) to Fe(III) facilitates in situ coagulation of inorganic contaminants. Lee et al. assessed the removal of phosphate by Fe(VI) using jar tests.[45] For an initial phosphate concentration of 3.5 mg/L, they reported that a Fe(VI) dose of 7.5 mg/L was sufficient to lower the phosphate concentration below 0.8 mg/L—the phosphate regulatory limit for wastewater discharge in Switzerland.[45] Furthermore, they observed that at a similar Fe dose (7.5 mg/L) in the form of $FeCl_3$ did not achieve similar results,[45] which demonstrates Fe(VI) superior coagulative properties.

Fe(VI) treatment of inorganic contaminants is achieved by sorption of the contaminants on Fe(VI) surface and sequestration within the structure of Fe(III) (hydr)oxides (i.e., γ-Fe_2O_3 and γ-FeOOH) products of Fe(VI) reduction (**Figure 1.3**). Prucek et al. evaluated the mechanisms of

removal of metals (i.e., Ni, Cu, Al, Cd, and Co) by Fe(VI).[46] They observed that while Cd only adsorbed on the surface of Fe(III) oxide/oxyhydroxide nanoparticles generated from Fe(VI) decomposition in water, the other metals (i.e., Co, Ni, Cu and Al) were either trapped within the crystal lattice of Fe(III) oxide phases or formed Fe-metal oxides complexes.[46] This led to a greater removal (>95%) of the latter metals as opposed to Cd (70%).[46] They identified that γ-Fe_2O_3 and γ-FeOOH nanoparticles formed from Fe(VI) reduction[78, 79] can trap small metal ions into nanoparticle tetrahedral sites, while larger metal ions are incorporated into octahedral sites.[46] Fe(VI) can also serve as an oxidant and sorbent for remediation of metals during water treatment. For example, removal of As and Mn in contaminated waters can occur via oxidation of As(III) and Mn(II) into As(V) and Mn(IV) phases followed by coagulation and precipitation.[50, 51, 80] X-ray photoelectron spectroscopy (XPS) analyses on Fe and Mn particles formed after reaction between Fe(VI) and Mn(II) revealed a binding energy peak at 49 eV similar to the Mn 3p peak observed at 49.1 eV for Mn(IV) (in the form of MnO_2).[51]

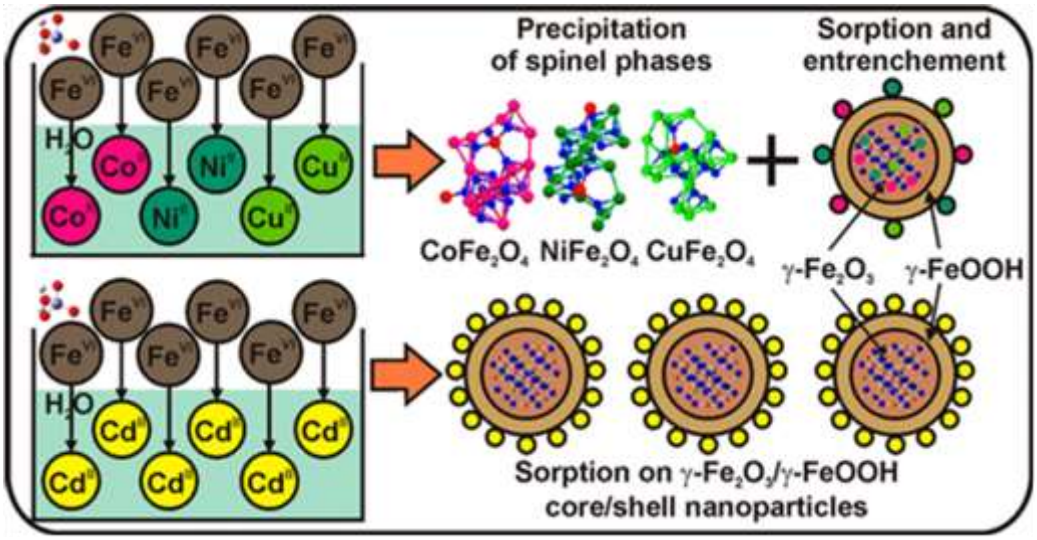

Figure 1.3. Scheme of the removal of metals by Fe(VI). Image taken from Prucek et al.[46]

1.3. Challenges in Ferrate Application

1.3.1. Effects of pH

While Fe(VI) is a very promising reactive species, its chemical instability limits feasibility for deployment in water treatment applications.[32] In aqueous solutions, Fe(VI) undergoes parallel and/or sequential reactions: (i) acid-base reactions to form $H_3FeO_4^+$, H_2FeO_4, $HFeO_4^-$, FeO_4^{2-}; (ii) decomposition into Fe(III) via Fe(V), Fe(IV), Fe(II) and H_2O_2/O_2 intermediates; (iii) reactions with water molecules; and (iv) oxidation reactions with contaminants. Fe(VI) redox potential and speciation dependence on pH can affect these reactions. Under acidic and neutral pH conditions (pH < 7.3), Fe(VI) exists as the short-lived protonated $H_3FeO_4^+$, H_2FeO_4, and $HFeO_4^-$ which rapidly decompose into Fe(III) species and molecular oxygen (**Figure 1.4**). Studies have reported that this decomposition starts with the dimerization of the protonated species to form a differate (FeO_7^{2-}) ion (**Figure 1.4B**, **Eqs. 2, 4-7**) which further decays into Fe(III) through Fe(V), Fe(IV), Fe(II) and H_2O_2/O_2 intermediates (**Figure 1.4B**). This rapid degradation hinders Fe(VI) effectiveness towards organic compound oxidation. Furthermore, the electrochemical reduction potential is 2.2 V at acidic pH and decreases to 0.7 V at alkaline pH (**Table 1.1**). Thus, Fe(VI) reactivity is significantly reduced at environmentally relevant pH (pH 6-9).

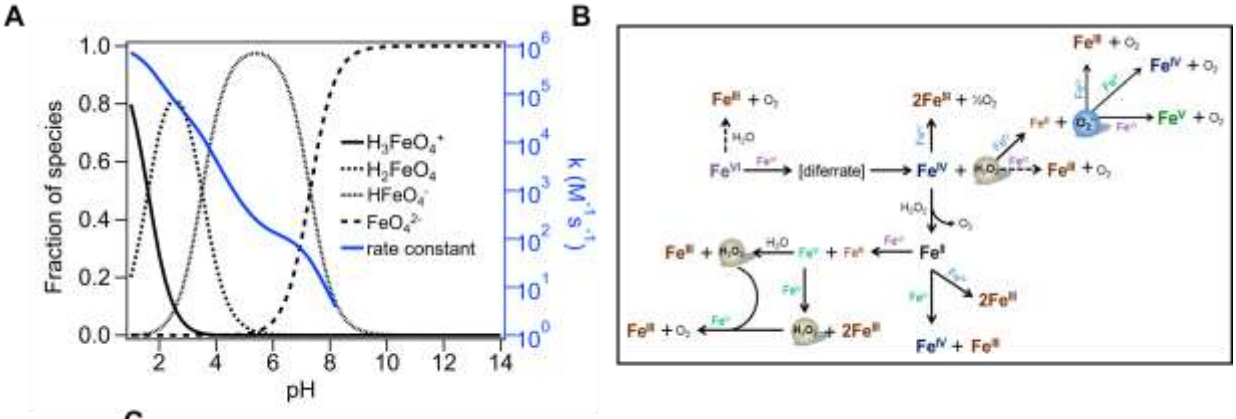

C

$2\ H_3FeO_4^+ \leftrightarrow [H_4Fe_2O_7]^{2+} + H_2O$	$k = (3.5\pm1)\times10^5\ M^{-1}\ s^{-1}$	(Eq. 2)
$H_4Fe_2O_7^{2+} + 2\ H^+ + 6\ H_2O \rightarrow Fe_2(OH)_2(H_2O)_8^{4+} + {}^3/_2O_2$	fast	(Eq. 3)
$H_3FeO_4^+ + H_2FeO_4 \leftrightarrow [Fe_2O_7]^{2-}$	$k \approx (3.5\pm1)\times10^5\ M^{-1}\ s^{-1}$	(Eq. 4)
$2\ H_2FeO_4 \leftrightarrow [Fe_2O_7]^{2-}$	$k = (1.5\pm0.5)\times10^4\ M^{-1}\ s^{-1}$	(Eq. 5)
$H_2FeO_4 + HFeO_4^- \leftrightarrow [Fe_2O_7]^{2-}$	$k \approx (1.5\pm0.5)\times10^5\ M^{-1}\ s^{-1}$	(Eq. 6)
$2\ HFeO_4^- \leftrightarrow [Fe_2O_7]^{2-} + H_2O$	$k = (250\pm50)\ M^{-1}\ s^{-1}$	(Eq. 7)

Figure 1.4. (**A**) Distribution of Fe(VI) species (black lines, right axis) and aqueous self-decay (blue line, left axis) as a function of pH (the pKa values for $H_3FeO_4^+$ ($pKa_1 = 1.6$), H_2FeO_4 ($pKa_2 = 3.5$) and $HFeO_4^-$ ($pKa_3 = 7.3$) were obtained from Rush et al.[74] and decay rate constants from Lee et al.[75] (**B**) Scheme of Fe(VI) self-decay as proposed by Sharma et al.[26] (**C**) Proposed reaction mechanisms for decay of Fe(VI) as proposed by Rush et al.[74]

1.3.2. Effects of Solution Composition

In addition to pH, Fe(VI) stability is affected by aqueous constituents (e.g., ions, dissolved organic carbon, nutrients) such as those commonly found in wastewater effluent (**Table 1.2**). The self-decay of Fe(VI) and its reduction into Fe(III) can be catalyzed by these constituents. Schreyer and Ockerman reported a rapid decrease in Fe(VI) concentration in aqueous solutions containing potassium chloride, potassium nitrate and sodium chloride salts, with the sodium chloride having the most impact; however the mechanisms underlying these observations were not discussed.[81] Divalent ions also exhibit negative effects on Fe(VI) stability.

Ma et al. measured O_2 generated from the decomposition of Fe(VI) in the presence of Ca^{2+} and observed increased dissolved O_2 levels as the Ca^{2+} concentration increased (**Figure 1.5**).[82] Density functional theory calculations revealed that the Ca^{2+} bridging of two Fe(VI) ions promotes the O–O coupling that onsets Fe(VI) self-decay.[44, 79, 82] Interestingly, Fe(III) can also catalyze the self-decay of Fe(VI)[81, 83] via a first-order heterogenous reaction.[83] However, the presence of solutes such as phosphate, borate and carbonate ions can impede the catalytic effect of cations on Fe(VI) decay.[83, 84] Interestingly, Fe(III) can also catalyze the self-decay of Fe(VI)[81, 83] via a first-order heterogenous reaction.[83] However, the presence of solutes such as phosphate, borate and carbonate ions can impede the catalytic effect of cations on Fe(VI) decay.[83, 84] These ions form complexes with the Fe(III) products of Fe(VI) reduction and reduce the surface area that would otherwise be available for further Fe(III) solid phases formation. Phosphate ions exhibit the greatest stabilization effect (**Figure 1.6**) because of their affinity toward Fe(III).[83]

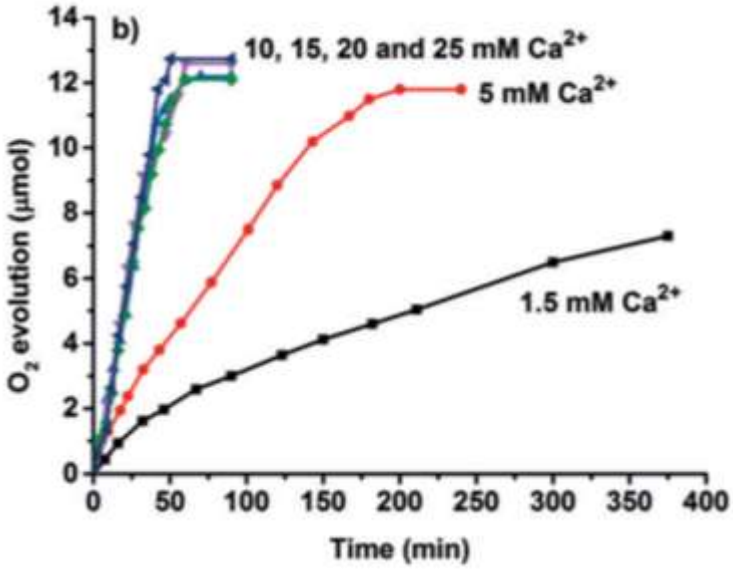

Figure 1.5. Effects of Ca on O_2 generation by Fe(VI) ($[K_2FeO_4]$ = 50 µM). The figure was taken from Ma et al.[82]

Table 1.2. Representative concentration ranges of aquatic species and pH in secondary wastewater effluent. DIC = dissolved inorganic carbon; DOC= dissolved organic carbon.

constituent	concentration	unit	references
Na^+	0.04-8.7	mM	Wang and Lan[85]
Ca^{2+}	0.03-1.3		Burton et al.[86]
Mg^{2+}	0.04-1.6		Azoulay et al.[87]
NO_3^-	0.01-0.4		Xu et al.[88]
Cl^-	1.4-9.9		Burton et al.[86]
PO_4^{3-}	0.001-0.009		Pinter et al.[89]
DIC	28-46.7	mM-C	Maizel et al.[90]
DOC	0.17-2.75		Griffith et al.[91]
pH	6.5-8.5		Lee et al.[17]

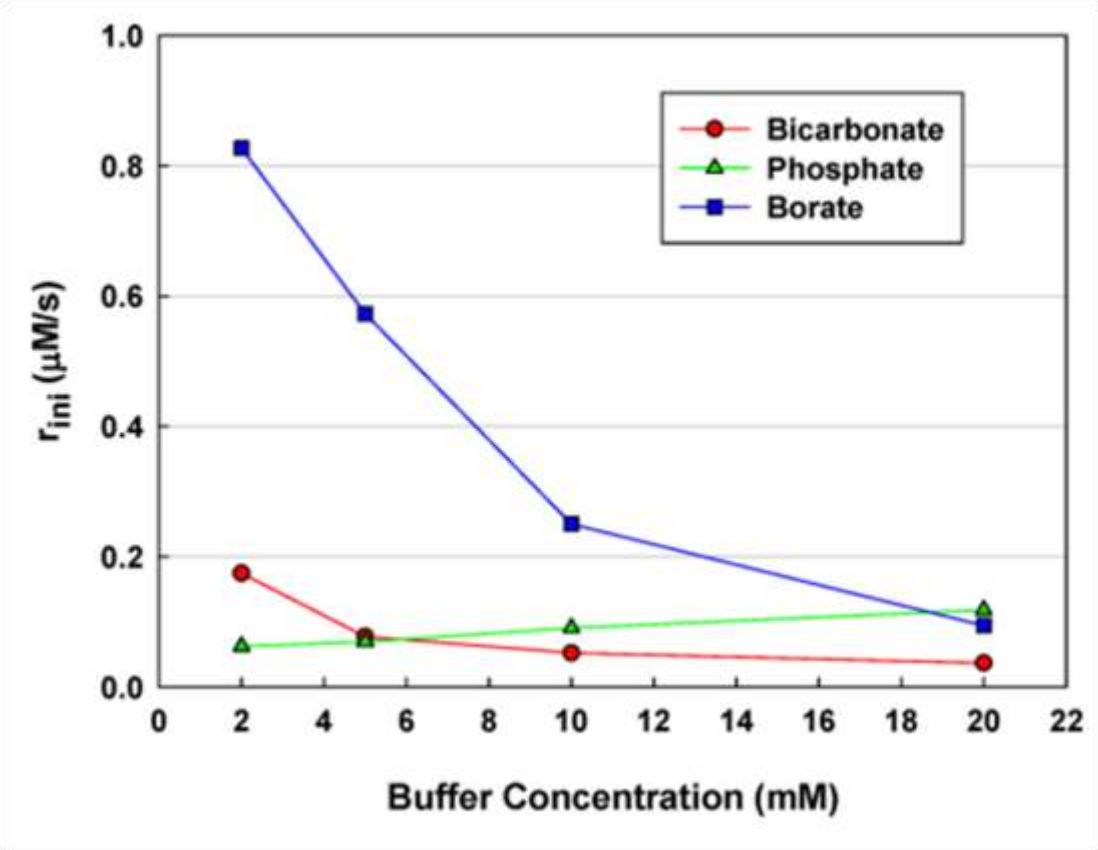

Figure 1.6. Effects of inorganic buffering ions on the decomposition rate of Fe(VI) (50 μM) at pH 7.5. Initial Fe(VI) decomposition (r_{ini}) is reported on the y-axis. Sodium salts (sodium bicarbonate, sodium borate decahydrate, sodium phosphate dibasic) of the ions were used. The figure is taken from Jiang et al.[83]

Consequently, Fe(VI) oxidation of organic compounds during water treatment can be impeded by solutes that promote Fe(VI) decay. In the presence of Ca^{2+}, Mg^{2+}, SO_4^{2-}, caffeine oxidation by Fe(VI) decreased by 11.8, 8.1 and 4.3% respectively.[92] Similarly, Feng et al. reported a decrease in the oxidation of flumequine in the presence of Ca^{2+} and Mg^{2+}.[39] They also observed decreased oxidation in the presence of Fe(III).[39] While fluorescence measurements indicated the complexation of Fe(III) and flumequine thus inhibiting Fe(VI) reaction with flumequine, no spectral changes were observed when Ca^{2+} and Mg^{2+} were present which indicates that these ions solely influenced Fe(VI) decay.[39] Contrary to these results, Wang et al. observed that the presence of Mg^{2+}, Ca^{2+}, K^+ and Na^+ enhanced the oxidation of acetaminophen by Fe(VI) with Mg^{2+} exhibiting the most enhancement.[93] The authors proposed that the metal cations promote the deprotonation of acetaminophen through metal complexation.[93] This phenomenon releases H^+ ions into solution which decreases the solution pH which will increase the oxidation capacity of Fe(VI).[93]

Additionally, Fe(VI) aqueous stability and reactivity are affected by dissolved organic carbon. Jiang et al. observed more Fe(VI) stability in natural waters compared to laboratory deionized water.[83] The authors hypothesized that dissolved natural organic matter (NOM) can coat and alter the surface of Fe(III) particles thus inhibiting further surface-promoted Fe(VI) decay.[83] Conversely, Deng et al. reported the opposite effect and observed a rapid decay of Fe(VI) in the presence of NOM.[94] They proposed that Fe(VI) decay in the presence of NOM is due to (i) reactions of Fe(VI) with NOM, (ii) Fe(VI) self-decay, and (iii) surface catalyzed decay of Fe(VI).[94] Thus the extent of NOM effects on Fe(VI) stability will depend on the extent of reactions with NOM moieties. Furthermore, these reactions can reduce Fe(VI) reactivity and decrease the oxidation of organic contaminants by Fe(VI) during water treatment. For example,

Feng et al. reported a 40% decrease in the removal efficiency of flumequine by Fe(VI) in the presence of 15 mg/L humic acid commonly present in wastewater.[95] Therefore, a pretreatment to remove NOM during wastewater treatment might be needed to optimize Fe(VI) treatment.

1.4. Ferrate Reactivity Stabilization by Silica

Researchers have explored different methods to overcome the limitations presented by Fe(VI) aqueous decomposition. Fe(VI) activation using chemicals[96, 97] and solid materials[98-100] have been investigated to stabilize Fe(VI) and increase the oxidation efficiency for organic compounds by Fe(VI).[98-100] Delaude and Laszlo tested different aluminosilicate materials as catalytic supports for the oxidation of benzyl alcohol by Fe(VI), and reported that the yield of the oxidation product benzaldehyde was greater (>90%) in the presence of a K10 montmorillonite clay.[98] The authors hypothesized that the K10 clay provides a polar environment that can promote the adsorption of benzyl alcohol and subsequent oxidation by Fe(VI) on the clay surface.[98] Al-Abduly and Sharma reported a 22% increase in the oxidation of dibenzothiophene at pH 8 in the presence of silica (SiO_2) gels.[100] Under the same conditions (i.e., pH 8, presence of SiO_2 gels), Manoli et al. reported a 47% increase in the oxidation of caffeine compared to oxidation in the absence of SiO_2 gels.[99] Studies indicate that dissolved silicate (SiO_4^{2-}) can retard the oxidation of Fe(II) to Fe(III) by occupying sorption sites on Fe(III) oxides produced during Fe(VI) reduction, thus preventing the binding of Fe(II) to these sites and further oxidation of Fe(II).[101] Similarly, Manoli et al. proposed that interactions between Fe(VI) and SiO_2 impede the self-decomposition of Fe(VI) and retards the electron transfer between Fe species (Fe(V), Fe(IV), Fe(III) and Fe(II)), thereby increasing Fe(VI) reactivity toward organic compounds. These studies clearly demonstrate the ability of SiO_2 gels to stabilize Fe(VI), which could expand applicability of ferrate for water treatment. However, the role of the SiO_2 gels is not well

understood. Furthermore, the use of silica gels to retard Fe(VI) reduction during treatment will create an additional solids waste stream that will need to be separated and/or replaced once ferrate is consumed. The application of SiO_2 gels water treatment systems with infiltration processes can be challenging due to the high water retention capacity of SiO_2 gels.[102] Therefore, more effective stabilization methods are needed to overcome the limitations of SiO_2 gels and promote the application of SiO_2 stabilized Fe(VI) in water treatment.

1.5. Dissertation Objectives and Overview

The research investigates the ability of SiO_2 to stabilize Fe(VI) to develop a novel, Fe(VI)-coated sand media for wastewater effluent treatment. Given the multimodal properties of Fe(VI) (i.e., oxidant, disinfectant, and coagulant), previous studies hypothesized that the use of Fe(VI) could reduce economical and spatial costs for water treatment plants by combining pre-disinfection, oxidation, and coagulation into one unit.[103] Similarly, the use of a Fe(VI)-coated sand media could be beneficial in water treatment systems that include filtration processes. Sand—composed of >80% SiO_2 content[104]—is a widely used filtration media in (de)centralized water treatment. Particularly, Fe(VI)-coated sand would be an excellent candidate for treatment media to provide the simultaneous oxidation of organic pollutants and adsorption of heavy metals while maintaining high hydraulic conductivity.

Chapter 2 presents a synthesis method for the Fe(VI)-coated sand composite media as well as its physicochemical characterization. A proof-of-concept study was also performed to evaluate the Fe(VI)-coated sand capacity for oxidation of phenol—a model wastewater contaminant—and the Fe(VI)-coated sand performance was compared to that of Fe(VI) powder. This work was published in *Journal of Materials Chemistry A*. In chapter 3, we assessed the Fe(VI)-coated sand reactivity in more complex matrices by evaluating the effect of pH and wastewater effluent ions

on the treatment of multiple contaminants (i.e., acetaminophen, benzotriazole, and sulfamethoxazole, copper, lead, zinc). These results are included in a manuscript recently accepted for publication in the *Journal of ACS Environmental Au*. In chapter 4, we probed the effects of effluent organic matter on the reactivity of the Fe(VI)-coated sand in a synthetic wastewater effluent. In chapter 5, applications of the Fe(VI)-coated sand in water treatment systems as well avenues for future research are discussed.

Chapter 2. Synthesis of Ferrate (Fe(VI))-coated Sand for Stabilized Reactivity and Enhanced Treatment of Phenol

This chapter was previously published as: Okaikue-Woodi, F. E. K. and Ray J. R. Synthesis of Ferrate(Fe(VI))-coated sand for stabilized reactivity and enhanced treatment of phenol. *J. Mater. Chem. A* **2023**, 11, 13550-13563. doi.org/10.1039/D3TA01950K.

ABSTRACT

Fe(VI)-coated sand was synthesized by coating potassium ferrate onto sand modified with a tetraethyl orthosilicate precursor. The mass of Fe(VI) leached from the media surface increased with increasing pH (pH 7–9). Furthermore, Fe(VI) decay was faster in a borate buffer (k = 2.22 mg L^{-1} hr^{-1}) than in a phosphate buffer (k = 3.39 mg L^{-1} hr^{-1}). Removal of 219±12 µg/L phenol—a representative wastewater organic compound—was achieved at a faster rate by the composite than by application of aqueous K_2FeO_4 powder (51% removed after 5 min compared to 37%). Decomposition of Fe(VI) from the composite surface in the presence of methyl phenyl sulfoxide (PMSO) suggests that reactive Fe(V) and Fe(IV) formation occurs at a faster rate than with K_2FeO_4 powder addition. In the presence of PMSO, phenol removal was approximately 1.1 times higher, which suggests Fe(V)/Fe(IV) involvement. This novel, cost-effective and eco-friendly media presents a viable alternative for more feasible deployment of Fe(VI) in water treatment systems.

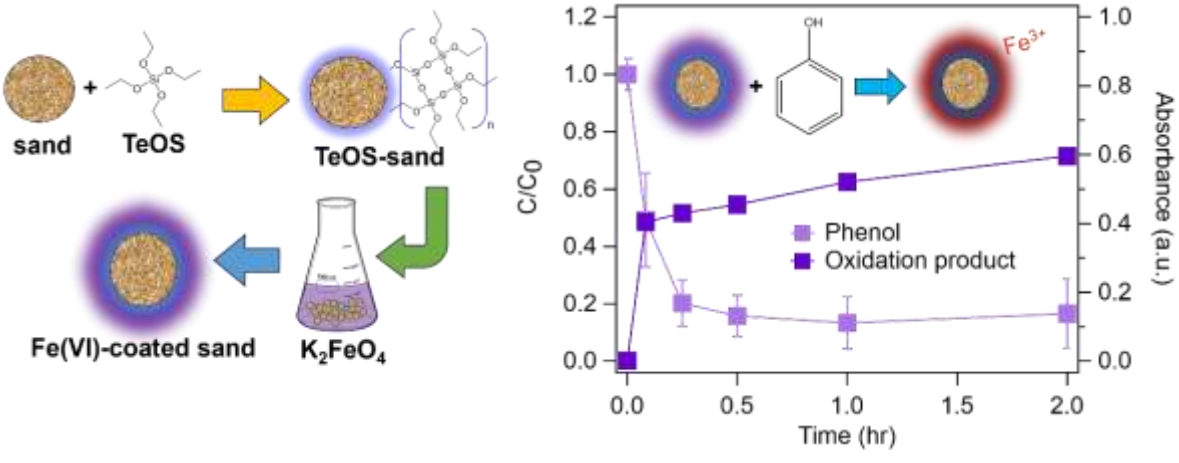

2.1. Introduction

Chemical oxidation is a critical process in water treatment to facilitate the destruction of harmful trace organic compounds such as pharmaceuticals and personal care products, pesticides, antibiotics, and industrial chemicals. Traditionally, chemical oxidation is achieved by addition of ozone[21, 105] or chlorine[21, 106] due to their potential for disinfection. However, the application of these chemicals can lead to the formation of harmful transformation products (e.g., halogenated byproducts[5, 18, 62, 107, 108]). For example, studies have reported increased estrogenic activity after ozonation[109, 110] or chlorination[109] of estrogenic compounds (e.g., bisphenol A) found in surface waters. Gomes et al. assessed the oxidation of a mixture of parabens—used as antimicrobial and preservatives in pharmaceuticals and personal care products—and reported quinone by-products with higher toxicity to *D. magna*, which also demonstrates the risks associated with use of conventional chemical oxidants.[111]

Ferrate (Fe(VI)) has been explored as an alternative chemical to conventional oxidants. Fe(VI) is an environmentally benign iron oxyanion with a standard oxidation potential (E^0) of 2.2 V, which is greater than the oxidation potentials of chlorine (E^0 = 1.36 V)[55] and ozone (E^0 = 2.08 V).[55] Additionally, compared to chlorine and ozone, Fe(VI) is less reactive towards bromide[58, 112] and has been shown to reduce the formation of brominated transformation byproducts during pre-oxidation of surface waters.[61, 62, 112] Furthermore, the chemical reduction of Fe(VI) leads to the formation of naturally occurring, non-toxic ferric (i.e. Fe^{3+} or Fe(III)) species[113, 114] which have been used as coagulants[55, 56] and adsorbents[55, 57] in water treatment. Fe(VI) has been investigated in numerous studies with a demonstrated ability to remediate a wide range of organic compounds (e.g., pharmaceuticals,[36, 38-40, 42, 115] herbicides,[43] and other micropollutants[31, 44, 45]). The oxidation of organic compounds by Fe(VI) occurs via (i) a 1 e^- transfer to form Fe(V) followed by a 2 e^- transfer to form Fe(III); (ii) a 2 e^- transfer to form Fe(II)

through a Fe(IV) intermediate; (iii) reactions of Fe(V) and Fe(IV) with the compound; and (iv) an oxygen atom transfer to the compound.[32, 68] Fe(VI) has high selectivity toward compounds with electron-donating moieties, but minimal reactivity toward compounds with electron-withdrawing moieties.[42] In addition, Fe(VI) has proven to be an effective coagulant[46-48, 51] and disinfectant[48, 53, 103] in water treatment. Therefore, the large standard oxidation potential and multifunctionality of Fe(VI) make it an attractive chemical for water treatment.

While Fe(VI) is a very promising, benign treatment chemical, its deployment in water treatment applications is hindered by its aqueous properties. As the stability of the aqueous

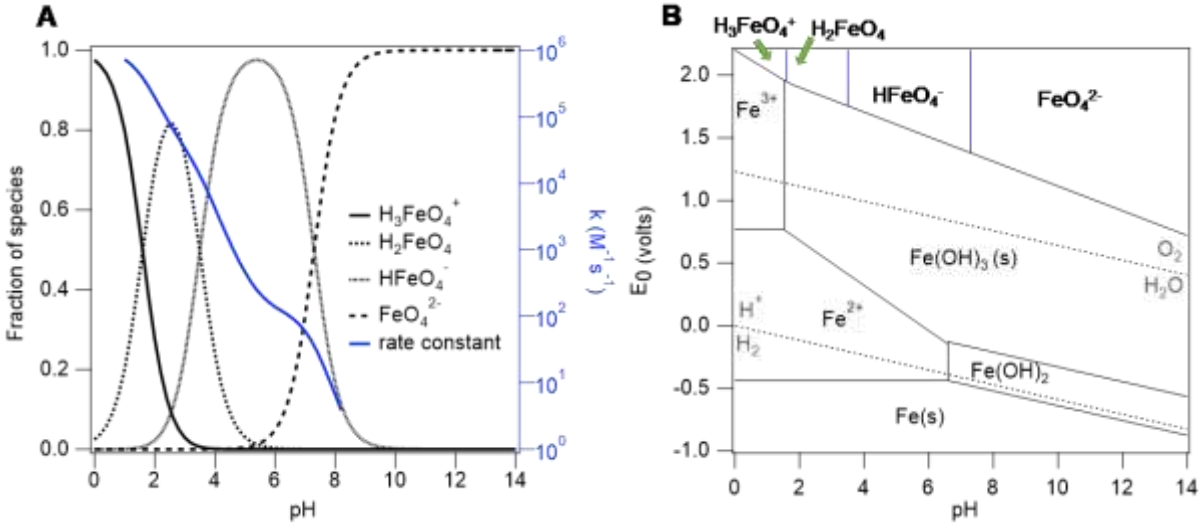

Figure 2.1. (A) Speciation of Fe(VI) (left axis, black lines) and aqueous Fe(VI) self-decay rate (right axis, blue line) as a function of pH. (**B**) Distribution of the standard potential of iron species including Fe(VI) species. The pKa values: $H_3FeO_4^+$ (pKa = 1.6); H_2FeO_4 (pKa = 3.5); $HFeO_4^-$ (pKa = 7.3) were obtained from Rush et al.,[74] and decay rate constants from Lee et al.[75] Data for the standard potentials was obtained from Pogliani et al.[130] and Wulfsberg.[131]

Fe(VI) chemical structure increases with solution pH, its oxidation potential decreases. Under acidic conditions, Fe(VI) exists as the short-lived and highly reactive protonated species $H_3FeO_4^+$, H_2FeO_4, and $HFeO_4^-$ (**Figure 2.1**) which undergo hydrolysis reactions to form Fe(III) species via formation and decomposition of intermediate species Fe(V) and Fe(IV) phases.[78, 116,

[117] Under these conditions, Fe(VI) undergoes a kinetically fast decomposition (**Figure 2.1A**). In alkaline solutions, Fe(VI) exists as the stable and less reactive deprotonated species FeO_4^{2-} (**Figure 2.1**) which also reacts with water to form Fe(III) via Fe(V) and Fe(IV) intermediate species formation.[118] Consequently, these hydrolysis reactions compete with Fe(VI)-contaminant reactions during water treatment.

In recent years, researchers have investigated methods to increase the Fe(VI) oxidizing power at environmentally relevant pH (pH 6-9).[71, 119-124] For example, in addition to water, Fe(VI) reactions with organic compounds also generates Fe(V) and Fe(IV) intermediate species via one-electron and two-electron transfer respectively. Fe(V) and Fe(IV) species are reportedly two to four orders of magnitude more reactive than Fe(VI),[125] but are highly unstable and can quickly react with water to self-decompose.[44, 116, 117, 126] Thus, enhancing reactions between the short-lived, unstable Fe(V) and Fe(IV) species and the organic compounds would improve their oxidation by Fe(VI). To this end, researchers have employed activation agents such as sulfur(IV)-based reductants[127-130] and silica (SiO_2)[68, 131] to catalyze Fe(V)/Fe(IV) production. For example, Al-Abduly and Sharma reported a 22% increase in the oxidation of dibenzothiophene in the presence of SiO_2 gels at pH 8.[131] Under the same conditions (i.e., pH 8, presence of SiO_2 gels), Manoli et al. reported a 47% increase in the oxidation of caffeine compared to oxidation in the absence of SiO_2 gels.[68] The authors proposed that interactions between Fe(VI) and SiO_2 promotes the generation of Fe(V) and Fe(IV) species, and retards the self-decomposition of Fe(VI) to Fe(V) and Fe(IV) species, thereby increasing their exposure to organic compounds.[68] During Fe(VI) oxidation of organic compounds, redox reactions between Fe(VI) and lower valence iron species (e.g., Fe(II)) can occur (e.g., Fe(VI) + Fe(II) → Fe(V) + Fe(III); Fe(IV) + Fe(II) → 2 Fe(III))[32] which will limit Fe(VI) exposure to organic compounds and decrease

Fe(VI) treatment efficacy. Studies have shown that dissolved silicate (SiO_4^{2-}) can retard the heterogeneous oxidation of Fe(II) to Fe(III) by occupying sorption sites on Fe(III) oxides.[132] Thus, the presence of SiO_2 would decrease the rate of redox reactions between iron species during Fe(VI) treatment of organic compounds. In this study, we exploit the stabilization properties of SiO_2 to develop a novel, Fe(VI)-coated sand media for water treatment. Given the multimodal properties of Fe(VI) (i.e., oxidant, disinfectant, and coagulant), researchers hypothesize that the use of Fe(VI) could reduce economical and spatial costs for water treatment plants by combining pre-disinfection, oxidation, and coagulation into one unit.[103] Therefore, the use of a Fe(VI)-coated sand media could be beneficial in water treatment systems that include filtration units as sand (composed of >80% SiO_2 content[133]) is a widely used filtration media. To assess the oxidative capacity of the novel Fe(VI)-coated sand, we will use phenol as a model organic compound as many naturally occurring and anthropogenic contaminants detected in wastewater effluents[42, 134] and surface waters[42, 135, 136] contain phenolic moieties (e.g., natural organic matter, halogenated phenols, alkylphenols, and steroid estrogens). The objectives of this study are to: (1) establish a synthesis for the Fe(VI)-coated sand media and characterize its properties; (2) assess the capacity of Fe(VI)-coated sand for the treatment of organic contaminants, and (3) elucidate the mechanisms underlying the oxidation process and the role of SiO_2 stabilization.

2.2. Materials and Methods

2.2.1. Chemicals

All chemicals were ACS grade and higher unless stated otherwise. Calcium hypochlorite ($Ca(OCl)_2$), ferric nitrate nonahydrate ($Fe(NO_3)_3 \cdot 9\ H_2O$), and potassium hydroxide (KOH) were purchased from Fisher Scientific (Waltham, MA) and used in the synthesis of potassium ferrate (K_2FeO_4). Pentane (Sigma Aldrich, MO), methanol (JT Baker, NJ), and dichloromethane (Sigma

Aldrich) were used as organic solvent washes of the K_2FeO_4 solid. The Ottawa sand composite substrate was purchased from VWR (Radnor, PA). Tetraethyl orthosilicate (TeOS, Sigma Aldrich, MO) and nitric acid (HNO_3, Fisher Scientific, MA) were used in the modification of the sand prior to Fe(VI) coating. Trace metals grade HNO_3 was purchased from Fisher Scientific for total Fe measurements. Sodium tetraborate anhydrous ($Na_2B_4O_7$, Across Organics, Belgium), sodium phosphate dibasic heptahydrate ($Na_2HPO_4 \cdot 7H_2O$, VWR, PA), sodium phosphate monobasic monohydrate ($NaH_2PO_4 \cdot H_2O$, VWR, PA), acetic acid (Fisher Scientific, MA), sodium hydroxide (NaOH, Fisher Scientific, MA), and hydrochloric acid (HCl, Sigma Aldrich, MO) were used to prepare buffer solutions. Phenol (Sigma Aldrich, MO), methyl phenyl sulfoxide (PMSO, Sigma Aldrich, MO), methyl phenyl sulfone ($PMSO_2$, Sigma Aldrich, MO), and sodium sulfite anhydrous (Na_2SO_3, Fisher Scientific, MA) were used in the organic compound removal experiments. 2,2'-azinobis-(3-ehtylbenzothiazoline-6-sulfonate) (ABTS), 3-(2-Pyridyl)-5,6-diphenyl-1,2,4-traizine-4',4''-disulfonic acid sodium salt (ferrozine), ammonium acetate (Sigma Aldrich, MO), hydroxylamine hydrochloride (Beantown Chemical, NH), and potassium thiocyanate (KSCN, Fisher Scientific, MA) were purchased from Sigma Aldrich for measurements of aqueous Fe(VI), Fe(II), and Fe(III). High performance liquid chromatography (HPLC) grade formic acid (Agilent Technologies, CA), acetonitrile (Fisher Scientific, MA) and water (Fisher Scientific, MA) were used for HPLC analyses. All experiments were conducted using ultrapure Milli-Q water (resistivity: 18.2 mΩ).

2.2.2. Synthesis of Fe(VI)-coated sand

The Fe(VI)-coated sand was synthesized by adding sand to a solution of potassium ferrate. First, the Ottawa sand (30-40 mesh, >90% SiO_2) was washed with 1 M HNO_3 for 24 hours and rinsed with deionized water until the pH of the rinse solution was within pH 6-8. The washed sand was then dried at 105 °C for 24 hours in a VWR 1350G oven (Radnor, PA). To promote

binding of ferrate to the sand surface, 15 mL of TeOS was added to 30 g of pre-washed sand, mixed for 3 hours, and dried at 105 °C for 24 hours in a VWR 1350G oven. The TeOS modified sand, designated as **TeOS-sand**, was added to the potassium ferrate (K_2FeO_4) solution. The stability of the TeOS on the sand surface was tested by sonicating 15 mg of TeOS-sand in a 15 ml of 10 mM $Na_2B_4O_7$ buffer and analyzing the leachate via UV-Vis spectroscopy using a Shimadzu UV-2700 spectrophotometer (Kyoto, Japan). The resulting spectrum was compared to the spectrum of a 4 mL TeOS solution obtained on the same spectrophotometer. Another TeOS-sand was also synthesized by mixing the TeOS (15 mL) and cleaned sand (30 g) for 24 hours before drying.

The K_2FeO_4 solution was prepared via the wet oxidation process following a method adapted from Guan et al. (more information provided in **Appendix A1**).[137] A saturated solution of 13 M KOH was prepared, chilled, and stored at 4 °C throughout the synthesis to maintain cold temperature conditions. Approximately 15 g of $Ca(OCl)_2$ was added to 25 mL of the saturated KOH solution, then the mixture was stirred for 30-60 min and filtered using a Whatman glass microbore filter (grade GF/A) paper to obtain a yellow solution of potassium hypochlorite. An additional 20 mL of the saturated KOH solution was added to the yellow filtrate and the mixture was placed in an ice bath for 20-30 min to precipitate potassium chloride. The potassium chloride suspension was further filtered with a GF/A filter paper, then 8 g of pulverized ferric nitrate was added in small portions (~0.50 g/min) for 15 min to the filtrate solution under cooling conditions (4 °C) to form K_2FeO_4. A VWR recirculating chiller was used to maintain the temperature of the potassium ferrate throughout the synthesis. The generated solution of potassium ferrate was stirred for an hour before the addition of 50 mL of saturated KOH. The solution was vigorously stirred at 500 rpm for 5 min and left to stand for 30 min. Next, 25 g of

the TeOS-sand was added to the K_2FeO_4 solution and stirred for 24 hours at 4 °C to allow the Fe(VI) to coat the sand surface. The K_2FeO_4 supernatant was decanted, and the synthesized Fe(VI)-coated sand was centrifuged at 4000 rpm for 10 min to remove the excess solution before being dried in a VWR vacuum oven pumped with a RV12 Edwards pump for more than 24 hours. The Fe(VI)-coated sand was stored under vacuum when not in use to limit exposure to air and prevent ferrate decomposition. The Fe(VI)-coated sand was synthesized by adding sand to a solution of potassium ferrate. First, the Ottawa sand (30-40 mesh, >90% SiO_2) was washed with 1 M HNO_3 for 24 hours and rinsed with deionized water until the pH of the rinse solution was within pH 6-8. The washed sand was then dried at 105 °C for 24 hours in a VWR 1350G oven (Radnor, PA). To promote binding of ferrate to the sand surface, 15 mL of TeOS was added to 30 g of pre-washed sand, mixed for 3 hours, and dried at 105 °C for 24 hours in a VWR 1350G oven. The TeOS modified sand, designated as **TeOS-sand**, was added to the potassium ferrate (K_2FeO_4) solution. The stability of the TeOS on the sand surface was tested by sonicating 15 mg of TeOS-sand in a 15 ml of 10 mM $Na_2B_4O_7$ buffer and analyzing the leachate via UV-Vis spectroscopy using a Shimadzu UV-2700 spectrophotometer (Kyoto, Japan). The resulting spectrum was compared to the spectrum of a 4 mL TeOS solution obtained on the same spectrophotometer. Another TeOS-sand was also synthesized by mixing the TeOS (15 mL) and cleaned sand (30 g) for 24 hours before drying.

The K_2FeO_4 solution was prepared via the wet oxidation process following a method adapted from Guan et al. (more information provided in **Appendix A1**).[137] A saturated solution of 13 M KOH was prepared, chilled, and stored at 4 °C throughout the synthesis to maintain cold temperature conditions. Approximately 15 g of $Ca(OCl)_2$ was added to 25 mL of the saturated KOH solution, then the mixture was stirred for 30-60 min and filtered using a Whatman glass

microbore filter (grade GF/A) paper to obtain a yellow solution of potassium hypochlorite. An additional 20 mL of the saturated KOH solution was added to the yellow filtrate and the mixture was placed in an ice bath for 20-30 min to precipitate potassium chloride. The potassium chloride suspension was further filtered with a GF/A filter paper, then 8 g of pulverized ferric nitrate was added in small portions (~0.50 g/min) for 15 min to the filtrate solution under cooling conditions (4 °C) to form K_2FeO_4. A VWR recirculating chiller was used to maintain the temperature of the potassium ferrate throughout the synthesis. The generated solution of potassium ferrate was stirred for an hour before the addition of 50 mL of saturated KOH. The solution was vigorously stirred at 500 rpm for 5 min and left to stand for 30 min. Next, 25 g of the TeOS-sand was added to the K_2FeO_4 solution and stirred for 24 hours at 4 °C to allow the Fe(VI) to coat the sand surface. The K_2FeO_4 supernatant was decanted, and the synthesized Fe(VI)-coated sand was centrifuged at 4000 rpm for 10 min to remove the excess solution before being dried in a VWR vacuum oven pumped with a RV12 Edwards pump for more than 24 hours. The Fe(VI)-coated sand was stored under vacuum when not in use to limit exposure to air and prevent ferrate decomposition.

2.2.3. Characterization of the Fe(VI)-coated sand media

2.2.3.1. Detection of Fe(VI) on the media surface

In an alkaline solution, Fe(VI) has an absorption peak at 510 nm.[138] The presence of the Fe(VI) on the Fe(VI)-coated sand surface was determined via UV-Vis spectroscopy. The Fe(VI)-coated sand was placed in a 5 mM Na_2HPO_4/1 mM $Na_2B_4O_7$ solution (pH 9.25) and sonicated for 5 min to desorb Fe(VI) from the coated sand surface for direct UV-Vis measurement of the Fe(VI) leachate. The leachate solution was reacted with ABTS following a method by Lee et al.[139] to measure the absorbance corresponding to the formation of an $ABTS^{\cdot+}$ radical at 415 nm (more information provided in **Appendix A2**).

2.2.3.2. Fe coating density on the media surface

The total Fe mass coated on the sand was measured via inductively coupled plasma orbital emission spectrometry (ICP-OES) using a Perkin Elmer Optima 8300 Inductively Coupled Plasma-Optical Emission Spectrophotometer (ICP-OES) (Perkin Elmer, Whatman, MA) (more information provided in Appendix A2). The Fe(VI)-coated sand was placed in a 1% HNO_3 solution and sonicated for 5 min to leach all the Fe coating. The leachate was further diluted with the 1% HNO_3 solution before ICP-OES analysis.

2.2.4. Stability of the Fe(VI) coating on the sand surface

2.2.4.1. Aqueous stability

Batch experiments were conducted to evaluate the aqueous stability of the Fe(VI)-coated sand and the desorption of Fe(VI) from the media surface. Approximately 50 mg of Fe(VI)-coated sand was added to 50 mL of 10 mM Na_2HPO_4/NaH_2PO_4 or 10 mM $Na_2B_4O_7$ buffer and stirred at 40 rpm. The buffer solutions were adjusted to pH 7, 8, 9 using HCl or NaOH to determine the effects of solution pH on Fe(VI) stability. At designated time intervals, aliquots of the samples were filtered using 0.2 µm, 25 mm diameter cellulose acetate syringe filters. Aqueous concentrations of Fe(VI) were determined using the ABTS method[139] and aqueous total Fe using ICP-OES (see **Appendix A2**). Preliminary tests revealed that Fe(VI) and Fe(III) were the dominant Fe species in solution when the Fe(VI)-coated sand was placed in buffered solutions (pH 9) (**Figure A1B-C**); thus, aqueous Fe(III) concentrations were calculated as the difference between the measured total Fe and Fe(VI).

The aqueous stability of Fe(VI) in the absence of silica stabilization was also assessed for comparison with the Fe(VI)-coated sand. A stock solution of K_2FeO_4 powder (synthesis in **Text S1**) was diluted to approximately 21 mg/L in 10 mM $Na_2B_4O_7$ buffer at pH 9 and stirred at 40 rpm. At designated times, a 1 mL aliquot was taken and filtered using 0.2 µm, 25 mm diameter

cellulose acetate syringe filters, then residual Fe(VI) concentrations were determined using the ABTS method.[139]

2.2.4.2. Media storage stability

Total Fe and aqueous Fe(VI) measurements were taken at designated time intervals (t = 1, 3, 5, 7, and 11 days) after Fe(VI)-coated sand production to quantify Fe coating on the sand surface and to assess the media stability during storage. At each sampling time, approximately 3 g/L of Fe(VI)-coated sand was removed from the vacuum oven and placed in a 5 mM Na_2HPO_4/1 mM $Na_2B_4O_7$ solution (pH 9.25) and sonicated for 5 min to desorb Fe(VI) from the coated sand surface. The leachate solution was then reacted with ABTS to determine the aqueous Fe(VI) concentration. The same coated sand dose (3 g/L) was simultaneously measured and placed in a 1% HNO_3 solution and sonicated for 5 min before total Fe measurements.

2.2.5. Phenol removal experiments

Initial experiments (see **Appendix A3**) evaluating the effect of buffering ions on the oxidation of PMSO by Fe(VI)-coated sand revealed a higher oxidation capacity of Fe(VI)-coated sand in the borate buffer thus, remaining experiments were conducted in the borate buffer. Sulfoxides (e.g., dimethyl sulfoxide (DMSO), PMSO) are known to be oxidized by high-valent iron to produce their corresponding sulfones (e.g., dimethyl sulfone ($DMSO_2$), $PMSO_2$) through an oxygen atom transfer step.[140] Thus, PMSO is an excellent probing compound to evaluate the media reactivity under different experimental conditions. Batch experiments to evaluate the Fe(VI)-coated sand media capacity for phenol treatment were conducted in 10 mM $Na_2B_4O_7$ buffer at pH 9 in media bottles wrapped with aluminum foil to maintain dark conditions.

The effect of Fe(VI)-coated sand dose on phenol removal was determined to identify the optimal media dose for water treatment. Different amounts (i.e., 22.8±1.1, 42.6±0.8, and 80.7±1.0 mg) of Fe(VI)-coated sand were added to 20 mL solutions of 10 mM $Na_2B_4O_7$

containing phenol (236±0.6 µg/L) to obtain media doses of 1, 2, and 4 g/L. The mixtures were shaken for 30 min at 40 rpm. Then, a 2 mL aliquot was quenched with 20 µL of 500 mM Na_2SO_3 to stop the reaction between Fe(VI) and phenol. The mixture was filtered with a 0.2 µm, 25 mm diameter cellulose acetate syringe filter to measure residual phenol using high performance liquid chromatography (HPLC) methods. Details of the HPLC method are provided in **Appendix A4**.

Removal kinetics experiments were initiated by adding approximately 200 mg of Fe(VI)-coated sand to 100 mL of a 10 mM $Na_2B_4O_7$ buffer solution containing phenol. At designated time intervals, an aliquot of 2 mL was sampled and pretreated as above before HPLC analysis. An additional aliquot of 1 mL was taken simultaneously to measure aqueous Fe(VI) concentration by the ABTS method.[139] Another 1 mL aliquot was further diluted with a 10 mM $Na_2B_4O_7$ buffer solution and quenched with HNO_3 (trace metals grade) to measure total aqueous Fe by ICP-OES. A 4 mL aliquot was also taken and filtered with a 0.2 µm, 25 mm diameter cellulose acetate syringe filter for UV-Vis scanning between 200-650 nm for detection of oxidation products with absorbances outside of the range of the HPLC diode array detector.

The removal of phenol by Fe(VI) powder was also investigated to compare the performance of the Fe(VI)-coated sand media against Fe(VI) powder in the absence of silica stabilization. Fe(VI) stock solution (i.e., in the absence of sand) was freshly prepared by diluting approximately 12.6 mg/L of K_2FeO_4 powder (synthesis details in **Appendix A1**) in 10 mM $Na_2B_4O_7$ buffer. The stock solution was used within 15 min of preparation to minimize Fe(VI) self-decay. 10 mL of the stock solution was added to 90 mL of a 10 mM $Na_2B_4O_7$ buffer solution containing phenol to initiate phenol removal. All experiments were conducted in duplicates or triplicates.

2.2.6. Evaluation of Fe(VI)-coated sand oxidation mechanisms

To assess the media reactivity toward multiple organic compounds and probe oxidation mechanisms, phenol removal by Fe(VI)-coated sand was assessed in the presence of PMSO. Fe(VI)-coated sand (2 g/L) was added to pH 9 borate buffer solutions containing PMSO and phenol at different concentrations (250 µg/L or 500 µg/L phenol and 400 µg/L or 800 µg/L PMSO). Aliquots were sampled and analyzed as described in *Section 2.5*. HPLC samples were analyzed for phenol, PMSO and $PMSO_2$). All experiments were conducted in duplicates or triplicates.

2.3. Results and Discussion

2.3.1. TeOS sand surface modification increases Fe(VI) coating density

Spectroscopic characterization of modified sand surfaces indicates greater Fe(VI) coating densities in the presence of TeOS. The Fe(VI)-coated sand synthesis method proposed in this study generates a purple-grey sand product (**Figure 2.2A**) which displays a dark purple color when placed in aqueous solution (**Figure 2.2B**). The purple color is indicative of the Fe(VI) speciation.[141] UV-Vis measurements confirmed the presence of Fe(VI) on the sand surface (**Figure A1A**). Direct measurements of the leachate after the Fe(VI)-coated sand was added to a phosphate/borate buffer (5 mM Na_2HPO_4/1 mM Na_2B4O_7) solution shows a maximum absorbance at 509 nm (**Figure A1A**) confirming the presence of Fe(VI) on the coated sand surface.[138] Furthermore, the reaction between the leachate and ABTS generated the expected $ABTS^{\cdot+}$ radical[139] as evidenced by the absorbance peak at 415 nm (**Figure A1A**). Fe(VI) reacts rapidly with ABTS via a one-electron transfer mechanism to produce the stable radical $ABTS^{\cdot+}$. The $ABTS^{\cdot+}$ absorbance at 415 nm is then used to calculate aqueous Fe(VI) concentration.

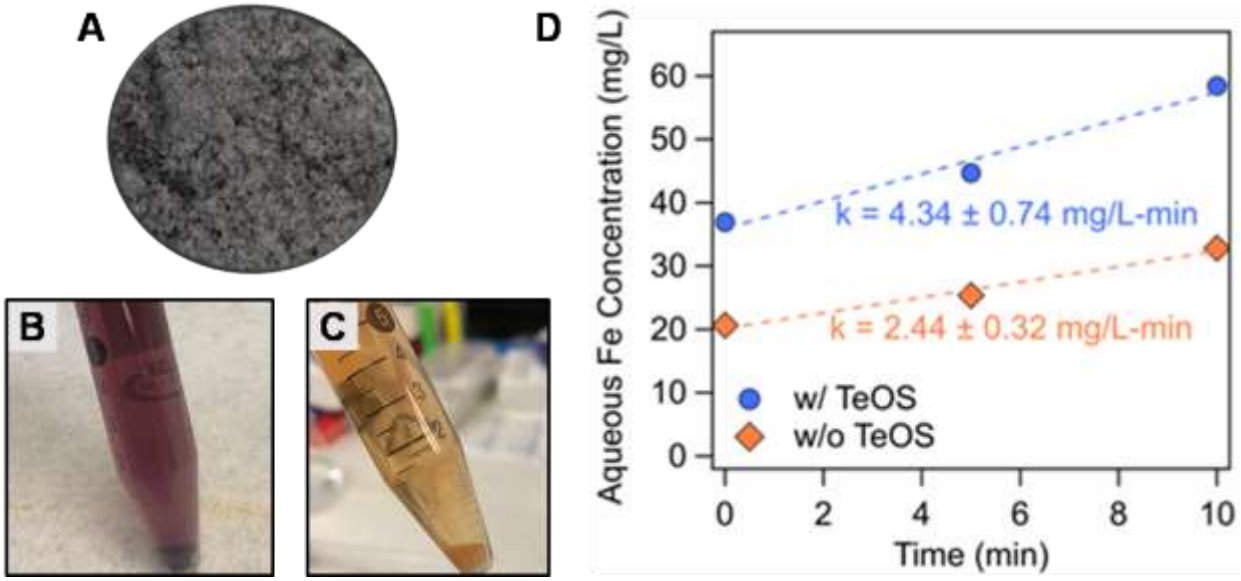

Figure 2.2. (**A**) As-prepared Fe(VI)-coated sand with TeOS-sand modification. (**B**) 20 g/L Fe(VI)-coated sand added to 5mM Na_2HPO_4/1mM NaB_4O_7 solution at time t=0 and (**C**) at t=180 min indicating Fe(VI) (purple) reduction to Fe(III) (orange) phases. (**D**) Total Fe leached from the Fe(VI)-coated sand prepared with and without TeOS-sand modification (3-hr reaction).

TeOS modification of the sand prior to Fe(VI) coating increased Fe(VI) binding to the sand surface (**Figure 2.2D**). TeOS is a well-known silica precursor[142, 143] that has been used to stabilize iron oxide particles.[144] ICP-OES analysis of the temporal Fe leached from the Fe(VI)-coated sand revealed that Fe(VI)-coated sand synthesized with TeOS-sand had approximately 44% higher initial Fe loading (**Figure 2.2D**) than media prepared with unmodified sand, indicating a higher Fe coating density in the presence of TeOS. Furthermore, ICP-OES analysis of acid-treated leachate—which revealed the maximum Fe loading on the sand surfaces—from the TeOS modified and unmodified sand surfaces (**Figure A2**) confirm that TeOS modification increases Fe coating mass. Additionally, spectroscopic analysis revealed a stable TeOS coating (i.e., no leaching of TeOS) on the sand surface (**Figure A3**). The UV-Vis spectrum of the

supernatant of TeOS-sand sonicated in the 10 mM borate buffer did not show an absorbance peak at 292 nm as corresponding to the presence of TeOS (**Figure A3**).

2.3.2. Solution pH and buffering ions govern Fe(VI)-coated sand stability

Analysis of Fe(VI) leaching kinetics suggests that the media Fe(VI) aqueous stability increases with increasing pH. Leaching experiments were conducted with the Fe(VI)-coated sand in buffered solutions (10 mM phosphate and 10 mM borate) at pH 7, 8, and 9 to evaluate the effect of pH and inorganic ions on the aqueous stability of the media (**Figure 2.3 & Figures A4-5**). Initially, the Fe(VI)-coated sand was sonicated in 1% HNO_3 to desorb all the Fe from the coated sand surface and to quantify the total Fe coating density on the media. This total Fe (9.4±0.8 mg/L) is designated as the maximum total Fe coating on the sand. The maximum total Fe concentration was greater than the aqueous total Fe concentrations at time t (t = 5-180 min) suggesting that Fe(VI) desorption from the coated sand is not instantaneous (**Figure 2.3 & Figure A5**). Previous studies have proposed that organic contaminant oxidation can be improved by a slow release of Fe(VI) into solution during water treatment[145-147] or multi-step dosing of Fe(VI).[39, 148] These two application methods limit Fe(VI) self-decay and increase Fe(VI) exposure to organic contaminants.[44] Similarly, a delayed desorption of Fe(VI) from the coated sand surface presents an opportunity for improved treatment of organic contaminants during water treatment. In solution, the Fe(VI)-coated sand media would consist of: (i) aqueous Fe(VI) leached from the sand surface; (ii) aqueous Fe(III) leached from the sand surface or produced from aqueous Fe(VI) decay; (iii) Fe(III) solids suspended in solution; and, (iv) Fe(VI) and/or Fe(III) bound to the sand surface. Thus, contaminant removal can occur simultaneously via reactions with Fe(VI) and Fe(III) in different phases and configurations. Further investigations on the coated sand surface and the Fe(III) phases produced are needed to differentiate these

phases and elucidate mechanisms by which contaminants are removed on the Fe(VI)-coated sand surface.

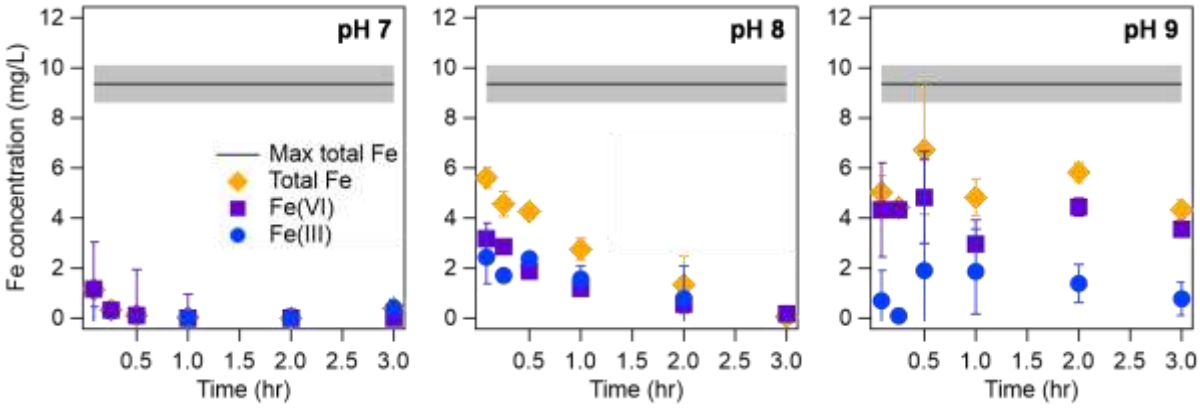

Figure 2.3. Kinetics of Fe(VI), Fe(III) and total Fe leached from 1 g/L Fe(VI)-coated sand into a 10 mM $Na_2B_4O_7$ solution at pH 7, 8, 9 as a function of time. Max total Fe refers to the maximum mass of Fe that would leach of the surface of Fe(VI)-coated sand. This was determined by mixing 1 g/L Fe(VI)-coated sand into 1% HNO_3 and measuring total Fe in solution. Total Fe refers to the total Fe leached into solution at a given time.

The Fe(VI)-coated sand exhibited slower decomposition kinetics at circumneutral pH. Previous studies reported that Fe(VI) was the most stable in aqueous solutions buffered at pH 9.2-9.4, but experienced a kinetically fast decay below this pH range.[149] Our Fe(VI) stability tests also confirm that the Fe(VI) leached from the Fe(VI)-coated sand was more stable at pH 9 than at pH 7 and 8. Aqueous decomposition of Fe(VI) was minimal at pH 9 (**Figure 2.3 & Figure A5)**. The aqueous Fe(VI) decay rates in the borate buffer were estimated at 355.4, 0.82, 0.004 mg^{-1} L^{-1} hr^{-1} at pH 7, 8, 9 respectively (**Figure A6**). At pH 7, the dominant Fe(VI) species is $HFeO_4^-$ (~67%) (**Figure 2.1**) which has a higher oxidizing potential[150, 151] than the deprotonated FeO_4^{2-}. The high oxidizing potential of the dominant $HFeO_4^-$ species and fast reactions with water result in the instability of aqueous Fe(VI) at pH 7 (**Figure 2.3 & Figure A4-5).** The self-decay of aqueous Fe(VI) was lessened at pH 8 (**Figure 2.3 & Figure A5)** and can be attributed to the dominant species, FeO_4^{2-} (~83%) (**Figure 2.1**) being less reactive than the $HFeO_4^-$ species.[150]

Due to the increased production of Fe(III) at pH 7 and 8, we hypothesize that sorption and coagulation are the major mechanism of contaminant removal whereas at pH 9, oxidation of organic compounds may be the more dominant treatment mechanism. At pH values where Fe(VI) decays faster, the treatment of organic contaminants by the Fe(VI)-coated sand media may occur by these pathways: (i) physical adsorption of the contaminants on the coated sand surface followed by oxidation by surface-bound Fe(VI) species, (ii) sorption to surface-bound Fe(III) particles; (iii) limited oxidation by Fe(VI) in the aqueous phase, and (iv) sorption and coagulation with Fe(III) particles in the aqueous phase. Characterization of optimized Fe(VI) stability is important in determining the operating conditions of Fe(VI)-coated sand application for which contaminant treatment is maximized and will be explored in future studies.

The aqueous stability of the Fe(VI)-coated sand is also affected by the buffering ions (**Figure 2.3 & Figure A4-5)**. At pH 8 and 9, aqueous Fe(VI) and total aqueous Fe concentrations were lower in the borate buffer than in the phosphate buffer (**Figure 2.3** & **Figure A5**). At pH 8, the total aqueous Fe concentration in the borate buffer within 0.5 hour of mixing was 4.26±0.27 mg/L and 7.43±0.76 mg/L in the phosphate buffer. Additionally, we noted that total Fe concentrations at pH 7 and 8 were constant in the phosphate buffer (**Figure A5**), yet the Fe concentration decreased with time in the borate buffer except at pH 9 (**Figure 2.3**). These results imply that while Fe desorption from the media surface is lessened in the borate buffer, Fe(VI) decay was enhanced. A linear regression fitted to the measured Fe(VI) concentrations in both buffered solutions at pH 8 shows that the slope for the borate buffer was 65% smaller than the slope for the phosphate buffer (**Figure A7**) indicating that Fe(VI) decay was slower in the phosphate buffer. This is in agreement with previous studies where Fe(VI) self-decay at pH 7.5 was slower in a 10 mM phosphate buffer than in a 10 mM borate buffer.[83] The results of the

leaching experiments suggest faster Fe(VI) decay would occur when the Fe(VI)-coated sand media is placed in certain pH and buffering conditions. In particular, water chemistries that favor the presence of Fe(III) would promote rapid decay of Fe(III) due the catalytic effect of Fe(III) species on Fe(VI) self-decay.[81, 83] The presence of Fe(III) in solution will result in a decrease in solution pH,[152] thus increasing the Fe(VI) oxidizing potential (via formation of protonated Fe(VI) species and reactive intermediate species) and promoting reactions with water molecules which would catalyze further decay of Fe(VI).[153] However, phosphate ions can form metal complexes with Fe(III) and prevent the formation of iron colloids and solids,[83, 154] thus impeding the Fe(III) catalytic effect on Fe(VI) decay. This complexation behavior can explain the reduced Fe(VI) decay observed in the phosphate buffer in this study (**Figure A7**). In the absence of phosphate ions, Fe(III) particles aggregate to form larger particles.[83, 154] Thus, the temporal decrease in total Fe observed at pH 7 and 8 in the borate buffer (**Figure 2.3**) can be attributed to these larger particles being removed by filtration which was done prior to ICP-OES analysis of the samples.

Further stability tests indicate that the proposed synthesis method generates a stable and viable media. We assessed the stability of Fe(VI) when K_2FeO_4 powder is dissolved in the borate buffer at pH 9 (**Figure A8**). Results revealed that in this system, Fe(VI) decays faster at a rate of 1.14 mg L^{-1} hr^{-1} compared to the Fe(VI)-coated sand where Fe(VI) decay was estimated at 0.23 mg L^{-1} hr^{-1}. This result validates the SiO_2 stabilization effect on Fe(VI). Additionally, the stability of the stored media was assessed by determining changes in total Fe and Fe(VI) on the sand surface at time t (in days) after the media was produced (**Figure A9**). The total measured Fe varied between 5.69±0.99 to 7.39±1.01 mg Fe/g sand. The degree of variability could be due to slight differences in coating density at different sites on the sand surface. Fe(VI) concentrations

(~2.43 mg Fe(VI)/g sand) remained constant for up to 7 days after media production then slightly decreased (1.29 mg Fe(VI)/g sand) after 7 days.

2.3.3. Silica stabilized Fe(VI) improves the treatment of phenol

While phosphate ions reduces Fe(VI) self-decay, studies have reported that their presence in solution leads to decreased oxidation of organic compounds by Fe(VI).[155] Huang et al. observed removal efficiencies of 97%, 90%, and 95% of carbamazepine, diclofenac, and ciprofloxacin respectively in unbuffered river waters but only 85%, 74%, and 82% removal of these compounds in phosphate buffered river waters.[155] The oxidation of organic compounds by Fe(VI) occur via (i) reactions between Fe(VI) and the compounds to form Fe(V) or Fe(IV), which are more reactive than Fe(VI); and, (ii) further reactions between the compounds and Fe(IV)/Fe(V).[32, 68] However, phosphate ions can react with Fe(V) through a nucleophilic attack to form metal complexes which would lead to a decrease in Fe(V) reactivity and thus reduce the oxidation of organic compounds.[155] On the other hand, borate ions have lower reactivity towards Fe species.[83, 84, 126] Our observations on the oxidation of PMSO by Fe(VI)-coated sand in 10 mM phosphate and borate buffer corroborated these findings (**Figure A10**). The oxidation efficiency of PMSO in the borate buffer was 93% (**Figure A10B**) but only 26% (**Figure A10A**) in the phosphate buffer under the same experimental conditions (i.e., pH 9, 2 g/L Fe(VI)-coated sand and 1 hour reaction time). The lower concentration of $PMSO_2$ observed in the phosphate buffer reaction system confirms the negative effect of phosphate ions on Fe(VI) reactivities (**Figure A10**).

Phenol removal increased with Fe(VI)-coated sand dose. The Fe(VI)-coated sand dose used in this study was determined by assessing the effect of different media doses (i.e., 1, 2 and 4 g/L) on the removal of phenol. Our results indicate that removal of phenol improved with increasing media doses and plateaued after 2 g/L (**Figure 2.4**). At this dose, 97% removal of phenol at an

initial concentration of 236 µg/L was achieved. Thus, a dose of 2 g/L was chosen for further experiments.

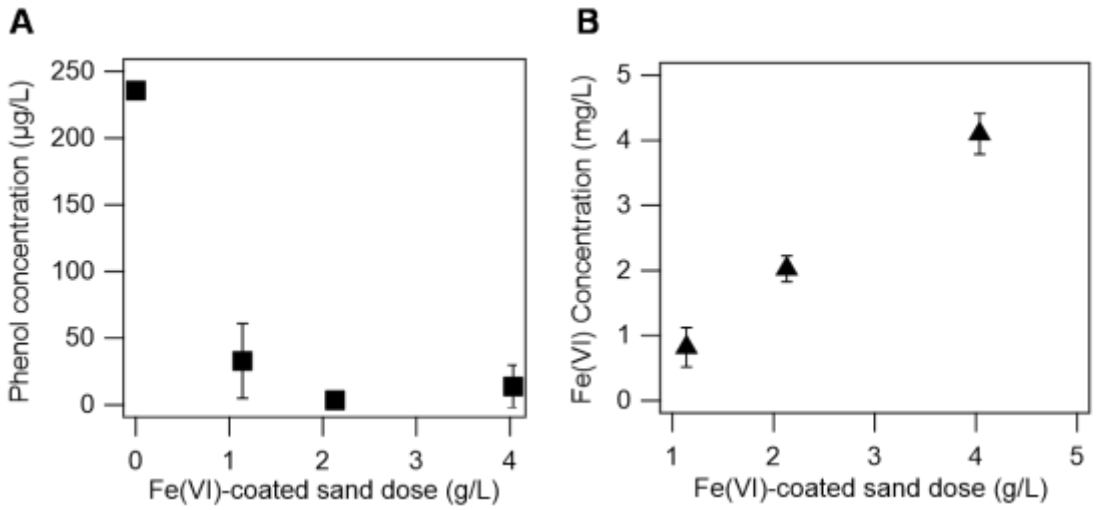

Figure 2.4. (A) Effect of Fe(VI)-coated sand dose on the removal of 236±0.6 µg/L phenol in 10 mM borate buffer pH 9 and **(B)** the measured Fe(VI) concentration remaining in solution after 30 min of reaction with phenol treatment.

Coating Fe(VI) onto the sand substate enhances its treatment capability toward organic compounds. The removal of phenol by the Fe(VI)-coated sand was compared to removal by the as-prepared K_2FeO_4 powder application (**Figure 2.5 & A11**). Both media had similar removal efficiencies (85% for as-prepared K_2FeO_4 powder and 83% for Fe(VI)-coated sand) of phenol at the end of the reaction time (2 hour); however, phenol removal was faster by the Fe(VI)-coated sand (**Figure 2.5 & A11**). After 5 min, the removal of phenol by Fe(VI)-coated sand was 51%, but only 37% by the as-prepared K_2FeO_4 powder. This accelerated treatment by Fe(VI)-coated sand could lead to rapid degradation of organic contaminants which has economic benefits for water treatment plants. Under the experimental conditions of this study (i.e., 2 g/L Fe(VI)-coated sand and 12.6 mg/L as-prepared K_2FeO_4 powder), we observed higher aqueous Fe(VI) concentrations (5.76-9.77 mg/L) in the Fe(VI)-coated sand system than in the as-prepared

K_2FeO_4 powder (0.28-1.87 mg/L), which could explain the enhanced treatment of phenol by Fe(VI)-coated sand. Previous studies have reported increased oxidation of organic compounds as Fe(VI) doses increase.[68, 156] However, we observed a faster decay of aqueous Fe(VI) in the as-prepared K_2FeO_4 powder system compared to the Fe(VI)-coated sand system (**Figure 2.5A2-B2**). We hypothesize that the slower decay of Fe(VI) in the Fe(VI)-coated sand indicates more Fe(VI) available in solution for longer periods of time, suggesting that more organic compounds could be treated simultaneously by the Fe(VI)-coated sand. The slower Fe(VI) decay in the Fe(VI)-coated sand system also confirms the SiO_2 stabilization effect on Fe(VI) reactivity. Furthermore, reduced decay rates of aqueous Fe(VI) also generate lower quantities of Fe(III) particles in solution which could decrease the frequency for Fe(III) sludge disposal post-treatment. Based on our hypothesis in *Section 2.3.2*, we speculate that phenol removal by Fe(VI)-coated sand would be threefold: removal in the aqueous phase, sorption/coagulation with Fe(III) solids, and removal on the sand surface. Further investigations are needed to characterize and decouple these removal mechanisms. For example, Huang et al. reported that the oxidation of phenol by Fe(VI) leads to the formation of a quinone and biphenol products via a phenoxy radical.[157]

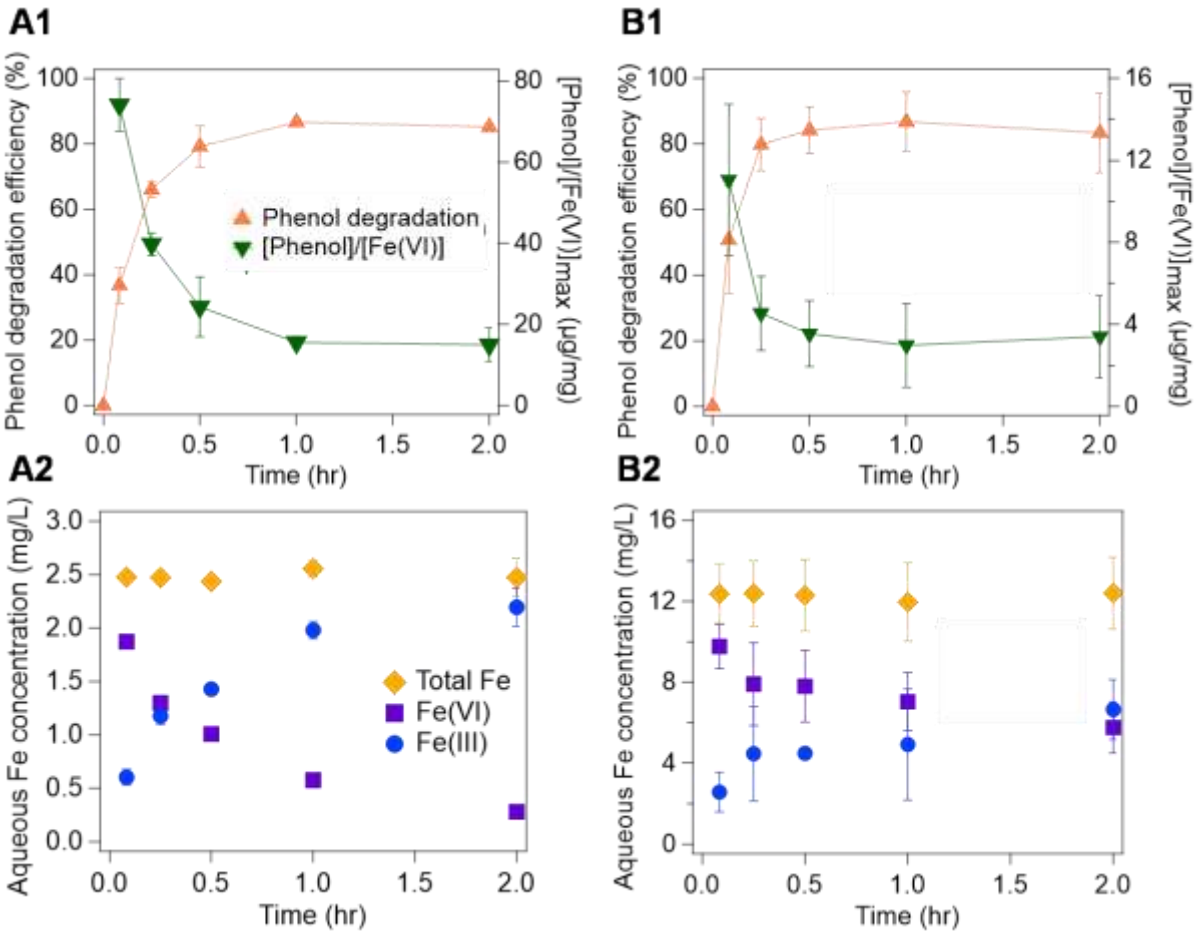

Figure 2.5. Degradation of of 219±12 µg/L phenol in 10 mM borate buffer pH 9 by (**A**) 12.6 mg/L Fe(VI) powder and (**B**) 2 g/L Fe(VI)-coated sand. (top) phenol removal efficiency (left axis) and phenol to maximum aqueous Fe(VI) concentrations ratio (right axis) with time; Fe(VI) concentration at 5 min was taken as the maximum aqueous Fe(VI) concentration, (bottom) changes in aqueous Fe.

UV-Vis measurements indicate the potential formation of oxidation products (**Figure A12**). We observed a sharp peak at 307 nm, a small shoulder peak near 350 nm, and a broad peak in the range of 430-630 nm with maximum absorbance near 500 nm (**Figure A12**). These peaks were not seen in the spectrum of a phenol blank solution (**Figure A12**). We suspect that the broad peak around 500 nm could be attributed to Fe(VI) which has an absorbance at 509 nm (**Figure A1A**) rather than an oxidation product. The minimal change in the absorbance values at this peak (**Figure A12**) aligns with the stable aqueous Fe(VI) concentration observed during phenol

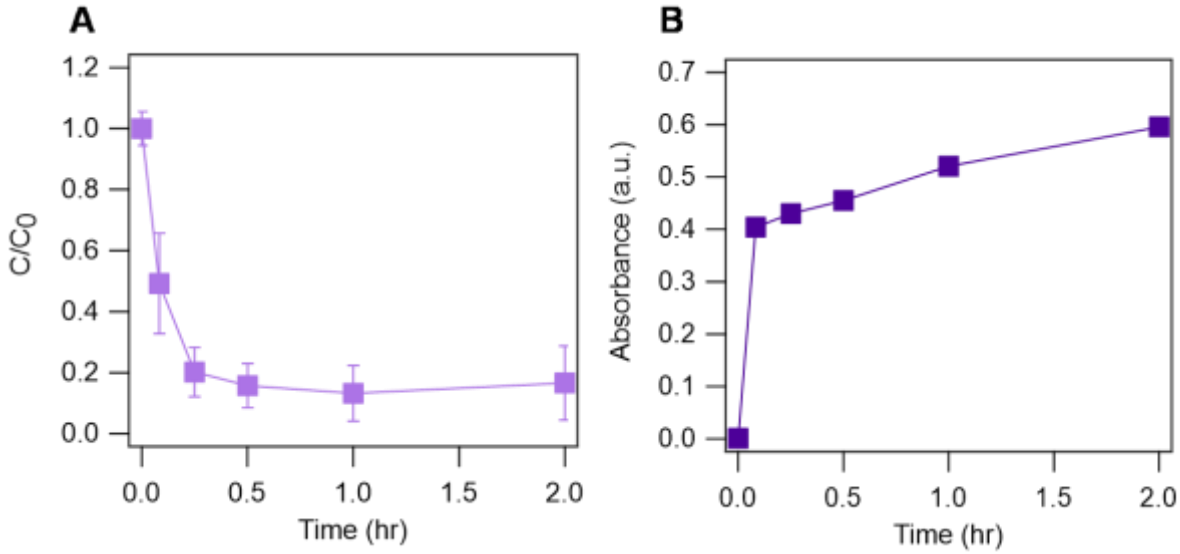

Figure 2.6. (A) Degradation of 219±12 µg/L phenol by 2 g/L Fe(VI)-coated sand in 10 mM borate buffer pH 9 and **(B)** subsequent formation of the oxidation product with maximum absorbance at 307 nm.

treatment by Fe(VI)-coated sand (**Figure 2.5B2**). The absorbance peak at 307 nm may be attributed to an oxidation product. The continuous increase in absorbance values at this peak indicates increased formation of the oxidation product as phenol degradation progresses (**Figure 2.6 & A12**). Chen et al. reported the oxidation of phenol via hydroxylation of the benzene ring which forms a hydroquinone intermediate product that further converts into p-benzoquinone and other oxidation products.[158] UV-Vis measurement of hydroquinone in 10 mM borate buffer

showed absorbance peaks at 290, 316, 403 and 428 nm (**Figure A12**). Previous studies have reported absorbance peak at 293 nm[159] and 289 nm[160] for hydroquinone. We speculate that the oxidation product formed in this study may be a quinone product. However, further analyses and more targeted analytical tools (e.g., mass spectrometry, gas chromatography) will be performed to monitor and identify all oxidation products found.

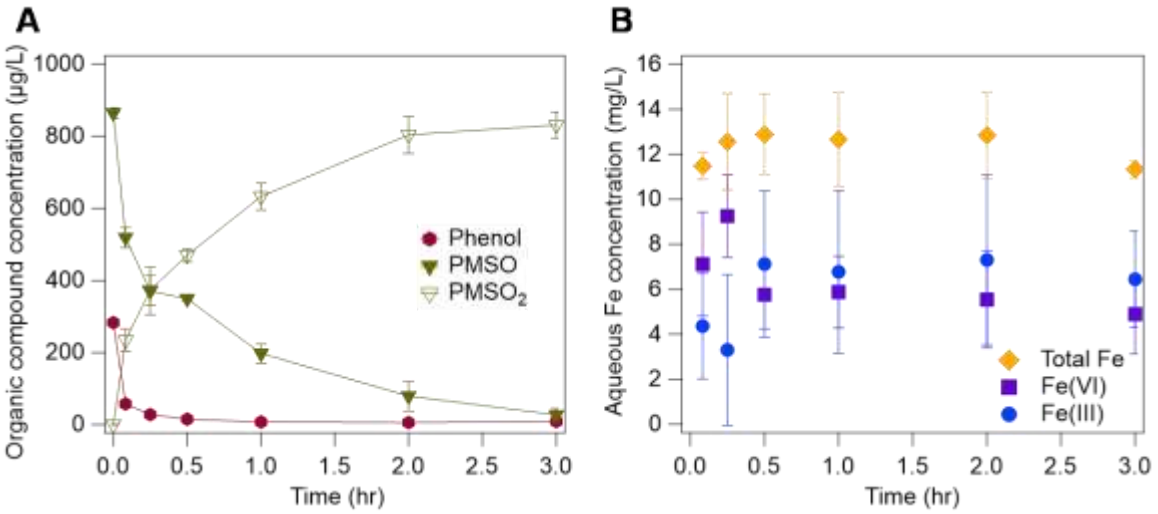

Figure 2.7. (**A)** Removal of 283±2.1 µg/L phenol and 865±15 µg/L PMSO by 2 g/L Fe(VI)-coated sand. (**B**) Changes in aqueous Fe concentration.

Fe(VI)-coated sand had greater reactivity towards phenol in the presence of PMSO (**Figures 2.7 & A13**) which indicates an increased presence of reactive species. The removal capacity of Fe(VI)-coated sand for phenol and PMSO was assessed using different concentrations of the organic compounds (i.e., 283 µg/L phenol and 865 µg/L PMSO; 245 µg/L phenol and 394 µg/L PMSO; and, 520 µg/L phenol and 739 µg/L PMSO). In the absence of PMSO, phenol removal by Fe(VI)-coated sand was estimated at 51% within 5 min (**Figure 2.5**), whereas in the presence of PMSO, the removal efficiency was 80-97% (**Figures 2.7 & A13**). The increased removal of phenol in the presence of PMSO suggests the formation of other reactive species (i.e., Fe(V), Fe(IV)), as a result of the reaction between Fe(VI)-coated sand and

PMSO.[161] The complete oxidation of PMSO to $PMSO_2$ (**Figure 2.7**) in this study indicates the presence of Fe(V) and Fe(IV) species and no other reactive species (i.e., H_2O_2) which would oxidize PMSO into other products.[140] Consequently, Fe(V) and Fe(IV) yield will increase due to their production from Fe(VI) self-decay and Fe(VI) reaction with PMSO thereby increasing phenol removal. These results also corroborate previous hypotheses[68, 71] regarding the SiO_2 effects on rapid formation of Fe(V) and Fe(IV) in Fe(VI) systems. Thus, in multi-pollutants systems, the combination of greater Fe(VI) reactivity promoted by SiO_2 and Fe(V)/Fe(IV) production from Fe(VI) reactions could result in more effective treatment than in aqueous K_2FeO_4 powder systems.

2.4. Conclusion

This study demonstrates a novel Fe(VI)-coated sand water treatment media application for organic contaminant removal. A synthesis method is proposed to produce a viable and stable Fe(VI)-coated sand composite. The initial coating of the sand with tetraethyl orthosilicate yielded a Fe(VI)-coated sand media with higher Fe (44%) bound to the surface and a greater binding attachment than media produced without sand modification. Water chemistries (i.e., pH and buffers) were explored to determine their effect on the rate of Fe(VI) decomposition and leaching from the media surface. The Fe(VI) self-decay was accelerated at pH 7 ($k = 3.87$ mg^{-1} L^{-1} hr^{-1}) and slowed with increasing pH ($k = 0.04$ mg^{-1} L^{-1} hr^{-1} at pH 9). Borate ions promoted a faster decay ($k = 2.22$ mg L^{-1} hr^{-1}) of the media compared to phosphate ions ($k = 3.39$ mg L^{-1} hr^{-1}). Treatment of phenol by the Fe(VI)-coated sand and by K_2FeO_4 powder revealed that the composite media had a removal capacity that is 1.4 times greater than that of Fe(VI) powder. Furthermore, the fast and complete removal of phenol (with initial concentrations of 245-283 µg/L) in the presence of PMSO (with initial concentrations of 394-865 µg/L) compared to the

incomplete removal of phenol in the absence of PMSO indicates an increased production of highly reactive Fe(V) and Fe(IV) intermediate species.

Removal of organic compounds by the media is expected to be three-fold: removal by aqueous Fe(VI), removal by suspended Fe(III) particles, and removal on sand surface. Further testing is needed to distinguish these different mechanisms and better understand the Fe(VI)-coated sand functionality.

Coating Fe(VI) onto a sand surface presents an opportunity for increasing Fe(VI) stability and for better deployment of Fe(VI) in water treatment applications. Previous studies have reported advantages of heterogeneous Fe(VI) applications.[123, 162, 163] This study offers an environmentally benign media that would be applicable to treatment systems (e.g., advanced wastewater systems) where sand filtration systems are already in use. Our Fe(VI)-coated sand media limits the need for solid substrates like SiO_2 gels that may require post-treatment disposal. The reduction of Fe(VI) to Fe(III) after treatment and the potential for synergistic treatment processes (i.e., oxidation, coagulation, disinfection, and filtration) due to Fe(VI) multimodal properties make this novel Fe(VI)-coated sand a cost-effective and eco-friendly water treatment media suitable for deployment in many water treatment applications. Currently, there are commercialized processes in place for on-site Fe(VI) production at water treatment facilities, which eliminates transportation costs. These cheaper Fe(VI) production methods coupled with the inexpensive cost of sand ($33/kg) and TeOS ($64/L) make the Fe(VI)-coated sand synthesis a cost-effective process.

Chapter 3. Simultaneous Oxidation of Trace Organics and Sorption of Trace Metals by Ferrate (Fe(VI))-coated Sand in Wastewater Effluents

This chapter is currently in press as: Okaikue-Woodi, F. E. K., Morales Lumagui, R. and Ray J. R. Simultaneous oxidation of trace organics and sorption of trace metals by ferrate (Fe(VI))-coated sand in synthetic wastewater effluent. *ACS Environ. Au* **2024**. doi.org/10.1021/acsenvironau.4c00024

ABSTRACT

Here, we assessed the potential of the media for treatment of acetaminophen (ACM), benzotriazole (BZT), sulfamethoxazole (SMX), copper (Cu), lead (Pb), and zinc (Zn)—common contaminants found in wastewater effluents—in ultrapure and synthetic wastewater. Fe(VI)-coated sand reactivity was influenced by the solution pH and the aqueous chemistry. For example, removal of Pb improved by 39% in the presence of trace organics indicating that trace metals removal was enhanced by Fe(III) phases formed during Fe(VI) reactions with trace organics. While oxidation of trace organic compounds increased as pH decreased, trace metals sorption was more favorable at higher pH (i.e., pH 8 and 9). The oxidation efficiency of trace organics by the medium was the highest for ACM and SMX; BZT degradation was limited due to formation of Cu–BZT complexes. Batch tests in synthetic wastewater effluent solutions revealed the presence of divalent cations (i.e., Ca^{2+} and Mg^{2+}) can catalyze Fe(VI) self-decay and promote Fe(III) production and subsequent trace metal removal; however, oxidation of trace organics was hindered in this matrix. This study highlights the potential for Fe(VI)-coated sand application for treatment of complex matrices more representative of natural and engineered aquatic systems.

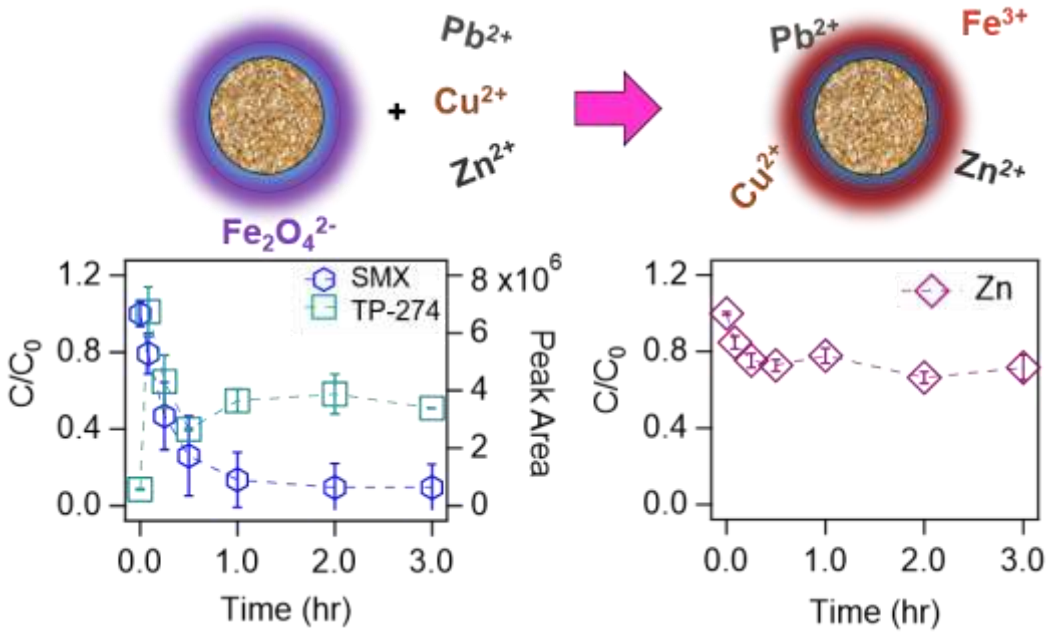

3.1. Introduction

Due to water shortages, wastewater effluent is increasingly considered for augmentation of water resources.[7] Treated wastewater discharges into nearby water bodies that often serve as downstream drinking water sources. Additionally, wastewater effluent can be injected into aquifers to recharge groundwaters and replenish drinking water aquifers.[7] However, processes used in conventional wastewater treatment plants have variable effectiveness for removal of trace contaminants prior to discharge.[4, 164] Studies have reported the presence of contaminants such as heavy metals[3, 9, 165] and organic compounds (e.g., antibiotics[4, 166], prescription drugs[4, 10], industrial chemicals[164]) in wastewater effluents. The increasing presence of these contaminants in wastewater effluent discharges and in reclaimed wastewater due to anthropogenic activity and overuse of chemicals may cause acute and chronic risks to human health and aquatic life,[10, 167] and jeopardizes the safety of wastewater reuse and aquifer recharge efforts. For example, Ferrari et al. detected diclofenac, carbamazepine, and clofibric acid in real wastewater effluent solutions

and reported chronic effects when invertebrates obtained from laboratory cultures were exposed to the wastewater effluent solutions.[168] Therefore, advanced treatment of wastewater effluents is necessary to decrease the trace contaminant load to receiving waters.

Many advanced (oxidation) treatment processes (e.g., ozonation, Fenton processes, UV irradiation, reverse osmosis membrane filtration) have been proposed and investigated to enhance contaminant removal and degradation during wastewater treatment. Ferrate [Fe(VI)] is a multifunctional iron oxide capable of oxidation,[55, 114] coagulation[46, 55] and disinfection[53, 56] with a standard oxidation potential (E^0) of 2.2 V, which is greater than the oxidation potential of chlorine (1.36 V)[55], a commonly used disinfectant and oxidant. For example, Yang et al. observed more than 90% removal of trace organic compounds by Fe(VI) in secondary wastewater effluent.[42] Additionally, Fe(VI) is considered an environmentally benign chemical because it reduces into non-toxic Fe(III) species during application,[113, 114] which is often used as coagulants[55, 56] and adsorbents[55, 57] in water treatment. However, the use of Fe(VI) as a water treatment technology for contaminant destruction is limited due to its chemical instability in solution. As the solution pH increases to alkaline pH ranges (pH > 7.3) the Fe(VI) aqueous stability increases; however, its oxidizing power decreases.[169] Previous studies have proposed methods to increase Fe(VI) oxidizing power at environmentally relevant pH and accelerate the oxidation of organic contaminants.[68, 119-123] In our previous work, we proposed and developed a Fe(VI)-coated sand composite media that leverages SiO_2 stabilization properties for enhanced water treatment applications.[169] We observed 51% oxidation of phenol by the Fe(VI)-coated sand within 5 min of treatment compared to 37% when aqueous Fe(VI) powder was applied which indicates enhanced oxidation efficacy by immobilizing Fe(VI) on the sand surface.[169] Therefore, applying the Fe(VI)-coated sand media presents an opportunity for advancing water treatment

processes with additional capabilities (i.e., oxidation, coagulation, and disinfection) due to the multimodal properties of Fe(VI). While our previous study indicated that the application of the Fe(VI)-coated sand media would be effective to degrade phenolic compounds in wastewater, there are many other types of chemical contaminants present in wastewater. Therefore, a better assessment of the Fe(VI)-coated sand performance should include more complex and varied matrices and contaminants.

In this study, we investigated the potential of Fe(VI)-coated sand media for advanced treatment of multiple contaminant classes and more environmentally representative aquatic matrices. Specifically, we evaluated the removal of trace metals (i.e. copper, lead, and zinc) and organic compounds (i.e., acetaminophen, sulfamethoxazole, benzotriazole) commonly found in wastewater effluents. Copper (Cu), lead (Pb) and zinc (Zn) can enter wastewater from industrial sources (e.g., paper mills, textiles, paints, oil refining)[9, 170] and household products (e.g., detergents).[165, 170] Acetaminophen (ACM) is a widely used non-prescription drug that has been widely detected in aquatic environments.[4, 171, 172] Sulfamethoxazole (SMX) is an antimicrobial widely used in human and veterinary medicine[12, 13] and has been detected in wastewater effluents.[12, 173] Benzotriazole (BZT) is used as an anticorrosion agent and has also been detected in wastewater effluents.[41, 174] An advantage of Fe(VI) is its reduction into Fe(III) species, thus making it possible for the dual treatment of organic and inorganic contaminants by Fe(VI) in a single unit process. Therefore, the specific objectives of this study are to: (1) assess the capacity of the Fe(VI)-coated sand for the treatment of a wider range of contaminants; (2) understand competitive removal of organic and inorganic contaminants; and, (3) characterize the effects of wastewater effluent matrix on the Fe(VI)-coated sand treatment rates.

3.2. Materials and Methods

3.2.1. Chemicals

Acetaminophen (Spectrum Chemical MFG Corp, NJ), 1,2,3-Benzotriazole (TCI America, OR), Sulfamethoxazole (TCI America, OR), Copper(II) chloride anhydrous (Thermo Fisher Scientific, WA), Lead(II) chloride (Thermo Fisher Scientific, WA), Zinc(II) chloride anhydrous (Thermo Fisher Scientific, WA) and sodium sulfite anhydrous (Na_2SO_3, Fisher Scientific, MA) were purchased to assess contaminant removal by the media. Details of all other chemicals used in this study can be found in **Appendix B1** (in the Supporting Information). All experiments were conducted using ultrapure Milli-Q water (resistivity: 18.2 MΩ-cm).

3.2.2. Synthesis and surface characterization of Fe(VI)-coated sand

Fe(VI)-coated sand was synthesized as described in Okaikue-Woodi and Ray.[169] Briefly, Ottawa sand, initially coated with tetraethylorthosilicate (TeOS), was added to a K_2FeO_4 solution and stirred for 24 hours at 4 °C.[169] The wet Fe(VI)-coated sand composite was dried under vacuum.[169] Surface analyses of the media were conducted to complement aqueous in situ characterization analyses reported in our previous study.[169] Scanning electron microscopy (SEM) imaging of the Fe(VI)-coated sand morphology was measured with a FEI (Hillsboro, OR) Sirion XL30 SEM instrument following platinum sputtering of the media to increase electrical conductivity. The elemental composition at the surface of the Fe(VI)-coated was also evaluated via SEM energy dispersive X-ray spectroscopy (SEM-EDS) following carbon coating of the media. X-ray diffraction measurements were recorded on a Brucker (Billerica, MA) D8 Discover X-ray diffractometer operated at 50 kV and 1000 μA. The scanning parameters were a 11° 2θ step size and 60 seconds/step over a 0–93° 2θ Cu Kα angular range.

3.2.3. Removal of trace metals and organics in ultrapure water

Batch experiments were conducted to evaluate the Fe(VI)-coated sand removal capacity of the contaminants in a pure water matrix containing only 10 mM sodium borate buffer. Stock solutions of each contaminant were prepared in Milli-Q water except for SMX, which was prepared in methanol. An intermediate SMX stock was prepared in water from the concentrated methanol stock. All experiments were conducted in triplicates and samples were shaken on a Fisherbrand™ multi-purpose tube rotator (Fisher Scientific, Waltham, MA) at 40 rpm.

The efficacy of the Fe(VI)-coated sand was evaluated in multiple contaminant systems and at different pH values (pH 7.5 and 9). These pH values were chosen to assess the Fe(VI)-coated sand reactivity when its aqueous stability is high (i.e., at pH 9) and at environmentally relevant pH (i.e., pH 7.5). A pH range of 6.5–8.5 is typical of wastewater effluent.[17, 89] Additionally, an assessment of pH effects on the aqueous stability of the Fe(VI)-coated sand demonstrated that the Fe(VI)-coated sand was more stable at pH 9, as reported in our previous publication.[169] Batch kinetics experiments were conducted in four different phases: (i) all trace organics in a pH 9, 10 mM sodium borate buffer solution (**O9 system**); (ii) all trace metals in a pH 9, 10 mM sodium borate buffer solution (**M9 system**); (iii) trace organics and metals together in a pH 9, 10 mM sodium borate buffer solution (**MO9 system**); and, (iv) trace organics and metals together in a pH 7.5, 10 mM sodium borate buffer solution (**MO7.5 system**). The concentration of the contaminants was targeted at 500 µg/L each and the dose of the Fe(VI)-coated sand was 2 g/L for all reaction systems explored in this study. This dose (2 g/L) of Fe(VI)-coated sand was previously found to maximize removal of phenol.[169] At designated time intervals, a 2 mL aliquot of samples containing the organic compounds was quenched with 20 µL of 500 mM Na_2SO_3 to stop the reaction between Fe(VI) and the organic compounds, then filtered with a 0.2 µm, 25 mm diameter cellulose acetate syringe filter before analysis using high performance liquid

chromatography (HPLC) methods (**Appendix B2**). 500 µL of LC-MS grade methanol was added to 500 µL of the quenched and filtered aliquot for high-resolution mass spectrometry (HRMS) analyses (**Appendix B3**) to determine transformation products of the organic compounds. For all samples, a 3 mL aliquot was taken and filtered with a 0.2 µm, 25 mm diameter cellulose acetate syringe filter, then 1 mL of the aliquot was used to the measure aqueous Fe(VI) concentration via the 2,2'-azinobis-(3-ehtylbenzothiazoline-6-sulfonate) (ABTS) colorimetric method[139] via UV-Vis spectroscopy using a Shimadzu UV-2700 spectrophotometer (Kyoto, Japan). The remaining aliquot was diluted with 10 mM sodium borate buffer solution and acidified to 2% trace metal grade nitric acid for inductively coupled plasma orbital mass spectrometry (ICP-MS) analysis using a PerkinElmer Nexion 2000B inductively coupled mass spectrometer (Waltham, MA).

Control experiments in the absence of the Fe(VI)-coated sand were conducted to assess the stability and the reactivity of the trace metals and organics in solution for all four reaction systems. In addition, the role of Fe(III) phases in the Fe(VI)-coated sand reactivity was evaluated. A weighted amount (1.3±0.1 mg) of $Fe(NO_3)_3 \cdot 9H_2O$ was added to 50 mL of either a pH 9, 10 mM sodium borate buffer solution or a pH 7.5, 10 mM sodium borate buffer solution containing all the trace metals and trace organics. The final Fe(III) concentration (26±1.8 mg/L) in solution was chosen as an overestimate of the total Fe concentration (12.6±5.1 mg/L) possible in solution if all of the Fe were to leach from the sand surface. At designated times, aliquots are taken and filtered prior to ICP-MS and HPLC analyses. The results from our previous study indicated that Fe(VI)-coated sand enhanced removal and oxidation of phenol compared to application of Fe(VI) powder. Therefore, this study did not compare treatment of the select contaminants with Fe(VI) powder.

3.2.4. Removal of trace metals and organics in a synthetic wastewater effluent matrix

Batch kinetics experiments were also conducted under synthetic wastewater (SWW) effluent conditions to characterize the effects of wastewater effluent matrix on the Fe(VI)-coated sand treatment capacity for the select trace contaminants. The matrix was prepared based on wastewater effluents (real and synthetic) composition reported in literature.[86, 89, 175-177] The SWW composition included: $NaHCO_3$ (96 mg/L), NaCl (83 mg/L), $MgCl_2{\cdot}6H_2O$ (19 mg/L), $Mg(NO_3)_2{\cdot}6H_2O$ (10 mg/L), $CaCl_2{\cdot}2H_2O$ (89 mg/L), $Ca(NO_3)_2{\cdot}4H_2O$ (10 mg/L), and Na_2HPO_4 (1 mg/L). The detailed composition of the synthetic matrix is included in **Table B4**. Batch experiments were conducted by adding approximately 100 mg of Fe(VI)-coated sand in 50 mL of SWW in 50-mL polypropylene centrifuge tubes containing roughly 500 µg/L of ACM, BZT, SMX, Cu, Pb, Zn each. At designated time intervals, aliquots were sampled and analyzed as described in *Section 3.2.3*.

3.3. Results and Discussion

3.3.1. Surface analyses confirm Fe coating on the sand surface

SEM images indicate that Fe(VI) coating alters the surface morphology of the Ottawa sand (**Figure 3.1**). The noncoated Ottawa sand (**Figure 3.1A**) surface roughness increased following the TeOS and Fe(VI) coating (**Figure 3.1B**). Elemental analysis of the surface composition indicated mostly Si (32.5%) and O (54.5%) for the unmodified Ottawa sand (**Figure 3.1**) which confirms the expected high SiO_2 content of the sand structure.[133] The carbon detected on the Ottawa sand can be attributed to the carbon coating sample preparation done prior to analysis to reduce electrical charge on the non-conductive sand samples. On the Fe(VI)-coated sand surface, K (33.7%), Cl (1%) and Fe (1.7%) were detected confirming the successful coating of the potassium ferrate (K_2FeO_4).

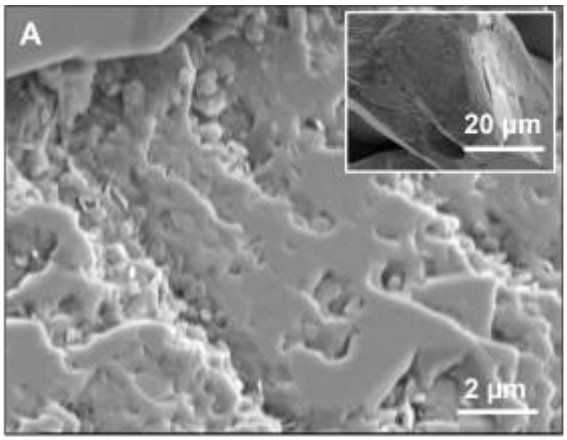

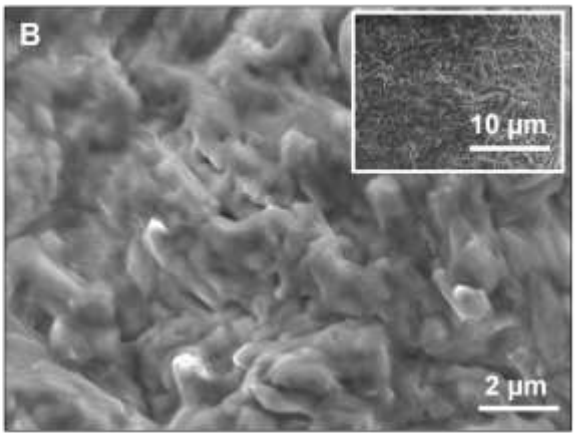

Elements	Minimum weight %	Maximum weight %	Average weight %	Standard deviation
Si	22.0	38.7	32.5	4.7
O	42.1	60.4	54.5	5.3
C	8.3	21.3	11.9	4.4
N	0.3	2.2	1.0	0.5

Elements	Minimum weight %	Maximum weight %	Average weight %	Standard deviation
Si	3.6	40.8	16.9	11.6
O	36.4	57.4	46.5	7.0
Fe	0.0	6.5	1.7	2.4
K	1.8	53.5	33.7	16.7
Cl	0.6	1.8	1.0	0.4

Figure 3.1. SEM images of (A) noncoated Ottawa sand and (B) Fe(VI)-coated sand. The insets are SEM images at lower magnification. The adjoining tables report elemental composition by weight percent on the medium surface.

The XRD analysis confirmed Fe coating on the sand surface (**Figure B2**). An increase in peaks was observed in the XRD pattern of the Fe(VI)-coated sand compared to the noncoated Ottawa sand and TeOS-sand, suggesting the presence of a new component (i.e. Fe(VI)) on the sand surface. Additional physicochemical characterization of the Fe(VI)-coated sand was performed in our previous study[169] which confirmed the presence of Fe(VI) on the sand surface.

3.3.2. In-situ formation of Fe(III) enhances removal of trace metals

The Fe(VI)-coated sand exhibited lower reactivity and removal efficiency towards the trace metals compared to trace organics. Furthermore, the reactivity towards Pb was greater than that of Cu and Zn. The batch adsorption results suggest that the trace metals are removed via interaction with Fe(III) particles generated during the reduction of leached Fe(VI) in the reaction

solution (**Figure 3.2 and Figure B3**). For example, 100% removal of Pb and 94% removal of Zn (**Figure B3A2**) after the 3-hr reaction in the test evaluating Fe(III) removal capacity (i.e., Fe(III) solids only) was observed; whereas, the Fe(VI)-coated sand treatment in the **MO9 system** only yielded 61% removal of Pb and 28% for Zn after 3-hr reaction (**Figure 3.2B**). Additionally, the removal of Pb and Zn by Fe(VI)-coated sand was achieved at 23% and 26% in the **M9 system** absent trace organics (**Figure 3.2A**). These data suggest that Fe(III) phases formed as a result of oxidation of trace organics and subsequent Fe(VI) reduction can increase Pb and Zn removal. At pH 9, Fe(VI) is stable and reacts slowly with water to form Fe(III),[169] but this reduction can be accelerated in the presence of organic compounds reacting with the Fe(VI). This is evidenced by the slower decrease in aqueous Fe(VI) concentrations seen in the **M9 system** (**Figure B4A**) compared to the faster decrease in the **O9** (**Figure B4B**) and **MO9 systems** (**Figure B4C**) when trace organics are present. The enhanced removal of metals in the presence of organic compounds validates the multifunctional properties of Fe(VI)-coated sand as an oxidant and coagulant.

Visual MINTEQ analysis suggests that Pb removal is governed by its chemical speciation in solution. In the pH 9, 10 mM borate buffer, Visual MINTEQ analysis indicates that $Pb(OH)_2$ is oversaturated in solution (**Table B2B**) which could contribute to precipitate formation. In the **M9** control samples (i.e., no Fe(VI)-coated sand), the removal of Pb after 3 hours was 1.6 times greater than in the **M9 system**. Thus, we hypothesize that the removal of Pb within the pH 9, 10 mM borate buffer system was predominantly facilitated by sample filtration of precipitates prior to ICP-MS measurements. We further posit that processes governing trace metals removal in our treatment systems could be three-fold: (1) removal via filtration of solid phase precipitates

formed due to oversaturation; (2) sorption to aqueous Fe(III) phases generated during reduction of leached aqueous Fe(VI); and, (3) sorption onto the Fe-coated sand surface.

Trace metals removal by the Fe(VI)-coated sand decreased as pH, especially in the case of Zn. Previous studies have reported an increase in metals removal by Fe(VI) as pH increases due favorable electrostatic interactions between the trace metals and in-situ Fe(III) phases.[46, 74] The same trend was observed in our study (**Figure 3.2**). In the **MO7.5 system**, the removal efficiencies of Zn and Pb decreased by 7% and 14% compared to removal in the **MO9 system**. The isoelectric point of Fe(III) (hydr)oxide species is between pH 7–8.5;[178] thus we hypothesize that at pH 9, the removal of Pb is driven by electrostatic interactions of the abundant $Pb(OH)^+$ species (**Table B2A**) and the negatively charged Fe(III) (hydr)oxide surfaces. Furthermore, at pH 9, Fe(VI) exists predominantly as FeO_4^{2-} (**Figure B1**),[116, 169] which could also interact electrostatically with $Pb(OH)^+$ species. In the case of Zn, the abundant species at pH 9 is $Zn(OH)_2$ suggesting removal via physical sorption of Zn either on the media surface or within Fe(III) (hydr)oxide lattices. Conversely, at pH 7.5, Pb^{2+} and Zn^{2+} are the more abundant species and may sorb weakly to the neutral Fe(III) (hydr)oxides surface. The pH effect on metals removal in the Fe(VI)-coated sand treatment systems is also mirrored in the Fe(III) reaction systems (**Figure B3**). After the 3-hr reaction with Fe(III), the removal of Zn increased from 31% at pH 7.5 to 94% at pH 9 (**Figures B3A1 and B3A2**).

Interestingly, Cu removal was greater in the control experiments absent Fe(VI)-coated sand, regardless of solution pH (**Figure B5**). Visual MINTEQ analysis reports CuO and $Cu(OH)_2$ as the oversaturated mineral phases present in solution, thus the high removal efficiencies observed in the control samples could be attributed to the formation of these mineral phases which were removed during filtration. Furthermore, greater Cu removal efficiencies were

achieved in the **MO7.5** and **MO9** control systems. For example, the presence of trace organics in the MO9 control system led to a 58% increase in Cu removal, which suggests that Cu is interacting with the trace organics (discussed in more detail in *section 3.3.3*).

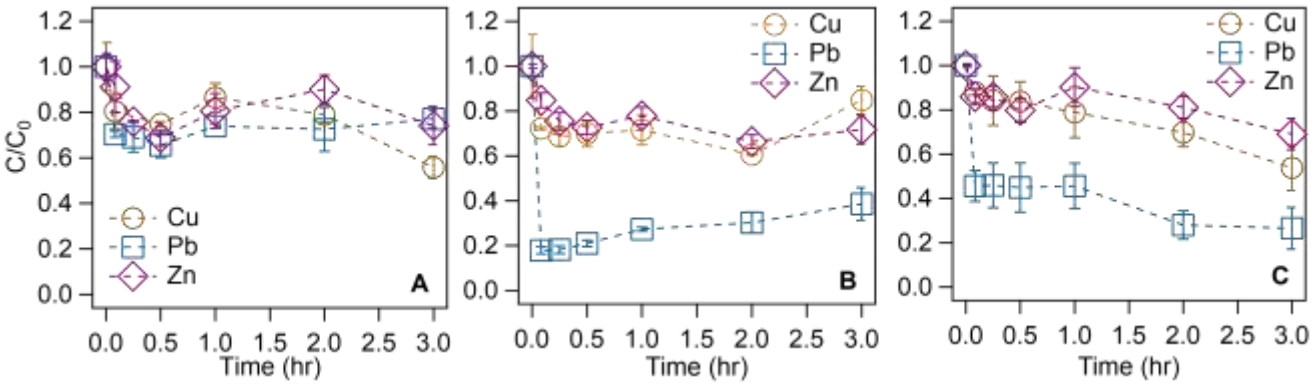

Figure 3.2. Removal of nominally 500 µg/L Cu, Pb, Zn (each) by 2 g/L Fe(VI)-coated sand (**A**) in the **M9 system**; and in the presence of nominally 500 µg/L ACM, BZT, and SMX (each) (**B**) in the **MO9** and (**C**) **MO7.5 systems.**

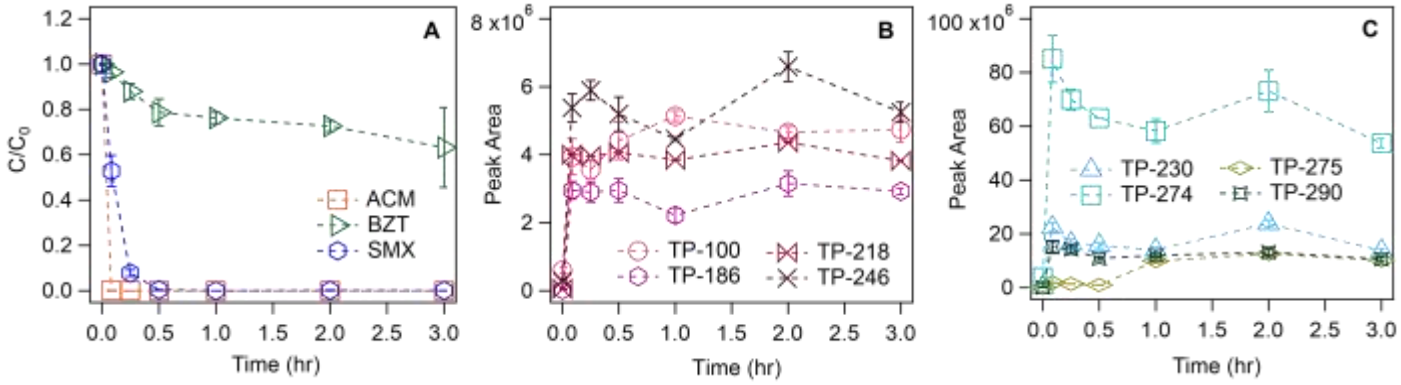

Figure 3.3. Normalized degradation of nominally 500 µg/L ACM, BZT, SMX (each) by 2 g/L Fe(VI)-coated sand in the **O9 system**; and (**B** and **C**) the formation of the most abundant transformation products as a function of time.

3.3.3. Solution pH and composition affect degradation of trace organics

Fe(VI)-coated sand exhibited a greater oxidation potential towards ACM and SMX compared to BZT. **Figures 3.3** through **3.5** indicate the oxidation of the three select trace

organics in this study by the Fe(VI)-coated sand and their corresponding transformation products identified using HRMS. For all of the test reaction systems, the degradation of ACM was complete and occurred rapidly (within 15 min, **Figures 3.3-3.55**). Oxidation efficiencies of 100% were achieved for SMX in the **O9** (**Figure 3.3**) and **MO7.5** reaction systems (**Figure 3.5**) and 90% in the **MO9 system** (**Figure 3.4**) after the 3-hr reaction. For BZT, the oxidation efficiency was 37% in the **O9 system** (**Figure 3.3**), but no removal was detected in the **MO9** and **MO7.5 systems** (**Figures 3.4-3.5**). The greater removal of ACM and SMX can be attributed to the high Fe(VI) selectivity towards electron-donating moieties such as phenols (present in ACM) and anilines (present in SMX). [42, 172]

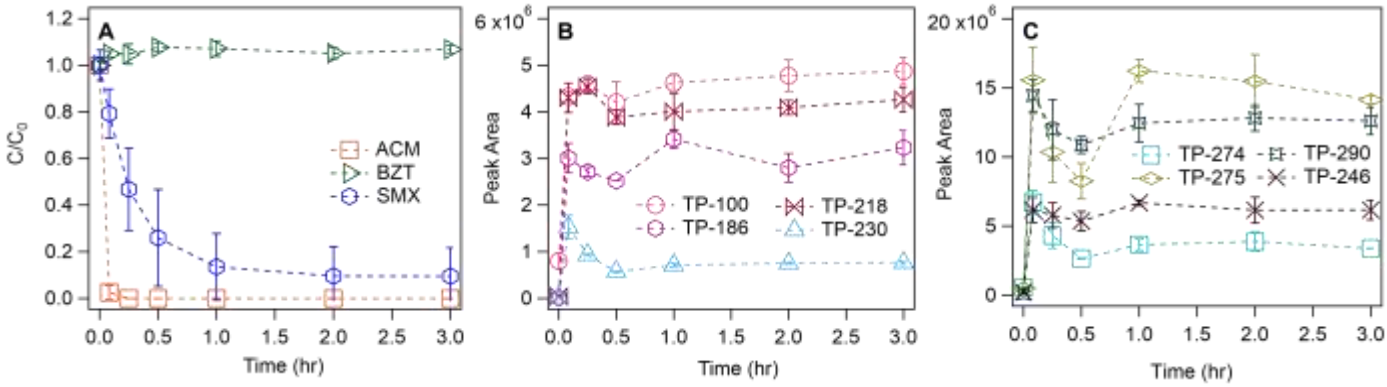

Figure 3.4. (**A**) Normalized degradation of nominally 500 µg/L ACM, BZT, SMX (each) by 2 g/L Fe(VI)-coated sand in the M**O9 system** in the presence of nominally 500 µg/L Cu, Pb, Zn (each); and (**B** and **C**) the formation of the most abundant transformation products as a function of time.

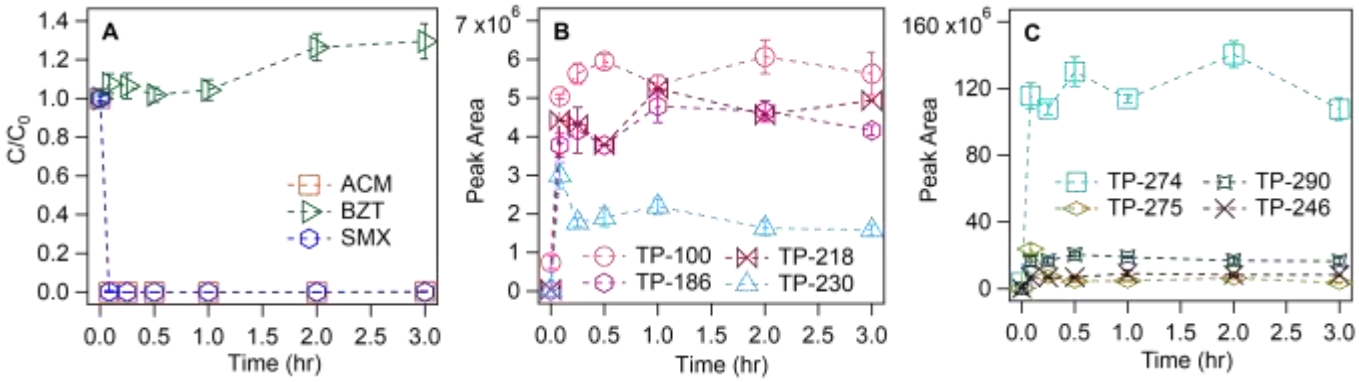

Figure 3.5. (**A**) Normalized degradation of nominally 500 µg/L ACM, BZT, SMX (each) by 2 g/L Fe(VI)-coated sand in the M**O7.5 system** in the presence of nominally 500 µg/L Cu, Pb, Zn (each); and (**B** and **C**) the formation of the most abundant transformation products as a function of time.

Solution matrix and pH were found to influence the oxidation potential of ACM and SMX by the Fe(VI)-coated sand. The presence of trace metals in the **MO9** system led to a 26% decrease in SMX oxidation capacity within 5 min of reaction compared to oxidation in the **O9 system** (i.e., absence of trace metals) (**Figures 3.3A and 3.4A**). The SMX oxidation capacity increased from 21% at pH 9 (**Figure 3.4A, MO9 system**) to 100% at pH 7.5 (**Figure 3.5A, MO7.5 system**) within 5 min of reaction. This difference can be explained by the differences in Fe(VI) chemical speciation at pH 7.5 compared to pH 9 (**Figure B1)**. At pH 7.5, Fe(VI) is comprised of 38.7% $HFeO_4^-$ and 61.3% FeO_4^{2-}.[169] $HFeO_4^-$ species are reported to have a higher oxidation potential than FeO_4^{2-} species[150, 151] which may result in greater degradation of ACM and SMX at pH 7.5. At pH 9, the degradation of the trace organics decreased (**Figure 3.4A**) which could be due to three effects: (1) the less reactive FeO_4^- species is dominant at this pH (i.e., 98%, **Figure B1**); (2) the presence of more contaminants in solution result in greater competition for Fe(VI); and, (3) Fe(VI) decays faster when there are more contaminants present. Results of aqueous Fe(VI) concentration evolution show that Fe(VI) decays faster in the **MO9** and **MO7.5** reaction systems containing all contaminants (**Figure B4C**) compared to the systems

containing one type of contaminant (**Figure B4B**). To enhance the decomposition of trace organics during wastewater treatment with more complex matrices containing multiple contaminant types, higher doses of Fe(VI)-coated sand or higher Fe(VI) mass loadings on the sand surface may be required. However, we note that within the 3-hr reaction period used in this study, removal efficiencies of 90% or greater were still achieved for ACM and SMX despite the mass of contaminants present.

BZT complexation with Cu inhibits its treatment by the Fe(VI)-coated sand. BZT is used as a corrosion inhibitor for Cu[179, 180] and has been reported to form metal complexes with Cu^{+} and Cu^{2+} through electron transfer between the BZT nitrogen atoms.[181, 182] The formation of Cu–BZT complexes has been leveraged in some studies to enhance BZT degradation in wastewater. For example, Zhang et al. investigated the use of a mesoporous Cu/MnO_2 composite to catalyze oxidation of BZT by hydrogen peroxide.[179] The oxidation of BZT by the MnO_2 was facilitated by the Cu–BZT complex formed on the catalyst surface.[179] However, in our study, the presence of Cu did not enhance BZT degradation (**Figures 3.4-3.55**). In the **O9 system**, we observed up to 37% removal of BZT after 3 hours of reaction (**Figure 3.3A**); however, in the **MO9** and **MO7.5 systems** containing metals, we observed an artificial increase in the measured aqueous BZT concentrations (**Figures 3.4A and 3.5A**). The increase was higher for the pH 7.5 condition after 2 hours of reaction. Furthermore, results from the control experiments (i.e., absence of media) for the **MO9** and **MO7.5** systems show a decrease in BZT concentrations (**Figures. B6B-D**) as well as in the presence of Cu only (**Figure B7**) which suggests the formation of the Cu–BZT complex. Cu–BZT complexes are reported to be insoluble in water,[181] thus we hypothesize that the Cu–BZT complexes formed in our systems are removed via filtration prior to HPLC analysis

which explains the lower concentrations obtained in the control experiments described above (**Figures. B6B-D and Figure B7**).

The Cu–BZT complexation is also made evident in the measured aqueous concentrations of Cu in the control experiments conducted in the absence of media (**Figure B5**). For example, in the **M9** control system, 36% Cu removal was observed; however, in the **MO9** control system, 98% Cu was removed after 3 hours of reaction in the presence BZT and the other trace organics. We hypothesize that the reaction between the Cu–BZT complexes and the Fe(VI)-coated sand media leads to the decomplexation of the Cu–BZT and release of aqueous Cu and BZT into solution. Previous studies have reported the successful removal of metal complexes by Fe(VI).[74, 77, 183, 184] For example, Tiwari et al.[77] investigated the removal of iminodiacetic acid (IDA) complexes with Cu(II), Ni(II) and Cd(II) at pH 8, 9 and 10. They reported a removal efficiency of up to 80% of total organic carbon when the concentrations of Cd(II)-IDA and Ni(II)-IDA were 0.3 mM.[77] The removal of the metal complexes in their study was hypothesized to be initiated by the decomplexation by Fe(VI) followed oxidation of the IDA.[77] Further removal of the freed metals by Fe(VI) was also reported.[77] In this study, while we observed the decomplexation of the Cu–BZT complex as evidenced by the increase in aqueous BZT concentration, the free BZT did not react further with Fe(VI). This could be due to the lesser Fe(VI) affinity towards BZT, which was observed in **Figure 3.3**. Further investigations with higher doses of the Fe(VI)-coated sand media or lower concentrations of contaminants could be explored to determine whether the decoupled BZT could be degraded when there is more Fe(VI) available in solution.

Table 3.2. Structures and properties of select trace organic compounds and metals used in this study.[185-189]

trace organic compounds	sources	structure	pKa	Log K_{ow}

acetaminophen (ACM)	analgesic drug (Zhang et al.[185])	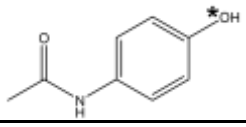	9.71 (Li et al.[171])	0.46 (Snyder et al.[186])
benzotriazole (BZT)	anti-corrosion agent, UV-inhibitors (Mawhinney et al.[174])	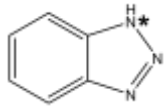	pKa_1 = 1.6 pKa_2 = 8.6 (Xu et al.[187])	1.23 (Hart et al.[188])
sulfamethoxazole (SMX)	antimicrobial drug (Dodd et al.[12])	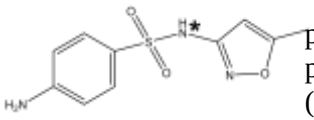	pKa_1 = 1.7 pKa_2 = 5.6 (Dodd et al.[12])	0.89 (Snyder et al.[186])

trace metals	**sources**	**matrix pH**	**speciation**	**% abundance**
copper	fertilizers, paints, oil refining, mining (Khan et al.[9])	9	$Cu(OH)_2$ (aq) (*$Cu(OH)_2$(s), CuO(am, c)*)	57.1
		7.5	Cu^{2+}	46.1
			$CuOH^{+}$	45.6
			(*CuO (am, c)*)	
lead	lead-based batteries, paints (Chowdhury et al.[189]); fertilizers (Das et al.[165])	9	$Pb(OH)^{+}$ (*$Pb(OH)_2$(s)*)	73.5
		7.5	Pb^{2+} (*$Pb(OH)_2$(s)*)	55.7
zinc	oil refining, textiles, rubber products (Das et al.[165])	9	$Zn(OH)_2$ (aq) *(ZnO)*	86.0
		7.5	Zn^{2+}	95.8

The (*****) on the structures show the moieties that can be deprotonated or protonated at the pH values used in this study. The mineral phases in italics are the oversaturated mineral phases for the metal species as determined by Visual MINTEQ at the given pH.

3.3.4. Trends in transformation product formation validates oxidation mechanisms of the trace organics

HRMS results were analyzed as described in **Appendix B3**. Based on this analysis, 85 transformation products (TPs) were identified in the **O9 system** (**Table B5**), 46 TPs in the **MO9 system** (**Table B6**) and 72 TPs in the **MO7.5 system** (**Table B7**). The lower number of TPs

detected in the trace metal-containing systems support the findings discussed in *Section 3.3* when a decrease in oxidation efficiency of the trace organics in the presence of metals was observed. We recognize that the large pool of TPs detected could be due to the inclusion of multiple fragments from the same parent compounds and additional steps are needed to further isolate the transformation products. However, we note that the primary objective of this study is to assess the reactivity of the Fe(VI)-coated sand media in complex matrices; therefore, further analyses were not conducted to identify the structures of the TPs nor to deduct oxidation pathways.

The higher peak areas observed for TPs in the **O9** and **MO7.5** corroborate the solution pH and matrix effects on the oxidation efficiency of the trace organics by the Fe(VI)-coated sand. While over 40 TPs were identified in reaction systems containing trace organics, eight TPs were portrayed in **Figures 3.3–3.5** because they were formed at the highest yield: TP-100, TP-186, TP-218, TP-230, TP-246, TP-274, TP-275, TP-290 (**Figures 3.3–3.5**). For all eight featured TPs, we observed a sharp increase (by 2 orders of magnitude or greater) in peak area after 5-min of reaction, which confirms the fast reactivity of the Fe(VI)-coated sand towards the trace organics. Additionally, all the featured TPs except for TP-230 and TP-275 exhibited an increase in peak area at pH 7.5 (**Figure 3.5B-C**) emphasizing the greater reactivity of Fe(VI) at pH 7.5 due to the $HFeO_4^-$ species. However, for TP-230, we observed more than an 85% decrease in peak area in the presence of trace metals at both pH values (**Figures 3.4B and 3.5B**). Furthermore, the maximum peak area obtained in the presence of the trace metals (in the **MO9** and **MO7.5 systems**) was recorded at 5-min of reaction which indicates that TP-230 formed within 5-min of treatment then subsequently decreased. These results suggest that the presence of trace metals inhibits the formation of TP-230, or that the trace metals react with TP-230 to form metal complexes. Additionally, the TP-275 peak area after 5-min of reaction in the **MO7.5 system** was

35% greater than the peak area in the **MO9 system**; however, after 3 hours of reaction, the peak area in the **MO7.5 system** was 74% less than the peak areas in the **MO9 system**. This implies that the formation of TP-275 is a pH-dependent reaction, and that TP-275 may be undergoing reactions with the trace metals.

In the **MO9** and **MO7.5 systems**, BZT oxidation did not occur suggesting that TP-275 is a transformation product of either ACM or SMX. Furthermore, under pH 7.5 and 9 conditions, SMX is deprotonated whereas ACM is protonated (see **Table 3.1**). Thus, we hypothesize that TP-275 is a transformation product of SMX that can react with the positively charged metal species via electrostatic interactions. In particular, at pH 7.5 in the **MO7.5 system**, Cu, Pb and Zn exist predominantly as Cu^{2+}, Pb^{2+}, Zn^{2+} (**Table B3A**), thus complexation between these cations and a negatively charged transformation product may explain the significant decrease in peak area in the **MO7.5 system**. Future work will be performed to identify these compounds and elucidate their fate in our treatment systems.

Comparing the trends in the TP yields with the measured oxidation efficiencies of the trace organics suggests that TP-100, TP-186, TP-218 and TP-246 are potential oxidation products of ACM, whereas TP-274 and TP290 may be oxidation products of SMX. While we recorded a slight increase in peak area at pH 7.5 for TP-100, TP-186, TP-218, and TP-246 (**Figure 3.5**), their peak areas were relatively similar across the test reaction systems (i.e., **O9**, **MO9**, and **MO7.5** in **Figures 3.3B, 3.4B** and 3.5**B**). For example, the peak areas for TP-218 after 3 hours of reaction were 3.82×10^6 in the **O9 system**, 4.26×10^6 in the **MO9 system**, and 4.94×10^6 in the **MO7.5 system**. The consistent formation of these TPs at similar quantities aligns with the comparable oxidation capacity observed for ACM across the three reaction systems containing trace organics (**Figures 3.3A-3.5A**). Oxidation of organic compounds by Fe(VI) occurs via

electrophilic attack of electron rich moieties (e.g., phenols, amines, anilines and olefins).[32, 44, 68] Thus, we hypothesize that Fe(VI) oxidation of ACM and SMX will occur with their phenolic and aniline moieties, respectively. For ACM, oxidation could proceed by separation of the amide moiety and phenol moiety followed by cleavage of the latter[190] to produce TP-100 (**Figure B8**). Additionally, oxidation of ACM could occur via hydrolysis. In neutral to alkaline solutions, Fe(VI) reacts with water to form $Fe(OH)_3$ and OH^-.[149] We suspect that the formation of OH^- could enhance hydrolysis of ACM at the benzene ring[190] to produce TP-186 (**Figure B8**). Conversely, the chemical structure of SMX can contribute to multiple oxidation pathways for reaction with Fe(VI) which can happen via the aniline group, the isoxazole group, or at the N–S bond (**Figure B9**).[42, 191] The hypothesized SMX TP-274 peak area decreased by 94% in the **MO9 system** compared to the **O9 system** after 3 hours of reaction. At environmental pH (i.e., the **MO7.5 system**), the TP-274 peak area increased by 50% compared to the peak area in the **O9 system**. The observed trends with respect to peak area magnitude correspond with the trends in SMX oxidation observed in the **MO9** (**Figure 3.4A**) and **MO7.5** (**Figure 3.5A**) reaction systems. Furthermore, the literature reports an oxidation product with m/z value of 276 during the oxidation of SMX by Fe(VI).[115, 191] We hypothesize that the TP-274 detected in our study is similar to this oxidation product reported in literature. The formation of this transformation product occurs through the cleavage and subsequent hydroxylation of the isoxazole moiety in SMX[191, 192] (**Figure B9**). It is further degraded via hydroxylation of the benzene ring to form a product with a reported m/z value of 292.[191, 192] We attribute this compound to TP-290 reported in our study (**Figure B9**).

3.3.5. Wastewater effluent constituents inhibit trace organic oxidation but promotes trace metals sorption

Trace organics removal by Fe(VI)-coated sand is reduced in the synthetic wastewater reaction system. After 3 hours of reaction with the media, only 7.24% removal of SMX was achieved (**Figure 3.6A**). While the oxidation efficiency of ACM remained high (98.4%) (**Figure 3.6A**), the degradation was slower in SWW compared to degradation in the borate buffer solutions (**Figures. 3.3-3.5**). Oxidation of BZT in the SWW was minimal, and, as before, we observed an artificial increase in the aqueous BZT concentration during the reaction period (**Figure 3.6A**). While some studies have reported no effect of inorganic ions (i.e., Na^+, Ca^{2+}, Cl^-, HCO_3^-) on Fe(VI) oxidation capacity,[68, 93] others have noted that the presence of these ions will impede ferrate oxidation.[39, 92] For example, Feng et al. observed a 10% decrease in flumequine oxidation by Fe(VI) in the presence of Ca^{2+} and Mg^{2+} ions[39] which was attributed to the catalytic effects of these cations on the self-decomposition of Fe(VI) in solution.[39, 82] Specifically, Ma et al. investigated the effect of Ca^{2+} on Fe(VI) decomposition at pH 9-10 and demonstrated that Ca^{2+} bridges FeO_4^{2-} ions to facilitate the formation of the diferrate intermediate[82] which undergoes reduction to produce Fe(III).[82, 117] The same effect is expected for other divalent ions present in the synthetic wastewater matrix (i.e., Mg^{2+}).[82] In the SWW treatment system, Fe(VI) consists of predominantly FeO_4^{2-} ions (83.4%); thus, we suspect that the Ca^{2+} and Mg^{2+} ions present will react with FeO_4^{2-} to catalyze Fe(VI) decomposition and decrease the oxidation of ACM and SMX.

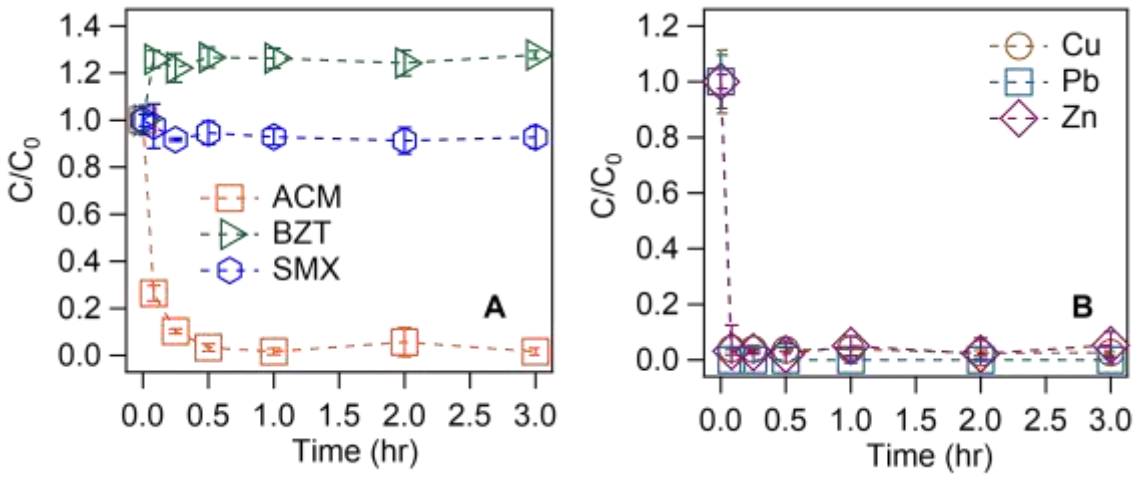

Figure 3.6. Removal of nominally 500 µg/L (each) of (**A**) ACM, BZT, SMX and (**B**) Cu, Pb, Zn by 2 g/L Fe(VI)-coated sand in synthetic wastewater solution as a function of time.

Conversely, the SWW constituents enhanced trace metals removal by the Fe(VI)-coated sand. Greater (>94%) and faster (within 5 min of reaction) removal efficiencies were recorded for all three trace metals in the SWW reaction system (**Figure 3.6B**) compared to the treatment systems in borate buffer. While the removal of Cu and Pb can be partially attributed to removal of solid phases through filtration, the removal of Zn is completely achieved by the media. In the SWW control samples absent Fe(VI)-coated sand, Zn removal did not occur (**Figure B4D**); however, the presence of the media led to a 94.7% removal of Zn in SWW (**Figure, 3.6B**). Therefore, while the self-decomposition of Fe(VI) by the Ca^{2+} and Mg^{2+} ions hindered transformation of trace organics within the SWW matrix, the faster generation of Fe(III) species in solution promoted trace metals removal. However, we observed that the total mass of leached, aqueous Fe(VI) in the SWW reaction system (**Figure B7**) was comparable to the leached mass in the **MO9 system** (**Figure B6C**) indicating that the effect of Ca^{2+} and Mg^{2+} might be limited to interferences with oxidative processes in our treatment systems.

The decreased oxidation efficiency of trace organics coupled with the enhanced removal of trace metals in the SWW matrix suggest a hierarchy in Fe(VI) reactivity toward contaminants

and co-existing ions. The significant difference in ACM and SMX oxidation efficiencies (**Figure 3.6A**) in the SWW matrix (91%) compared to the difference in oxidative removal of ACM and SMX in the **MO9** (10%) and **MO7.5** (no difference) **systems** demonstrates preferential affinity of the Fe(VI)-coated sand for ACM. Furthermore, the diminished oxidation efficiency of SMX and BZT in the SWW matrix indicates that Fe(VI) favorably reacts with hydrophilic and protonated ACM, divalent cations, and water molecules in the SWW system. Additionally, these three interactions boost formation of Fe(III) phases to significantly improve trace metals removal. These results further demonstrate the promising potential for Fe(VI)-coated sand for treatment of contaminants in complex matrices.

3.4. Conclusion

The Fe(VI)-coated sand composite media proved to be a highly effective treatment for Fe(VI) deployment in water treatment applications. The effect of water chemistries (i.e. pH and inorganic ions) and matrix complexity (i.e., multiple contaminants) on the reactivity of the Fe(VI)-coated sand was explored through batch tests. Treatment of ACM, SMX, BZT, Cu, Pb, and Zn at equal initial concentrations revealed that the Fe(VI) had a greater affinity for the trace organics, especially for ACM for which removal efficiency exceeded 90% under all experimental conditions tested. The presence of Cu in the treatment systems inhibited BZT removal due to the formation of Cu–BZT complexes. Therefore, if such complexes form in solution during application of Fe(VI)-coated sand, treatment of both complex components may be compromised. A faster removal of ACM and SMX was achieved at pH 7.5 compared to pH 9 indicating that the lower, environmental pH is favorable for trace organics oxidation due to the increased presence of $HFeO_4^-$ ions in solution. The removal of ACM and SMX decreased at pH 9 in the presence of trace organics and at pH 8 in the presence of trace metals and inorganics ions, suggesting that at

pH values where $HFeO_4^-$ ions exist in smaller quantities, the removal of trace organics may depend on the ratio of Fe(VI) species to contaminants. HRMS results indicated that removal of trace organics occurred via oxidation and showed a sharp increase by 2 or more orders of magnitude in the peak area of the transformation within 5 min of reaction, validating the high reactivity of the media towards the trace organics. While Cu and Pb removal was partially attributed to the removal of their mineral solid phases, Zn removal was solely via interaction with the Fe(VI)-coated sand. Thus, the increased removal of Zn in the presence of trace organics indicated that trace metals removal was achieved by Fe(III) formed in solution after Fe(VI) reaction with the trace organics.

This study demonstrates the potential for Fe(VI)-coated sand media for treatment of multiple contaminants in complex matrices such as in wastewater effluents. Here, we used concentrations that are higher than typical concentrations of trace organics and trace metals in the environment. We expect as with any chemical oxidant and coagulant, 100% removal or degradation of all contaminant types will not be achieved. Therefore, our goal was not to optimize the Fe(VI)-coated sand for contaminant remediation, but rather to evaluate its viability as treatment media. Future work exploring the treatment capabilities of the Fe(VI)-coated sand will probe removal of contaminants at environmentally relevant concentrations as well as in the presence of dissolved organic carbon to better assess the Fe(VI)-coated sand capacity for treatment. Additionally, we will also assess Fe(VI)-coated sand performance during column studies to mimic real-world treatment systems.

Chapter 4. Effects of Effluent Organic Matter on Ferrate (Fe(VI))-coated Sand Reactivity

4.1. Introduction

Wastewater effluents contain organic matter for which the composition depends on the source of the influent wastewater and the wastewater treatment processes.[193] The presence of the organic matter poses challenges for the discharge and further treatment of the effluent wastewater. Particularly, dissolved organic matter which constitutes more than 90% of effluent organic matter (EfOM)[193] has been linked to toxic effects on microorganisms in receiving waters. For example, Vazquez and Fatta-Kassinos evaluated the toxicity of wastewater samples from two sewage treatment plants on freshwater and saltwater microorganism (i.e., *Pseudokirchneriella subcapitata, Daphnia magna, Artemia salina, Vibrio fischeri*) and observed higher toxicity in the effluent wastewater compared to the influent samples and samples taken after secondary treatment.[194] The toxicity was higher in the summer season, which is concerning because of water reuse applications in Cyprus where the study was conducted, especially in summer when water demand is high. Additionally, the presence of organic matter can lead to the formation of disinfection byproducts in wastewater treatment plants where disinfection is done prior to discharge of the treated wastewater.[195] On the other hand, EfOM can aid to alleviate the toxicity of wastewater effluents. Studies have reported that effluent organic matter can complex metals in wastewater effluents thus reducing their bioavailability and toxicity to microorganisms in receiving streams.[196-198] Worms et al. observed a decreased intracellular Cd content in green alga *C. kesslerii* exposed to ultrafiltered and colloidal isolates from wastewater effluents.[196] Micropollutants (e.g. pharmaceuticals, personal care products, pesticides, endocrine disrupting compounds) that are not completely removed during wastewater treatment can also react with

EfOM via hydrophobic and hydrophilic interactions,[193] thus reducing their direct discharge into receiving waters.

The efficiency of water treatment technologies is affected by organic matter. For example, EfOM can impede treatment of organic pollutants, especially treatment via oxidation[21, 199] and adsorption processes.[200, 201] Steigerwald and Ray observed a 60% reduction in perfluorooctane sulfonate adsorption in the presence of EfOM when they evaluated a spent coffee ground biochar media for treatment of wastewater effluent.[200] The EfOM can sorb to adsorptive media, thus reducing sorption sites available for contaminants.[200, 201] Dissolved organic matter contains phenolic moieties that can react rapidly with chemical oxidants (e.g., ozone), thus reducing the availability of the oxidant for treatment of organic compounds. This inhibitory effect of organic matter is particularly concerning for wastewater treatment plants because adsorption onto activated carbon or advanced oxidation processes are often used as a final treatment step for wastewater prior to discharge.[7] Similarly, EfOM can impede trace organic compounds oxidation by ferrate (Fe(VI)). Initially proposed for drinking water treatment, Fe(VI) has gained increased attention for wastewater treatment. Researchers have investigated the effects of organic matter on Fe(VI) aqueous stability and reactivity,[68, 92, 199, 202] especially because of Fe(VI) sensitivity to water chemistries and composition. Manoli et al. observed a 15% decrease in removal of caffeine by Fe(VI) in a secondary effluent wastewater compared to removal in ultrapure water.[92] This decrease was even greater (31.4%) when acid-activated Fe(VI) was used,[122] confirming reactions between Fe(VI) and EfOM which would consume the Fe(VI) otherwise available for organic compounds oxidation.

In this study, we assess the effect of EfOM on the reactivity of the Fe(VI)-coated sand media in synthetic wastewater effluent. Specifically, we evaluate this effect on the removal of

trace metals (i.e. copper (Cu), lead (Pb), and zinc (Zn)) and organic compounds (i.e., acetaminophen (ACM), sulfamethoxazole (SMX), phenol (PHE)) commonly found in wastewater effluents. Humic acid, bovine serum albumin, sodium alginate and octanoic acid were chosen to mimic the humic, protein, carbohydrate and fat composition of typical EfOM. Our previous study (*Chapter 3*) indicated that the presence of divalent cations in the synthetic wastewater effluent (SWW) effluent solution reduced organic compounds oxidation while catalyzing Fe(VI) self-decay which promoted trace metal removal by the *in-situ* produced Fe(III). Here, we hypothesize that the combining effects of the EfOM reactions with Fe(VI) and divalent cations catalytic effects would further reduce the oxidation of the organic compounds. Furthermore, EfOM could complex the trace metals resulting in their increased sorption.

4.2. Materials and Methods

4.2.1. Chemicals

Bovine serum albumin lyophilized powder (96%), alginic acid sodium salt from brown algae, technical grade humic acid, octanoic acid (98%) were purchased from Sigma Aldrich and used to mimic composition of effluent organic matter constituent. Puriss p.a. grade potassium hydrogen phthalate monobasic was purchased from Sigma Aldrich (St. Louis, MO) and used to prepared organic carbon standards for total organic carbon analysis. Details of all other chemicals used in this study are as described in *Chapters 2 and 3, and Appendix A and B*. All experiments were conducted using ultrapure Milli-Q water (resistivity: 18.2 mΩ).

4.2.2. Evaluation of effluent organic matter effects on Fe(VI)-coated sand reactivity

Initial experiments to assess the effects of EfOM on Fe(VI)-coated sand reactivity were conducted in ultrapure water buffered at pH 9 with 10 mM $Na_2B_4O_7$ buffer. Approximately 100

mg of the Fe(VI)-coated sand was added to 50 mL of 10 mM $Na_2B_4O_7$ containing roughly 250 µg/L of phenol and synthetic EfOM in a 50-mL polypropylene centrifuge tubes. The synthetic EfOM (Syn-EfOM) was prepared as discussed in Motsa et al.[203] The composition included bovine serum albumin (2.5 mg/L), sodium alginate (2 mg/L), octanoic acid (0.5 mg/L), and humic acid (5 mg/L).[200, 203] At designated time intervals, a 2 mL aliquot was quenched with 20 µL of 500 mM Na_2SO_3 to stop the reaction between aqueous Fe(VI) and PHE and then filtered with a 0.2 µm, 25 mm diameter cellulose acetate syringe filter before analysis using high performance liquid chromatography (HPLC) methods (**Appendix C1**). A 4 mL aliquot was taken and filtered with 0.2 µm, 25 mm diameter cellulose acetate syringe filter and 1 mL of the aliquot was used for aqueous Fe(VI) measurements via the 2,2'-azinobis-(3-ehtylbenzothiazoline-6-sulfonate) (ABTS) colorimetric method[139] via UV-Vis spectroscopy using a Shimadzu UV-2700 spectrophotometer (Kyoto, Japan). 2 mL of the filtered aliquot was diluted with Milli-Q water before total organic carbon (TOC) measurements using a Shimadzu (Kyoto, Japan) TOC-L analyzer. Batch experiments were also conducted using Fe(VI) powder to compare the effects of the Syn-EfOM on the Fe(VI)-coated sand and the Fe(VI) powder. Fe(VI) powder synthesized in our laboratory was added to 50 mL solutions of 10 mM $Na_2B_4O_7$ containing 250 µg/L of phenol and the synthetic effluent organic matter. Aliquots were taken and analyzed as described above.

The effects of Syn-EfOM on the Fe(VI)-coated sand reactivity in a more complex matrix were investigated with batch experiments using a SWW solution containing the Syn-EfOM and 50 µg/L of ACM, SMX, PHE, Cu, Pb, Zn each. The synthetic wastewater composition was as described in *Chapter 3* and *Appendix B*. Aliquots were taken as above. Additionally, 500 µL of the filtered aliquot was further diluted with MilliQ-water and acidified to 2% trace metal grade

nitric acid for inductively coupled plasma orbital mass spectrometry (ICP-MS) analyses using a Perkin Elmer Nexion 2000B inductively coupled mass spectrometer (Waltham, MA).

Control experiments in the absence of Fe(VI)-coated sand and in the presence of Syn-EfOM were conducted to determine interactions between the trace metals and organics with the Syn-EfOM. Control experiments in the absence of Fe(VI)-coated sand and of the Syn-EfOM were also conducted.

All experiments were conducted in triplicates.

4.3. Results and Discussion

4.3.1. Production of Fe(V) and Fe(IV) species enhances degradation of trace organics in the presence of effluent organic matter

Phenol degradation by Fe(VI)-coated sand and Fe(VI) powder was enhanced in the presence of the synthetic effluent organic matter. After 5 min, the degradation efficiency of phenol was 79.4% by Fe(VI)-coated sand and 92.3% by Fe(VI) powder (Figure 4.1). These degradation efficiencies were higher than the efficiencies obtained in our previous study[169] where phenol degradation in the absence of Syn-EfOM was 51% by Fe(VI)-coated sand and 37% by Fe(VI) powder. Control experiments conducted in the absence of media revealed no loss of phenol in solution suggesting that there were no interactions with the Syn-EfOM. We suspect the involvement of Fe(V) and Fe(IV) reactive species in the increased degradation of phenol in our treatment system. Guo et al. observed enhanced oxidation of sulfamethoxazole and trimethoprim by Fe(VI) in the presence of natural organic matter.[204] They attributed this increase to the formation of Fe(V) and Fe(IV) from reactions between Fe(VI) and phenolic moieties in the natural organic matter.[204] We observed an initial decrease in TOC in both Fe(VI)-coated sand and the Fe(VI) powder systems (**Figure 4.1**), which could be due to the reaction between Syn-EfOM

and aqueous Fe(VI). Similar degradation of phenol by Fe(VI)-coated sand was observed in the SWW effluent matrix (**Figure 4.2**).

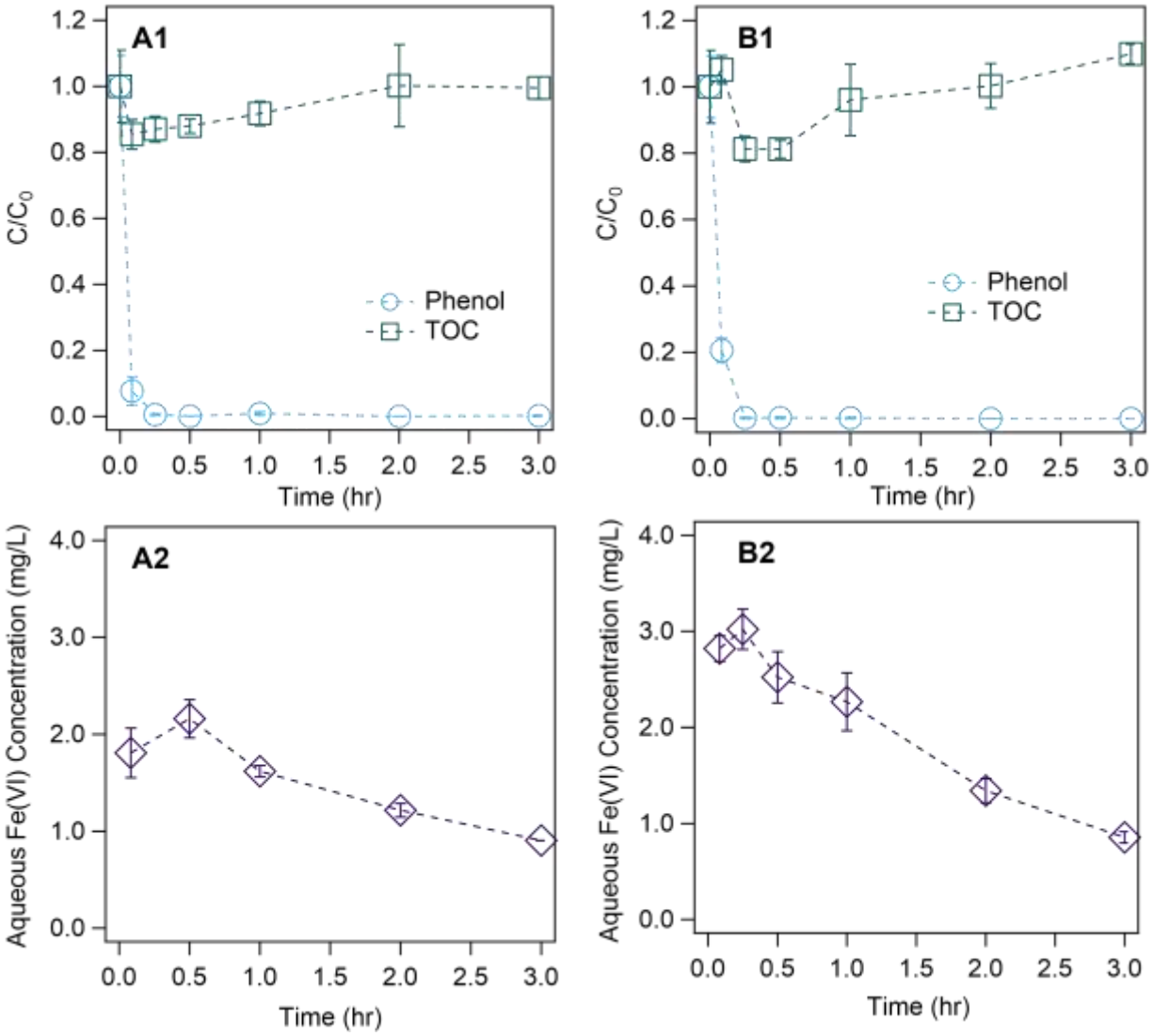

Figure 4.1. Degradation of nominally 250 µg/L phenol in 10 mM borate buffer pH 9 in the presence of nominally 10 mg/L synthetic effluent organic matter by (**A**) 12.6 mg/L Fe(VI) powder and (**B**) 2 g/L Fe(VI)-coated sand. (Top) Normalized degradation of phenol and total organic carbon, (**bottom**) changes in aqueous Fe(VI). The error bars represent the standard deviation from triplicate samples.

Production of Fe(VI) and Fe(V) species is further confirmed by near complete degradation of SMX in the treatment system. More than 80% degradation of SMX was achieved in the presence of media and control experiments indicate no interactions with the Syn-EfOM. Although the initial concentrations of trace organics used in this study (i.e., 50 µg/L) are significantly smaller than the concentrations (500 µg/L) from our previous study (*Chapter 3*), a comparison between these results hints at the presence of more reactive species in our treatment systems with EfOM. Previously, we observed minimal degradation of SMX in the synthetic wastewater effluent solution containing no EfOM. Compared to degradation of SMX in the 10 mM borate buffer pH 7.5 systems, results in the SWW (no Syn-EfOM) was explained by both the reduced quantities of $HFeO_4^-$ at pH values greater than 7.3 and the complexities of the SWW matrix which lowers the ratio of Fe(VI) to water components thus limiting its oxidation capacity (**Chapter 3**). In this work, we observed significant degradation of all three organic compounds despite the added layer of Syn-EfOM. Furthermore, aqueous Fe(VI) concentrations were similar in the treatment systems with and without contaminants (**Figure C3**). This suggests formation of Fe(V) and Fe(IV) and enhanced degradation of the trace organics.

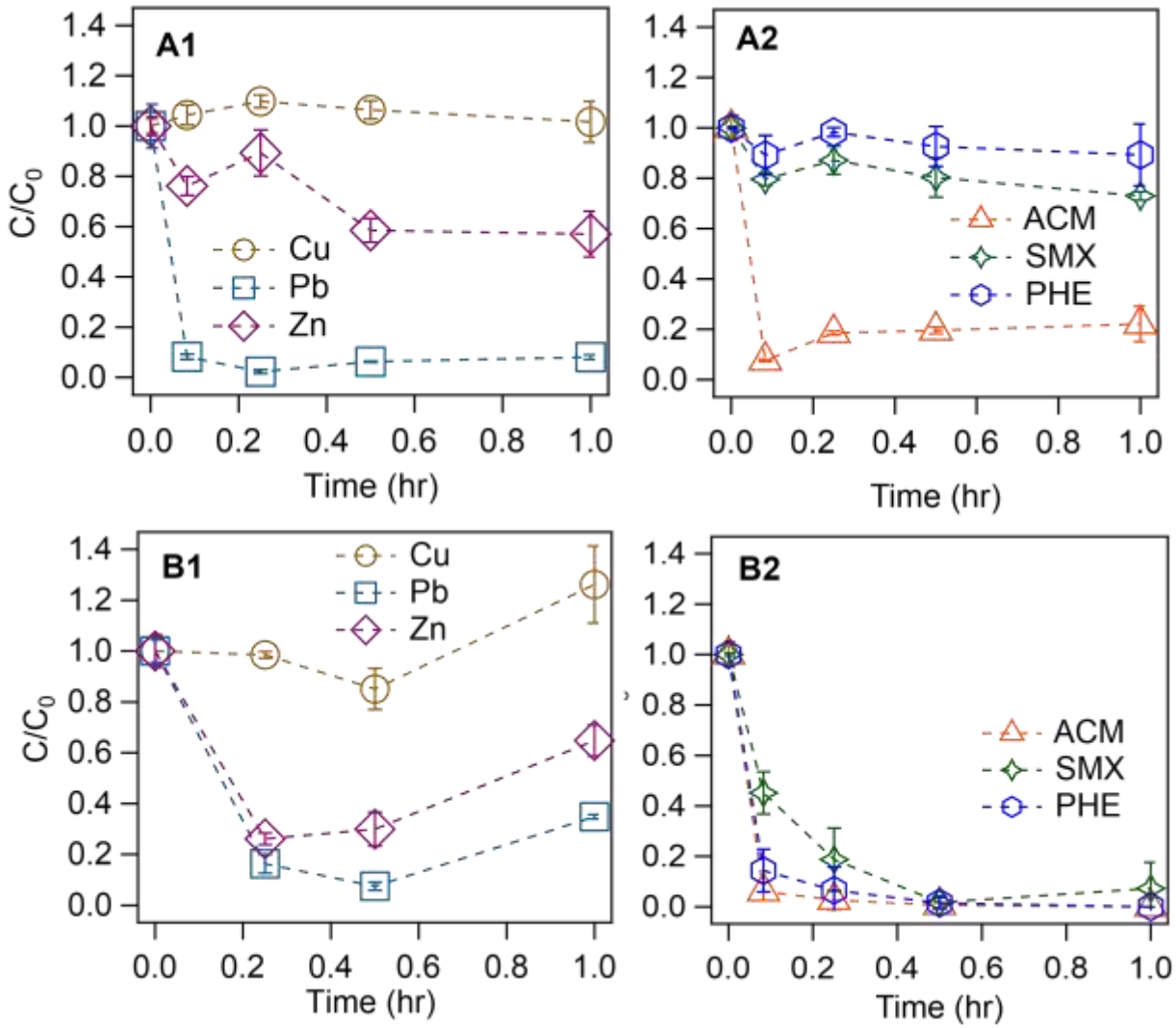

Figure 4.2. Normalized removal of (**left panel**) nominally 50 µg/L of Cu, Pb, and Zn each and (**right panel**) nominally 50 µg/L of ACM, PHE, SMX each in the synthetic wastewater effluent containing nominally 10 mg/L of synthetic effluent organic matter in (**A**) the absence and (**B**) the presence of 2 g/L of Fe(VI)-coated sand. The error bars represent the standard deviation from triplicate samples.

4.3.2. Complexation with effluent organic matter govern removal of trace metals

Removal of Pb in the synthetic wastewater effluent is primarily driven by interactions with the effluent organic matter. Similar removal efficiencies were observed for Pb in the absence (**Figure 4.2A1**) and presence (**Figure 4.2A2**) of Fe(VI)-coated in the synthetic wastewater effluent containing Syn-EfOM indicating that in the Fe(VI)-coated sand treatment

system, removal of Pb was due to removal by Syn-EfOM. Trace metals can complex with organic matter and sorb onto their surface; thus, we suspect that this complexation mechanism is the underlying factor for Pb removal. While Syn-EfOM achieves some level of removal (40% within 30 min) of Zn (**Figure 4.2A1**), the removal was more pronounced in the Fe(VI)-coated sand system where we observed 70% removal of Zn. Our previous study revealed that metals removal during treatment by Fe(VI)-coated sand was led by sorption to *in situ* formed Fe(III). These results indicate that trace metals removal in the SWW effluent containing Syn-EfOM could occur via: (1) complexation and sorption to Syn-EfOM, (2) in situ Fe(III) formed from

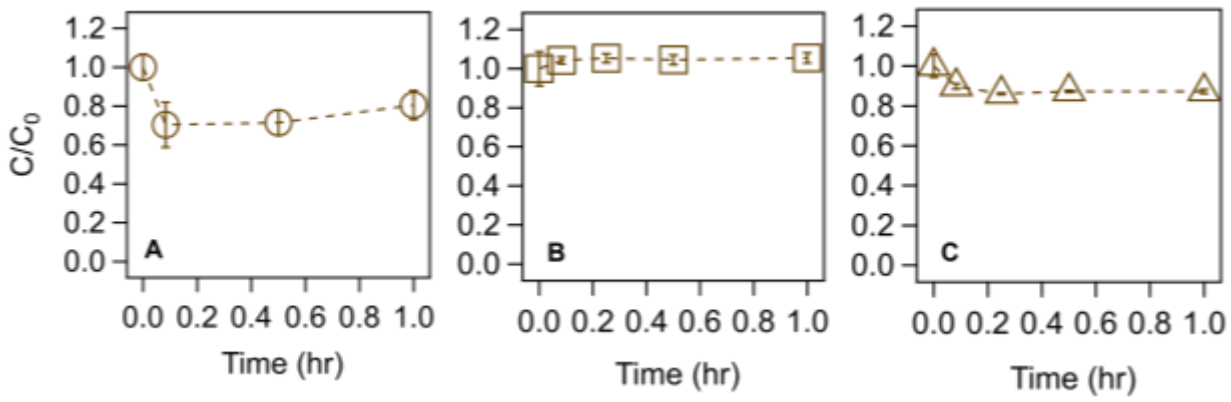

Figure 4.3. Changes in total organic carbon concentration in the synthetic wastewater effluent with (**A**) effluent organic matter in the presence of Fe(VI)-coated sand, (**B**) effluent organic matter and trace metals and trace organics in the absence of Fe(VI)-coated sand and (**C**) effluent organic matter and trace organics and trace metals in the presence of Fe(VI)-coated sand. The error bars represent the standard deviation from triplicate samples.

Fe(VI) self-decay, Fe(VI), Fe(V) and Fe(IV) reactions with organic compounds, and Fe(VI) reactions with Syn-EfOM.

Cu removal did not occur in the synthetic wastewater effluent system. Control experiments in the absence of Fe(VI)-coated sand show no loss of Cu in solution (**Figure 4.2A1**). Removal did not occur in the presence of Fe(VI)-coated sand either. In our previous

study (*Chapter 3*), Cu removal was mainly driven by its complexation with benzotriazole, which was not included in this study. However, we observed a 26% increase from the initial Cu concentration after 1 hr treatment in the Fe(VI)-coated sand system. Pb and Zn also exhibited an increase in concentration (**Figure 4.2A2**), hinting possible desorption and redissolution of these metals. We posit that the interactions (i.e., complexation, sorption) of the metals to the Syn-EfOM is immediate but can be limited by Fe(VI) reactions with Syn-EfOM. A recent study by Wang et al. reported that Fe(VI) and Mn(VII) do not mineralize EfOM during treatment of secondary wastewater effluent, but rather they convert some macromolecules of EfOM into smaller molecules.[199] Similarly, we observed minimal (<20%) reduction in TOC content in our treatment systems (**Figures 4.1 & 4.3**) indicating that complete mineralization of the Syn-EfOM did not occur. In our treatment systems, the changes in Syn-EfOM structural composition could change their interactions with the trace metals which could explain the sudden increase in their concentration.

4.4. Conclusion

Organic matter is ubiquitous in the environment and present in natural and engineered systems. Effluent organic matter especially can influence advanced treatment of wastewater effluent. Treatment of ACM, PHE, SMX, Cu, Pb, and Zn at environmentally relevant concentration by Fe(VI)-coated sand in the presence of Syn-EfOM revealed that Syn-EfOM can promote formation of reactive Fe(V) and Fe(IV) to enhance organic compounds degradation. Additionally, Syn-EfOM can remove Pb and Zn from solutions, however the possible changes in Syn-EfOM structure after reactions with Fe(VI) could lead to a redissolution of trace metals. Therefore, closer monitoring of the treated waters might be needed in facilities deploying Fe(VI)-coated sand for treatment of water containing EfOM and trace metals.

EfOM is comprised of many complex molecules and can differ depending on the source of the raw water. Thus, future studies that use real wastewater solutions are needed to fully comprehend the effects of EfOM on Fe(VI)-coated sand reactivity.

Chapter 5. Implications and Conclusions

The increasing presence of harmful chemicals in wastewater effluents due the inefficiency of conventional wastewater treatment plants poses challenges for wastewater reclamation and reuse applications that are increasingly being considered to address water shortage crises. This dissertation presents a novel Fe(VI)-coated sand composite media to enhance treatment of trace organics and metals in wastewater effluent. Batch studies showed that the Fe(VI)-coated sand stability and reactivity are affected by water chemistries. Significant degradation (>80%) of trace organics (i.e., phenol, acetaminophen, sulfamethoxazole) typically found in wastewater effluents was achieved whereas the removal of trace metals was only favored in systems where Fe(III) production was catalyzed. Despite Fe(VI) sensitivity to water chemistry, considerable level of contaminants removal was still achieved in the synthetic wastewater effluent matrix. This composite media offers an easier deployable method for Fe(VI)-coated sand in water treatment systems.

While this dissertation emphasized Fe(VI)-coated sand reactivity in a wastewater effluent matrix, this media has potential for diverse water treatment applications. For example, Fe(VI)-coated sand can be deployed in advanced water treatment plants to replace ozonation, sand filtration and activated carbon treatment often used in these facilities to treat secondary effluent before discharge or reuse.[7] The added filtration benefit of Fe(VI)-coated could be leveraged to remove solids during treatment. Then, an advanced filtration step (e.g., microfiltration, ultrafiltration, biologically active filtration) could follow to remove remaining particles that were not removed by the Fe(VI)-coated sand (**Figure D1**). Additionally, Fe(VI)-coated sand media can be beneficial for on-site decentralized wastewater treatment to alleviate treatment and operational costs on existing treatment plants. Due to its multifunctional properties as a coagulant, disinfectant and oxidant, researchers have proposed Fe(VI) as a one-step treatment

technology.[48, 205, 206] Similarly, the Fe(VI)-coated sand could be deployed as a one unit treatment process. If necessary, an additional coagulation/sedimentation step could be added to further remove soluble particles before discharge or reuse applications of the treated wastewater. For drinking water treatment, Fe(VI) can be deployed in sand filters and used for an advanced filtration treatment. The oxidative treatment that would then occur during filtration could reduce the need for chlorination.

Preliminary column studies were conducted to assess the Fe(VI)-coated sand performance during continuous flow treatment and revealed that the current synthesis method for the Fe(VI)-coated sand could introduce Fe(III) sludge in the treatment lines (**Figure D1-D3**), which would require solid-liquid separation technology. Column studies conducted to assess the media performance in infiltration systems resulted in fast leaching of the Fe(VI) off the sand surface (**Figure D2**). Column tests were conducted using short plexi glass columns (inner diameter = 1 cm, height = 5 cm) purchased from DWK Life Sciences (Milville, NJ) (**Figure D1**). PVC pipes, fittings, adapters purchased from McMaster Carr (Elmhurst, IL) were used for flow transport. The columns were packed with different ratios of Fe(VI)-coated sand media and uncoated Ottawa sand to achieve 0, 25 and 100 weight percent of Fe(VI)-coated sand. Approximately 0.5 g of silanized glass wool, purchased from MilliporeSigma (Bellevue, WA) was packed in the entrance of the column to prevent media loss. An Ismatec IPC 12-channel peristaltic pump was used to control the upward flow rate of 1 mL/min of water through the columns. A tracer test conducted on the 100% virgin sand packed columns using ABTS as the tracer indicated that the pore volume was 14.5±4.9 mL. The influent solution was composed of synthetic wastewater effluent matrix as described in *Chapter 3*, effluent organic matter as described in *Chapter 4*, and trace metals and trace organics at 50 µg/L each. As the influent solution flowed through the

column, we noticed Fe(VI) leaching off the sand surface and exiting the column. Sampling of the columns were done every two minutes; and the aliquots were quenched with 500 µL of 500 mM Na_2SO_3 to stop Fe(VI) reactions. The reactions between the quencher and Fe(VI) produced Fe(III) sludge visible in the effluent (**Figure D3**). This fast leaching of the Fe(VI) indicates binding agents that can form stronger interactions with the Fe(VI) to retain onto the sand surface for longer periods of time might be needed.

Future studies could explore enhancements or alternatives to the proposed synthesis method. Liu et al. developed a Fe(III)-encapsulating silica and amine modified sand using hydrolyzed TeOS and an aminosilane compound for phosphorous removal in wastewater.[143] The Fe(III) on this mesoporous sand could be oxidized to Fe(VI). Currently, the Fe(VI)-coated sand is synthesized by introducing the TeOS-sand to a slurry of potassium ferrate. However, preliminary regeneration tests suggest that the Fe(VI)-coated sand could be produced by oxidizing a Fe(III)-coated sand. During the column studies discussed above, the Fe(III) particles were not visible in the effluent solution after approximately 12-14 min (i.e., 1 PV) of sampling; however, the sands in the columns still display a slight orange color typically indicative of Fe(III) presence. Regeneration the media was attempted via two methods: (1) approximately 25 mL of KOCl solution prepared by reacting $Ca(OCl)_2$ and KOH as done during Fe(VI) synthesis (*Appendix A & Chapter 1*) was flowed at 1 mL/min through a column that had 100% Fe(VI)-coated sand, then the column was capped and left for approximately 24hr; (2) the sand was transferred from the column into a 50 mL centrifuge tube containing 25 mL of KOCl solution and stirred for approximately 24 hour before filtration. The regenerated media obtained through both methods were then placed in a vacuum oven. Visual characterization of the sands (**Figure D4**) shows a light pink, purple color which would indicate Fe(VI) speciation. This implies that Fe(III) already

present on a sand surface could be oxidized into Fe(VI) to form the Fe(VI)-coated sand. Additionally, a multilayer Fe(VI)-coated sand that introduces Fe(VI) to the treatment system sequentially could be explored. This composite would have a core of sand with multiple layers of Fe(VI) separated by layers of binding agent or binding agent and silica. Feng et al. reported that multiple addition of Fe(VI) led to complete degradation of fluoroquinolone (FQ) antibiotics compared to a single addition with Fe(VI):FQ molar ratio equivalent to the total molar ratio added during the multi-step treatment.[39] These possible avenues could result in more stable Fe(VI)-coated sand composite.

Appendix A: Supporting Information for Chapter 2

A1. Synthesis of potassium ferrate

The potassium ferrate (K_2FeO_4) solution was prepared via the wet oxidation process following a method adapted from Guan et al.[137] A saturated solution of 13 M KOH was prepared, chilled and stored at 4 °C throughout the synthesis to maintain cold temperature conditions. Approximately 15 g of $CaOCl_2$ was added to 25 mL of the saturated KOH solution. The mixture was stirred for 30-60 min and filtered using a Whatman glass microbore filter (grade GF/A) paper to obtain a yellow solution of potassium hypochlorite. An additional 20 mL of the saturated KOH was added to the yellow filtrate, and the mixture was placed in an ice bath for 20-30 min to precipitate potassium chloride. The potassium chloride suspension was further filtered with a GF/A filter paper. Then, 8 g of pulverized ferric nitrate was added slowly and in small portions to the filtrate solution under cooling conditions (5 °C) to form K_2FeO_4. A VWR recirculating chiller was used to maintain the temperature of the K_2FeO_4 throughout the synthesis. The generated solution of K_2FeO_4 was stirred for an hour before the addition of 6 g of KOH. The mixture was stirred for 20 min and left to cool for 40 min. Then the solution was centrifuged at 4000 rpm for 10 min. The supernatant solid was discarded and the solid frozen at -80 ˚C for 1 hr. The frozen solid was added to 50 mL of 3 M KOH solution pre-chilled at 4 ˚C. The mixture was shaken until the K_2FeO_4 solid thawed and dissolved in the KOH solution. The mixture was filtered into 150 mL of the saturated 13 M KOH solution and placed in an ice bath. The filtrate solution was left in the ice bath until solid particles started precipitating, then the filtrate was filtered. The solid K_2FeO_4 precipitate was washed subsequently with pentane (~250 mL), methanol (~ 100 mL) and dichloromethane (~20 mL). The final product was dried at 65 ˚C

for 4 hrs and stored in a desiccator for future uses. The purity of the Fe(VI) was determined as described in *section A2* below.

Fe(VI) stock solution was freshly prepared in 10 mM borate buffer (pH 9) and used within 15 min of preparation to minimize Fe(VI) self-decay.

A2. Quantification of Fe(VI) purity

The purity of Fe(VI) in the K2FeO4 powder was determined by measuring a K_2FeO_4 powder and dissolving in 5 mM Na_2HPO_4/1 mM $Na_2B_4O_7$ solution (pH 9.25). The Fe(VI) concentration was determined using the absorbance at 510 nm. This purity of Fe(VI) is then determined as the ratio of calculated Fe(VI) concentration to the theoretical measured K_2FeO_4 powder concentration. The purity of Fe(VI) in the K_2FeO_4 was estimated at approximately 88%.

The purity of Fe(VI) in the Fe(VI)-coated sand was also evaluated. This was achieved by taking an aliquot of K_2FeO_4 slurry obtained prior to sand addition and freeze-drying it. The dry product obtained was then used as K_2FeO_4 powder for purity calculation and the Fe(VI) purity was estimated at 8-9%.

A3. Quantification methods of aqueous Fe species

Aqueous Fe(VI) was measured using the ABTS colorimetric method.[139] Fe(VI) samples were reacted with 1.82 mM ABTS buffered at pH 4.2 with a 0.6 M acetate, 0.2 M phosphate buffer.[139] The absorbance of the mixture was determined at 415 nm and used to calculate Fe(VI) concentration.

Aqueous total Fe was determined using inductively coupled plasma – optical emission spectrophotometer (ICP-OES). Samples taken throughout the study for total Fe analysis were either in a buffer (i.e., 10 mM borate or phosphate) or in a 1% HNO_3 solution. The buffered samples were acidified with 1% HNO_3 before analysis. An internal standard solution of 100 µg/L

yttrium in 1% HNO_3 was added to all samples before analysis to normalize changes in Fe signals from the ICP-OES.

The measured aqueous Fe(II) concentration was determined using the colorimetric ferrozine method.[207] Samples taken during Fe leaching tests and organic compound removal experiments were reacted with 0.01 M ferrozine prepared in 0.1 M ammonium acetate. The absorbance of the mixture was measured at 562 nm. Fe(III) can also react with ferrozine to form the Fe-ferrozine complex with absorbance at 562 nm,[207, 208] thus the samples were further reduced by addition of 1.4 M hydroxylamine hydrochloride in 2 M HCl,[207] and buffered at pH 9.5 with 10 M ammonium acetate[207] for accurate analysis of Fe(II).

The aqueous Fe(III) concentration was determined using the colorimetric KSCN method. Fe(III) reacts with KSC to form a ferric thiocyanate complex.[157] Samples taken during Fe leaching tests and organic compound removal experiments were reacted with 0.2 M KSCN and measured at 476 nm with the UV-Vis spectrophotometer.

A4. Choice of buffer

The influence of buffering ions on the oxidation of PMSO by Fe(VI)-coated sand was investigated using 10 mM Na_2HPO_4/NaH_2PO_4 and 10 mM $Na_2B_4O_7$ buffers at pH 9. A dose of 2 g/L Fe(VI)-coated sand was added to the buffer solutions containing PMSO (700-740 µg/L) and the mixture was reacted for 1 hr. A 2 mL aliquot was taken at different sampling times and quenched with 20 µL of 500 mM Na_2SO_3 then filtered with 0.2µm, 25 mm diameter cellulose acetate (CA) syringe filters to measure residual PMSO and $PMSO_2$ using high performance liquid chromatography (HPLC) methods.

A5. HPLC Method

The concentrations of phenol, PMSO and $PMSO_2$ were quantified using a Dionex Ultimate 3000 HPLC equipped with a diode array detector and an Ascentis® C18 column (2.1 mm x 15 cm, 3 µm). The mobile phase was 0.1% formic acid in water (A) and acetonitrile (B). The compounds were separated in an isocratic mode of elution at 75% of 0.1% formic acid in water and 25% acetonitrile. The injection volume was 50 µL and the flow rate was 0.2 mL/min. The wavelength for each compound is given below.

Table A1. Wavelengths used for HPLC analysis of organic compounds.

Compounds	Wavelength (nm)	Retention time (min)
Phenol	271	8.99±0.12
PMSO	230	4.46±0.01
$PMSO_2$	265	7.64±0.08

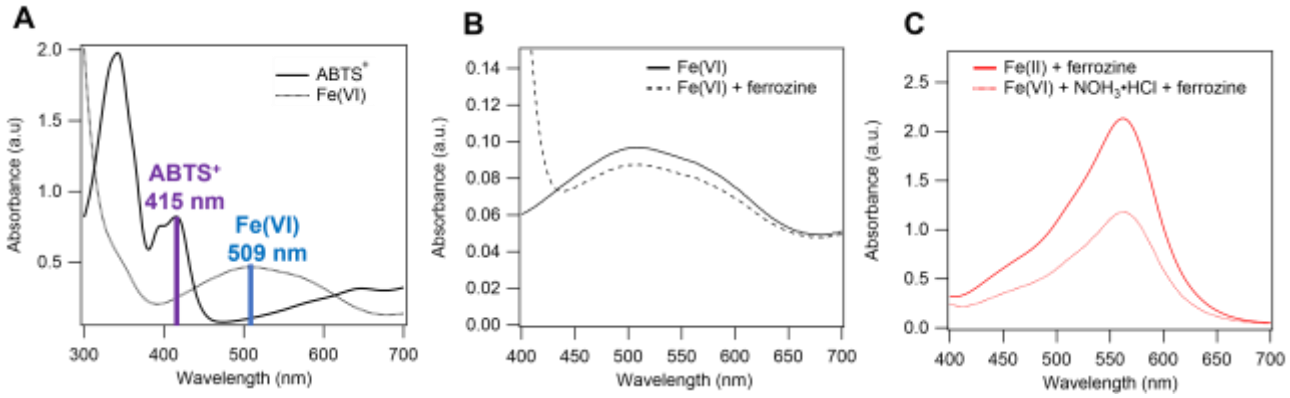

Figure A.1. Spectroscopic characterization of the Fe(VI)-coated sand. (**A**) UV-vis absorbance spectra of Fe(VI) leached from the Fe(VI)-coated sand (dashed line) and reacted with ABTS (solid line). (**B**) UV-vis absorbance of Fe(VI) leached from the media (solid line) and reacted with ferrozine (dashed line). (**C**) UV-vis absorbance of Fe-ferrozine complex formed with Fe(II) chloride (straight line) and with reduction of Fe(VI) (dashed line).

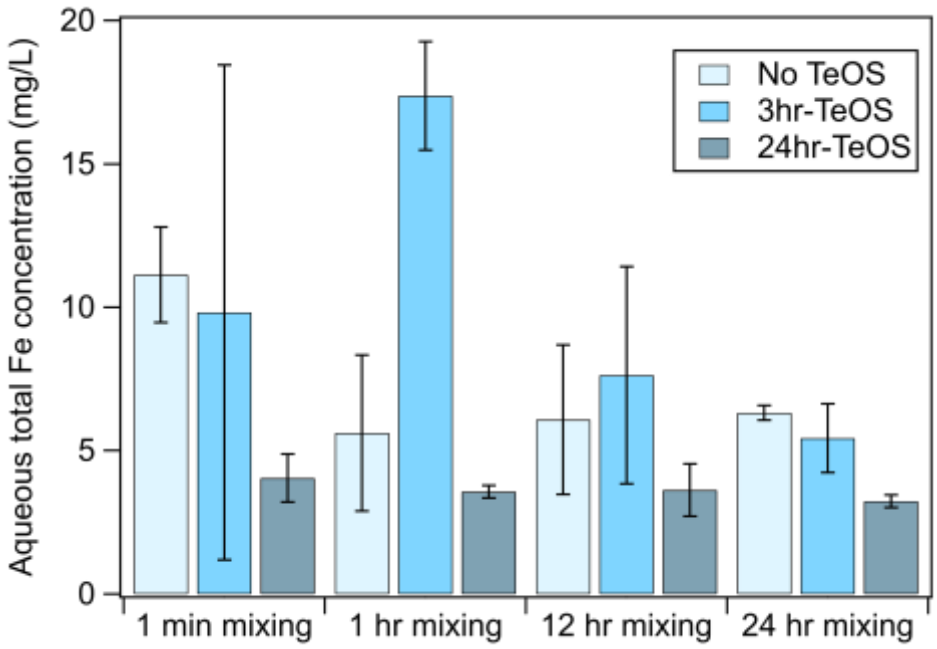

Figure A2. Total aqueous Fe concentration after 1 g/L Fe(VI)-coated sand was stirred in 1% HNO_3 for 1 min, 1 hr, 12 hrs and 24 hrs. The Fe(VI)-coated sand was prepared with virgin sand (no TeOS), 3hr-TeOS sand, and 24hr-TeOS sand.

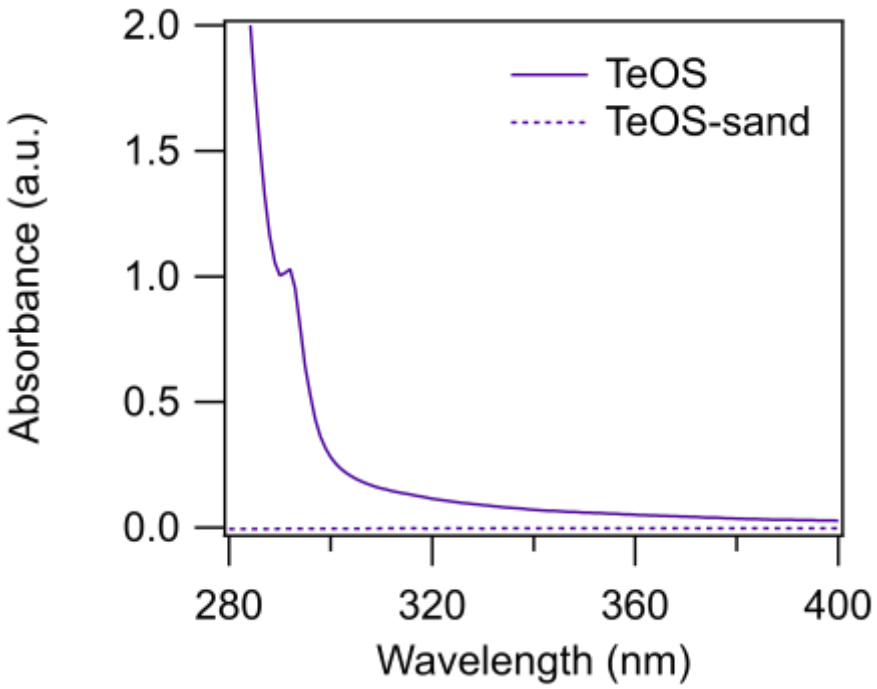

Figure A3. Spectroscopic analysis of TeOS stability on TeOS-coated sand. The UV-Vis spectrum of the supernatant of 1 g/L TeOS-coated sand (dashed line) placed in 10 mM borate buffer and sonicated was compared to the UV-Vis spectrum of TeOS (4 mL solution). The absence of a peak at 292 nm in the spectrum of the TeOS-sand indicates that TeOS did not leach from the TeOS-coated

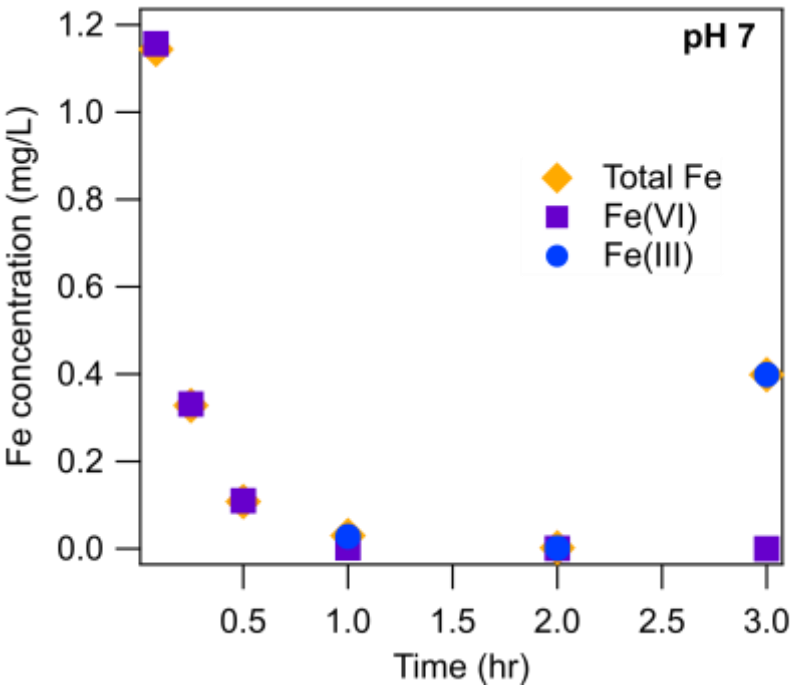

Figure A4. Kinetics of Fe(VI), Fe(III) and total Fe leached from 1 g/L Fe(VI)-coated sand into a 10 mM $Na_2B_4O_7$ solution at pH 7 as a function of time. Total Fe refers to the total Fe leached into solution at a given time.

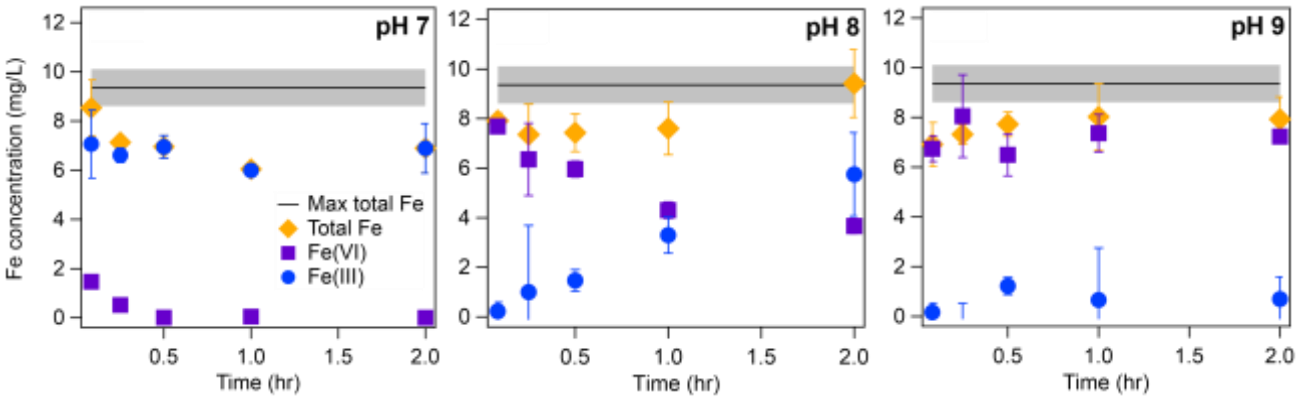

Figure A5. Decay kinetics of aqueous Fe(VI) from 1 g/L Fe(VI)-coated sand in a 10 mM 10 mM $Na_2B_4O_7$ at pH 7, 8, and 9. r^2 denotes the correlation coefficient of the fitted linear regression curve.

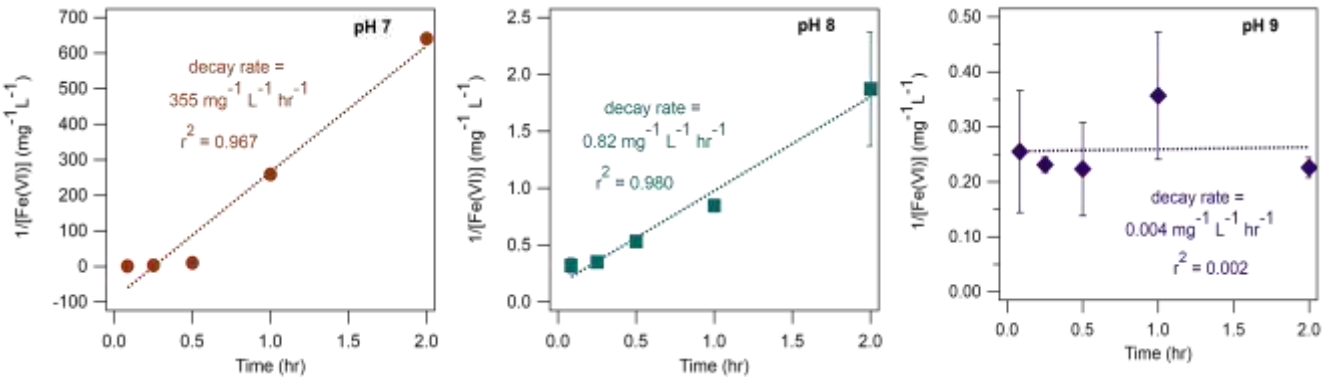

Figure A6. Kinetics of Fe(VI), Fe(III) and total Fe leached from 1 g/L Fe(VI)-coated sand with 3hr-TeOS sand modification into a 10 mM Na_2HPO_4/NaH_2PO_4 solution at pH 7, 8, 9 as a function of time. Max total Fe refers to the maximum mass of Fe that would leach of the surface of Fe(VI)-coated sand. This was determined by mixing 1 g/L Fe(VI)-coated sand into 1% HNO_3 and measuring total Fe in solution. Total Fe refers to the total Fe leached into solution at a given time.

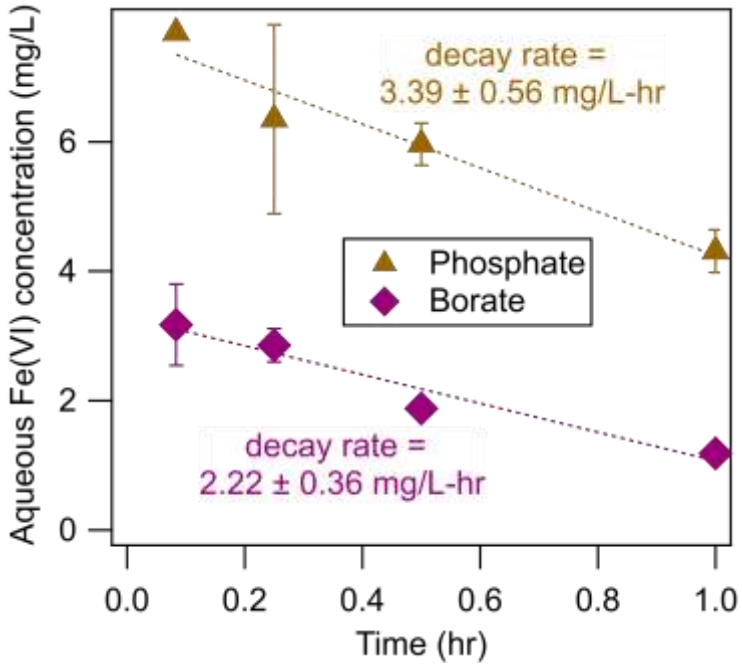

Figure A7. Aqueous Fe(VI) concentration leached from 1 g/L Fe(VI)-coated sand in a 10 mM Na_2HPO_4/NaH_2PO_4 and 10 mM $Na_2B_4O_7$ solution at pH 8.

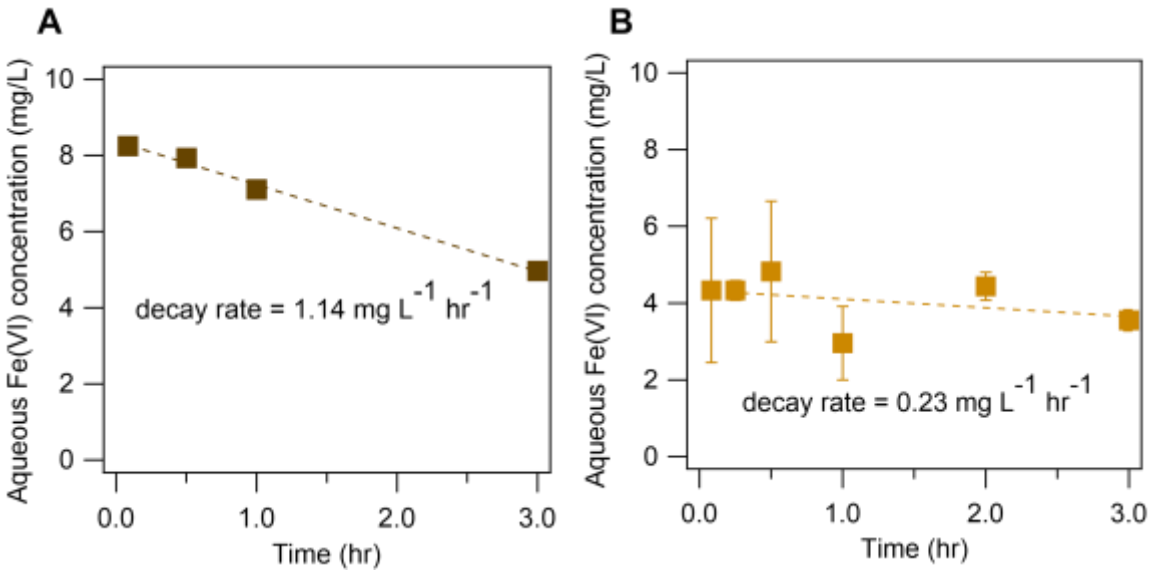

Figure A8. Decay of Fe(VI) in (A) 0.21 g/L K_2FeO_4 powder and (B) 1 g/L Fe(VI)-coated sand. The 0.21 g/L initial concentration of K_2FeO_4 was chosen to obtain a concentration of Fe(VI) that will be equivalent to the concentration of total Fe in the Fe(VI)-coated sand system.

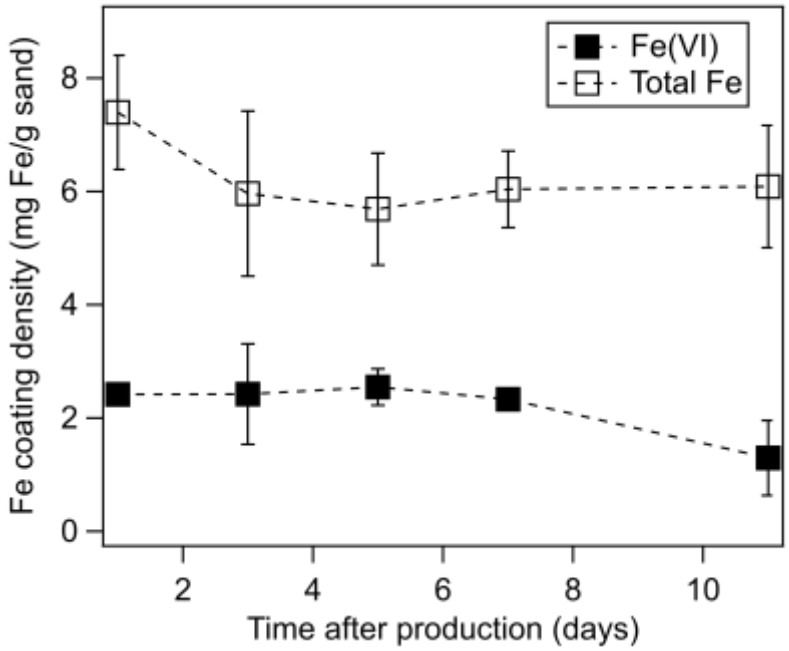

Figure A9. Total Fe and Fe(VI) coating mass leached from Fe(VI)-coated sand surface as a function of time. 3 g/L Fe(VI)-coated sand was mixed with 1% HNO_3 for the total Fe measurement. For the Fe(VI) coating mass determination, 3 g/L Fe(VI)-coated sand was mixed with 5 mM Na_2HPO_4/1mM NaB_4O_7 buffer.

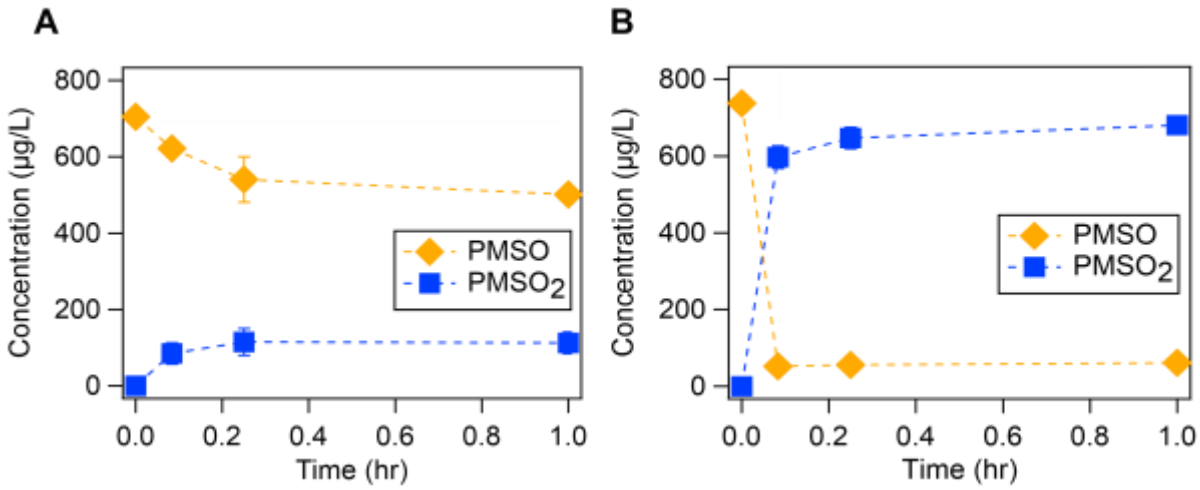

Figure A10. Oxidation of PMSO to $PMSO_2$ by 2 g/L Fe(VI)-coated sand in (**A**) 10 mM phosphate buffer and (**B**) 10 mM borate buffer at pH 9. The initial PMSO concentration was 705±20 µg/L PMSO in the phosphate buffer and 738±14 µg/L PMSO in the borate buffer.

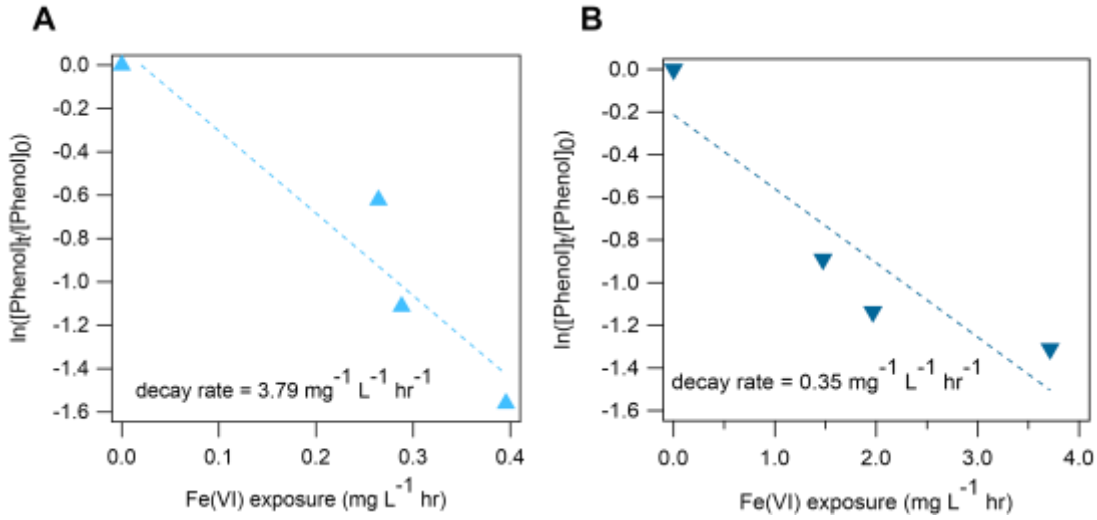

Figure A11. Linear fitting of the reaction kinetics of 219±12 µg/L phenol and (**A**) 12.6 mg/L Fe(VI) powder and (**B**) 2 g/L Fe(VI)-coated sand in 10 mM borate buffer pH 9.

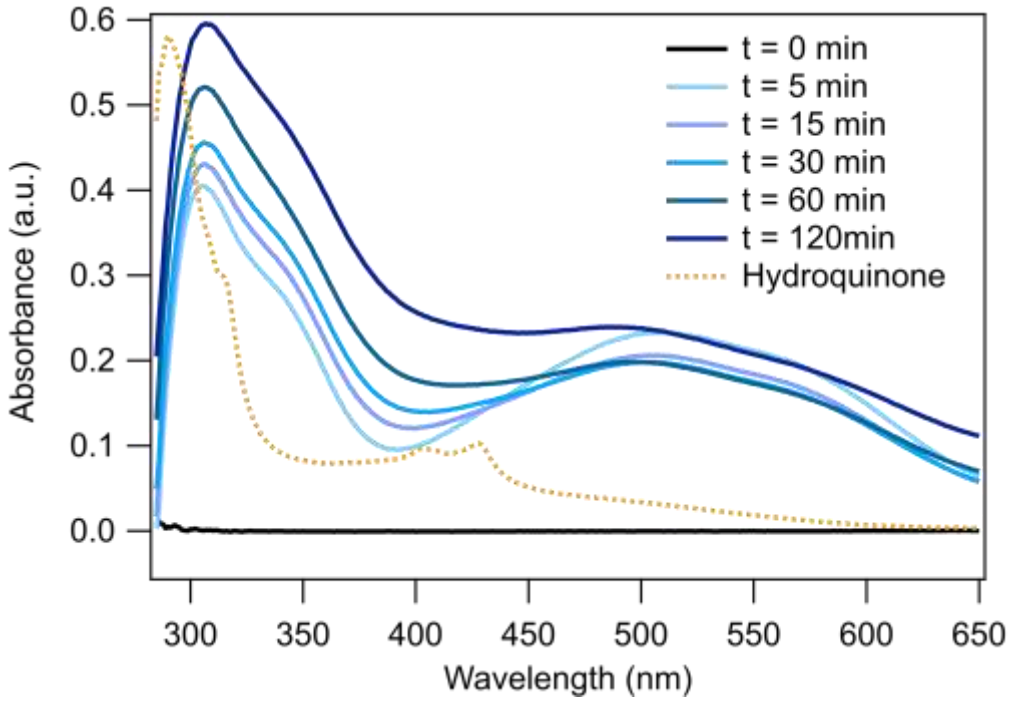

Figure A12. UV-Vis scans of 219±12 µg/L phenol reacted with 2 g/L Fe(VI)-coated sand in 10 mM borate buffer pH 9 measured at various time intervals within the 120-min and a hydroquinone blank solution.

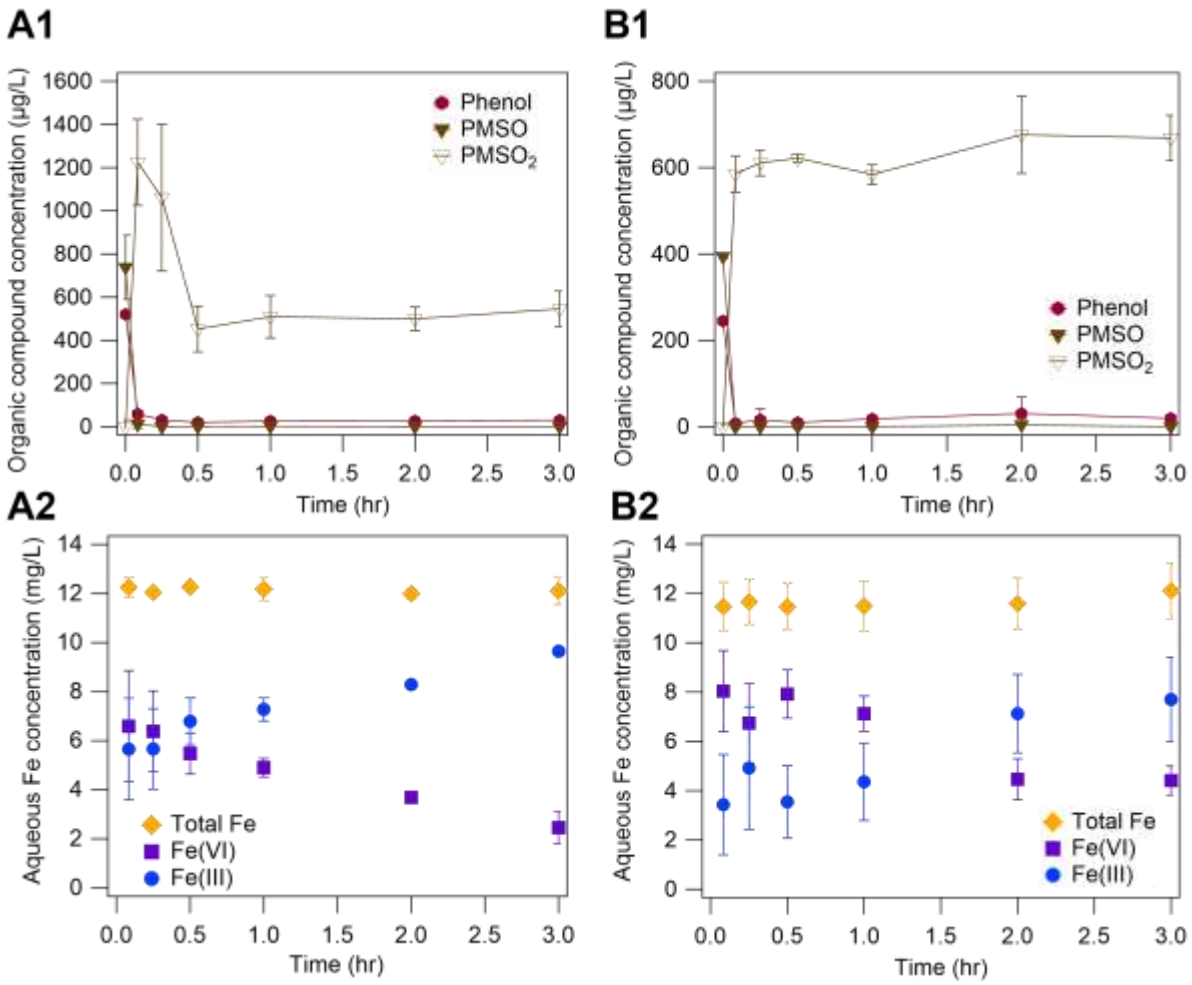

Figure A13. (**Row 1**) Degradation of phenol and oxidation of PMSO at different concentrations **A**. 520±8.1 µg/L phenol and 739±148 µg/L PMSO; **B**. 245±3.0 µg/L phenol and 394±4.7 µg/L PMSO) by 2 g/L Fe(VI)-coated sand and (**row 2**) the corresponding changes in aqueous Fe concentrations.

Appendix B. Supporting Information for Chapter 3

B1. Chemicals and materials

All chemicals were ACS grade and higher unless stated otherwise. Calcium hypochlorite ($Ca(OCl)_2$), ferric nitrate nonahydrate ($Fe(NO_3)_3 \cdot 9\ H_2O$), and potassium hydroxide (KOH) were purchased from Fisher Scientific (Waltham, MA) and used in the synthesis of potassium ferrate (K_2FeO_4). The Ottawa sand composite substrate was purchased from VWR (Radnor, PA). Tetraethyl orthosilicate (TeOS, Sigma Aldrich, MO) and nitric acid (HNO_3, Fisher Scientific, MA) were used in the modification of the sand prior to Fe(VI) coating as reported in Okaikue-Woodi and Ray.[169]

Trace metals grade HNO_3 was purchased from Fisher Scientific for total Fe measurements. Sodium tetraborate anhydrous ($Na_2B_4O_7$, Across Organics, Belgium), sodium phosphate dibasic heptahydrate ($Na_2HPO_4 \cdot 7H_2O$, VWR, PA), sodium phosphate monobasic monohydrate ($NaH_2PO_4 \cdot H_2O$, VWR, PA), acetic acid (Fisher Scientific, MA), sodium hydroxide (NaOH, Fisher Scientific, MA), and hydrochloric acid (HCl, Sigma Aldrich, MO) were used to prepare buffer solutions. 2,2'-azinobis-(3-ehtylbenzothiazoline-6-sulfonate) (ABTS) was purchased from Sigma Aldrich for colorimetric measurements of aqueous Fe(VI). High performance liquid chromatography (HPLC) grade formic acid (Agilent Technologies, CA), methanol (Fisher Scientific, MA) and water (Fisher Scientific, MA) were used for HPLC analyses. Optima™ liquid chromatography mass spectrometry (LCMS) grade methanol (Fisher Scientific, MA) was used for the high-resolution mass spectrometry analyses (HRMS).

Synthetic wastewater effluent solution was made using sodium bicarbonate ($NaHCO_3$, Fisher Chemical, MA), sodium chloride (NaCl, VWR, PA), sodium phosphate dibasic heptahydrate ($Na_2HPO_4 \cdot 7H_2O$, Fisher Chemical MA), magnesium chloride hexahydrate

($MgCl_2 \cdot 6H_2O$), magnesium nitrate hexahydrate ($Mg(NO_3)_2 \cdot 6H_2O$, Thermo Scientific, MA) calcium chloride dihydrate ($CaCl_2 \cdot 2H_2O$, Sigma Aldrich, MO), and calcium nitrate tetrahydrate ($Ca(NO_3)_2 \cdot 4H_2O$, Thermo Scientific, MA).

B2. HPLC Method

The concentrations of acetaminophen (ACM), benzotriazole (BZT), and sulfamethoxazole (SMX) were quantified using a Dionex Ultimate 3000 HPLC equipped with a diode array detector and an Ascentis® C18 column (2.1 mm x 15 cm, 3 µm). The mobile phase was 0.1% formic acid in water (A) and methanol (B). The compounds were separated in an isocratic method of elution at 81% of 0.1% formic acid in water, and 19% methanol. The injection volume was 50 µL and the flow rate was 0.2 mL/min. The wavelength for each compound is reported in **Table B1** below.

Table B1. Wavelengths used for HPLC analysis of organic compounds.

Compounds	Wavelength (nm)	Retention time (min)
ACM	244	6.19±0.03
BZT	260	18.0±0.09
SMX	266	22.0±0.13

B3. HRMS Method and Data Processing

The oxidation products of acetaminophen, benzotriazole and sulfamethoxazole were determined using an Agilent 1290 Infinity ultrahigh performance liquid chromatograph (UHPLC) coupled to an Agilent 6546 quadrupole time-of-flight high-resolution mass spectrometer (QTOF-HRMS; Santa Clara, CA, USA). A reverse-phase C18 column (Agilent ZORBAX Eclipse Plus 2.1×100 mm, 1.8 µm) with a C18 guard column (2.1×5 mm, 1.8 µm) was used for the UHPLC separation at 45 ºC with 5 µL injection volume (infused with 1 µL QTOF

internal standard during injection for QA/QC purpose) and a flow rate of 0.4 mL/min. The compounds were separated using a gradient elution with mobile phases of 0.1% formic acid in each of deionized water (A) and methanol (B) as follows: 5% B at 0-1 min, 50% B at 4 min, 100% B at 17-20 min, 5% B at 20.1 min; stop time 22.5 min; post-time 2 min. The flow rate was 0.4 mL/min. Full scan data were acquired under 10 GHz Extended Dynamic Range mode at a range of 100-1700 m/z.

The data analysis was initiated by isolating features with retention time between 2–18 min, mass-to-charge ratio (m/z) < 900 Da, and signal to noise (S/N) ratio greater than 10. Then, features for which the peak area was greater than 10,000 after reaction between the trace organics and the media were retained. The following condition was then set to further reduce the data: the average peak area in the control samples (time = 0 min) must be five times less than the average peak area in the samples taken after 5 min or 15 min or 30 min or 1 hour of reaction. The combination of features that fit this rule was further reduced by isolating features with peak area greater than 100,000 after 2 hours of reaction with the media. Then, features with relative standard deviation (RSD) greater than 50% at all time points were removed. Finally, the remaining features were checked manually to ensure that the peak area in the reaction samples were greater than the peak area in the control samples and the solvent (methanol) blanks. These exclusion criteria were set to eliminate artifacts from the dataset and to prioritize viable m/z values with peak area that showed significant increase from the control samples to the reacted samples. Replicate features with the same m/z values were eliminated by retaining the feature with the highest peak area. The final features are reported in **Tables B5-7** added as additional supporting information.

Table B2A. Trace metals speciation at pH 9 as calculated using Visual MINTEQ. Only species with abundance > 1% are reported.

	Speciation	**% abundance**
Cu	$Cu(OH)_2$ (aq)	57.1
	$CuOH^+$	31.0
	$Cu_3(OH)_4^{2+}$	6.3
	$Cu_2(OH)_2^{2+}$	2.29
	$Cu(OH)_3^-$	2.23
Pb	$PbOH^+$	73.5
	$Pb(OH)_2$ (aq)	23.3
	Pb^{2+}	2.95
Zn	$Zn(OH)_2$ (aq)	86.0
	$ZnOH^+$	6.82
	Zn^{2+}	6.87

Table S2B. Oversaturated mineral phases at pH 9 and their saturation index as calculated using Visual MINTEQ

Mineral	**Saturation index**
$Cu(OH)_2(s)$	1.27
$Pb(OH)_2(s)$	2.57
CuO (amorphous)	2.07
CuO (colloidal)	2.92
ZnO	0.16

Table B3A. Trace metals speciation at pH 7.5 as calculated using Visual MINTEQ. Only species with abundance > 1% are reported**.**

	Speciation	**% abundance**
Cu	Cu^{2+}	46.1
	$CuOH^{+}$	45.6
	$Cu_2(OH)_2^{2+}$	4.96
	$Cu(OH)_2$ (aq)	2.65
Pb	Pb^{2+}	55.7
	$PbOH^{+}$	43.8
Zn	Zn^{2+}	95.8
	$ZnOH^{+}$	3.0
	$Zn(OH)_2$ (aq)	1.20

Table B3B. Oversaturated mineral phases at pH 7.5 and their saturation index as calculated using Visual MINTEQ

Mineral	**Saturation index**
$Pb(OH)_2$ (s)	0.84
CuO (amorphous)	0.73
CuO (colloidal)	1.58

Table B4. Composition of synthetic wastewater effluent solution used in this study

Component	**Concentration**	**Unit**
Ca^{2+}	26	
Mg^{2+}	13	
Na^{+}	58.8	mg/L
Cl^{-}	100	
HCO_3^{-}	70	

NO_3^-	10
PO_4^{3-}	0.3
pH	8.0±0.1

Table B5 (not shown). All prioritized TPs from oxidation of organics by Fe(VI)-coated sand at pH 9 in absence of trace metals. This table is contained in the associated Microsoft Excel® spreadsheet.

Table B6 (not shown). All prioritized TPs from oxidation of organics by Fe(VI)-coated sand at pH 9 in presence of trace metals. This table is contained in the associated Microsoft Excel® spreadsheet.

Table B7 (not shown). All prioritized TPs from oxidation of organics by Fe(VI)-coated sand at pH 7.5 in presence of trace metals. This table is contained in the associated Microsoft Excel® spreadsheet.

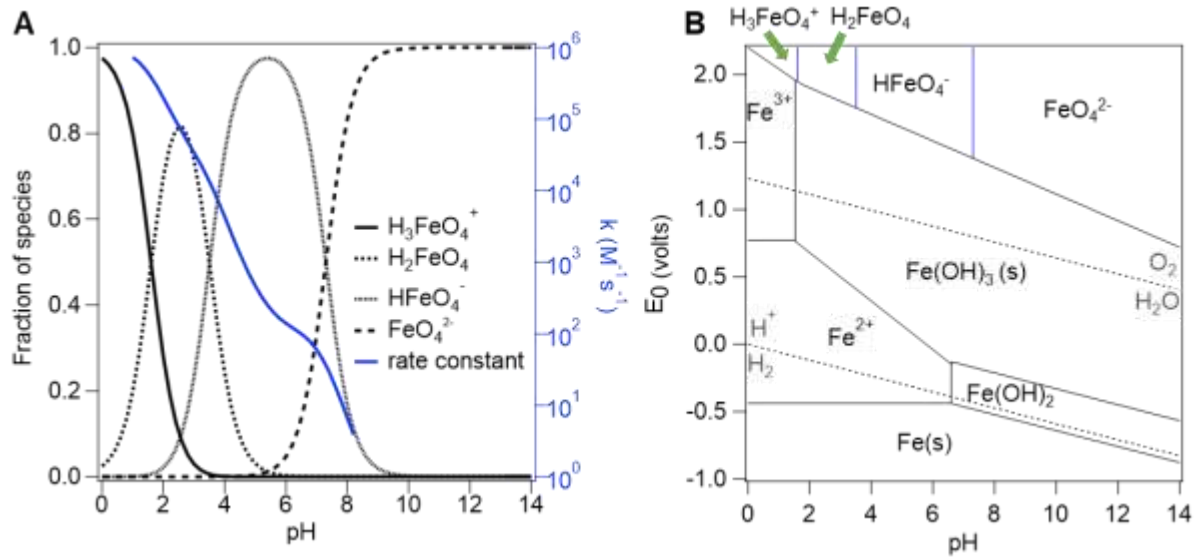

Figure B1. (**A**) Speciation of Fe(VI) (left axis, black lines) and aqueous Fe(VI) self-decay rate (right axis, blue line) as a function of pH. (**B**) Distribution of the standard potential of iron species including Fe(VI) species. The pKa values: $H_3FeO_4^+$ (pKa = 1.6); H_2FeO_4 (pKa = 3.5); $HFeO_4^-$ (pKa = 7.3) were obtained from Rush et al.[116] and decay rate constants from Lee et al.[126] Data for the standard potentials was obtained from Pogliani et al.[209] and Wulfsberg.[210]

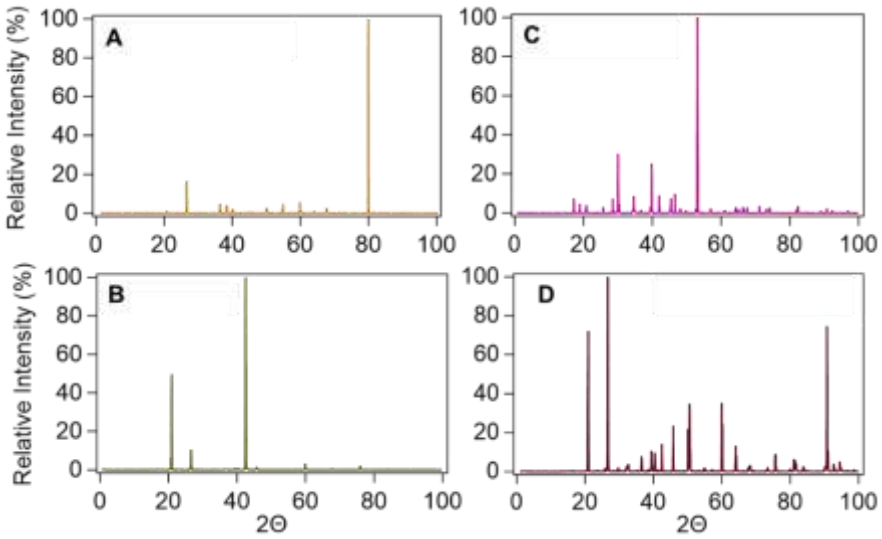

Figure B2. XRD measurements of (**A**) noncoated Ottawa sand, (**B**) TeOS-sand, (**C**) Fe(VI) powder and (**D**) Fe(VI)-coated sand

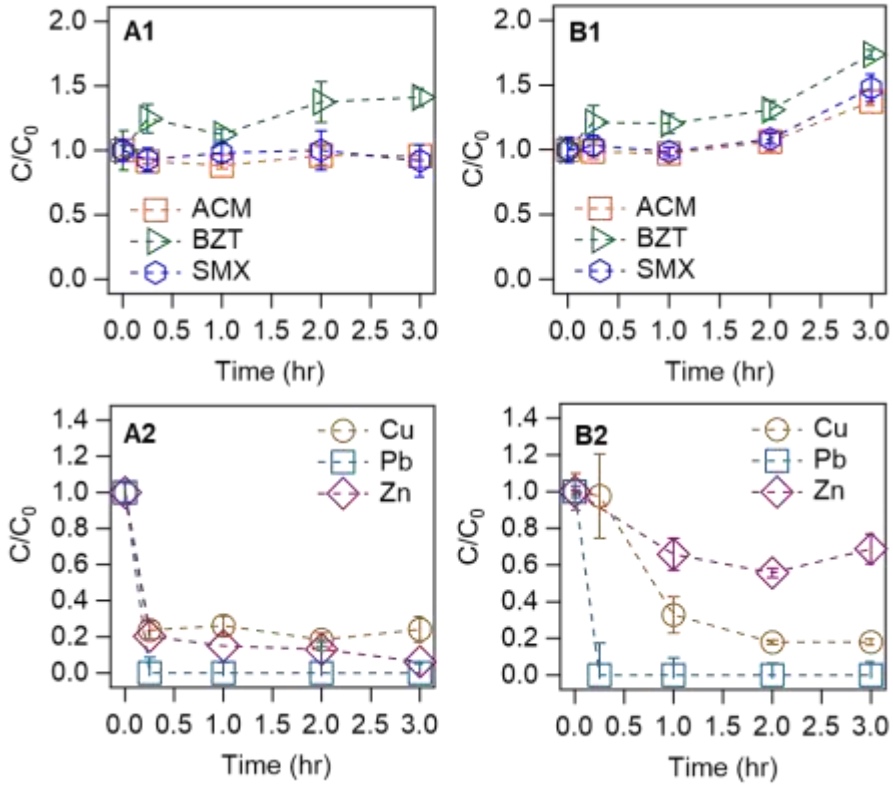

Figure B3. Normalized removal of nominally 500 µg/L trace organics (top) and trace metals (bottom) by 26±1.8 mg/L $Fe(NO_3)_3$ in the (**A**) **MO9 system** and (**B**) **MO7.5 system.**

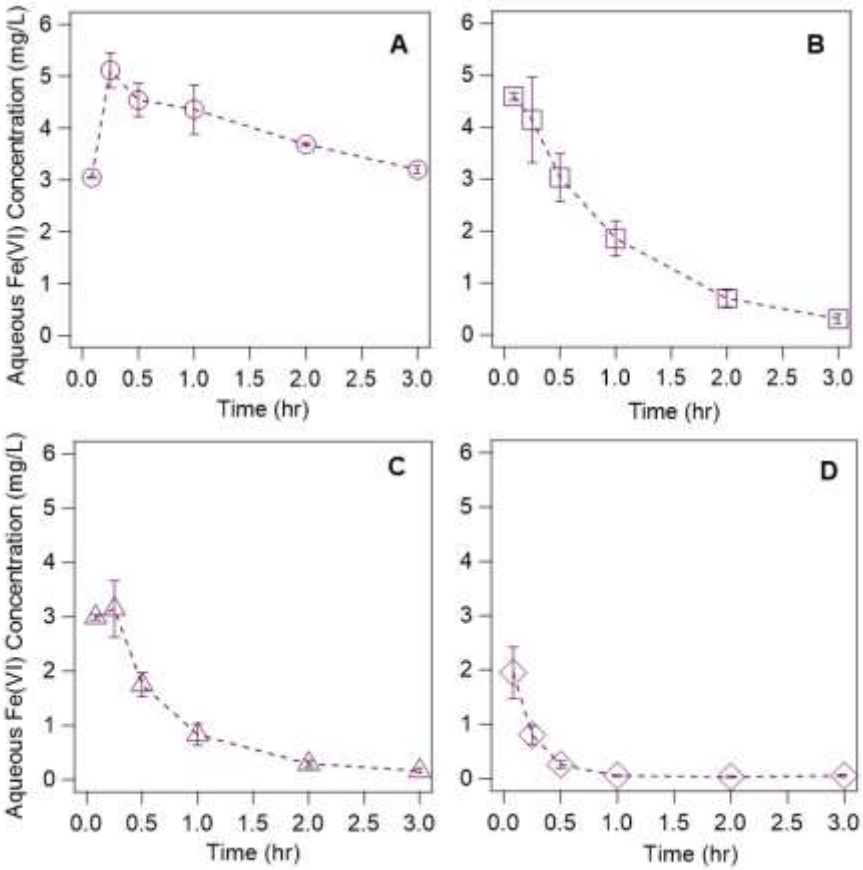

Figure B4. Changes in aqueous Fe(VI) concentrations during reaction in the (**A**) **M9 system**; (**B**) **O9 system**; (**C**) **MO9 system**; and the (**D**) **MO7.5 system**. The nominal concentration for each contaminant is 500 μg/L.

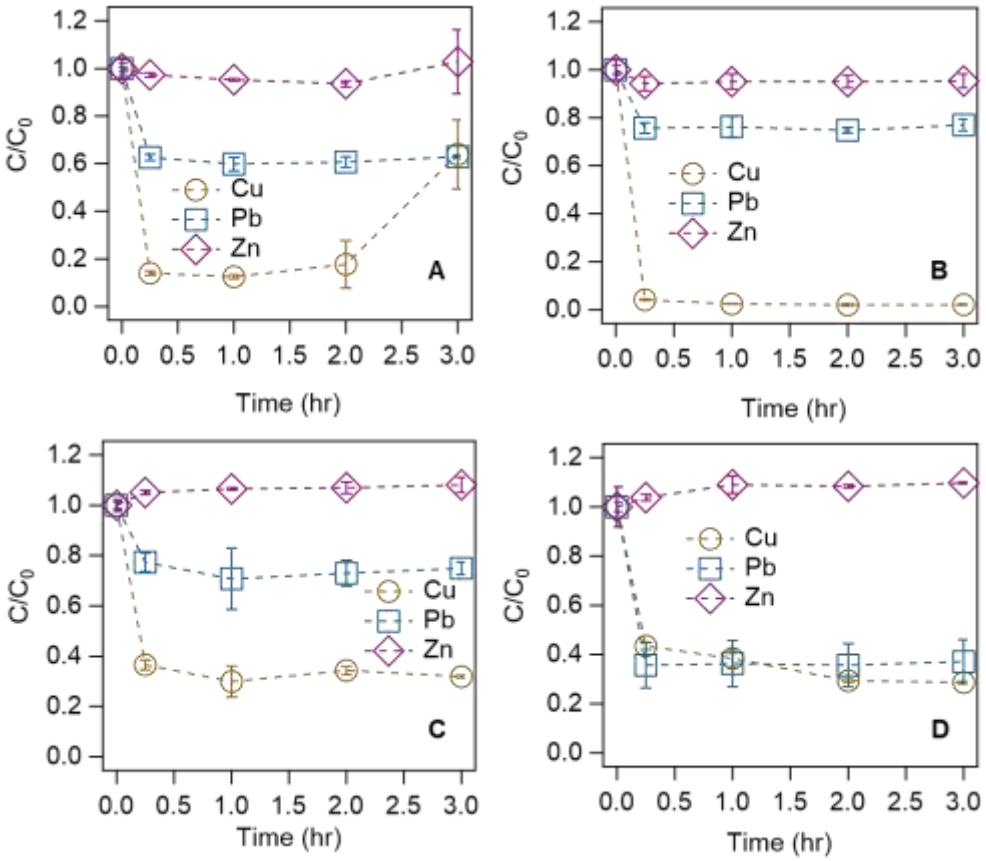

Figure B5. Results showing normalized loss of Cu, Pb, and Zn (i.e., control experiments with no media present) with (**A**) nominally 500 µg/L Cu, Pb, and Zn in 10 mM sodium borate buffer at pH 9; (**B**) nominally 500 µg/L Cu, Pb, and Zn in 10 mM sodium borate buffer at pH 9 in the presence of select trace organics (**C**) nominally 500 µg/L Cu, Pb, and Zn in 10 mM sodium borate buffer at pH 7.5 in the presence of select trace organics and (**D**) nominally 500 µg/L Cu, Pb, and Zn in the synthetic wastewater effluent solution in the presence of select trace organics.

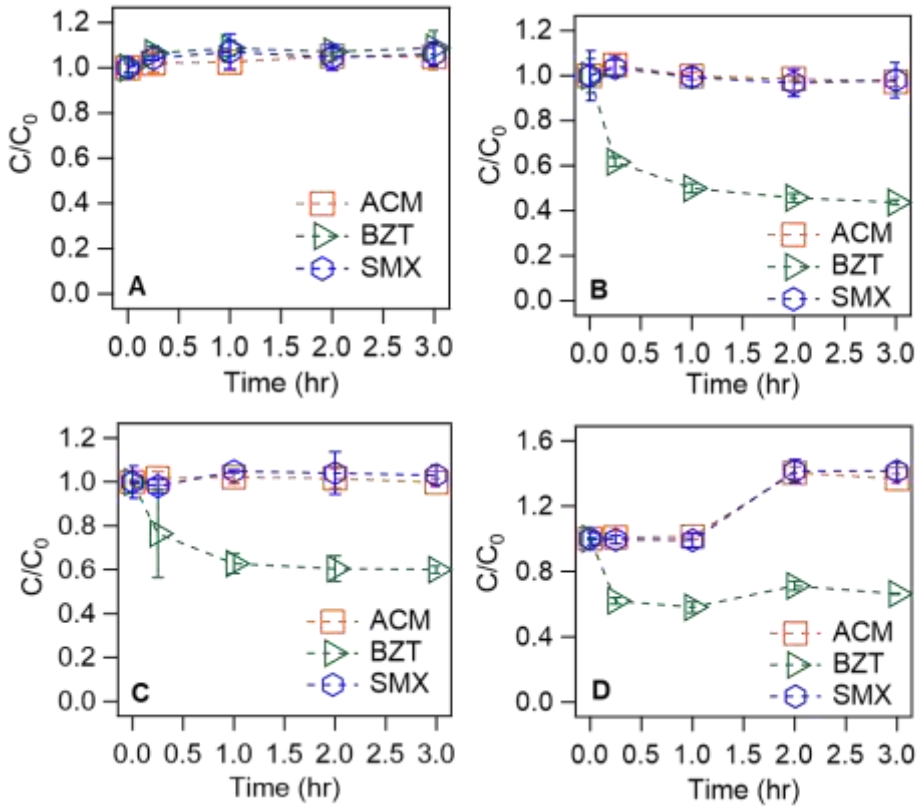

Figure B6: Results showing normalized loss ACM, BZT and SMX (i.e., control experiments with no media present) with (**A**) nominally 500 µg/L ACM, BZT, and SMX in 10 mM sodium borate buffer at pH 9; (**B**) nominally 500 µg/L ACM, BZT, and SMX in 10 mM sodium borate buffer at pH 9 in the presence of select trace metals (**C**) nominally 500 µg/L ACM, BZT, and SMX in 10 mM sodium borate buffer at pH 7.5 in the presence of select trace metals and (**D**) nominally 500 µg/L ACM, BZT, and SMX in the synthetic wastewater effluent solution in the presence of select trace metals.

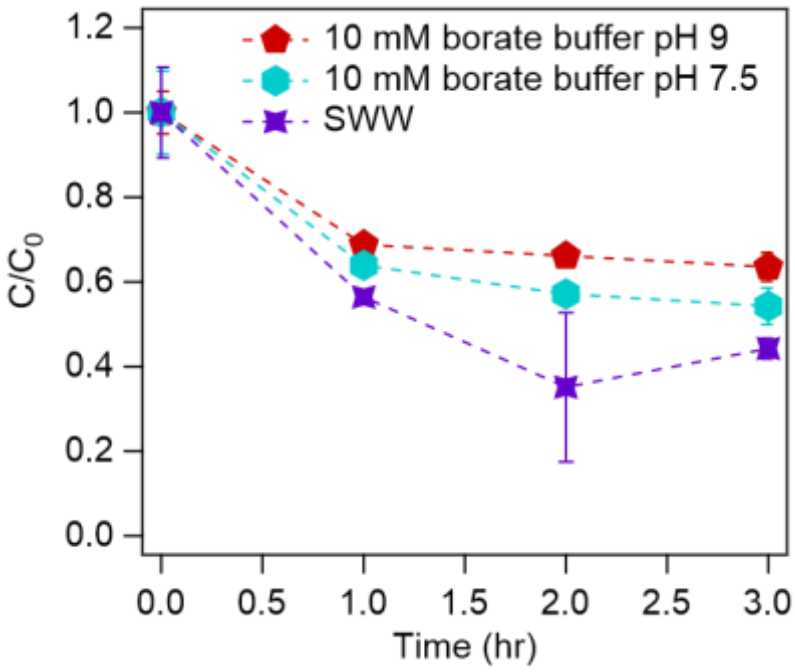

Figure B7. Control experiments (no media) with BZT and Cu under different experimental conditions. BZT initial concentrations were 427±21.4 µg/L in 10 mM $Na_2B_4O_7$ pH 9, 365±35.9 µg/L in 10 mM $Na_2B_4O_7$ pH 7.5, and 371±39.9 µg/L in the synthetic wastewater effluent (SWW) solution.

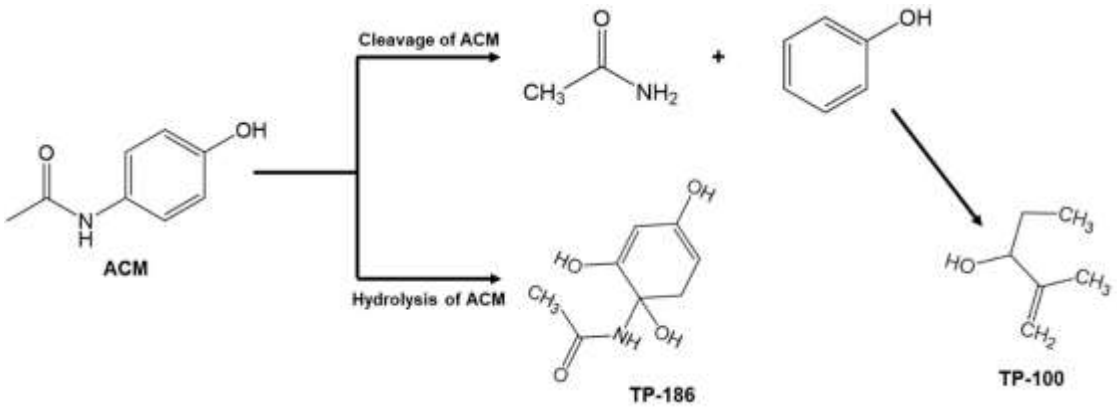

Figure B8. Possible oxidation pathways of ACM by the Fe(VI)-coated sand.

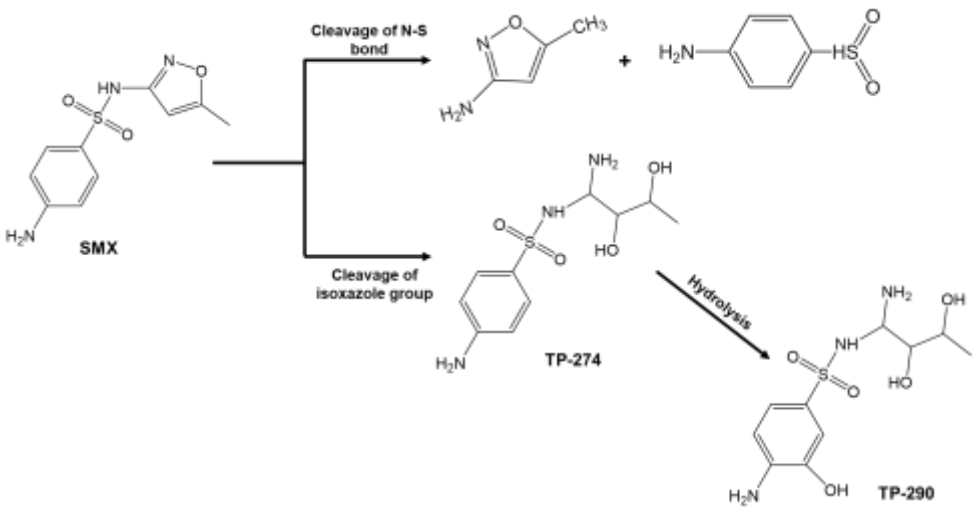

Figure B9. Possible oxidation pathways of SMX by the Fe(VI)-coated sand

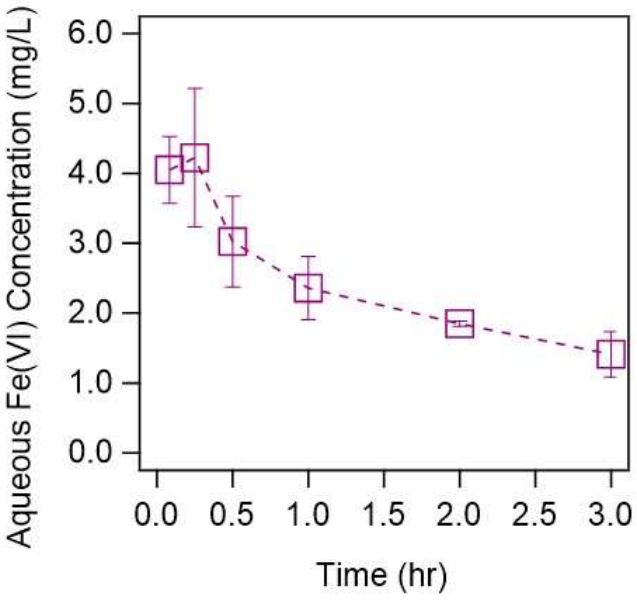

Figure B10. Changes in aqueous Fe(VI) concentrations during reaction with trace metals and trace organics at a nominal concentration of 500 μg/L in the synthetic wastewater effluent solution.

Appendix C. Supporting Information for Chapter 4

C1. HPLC Method

The concentrations of acetaminophen (ACM), phenol (PHE), and sulfamethoxazole (SMX) were quantified using a Dionex Ultimate 3000 HPLC equipped with a diode array detector and an Ascentis® C18 column (2.1 mm x 15 cm, 3 µm). The mobile phase was 0.1% formic acid (FA) in water (A) and 0.1% FA in methanol (MeOH) (B). The compounds were separated in an isocratic method of elution. The injection volume was 50 µL and the flow rate was 0.2 mL/min. The wavelength for each compound is reported in **Table C1** below.

Table C1. Wavelengths used for HPLC analysis of organic compounds.

Compounds	Solvent (FA in H2O:FA in MeOH, v/v)	Wavelength (nm)	Retention time (min)
ACM	80/20	244	5.76±0.04
PHE	70/30	271	10.6±0.01
SMX	70/30	268	8.11±0.03

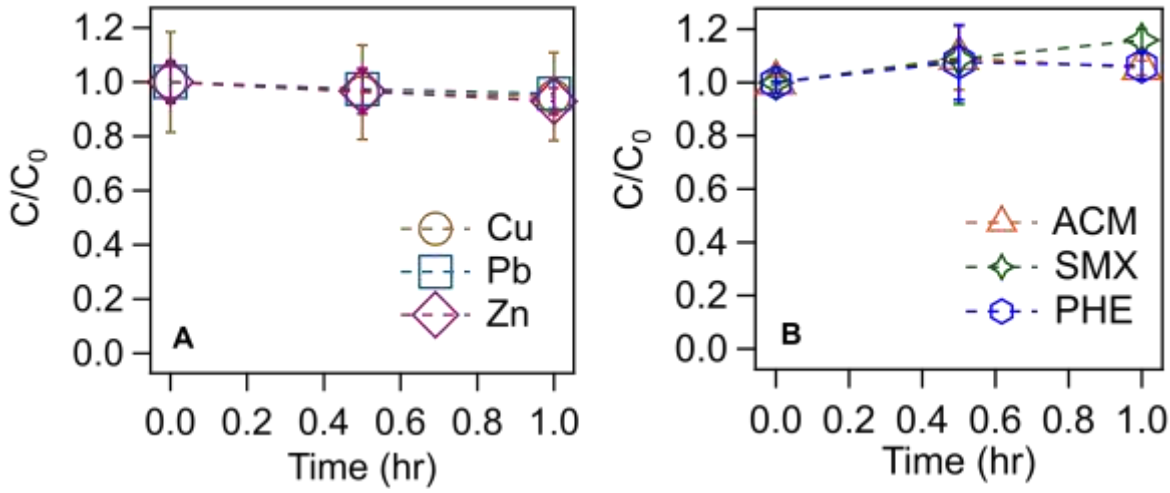

Figure C1. Results of control experiments with no media showing normalized loss of nominally 50 µg/L of (**A**) Cu, Pb, and Zn each and (**B**) ACM, PHE and SMX each in the synthetic wastewater effluent containing synthetic effluent organic matter.

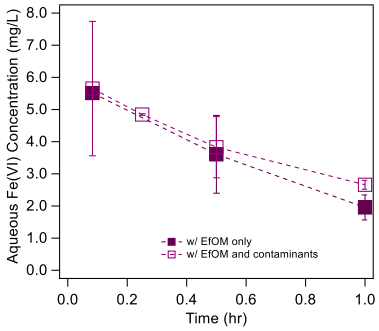

Figure C2. Changes in aqueous concentration of Fe(VI) in the synthetic wastewater effluent solution containing synthetic effluent organic matter with (open squares) and without (shaded squares) trace metals and trace organics. The error bars represent standard deviation.

Appendix D. Supporting Information for Chapter 5

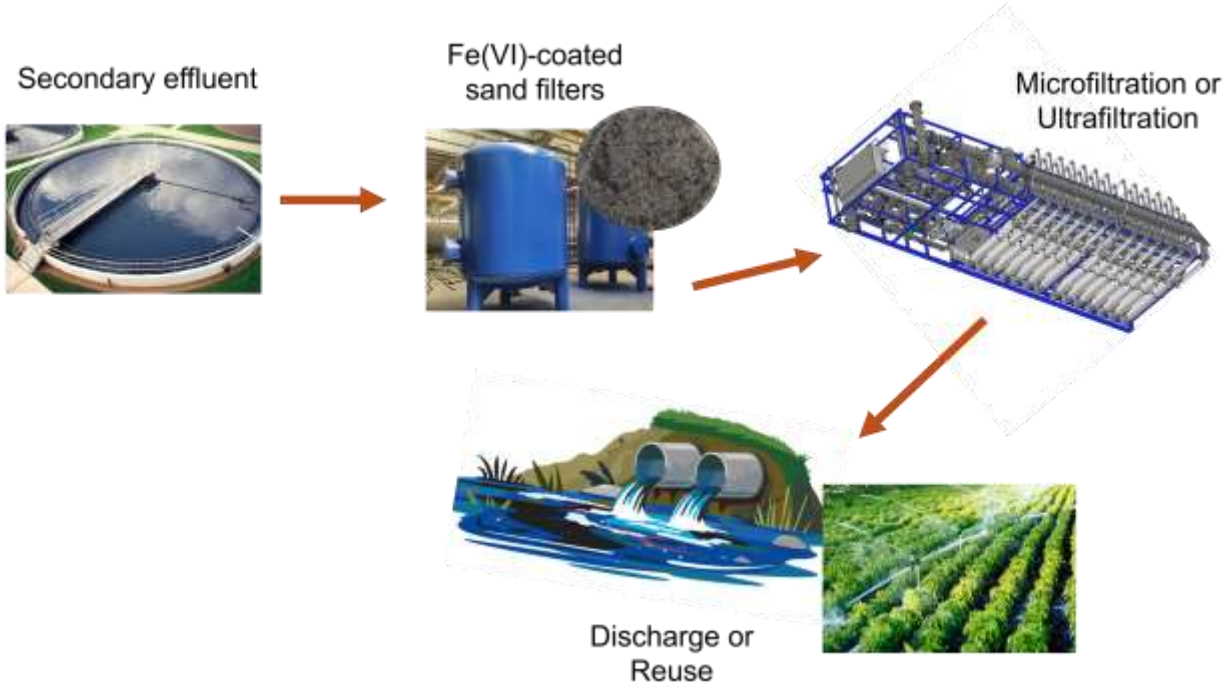

Figure D1. A proposed secondary wastewater effluent treatment train that employs Fe(VI)-coated sand.

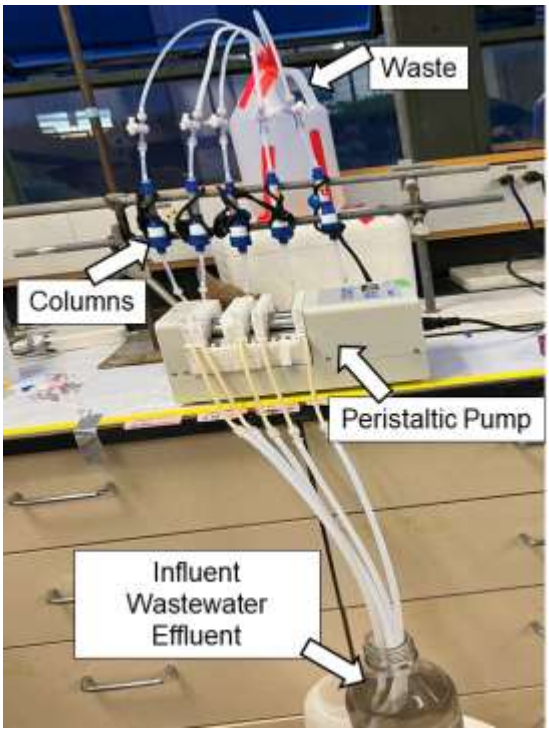

Figure D2. Column test set up

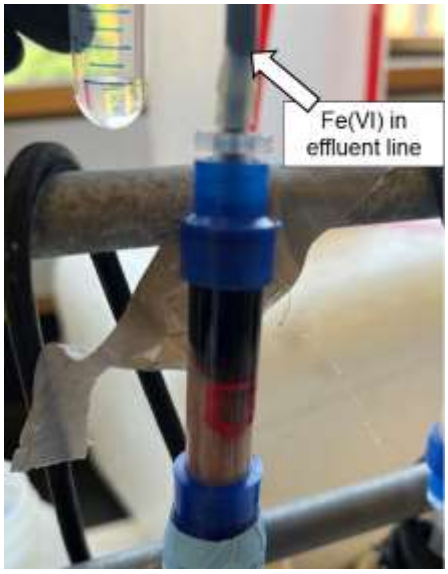

Figure D3. Image of the Fe(VI) leaching off the sand surface and exiting the column

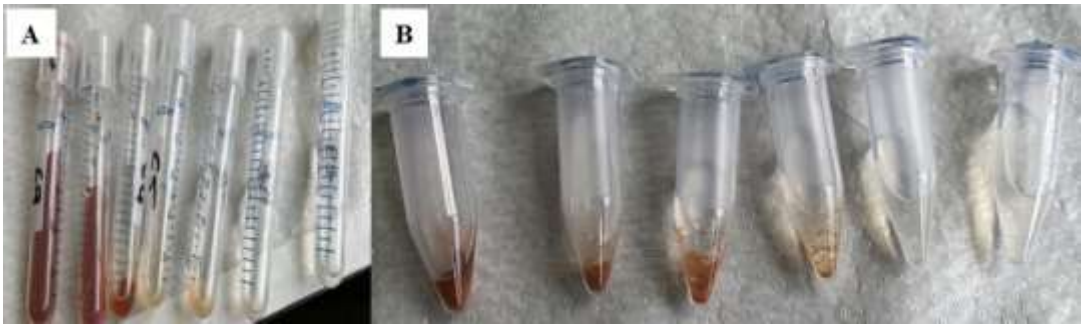

Figure D3. Image showing gradual decrease in Fe exiting the column with (**A**) 100 wt% Fe(VI)-coated and **(B**) 25 wt % Fe(VI)-coated sand

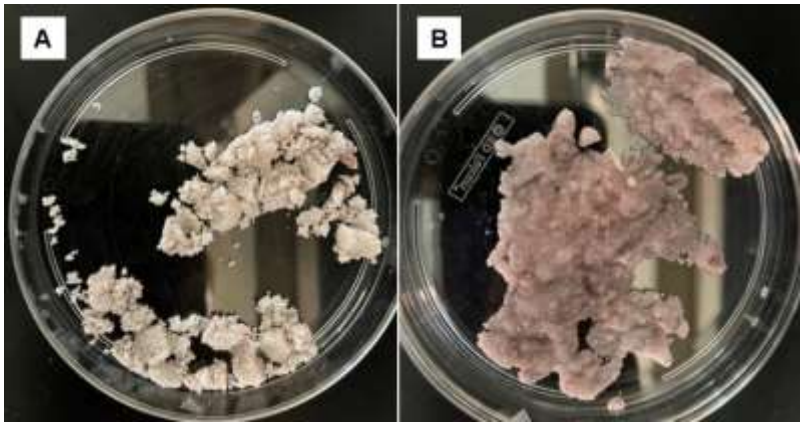

Figure D4. Regenerated Fe(VI)-coated sand via (**A**) method 1 and (**B**) method 2

Appendix E. A critical review of contaminant removal by conventional and emerging media for urban stormwater treatment in the United States

This appendix was previously published as: Okaikue-Woodi, F. E. K., Cherukumilli, K., Ray J. R. A critical review of contaminant removal by conventional and emerging media for urban stormwater treatment in the United States. *Water Res.* **2020**, 187, 116434. doi.org/10.1016/j.watres.2020.116434

ABSTRACT

Stormwater is a major component of the urban water cycle contributing to street flooding and high runoff volumes in urban areas, and elevated contaminant concentrations to receiving waters from contact with impervious surfaces. Engineers and city planners are investing in best management practices to reduce runoff volume and to potentially capture and use urban stormwater. However, these current approaches result in moderate to low contaminant removal efficiencies for certain classes of contaminants (e.g., particles, nutrients and some metals). This review describes options and opportunities to augment existing stormwater infrastructure with conventional and emerging reactive media to improve contaminant removal. This critical analysis characterizes media physicochemical properties and mechanisms contributing to contaminant removal, describes possible candidates for new engineered media, highlights lab and field studies investigating stormwater media contaminant removal, and identifies possible limitations and knowledge gaps in media implementation. Following this analysis, information is provided regarding factors that may contribute to or adversely impact urban stormwater treatment by media. The review closes with insights into additional research directions and important information necessary for safe and effective urban stormwater treatment using media.

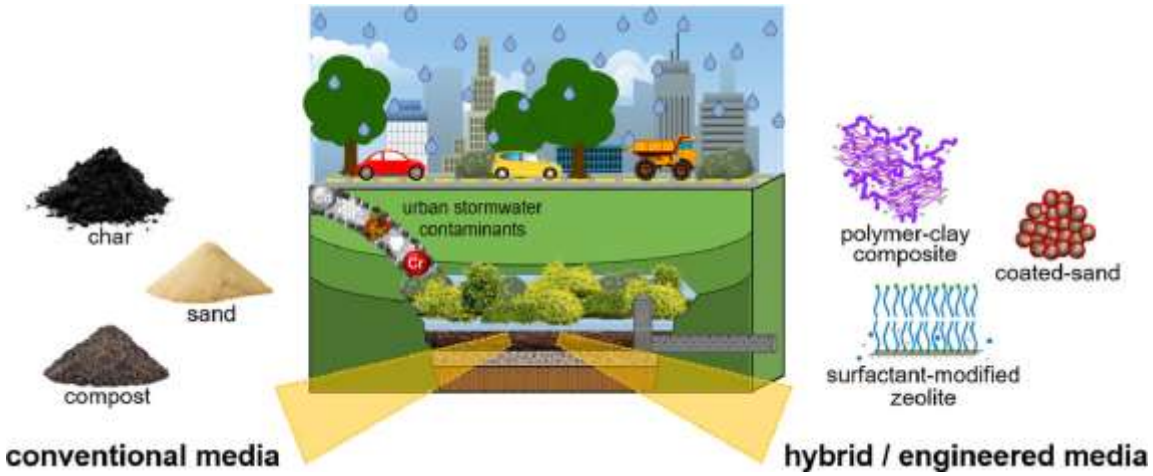

E1. Introduction

Stormwater management in urban areas has become a growing challenge for civil and environmental engineers and city planners. Increases in population, urbanization, and impervious surface coverage have led to subsequent increases in surface runoff volume[211] and decreases in local stormwater infiltration during natural and managed aquifer recharge.[212] Lack of appropriate stormwater management practices result in overflow of urban stormwater into receiving waters, streets, and building basements during storm events. Areas with combined sewer systems experience greater raw sewage and stormwater runoff during overflow events (**Figure E1**).

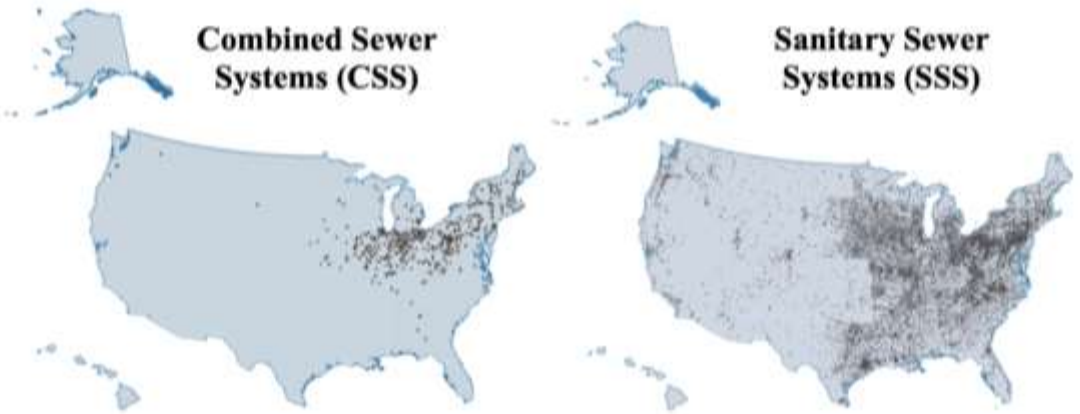

System Type	Number of Systems	Population Served	Estimated Annual Overflow Events	Overflow Volume Discharge
Combined Sewer (CSS)	1,100	43 million	43,000 - 60,000	850 billion gall
Sanitary Sewer (SSS)	20,428	164 million	23,000 - 75,000	3-10 billion gallons

Figure E1. Map of combined and sanitary sewer systems in the United States.[213] The adjoining table quantifies the number of these systems, the annual overflow events and discharge volume, and the number of people impacted by these overflow events.

In addition to high volumes of surface runoff and sewer overflow, another consequence of poorly managed and untreated urban stormwater is that it acts as a major pollution source to receiving waters due to elevated contaminant concentrations (**Table E1**). After storm events, hazardous contaminants in stormwater runoff are transported to local groundwater and surface water sources via interactions with impermeable surfaces (e.g., roads, roofs, etc.) and chemically-treated greenways (e.g., lawns, parks, etc.).[214] Contaminant groups typically found in urban stormwater include suspended solids, particulate-associated (e.g. bacteria, organic), and dissolved (e.g. nutrients, metals, ionic salts, organic compounds) species.[214-217] Some sources of these contaminants include: deposits from the atmosphere, roofing materials, metal pipes and gutters, pavement, emissions from combustion engines, tire/brake pad abrasion, gasoline, oil, and

brake fluid,[214-217] biocides, fertilizers, flame retardants.[215] The National Stormwater Quality Database compiled a list of multiple stormwater contaminants. In **Table E1**, we highlight representative contaminants and their concentrations. Suspended solids lead to increased turbidity and the build-up of sediments in receiving waters[218] which impact the quality of these waters. Nutrients in urban stormwater runoff[216] contribute to harmful algal blooms and eutrophication,[219] which was recently the second largest cause of United States water impairment affecting over 7,000 water bodies.[220] Additionally, the presence of metals, organic and biological contaminants in urban stormwater runoff will pollute receiving waters posing risks to aquatic and human health.[216, 221]

Table E1. Summary of national stormwater parameters and contaminant concentrations from the National Stormwater Quality Database.[222] Data was collected from 2001 – 2018 from over 5,000 urban runoff events. The values for urban stormwater contaminants are the collective average from six main urban land uses: 49% residential, 20% commercial, 13% industrial, 6% freeways, 6% institutional, and 6% open space.

Category	Constituent	Value	Unit
Physicochemical Parameters	pH	7.3 ± 0.8	
	TSS	133 ± 260	mg/L
	COD	77 ± 91	
	Oil and grease	10 ± 1	
	TKN	2.0 ± 3.5	
	$NO_2^- + NO_3^-$	0.9 ± 1.3	
	Total P	2.0 ± 3.5	
Metals	Zn	160 ± 356	µg/L
	Cu	26.5 ± 54.6	
	Pb	24.4 ± 60.6	
	Ni	7.2 ± 14.7	
	Cr	7.1 ± 13.5	

	Cd	1.5 ± 5.5	
Biological	Fecal coliforms	55151 ± 282910	#/100 mL
	Total petroleum hydrocarbons	3.9 ± 4.4	mg/L
Trace Organic Compounds*	benzene	84.7 ± 79.3	µg/L
	2-chloroethylvinylether	3.4 ± 2.6	
	chloroform	74.8 ± 159.5	
	dichlorobromoethane	0.8 ± 0.5	
	1,1-dichloroethane	0.6 ± 0.1	
	1,2-dichloroethane	1.5 ± 3.6	
	methyl chloride	5.2 ± 4.1	
	methylenechloride	12.2 ± 9.4	
	tetrachloroethylene	1.5 ± 1.0	
	toluene	1.5 ± 2.1	
	1,1,1-trichloroethane	2.4 ± 2.0	

*these 13 organic compounds were among those with the highest detection frequency

Stormwater best management practices (BMPs) offer a practical solution to reduce surface runoff volume and street flooding and provide some level of contaminant removal. Architects, city planners and engineers are thoughtfully implementing permeable pavement, rain gardens, and bioretention[223] and bioinfiltration basins[221, 224, 225] to increase hydraulic conductivity, which promotes groundwater recharge and prevents runoff backup in cities with high impervious surface coverage. Other countries, including the United States, may classify these systems as "low-impact developments" or "green stormwater infrastructure". For this review, we will refer to stormwater infrastructure as "BMPs". Existing BMPs designed for filtration (e.g., bioretention systems, wetlands, sand filters, and vegetated channels) typically employ native soil, vegetation and/or sand in their designs which help convey urban runoff from the street and retain large particulates (**Figure E1**).[221, 226] In regions of water scarcity, other BMP

options include urban stormwater capture by businesses and residences to create a local water source for non-potable applications such as landscape irrigation.[227, 228] Unfortunately, BMPs may be ineffective in reducing dissolved concentrations of nutrients, organic compounds, metals, and other contaminants in urban stormwater because they are primarily designed to mitigate impacts of high-volume during overflow events and to remove suspended solids and large particles.

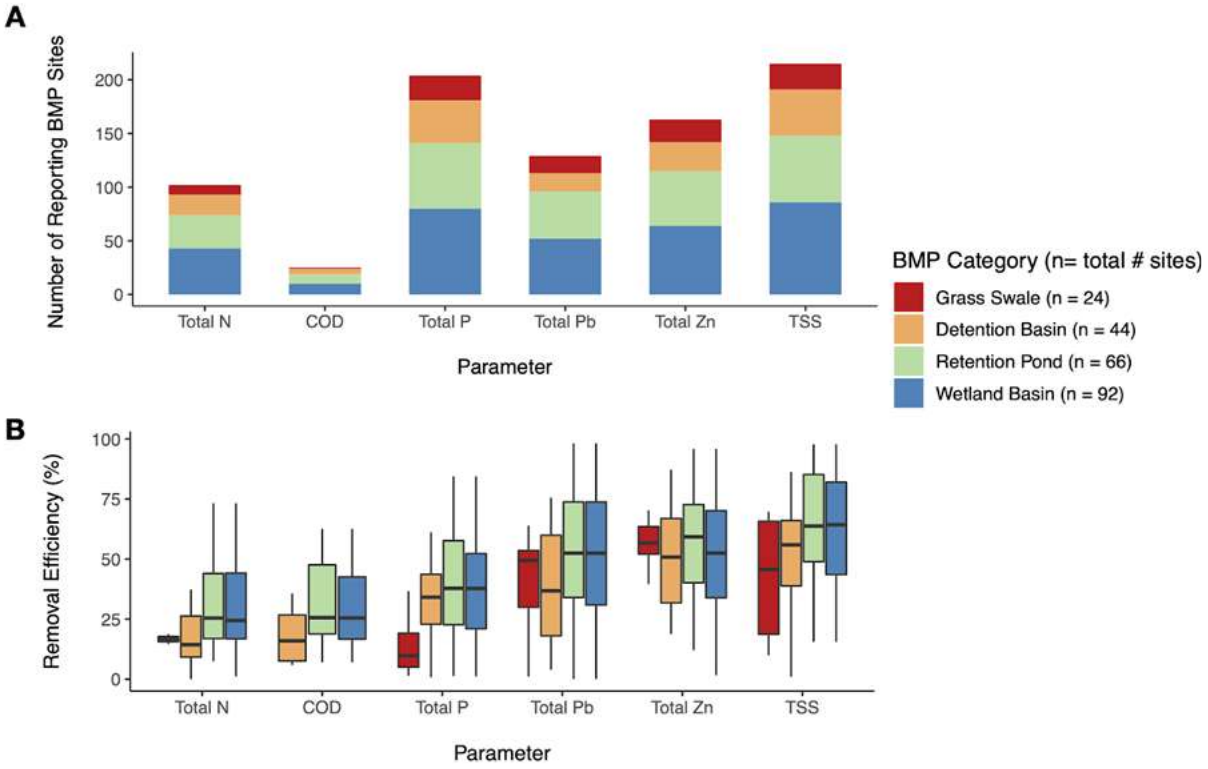

Figure E1. Synthesized data from the International Stormwater Best Management Practices (BMPs) Database[229] showing **(A)** number of sites reporting measurements and **(B)** the average removal efficiency of select, representative urban stormwater contaminants in grass swales, detention basins, retention ponds, and wetland basins. The boxplots in panel B were created by calculating the average removal efficiency for each unique BMP site reporting paired influent and effluent parameter

Figure E1A shows the performance of common stormwater BMPs reporting the influent and effluent concentrations of various pollutants during urban storm events. There is a wide range in the total number of BMP sites reporting measurements in the database: 24 grass swales,

44 detention basins, 66 retention ponds, and 92 wetland basins. The majority of the BMPs in the database are located in the United States and the most common BMP sites reporting pollutant concentration data are retention ponds and wetland basins (**Figure E1A**). Across all BMP categories, there is large variability in the number of total reporting sites for each chemical parameter—for example, approximately 200 BMP sites report concentrations of phosphorus (Total P) and total suspended solids (TSS), whereas less than 25 BMP sites report chemical oxygen demand (COD) levels. The median removal efficiency ranges for the reported chemical parameters across all BMP categories are as follows: nitrogen (Total N) (14–25%), COD (16–26%), Total P (10–38%), Total Pb (37–52%), Total Zn (51–59%), and TSS (46–64%) (**Figure E1B**). For Total N, Total P, and COD, the median removal efficiency in all selected BMP categories is less than 40%. **Figure E1** suggests that: (1) more data is needed to accurately validate, compare and predict BMP contaminant removal capabilities; (2) BMP treatment efficacy is not reported for certain contaminants (i.e., especially trace organic compounds, **Table E5**; and (3) there is an opportunity and need to enhance the removal efficiency of all urban stormwater contaminants.

Amending existing BMPs with media can enhance contaminant removal from urban runoff while also promoting groundwater recharge and reducing discharge volume during overflow events. Additionally, media amendments are a more cost-effective option for enhanced contaminant removal when designing and/or maintaining new stormwater infrastructure, particularly where physical space is limited in urban areas. When combined with conventional media, novel engineered media can further reduce levels of contamination in urban stormwater runoff to surface water or recharged groundwater. Efficient planning and heavy financial support from cities and states is often required to achieve these goals. To better inform decisions made by

engineers and city planners regarding improved management, safer discharge or infiltration of urban stormwater, a synthesis and critical review of available stormwater media is needed.

In this review, we present an overview of two main types of media, conventional and emerging engineered media, for stormwater treatment in urban areas, where space constraints and contamination from industrial and other anthropogenic sources complicate stormwater management. These media will be further divided into organic and inorganic media, and composite media classifications (for engineered media). We discuss physicochemical properties of inorganic, organic, and composite materials affecting contaminant removal and present opportunities to functionalize media for targeting specific contaminants and/or enhancing removal. It is important to consider that the specific physicochemical properties of media may vary depending on how the media is prepared or synthesized. To better elucidate how media could be incorporated into existing and future stormwater infrastructure, we highlight key factors impacting contaminant removal (e.g., media characteristics, stormwater hydrology and composition) and provide recommendations for lab-scale media tests and material characterization. We conclude the review by providing insight into some potential challenges and uncertainties associated with performance and implementation of engineered media for stormwater management applications.

E2. Conventional Stormwater Remediation Media

Here, we highlight research conducted in the United States to assess the potential of different conventional media for stormwater pollutant removal. A majority of the studies were conducted using synthetic stormwater in lab-scale column and batch experiments, and a few studies report contaminant removal in columns treating real urban stormwater under field conditions (**Table E5**).

Figure E2 reports the removal efficiencies of conventional media to treat various stormwater contaminants, with a majority of the studies focused on the removal of nutrients and metals. A majority of the media categories exhibit a high removal efficiency (>75%) for solids (volatile and total suspended solids). There are notable differences between the types of contaminants removed and the nature of the media. For example, inorganic media like zeolites and iron-based media have similar removal efficiencies for solids, pathogens, nutrients, metals and hydrocarbons; whereas, organic media have higher removal efficiencies for organic contaminants compared to inorganic media. In contrast to both organic and other inorganic media, sand has a lower removal efficiency with respect to organic contaminants (excluding hydrocarbons), metals, nutrients, and pathogens. Across all media categories, similar removal efficiencies were observed for hydrocarbons, while nutrient removal varies across media categories.

E2.1. Organic materials

Multiple studies have evaluated the application of organic materials such as compost, mulch, wood, activated carbon, biochar, peat and agricultural wastes for stormwater treatment.[230-250] The retention and removal of stormwater pollutants by carbonaceous media is aided by their high organic matter content and reactive functional groups (e.g., carboxyl, carbonyl, hydroxyl, phenolic, amino, and sulfonyl). For example, metals removal by organic media was hypothesized to correlate to the amount of oxygen-containing moieties (e.g., carboxyl and hydroxyl) present on the surface.[239, 251] The large degree of hydrophobicity and porosity of organic media can also facilitate removal of organic compounds.[252] Organic media can also improve biotransformation of organic contaminants by serving as excellent substrates for microbial growth.

E2.1.1. Biochar

In our review of stormwater treatment media literature, we found that biochar was the most well-studied media with reports covering a wide range of stormwater contaminants (**Figure E2, Tables E2 and E5**). Biochar and activated carbon are among the most commonly used organic materials for water treatment applications. Chars possess large porosities and acidic functional groups to remove organic compounds via diffusion[253] and complexation of metals, respectively.[254] They are produced from raw biomass with a high content of readily available carbon. Biochar is produced through low-oxygen thermochemical processing of raw biomass, which increases the overall surface area and number of active sites for the diffusion and adsorption of pollutants.[251, 255] Activated carbon requires additional steps employing oxygen or strong acids to activate the charred biomass. [251, 255] Variations in the physical and chemical properties of different precursor biomass feeds and thermochemical conditions used to produce biochar and activated carbon impact their removal capacities for different contaminants.[248, 249, 251] For example, batch experiments show that despite its lower surface area, granular activated carbon (GAC) produced from rice byproducts has higher affinity to Cu and Zn than nutshell-sourced GAC under the same conditions.[249] Additionally, Mohanty et al. observed that low temperature biochar exhibited greater removal of *E. coli* during stormwater infiltration studies and only 1% remobilization after intermittent flow compared to 3% remobilization using high temperature biochar.[238]

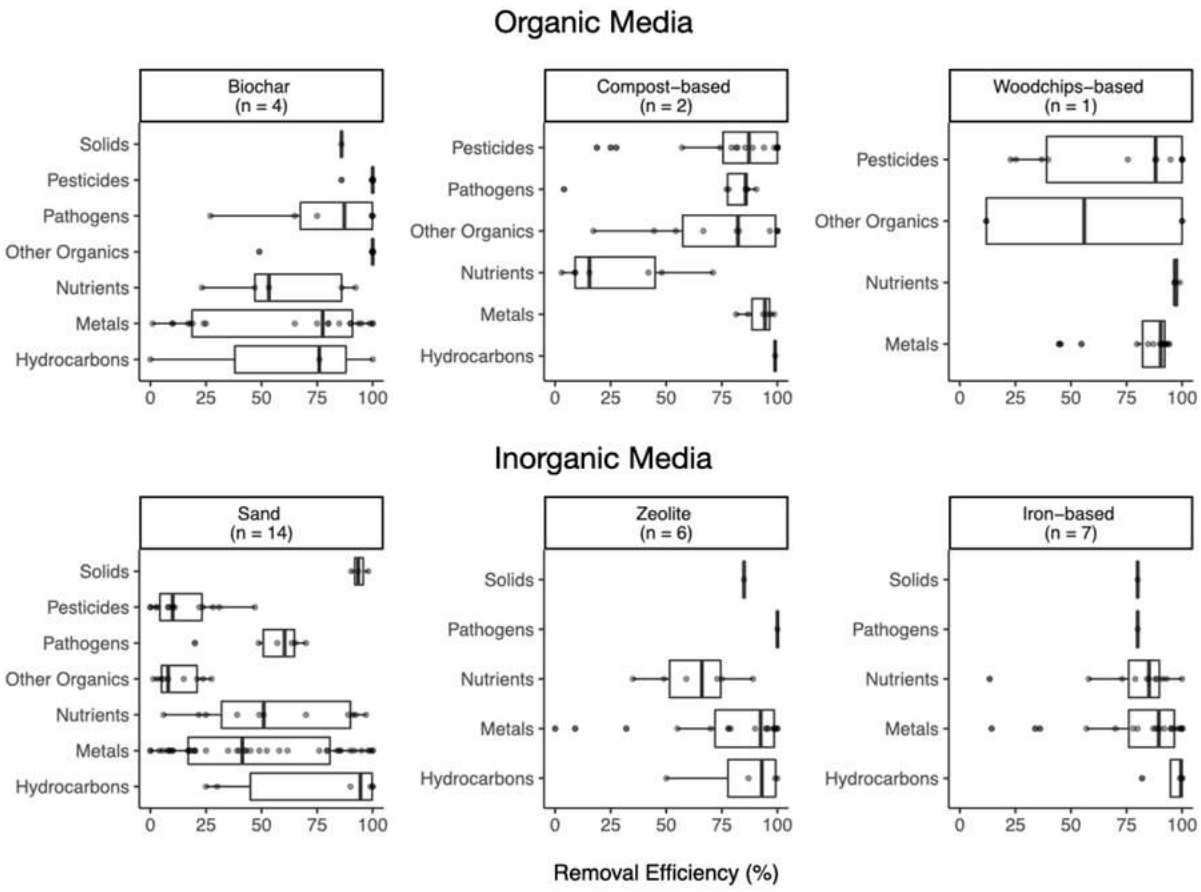

Figure E2. Boxplots show the range of reported or calculated removal efficiencies of conventional organic and inorganic media for different stormwater contaminant categories tested in 18 different studies (indicated by individual points for each specific media/contaminant pair). General media categories refer to grouped materials as follows: compost-based media (compost only and compost mixed with either sand, biochar, or activated carbon); woodchips-based (woodchips only and woodchips mixed with straw mulch or biochar); and iron-based (iron filings and iron filings mixed with sand, and iron hydroxides). General contaminant categories refer to grouped contaminants as follows: solids (total suspended and volatile suspended solids); pesticides (diuron, atrazine, fipronil, 2,4-dichlorophenoxyacetic acid, simazine, oryzalin and prometon); pathogens (*E. coli*, *Enterococcus faecalis*, total coliforms and fecal coliforms); other organics (tris(3-chloro-2propyl)phosphate, tris(2-chloroethyl)phosphate, perfluorooctanoic acid, perfluorooctanesulfonic acid, benzotriazole, 1H-benzotriazole, 5-methyl-1H-benzotriazole, and total organic carbon); nutrients (total P, orthophosphates, total P, total Kjeldahl nitrogen, NH_4^+, and NO_3^-); metals (As, Cd, Cu, Cr, Ni, Pb and Zn); and hydrocarbons (total petroleum hydrocarbons, motor oil, naphthalene, phenanthrene and benzo(a)pyrene)

Biochar is particularly effective at removing organic contaminants and pathogens (**Figures E2 and E3**), many of which are persistent in stormwater BMPs.[215, 256] Ulrich et al. and Ray et al. evaluated biochar produced from gasification of pinewood for the simultaneous removal of multiple organic contaminants in synthetic stormwater matrices.[242, 247] Ray et al. used a biochar dose of 3 wt% (with sand) for column filtration of a synthetic stormwater solution containing 10 µg/L (each) of seven representative organic contaminants and observed complete removal of 2,4-dichlorophenoxyacetic acid, tris(2-chloroethyl)phosphate, diuron, fipronil, perfluorooctanoic acid and perfluorooctanesulfonic acid (select organic compounds shown in **Figure E3A1**) and 80–100% atrazine removal.[242] The presence of DOC (5 mg-C/L) in a mirrored study did not significantly alter the performance of biochar during treatment (**Figure E3A2**). Ulrich et al. also reported 70–100% removal of prometon, benzotriazole, atrazine, diuron and tris(3-chloro-2-propyl) phosphate for over 428 pore volumes with initial contaminant concentrations of 20 µg/L (each) and 10 mg-C/L of dissolved organic carbon (DOC) using a biochar dose of only 0.2 wt%.[247] These studies suggest that the biochar high surface area (351 m^2/g) and functional groups were enough to overcome competing sorption and complexation sites of organic compounds, DOC and/or metals (select metals shown in **Figures E3A1 and E3A2**). The high removal (>99%) of these metals (except As and Cr) and organic contaminants suggest that multiple stormwater contaminants can be effectively and simultaneously removed if a sufficiently large surface area (>300 m^2/g) biochar is used. The large, hydrophobic biochar surface area also provides an anchor attracting pathogens like *E. coli* to attach overcoming electrostatic repulsive forces and facilitating efficient removal during stormwater infiltration.[238]

While biochar exhibits moderate to high removal efficiency (> 50%) for most contaminants (**Figures E2 and E3**), more research is needed to better predict removal of

contaminants with different phases and under more realistic stormwater conditions. Several studies have evaluated biochar's ability to remove multiple types of contaminants simultaneously.[230, 242, 248] For example, Reddy al. evaluated the simultaneous removal of nutrients (NO_3^- and TP), metals (Cd, Cr, Cu, Pb, Ni and Zn) and hydrocarbons (phenanthrene, naphthalene, and benzo(a)pyrene) by biochar in synthetic stormwater.[239] A stormwater matrix containing a mixture of contaminants would be a more realistic assessment of biochar performance allowing for comparative removal efficiencies of different contaminant categories to be better understood. As previously discussed, stormwater contaminants can exist as dissolved species and particulate-associated species. Therefore, the removal of some contaminants (e.g., nutrients, organic compounds, and metals) can be dictated by the behavior of particles in the stormwater and in the treatment systems. For example, organic contaminants and metals can react with natural organic matter (NOM) to form NOM-complexes and metals can form precipitates with sulfate, sulfides, and phosphate species. Although removal of solids by organic media such as biochar and GAC was evaluated in some studies[239, 244, 245, 250] (**Table E5**), further analysis is needed to assess the fraction of the solids associated with other dissolved stormwater contaminants.

Table E2. Summary of studies on media performance to remove various stormwater pollutants, physicochemical properties and removal mechanisms of media. It is important to consider that the specific physicochemical properties of media may vary depending on how the media is prepared or synthesized.

Media	Physicochemical properties	References	Study scale	Stormwater type	*Pollutants tested	Removal mechanisms
Biochar	High porosity; redox active sites; hydrophobic sites; oxygen-containing functional groups	Ashoori et al.[230]	Batch, column	Synthetic	Nutrients (NO_3^-, PO_4^{3-}); Metals (*Cd, Cu, Ni, Pb, Zn*); Trace organics (*FIP, DIU, ATR 1HB, 2,4-D, TCEP*)	Adsorption; hydrophobic interactions; electrostatic attraction; partitioning
		Mohanty et al.[238]	Column	Synthetic	Biological pollutants (*E. coli*)	
		Reddy et al.[239]	Column	Synthetic	TSS; Metals (*Cd, Cu, Cr, Ni, Pb, Zn*); Nutrients (NO_3^-, PO_4^{3-}); *Biological pollutants (E. coli)*; Trace organics (*NAP, PHE, BAP*)	
		Ulrich et al.[247]	Batch, column	Synthetic	Trace organics (*2,4-D, FIP, ATR, DIU, PRO, ORY, BEN, TCPP*)	
		Ulrich et al.[248]	Column	Synthetic	Trace organics (*2,4-D, FIP, ATR, DIU, PRO, ORY, SIM, 1HB, 5HB,TCEP, TCPP);* Nutrients (*TN, NO_3^-, DP*); Metals (*Cu, Zn*); Biological pollutants (*E. coli, total coliforms)*	
Sand	Negative surface charge; low	Barrett[257]	Field	Real	TSS; Metals (*Cu, Pb, Zn*); Nutrients (NO_3^-, *TKN, TP,*	Adsorption; physical filtration; straining;

surface area; low cation exchange capacity				*ortho-P*)	sedimentation; electrostatic attraction
	Barrett[258]	Field	Real	TSS; VSS; Nutrients (*TP, DP, TKN, NO_3^-, NO_2^-*), Metals (*Cu, Pb, Zn*); BOD; COD; Biological pollutants (*fecal coliform, fecal streptococcus*)	
	Erickson et al.[259]	Column	Synthetic	Nutrients (PO_4^{3-})	
	Erickson et al.[234]	Column	Synthetic	Nutrients (PO_4^{3-})	
	Mohanty et al.[260]	Column	Synthetic	Biological pollutants (*E. coli, Enterococcus faecalis*)	
	Mohanty et al.[238]	Column	Synthetic	Biological pollutants (*E. coli*)	
	Prabhukumar et al.[261]	Column	Synthetic	TSS; Metals (*Cd, Cr, Cu, Ni, Pb, Zn*); Trace organics (*NAP, PHE*); Nutrients (NO_3^-, PO_4^{3-}); Biological pollutants (*E. coli*)	
	Ray et al.[242]	Column	Synthetic	Metals (*Cd, Cu, Cr, As, Ni, Zn*); Trace organics (*ATR, DIU, FIP, 2,4-D, TCEP, PFOA, PFOS*)	
	Reddy et al.[262]	Batch	Synthetic	Nutrients (NO_3^-, PO_4^{3-})	
	Reddy et al. [263]	Batch	Synthetic	Metals (*Cd, Cr, Cu, Pb,*	

					Zn)	
		Reddy et al.[264]	Batch	Synthetic	Trace organics (*NAP, PHE*)	
		Reddy et al.[265]	Batch	Synthetic	Metals (*Cd, Cu, Cr, Ni, Pb, Zn*); Nutrients (NO_3^-, PO_4^{3-})	
		Smith[266]	Field	Synthetic	Nutrients (NH_4, NO_3^-, NO_2)	
		Ulrich et al.[248]	Column	Synthetic	Trace organics (*2,4-D, FIP, ATR, DIU, PRO, ORY, SIM, 1HB, 5HB, TCPP, TCEP)*; Nutrients (*TN*, NO_3^-, *DP*); Metals (*Cu, Zn*); Biological pollutants (*E.coli; total coliforms*)	
		Zarezadeh et al.[267]	Field	Real	TSS, VSS, Nutrients (NO_3^-, *ortho-P*); Heavy metals (*Cu, Pb, Zn*)	
Wood-based (Aspen wood, woodchips, mulch)	Hydrophobic sites; oxygen-containing functional groups	Ashoori et al.[230]	Batch, column	Synthetic	Nutrients (NO_3^-, PO_4^{3-}); Heavy metals (*Cd, Cu, Ni, Pb, Zn*); Trace organics (*FIP, DIU, ATR 1HB, 2,4-D, TCEP*)	Adsorption; complexation; precipitation of metals; biotransformation; filtration; hydrophobic interactions
		Boving and Zhang[232]	Batch, column	Synthetic	Trace organics (*NAP, FLU, ANT, PYR*)	
		Boving and Neary[231]	Field	Real	Trace organics (*NAP, FLU, ANT, PYR, PHE, CRY, BAP, ACY, ACE)*	

		Jang et al.[236]	Batch	Synthetic	Metals (*Cu, Pb, Zn*)	
		Ray et al.[241]	Batch, column	Synthetic	Metals (*Cu, Cd, Cr, Pb, Zn*); Trace organics (*NAP, FLA, 1,3-D, BBP, BAP*)	
		Ray et al.[240]	Batch	Synthetic	Metals (*Cu, Cr, Pb, Zn*); Trace organics (*NAP, FLA, 1,3-D, BAP, BBP)*	
		Syring et al.[245]	Batch, column, field	Synthetic, real	TSS; Metals (*Cu, Zn*)	
Compost-based	High humic content; water holding capacity; highly porous; high ion exchange capacity	Faucette et al.[235]	Column	Synthetic	Nutrients (*TN, (NO_3^-, TP*)	Adsorption; absorption; biotransformation; ion exchange
		Silvertooth et al.[244]	Batch, column, field	Synthetic, real	Metals (Cu, Zn)	
		Tobiason et al.[246]	Column	Synthetic	Metals (Zn)	
Zeolites	High surface area; negative surface charge; high ion exchange capacity; high water retention capacity; layered structure	Prabhukumar et al.[261]	Column	Synthetic	TSS; Metals (*Cd, Cr, Cu, Ni, Pb, Zn*); Trace organics (*NAP, PHE*); Nutrients (NO_3^-, PO_4^{3-}); Biological pollutants (*E. coli*)	Adsorption; ion exchange; complexation; electrostatic attraction; intercalation
		Reddy et al.[262]	Batch	Synthetic	Nutrients (NO_3^-, PO_4^{3-})	
		Reddy et al. [263]	Batch	Synthetic	Metals (*Cd, Cr, Cu, Pb, Zn*)	
		Reddy et al.[264]	Batch	Synthetic	Trace organics (*NAP,*	

					PHE)	
		Reddy et al.[265]	Batch	Synthetic	Metals (*Cd, Cu, Cr, Ni, Pb, Zn*); Nutrients (NO_3^-, PO_4^{3-})	
		Smith[266]	Field	Synthetic	Nutrients (NH_4, NO_3, NO_2)	
Iron-based (iron fillings; iron oxides)	High surface area; amphoteric surface hydroxyl groups	Erickson et al.[268]	Column, field	Synthetic, real	Nutrients (PO_4^{3-})	Oxidation; complexation; electrostatic attraction; adsorption
		Ernst Clayton et al.[269]	Column	Synthetic, real	Metals (*Cu, Zn*)	
		Prabhukumar et al.[261]	Column	Synthetic	TSS; Metals (*Cd, Cr, Cu, Ni, Pb, Zn*); Trace organics (*NAP, PHE*); Nutrients (NO_3^-, PO_4^{3-}); Biological pollutants (*E. coli*)	
		Reddy et al.[262]	Batch	Synthetic	Nutrients (NO_3^-, PO_4^{3-})	
		Reddy et al. [263]	Batch	Synthetic	Metals (*Cd, Cr, Cu, Pb, Zn*)	
		Reddy et al.[264]	Batch	Synthetic	Trace organics (*NAP, PHE*)	
		Reddy et al.[265]	Batch	Synthetic	Metals (*Cd, Cu, Cr, Ni, Pb, Zn*); Nutrients (NO_3^-, PO_4^{3-})	
Iron (hydr)oxide-	Amphoteric surface hydroxyl	Zhang et al.[270]	Column	Synthetic	Biological pollutants (*E.coli*)	Electrostatic attraction or attachment;

coated sand	groups; high surface area coating	Sansalone[271]	Column	Synthetic, real	Metals (*Cd, Cu, Pb, Zn*)	adsorption; complexation; co-precipitation of trace metals
		Mohanty et al.[260]	Column	Synthetic	Biological pollutants (*E.coli, E. faecalis*)	
Manganese oxide-coated sand	Amphoteric surface hydroxyl groups; high surface area coating	Liu et al.[272]	Column	Synthetic	Metals (*Cd, Cu, Pb, Zn*)	Electrostatic attraction or attachment; adsorption; complexation; redox reactions; co-precipitation of trace metals
		Charbonnet et al.[273]	Column	Synthetic	Trace organics (*BPA)*	
		Charbonnet et al.[274]	Column	Synthetic	Metals (*Cd, Cu, Pb, Zn*)	
		Grebel et al.[275]	Column	Synthetic	Trace organics (*BPA, 2MBT, OCP PRO, DIU, FLA)*	
Phoslock®	Layered bentonite clay; patent-protected	Randall and Bradford[276]	Column	Synthetic	Nutrients (*TP, TN, TKN, NO_3^-, PO_4^{3-}*; Metals (*Al, Cu, Fe, Mn, Ni, Pb, Zn*)	Intercalation and complexation
Graphene oxide-coated sand	High surface area coating; high porosity;	Vu and Wu[277]	Column	Synthetic, real	Trace organics (*CAF*); Metals (*Zn*); Nutrients (*PO_4^{3-}); Biological pollutants (*E.coli*)	Hydrophobic interactions; complexation; adsorption
		Ahmadi et al.[278]	Batch	Synthetic	Trace organics (*DCF*); Metals (*Cu*); Nutrients (*PO_4^{3-})*	
Polymer-clay composites	Positively charged; high cation exchange	Ray et al.[242]	Column	Synthetic	Trace organics (*ATR, 24D, DIU, PFOA, PFOS, TCEP, FIP*); Metals (*Cu, Zn, As,*	Adsorption; hydrophobic interactions;

capacity; swelling (depending on clay used)		*Cr, Pb, Cd*)	electrostatic interactions

*The pollutants are referenced using the following abbreviations: 1,3-D: 1,3-dichlorobenzene; 2,4-D: 2,4-diphenoxy acetic acid; 2MBT: 2-mercaptobenzothiazole; 1HB: 1-H-benzotriazole; 5HB: 5-H-benzotriazole; ACE: acenaphthene; ACY: acenaphthylene; ANT: anthracene; ATR: atrazine; BAP: benzo(a)pyrene; BBP: butyl benzyl phthalate; BEN: benzotriazole; BPA: bisphenol A; CAF: caffeine; CRY: chrysene; DIU: diuron; DCF: diclofenac; DP: dissolved phosphorus; FIP: fipronil; FLA: fluoranthene; FLU: fluorene; NAP: naphthalene; OCP: n-octylphenol; ortho-P: orthophosphate; ORY: oryzalin; PAH: polyaromatic hydrocarbons; PFOA: perfluorooctanoic acid; PFOS: perfluorooctanesulfonic acid; PHE: phenanthrene; PRO: prometon; PYR: pyrene; SIM: simazine; SUL: sulfamethoxazole; TCEP: tris(2-chloroethyl)phosphate; TCPP: tris(3-chloro-2-propyl)phosphate; TKN: total Kjedahl nitrogen; TN: total nitrogen; TP: total phosphorus; TPH: total petroleum hydrocarbons; TSS: total suspended solids; VSS: volatile suspended solids.

E2.1.2. Compost-based media

Compost has a high humic content, which can promote removal of metals through complexation and organic compounds through hydrophobic interactions.[233] Although compost alone has demonstrated capability of reducing stormwater runoff volume,[279] the possible leaching of organic matter and nutrients during high volume storm events makes compost an ineffective media. To mitigate this issue, compost can be mixed with media such as biochar or activated carbon that has a higher affinity to retain leached compounds. **Figure E2** shows that the removal of nutrients by compost-based media ranges between 9–71%. The values at the lower end of the boxplot were obtained in studies using only compost,[235] whereas the high removal efficiencies were obtained when compost was amended with either biochar or activated carbon.[248] Ulrich et al. reported that the addition of biochar to vegetated biofilters containing a mixture of sand and compost prevented leaching of total organic carbon (TOC), total dissolved phosphate (TDP) and TN, and increased diuron and tris(2-chloroethyl)phosphate by 6 and 83%.[248] Removal of TOC, TDP, TN and NO_3^- also increased by 80, 73, 86, and 68% respectively, in the presence of biochar.[248]

E2.1.3. Woodchips-based media

Woodchips are readily available and primarily used in denitrifying bioreactors for stormwater, wastewater and agricultural drainage treatment.[230, 280, 281] Woodchips can act as a source of carbon and as electron donors for denitrifying microorganisms. For example, Ashoori et al. reported a 99% removal efficiency of NO_3^- in column experiments employing woodchips which also assessed removal of metals (Cu, Cd, Pb, Ni, and Zn) and organic contaminants (diuron, 2,4-dichlorophenoxyacetic acid, tris(2-chloroethyl)phosphate, 1H-benzotriazole, atrazine and fipronil) in stormwater.[230] They reported average removal efficiencies of 80-94% for the metals, with the exception of Zn which exhibited poorer removal (45%). These estimates

were similar to the removal efficiencies observed when biochar was added at 33 wt% to the woodchips. The retention of metals was attributed to the formation of metal-sulfide precipitates in the presence of woodchips.[230] In contrast, the addition of the biochar enhanced the removal of the organic contaminants. Adsorption isotherms experiments revealed that woodchips sorption affinity towards the contaminants was significantly lower than the biochar sorption affinity—linear K_d sorption coefficient was estimated at 10–20 L/kg for woodchips and 10^5–10^6 L/kg for biochar. Thus, the application of a woodchips-biochar mixture in stormwater treatment systems can ensure the simultaneous removal of several contaminants (e.g., NO_3^-, metals and organic contaminants). However, a thorough analysis will be needed to choose an appropriate biochar. Woodchips are an efficient media because they have an extended bedlife; however, in this study, Ashoori et al. reported that biochar decreased the saturated hydraulic conductivity of the system by more than two-fold (i.e., 2.1 cm/s in woodchips-only columns and 0.5 cm/s in woodchips-biochar columns).[230] This decrease in hydraulic conductivity could lead to frequent clogging during stormwater infiltration.

Overall, current literature suggests that organic media can effectively capture stormwater contaminants. Nevertheless, a more complete analysis of their performance and potential for stormwater treatment applications is lacking.

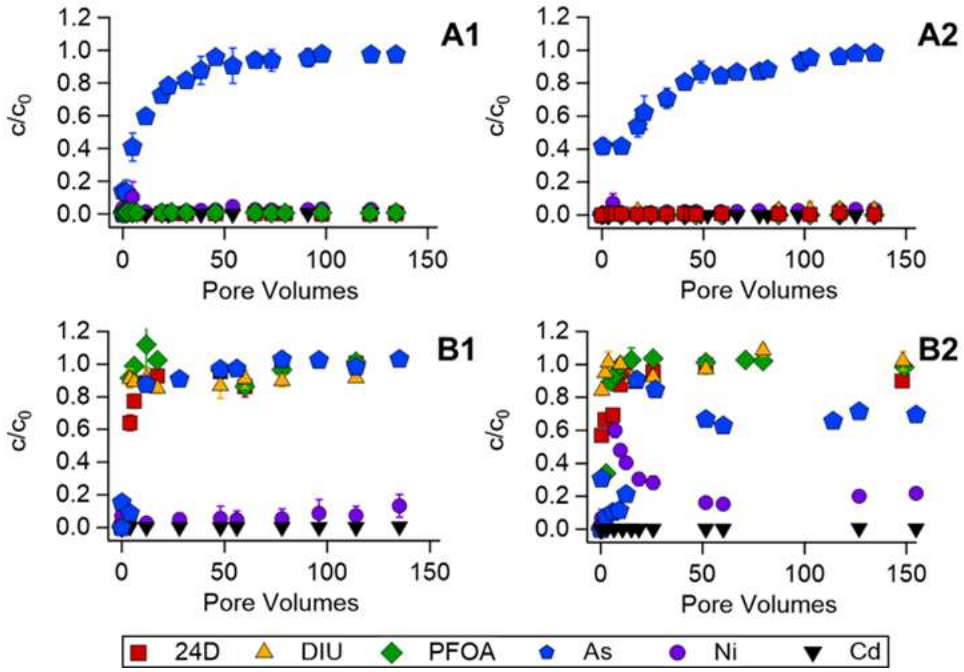

Figure E3. Column breakthrough results for removal of select metals and organic contaminants in columns amended with (A) 3 wt% biochar-97 wt% sand columns and columns with (B) virgin sand. The feed solutions contained 10 µg/L of each contaminant in (1) a synthetic stormwater matrix and in (2) the same synthetic stormwater matrix with 5 mg-C/L DOC. 24D = 2,4-dichlorophenoxyacetic acid. DIU = diuron, PFOA = perfluorooctanoic acid. The figure was created with permission from the authors.[242]

E2.2. Inorganic materials

In this review, the inorganic conventional media considered are mineral-based materials such as sand, zeolite, metal (hydr)oxides and other metal-based materials (e.g., iron filings). The presence of ionic species and hydroxyl moieties on the surface of these materials promotes sorption via electrostatic interactions and/or complexation of charged species such as nutrients (e.g., NO_3^-, NH_4^+, PO_4^{3-}), metals and organic contaminants.

E2.2.1. Sand

Coarse and silica-based materials like sand offer functional advantages to stormwater treatment systems because of their high hydraulic conductivities and ability to strain solids during infiltration. Beginning in the 1980s, the city of Austin, TX started using sand filters as an alternative BMP[233] equipped with a sedimentation basin designed to retain and slowly release stormwater runoff (90% of 24-h storm events).[257] Since then, sand filters have been commonly adopted in cities across the United States (e.g., Washington, DC and Seattle, WA) for stormwater management. They have a small land area requirement, which makes them convenient to use, especially for small development sites.[267, 282] Pollutant removal by sand filters is characterized by physical filtration, sedimentation, and straining.[233, 283] Both lab scale and field studies have been used to evaluate sand's ability to remove stormwater contaminants. Sand filters constructed near roadways in populous industrial cities exhibited high removal efficiency of stormwater solids (86–94%).[257, 267] Similar results of high (i.e., 98%) removal of TSS in lab-scale filters were also observed.[284]

Removal of other contaminants by sand, especially metals, varies greatly (**Figure E2**) and depends upon the metal speciation. Ray et al., Ulrich et al., and Prabhukumar et al. reported removal efficiencies greater than 80% for dissolved Cu (for different influent concentrations) in lab scale column experiments.[242, 248, 261] In contrast, Barret identified only a 6% and 39% reduction of dissolved Cu and Pb concentrations by sand filters, and 33% and 86% removal of total Cu and total Pb.[257] These conflicting findings suggest the need for more studies to assess removal efficiencies of different phases and speciation of contaminants during stormwater treatment.

The limited affinity of sand for dissolved contaminants is reflected in its low removal of organic contaminants (**Figures E2, E3A2** and **E3B2**). Ray et al. and Ulrich et al. reported removal efficiencies ranging from 0–47% for polar organic contaminants.[242, 248] **Figure E2** shows that sand can efficiently remove some hydrocarbons; however, these results were obtained from lab scale studies[261, 264] conducted under simplistic conditions using high contaminant concentrations which are not representative of typical concentrations found in natural stormwater (**Tables E1, E5**). For example, batch experiments conducted by Reddy et al. using sand and a synthetic solution of phenanthrene (30–1900 µg/L) and naphthalene (900–43000 µg/L) reported a removal efficiency of more than 90% for both compounds at all concentrations.[264] A survey of different runoff events in the United States estimated the maximum concentration of phenanthrene and naphthalene in urban runoff at 1 and 29 µg/L, respectively.[285] A study with lower, field relevant organic compound concentrations is necessary to properly assess sand removal capacity for these compounds. The aforementioned studies and results in **Figure E2** suggest that sand alone will be ineffective for urban stormwater treatment containing dissolved contaminants and a wide variety of other contaminants.

E2.2.2. Clays and Zeolites

Clay minerals and zeolites are naturally occurring minerals with great potential for water and wastewater treatment due to their high surface area, high affinity and selectivity for metals, low cost, abundance, and low toxicity. Studies investigating the utilization of clay minerals as treatment media for stormwater have focused primarily on zeolites. Both clays and zeolites can be purchased and synthesized at the laboratory scale,[286] which offers the advantage of being readily available.

Figure E2 shows that zeolites have moderate to high affinity for solids, pathogens, metals, nutrients and hydrocarbons. Zeolites are crystalline hydrated aluminosilicates with high surface area, ion exchange capacity, and water retention capacity.[266] Their high surface area provides an abundance of active sites onto which pollutants can adsorb. The porous and molecular sieve characteristic of zeolites can promote the structural sequestration and intraparticle diffusion of stormwater contaminants such as small neutral organic compounds.[233, 287] Zeolites with high silica content are favorable for the sorption of some organic contaminants (e.g., pharmaceuticals, pesticides) due to their high Si/Al ratio, which promotes strong hydrophobic interactions between zeolite surfaces and organic contaminants.[287, 288] The Si^{4+} and Al^{3+} in the structural framework of zeolites creates a net negative charge that attracts common stormwater cations (e.g., Ca^{2+}, Mg^{2+}, Na^{+}, and K^{+}), which can be exchanged with cationic trace metals.[289, 290] For example, Prabhukumar et al., reported a removal efficiency of 78-96% for cationic metals (Cd, Cu, Ni, Pb, and Zn) by zeolite as opposed to a removal efficiency of 55% for anionic Cr.[261] Reddy et al. also observed low removal efficiencies (5-9%) of Cr.[263] The permanent negative surface charge of zeolites leads to the repulsion of negatively charged species, thus limiting their sorption[233] while promoting the sorption of positively charged species. However, in zeolites with high silica contents, the negative charge is minimal thus limiting their sorption capacity for cations. Instead, zeolites with high silica content can be used for the sorption of some organic contaminants. Their high Si/Al ratio promotes strong hydrophobic interactions between their surfaces and organic contaminants.[287, 288]

Zeolites are also good candidates for nutrient removal and denitrification in stormwater (**Figure E2**). Zeolites can sequester NH_4^{+} through ion exchange, and NO_3^{-} and PO_4^{3-} through formation of metal complexes and precipitates. Additionally, their large surface area and ion

exchange capacity promotes the attachment of microorganisms[266, 291] enhancing denitrification. A pilot study evaluating the performance of zeolite as a biofiltration media for NH_4^+ removal observed that the average initial NH_4^+ level (0.78 mg/L) decreased by 93% under steady flow operation and by 98% during a high flow event followed by a 40-d dry period.[266] A close monitoring of the nitrogen and oxygen profiles in the biofilter showed that as levels of NH_4^+ and oxygen declined, NO_3^- and NO_2^- increased in the effluent which suggests nitrification occurred. A parallel sand control biofilter in the same study exhibited an average removal efficiency of 87% for NH_4^+. Both biofilters accumulated similar amounts of NO_3^- and NO_2^-, suggesting that in addition to denitrification, NH_4^+ could be removed through ion exchange in the zeolite biofilter. Compared to zeolite, sand has much lower surface area and cation exchange capacity[221] which limit adsorption sites and ion exchange processes occurring at the sand surface. This study indicates that zeolite can sustain performance through typical storm events and would be an excellent candidate in stormwater infiltration systems where NH_4^+ removal is the main priority.

E2.2.3. Iron-based media

Like zeolites, iron-based materials exhibit high removal efficiencies for solids, pathogens, metals, nutrients, and hydrocarbons (**Figure E2**). Metal oxides and metal-based materials are favorable for the attenuation of metal contaminants[261, 263, 265, 269] because of chemical properties facilitating ion exchange, surface precipitation, redox and complexation processes.[292-294] For example, Reddy et. al report removal efficiencies of 51–100% for Cd, Cu, Pb, Ni, Cr and Zn in batch experiments using a synthetic stormwater solution and iron filings--byproducts of the grinding or milling of iron material primarily consisting of iron (hydr)oxide minerals.[263] Prabukhumar et al. also reported similar removal efficiency (57–100%) during column experiments using iron filings.[261] These high removal efficiencies could be due to the high initial concentrations (5-500 mg/L) of the metals used in these studies. In contrast, column experiments

using natural highway runoff to assess granular ferric hydroxide capacity to remove metals report average removal efficiencies of 14 and 34% for Cu (initial concentration: 36 µg/L) and Zn (initial concentration: 50 µg/L).[269] Breakthrough (i.e., the ratio of influent to effluent concentration, $c/c_0 > 0$) for both Cu and Zn occurred within 5000 pore volumes, but the media was not saturated within the experimental period (98000 pore volumes).[269]

Compared to sand and zeolites, iron-based media exhibit greater removal efficiencies for nutrients (**Figure E2**). Mixtures of sand and iron filings at doses of 7.2 and 10.7 wt% along the trenches of a wet detention basin reduced PO_4^{3-} concentrations by 29–90%.[268] Erickson et al. also conducted column experiments with different doses of iron filings. In the absence of iron filings, sand sorption capacity for PO_4^{3-} was exhausted at a column depth less than 10 m, whereas a 5 wt% iron filing dose did not result in the exhaustion of the media sorption capacity even after 200 m of treated depth.[268] Furthermore, the authors reported that the hydraulic conductivity in the iron-sand columns did not change significantly as the iron filings fraction increased from 0.3 to 5 wt%. Thus, iron filings can be applied in BMPs (e.g., bioretention ponds, grass swales) where PO_4^{3-} removal is low (**Figure E1**) to minimize risk of PO_4^{3-} leaching. The limited reactivity of sand to dissolved contaminants resulted in minimal sorption of PO_4^{3-} in the Erickson et al. study.[268] In contrast to sand, the high surface area of iron-based media (and other metal oxides) presents numerous active sites for the adsorption of PO_4^{3-}, which can sorb to iron filings through the formation of iron phosphate precipitates or ligand exchange with iron (hydr)oxides.[221, 262]

Overall, zeolites and iron-based media possess great potential for pollutant removal and using them in stormwater treatment systems would ensure better water quality. However, they reportedly have low hydraulic conductivities compared to sand.[295] This could lead to rapid

clogging, flooding, and inhibit groundwater recharge. Careful considerations like these are needed in choosing media for stormwater treatment. In *section E4*, we discuss the influence of media properties in greater detail.

E3. Composite Engineered Media for Enhanced Urban Stormwater Treatment

To maximize the removal of trace contaminants in urban stormwater and protect receiving waters, conventional materials may not be sufficient. Researchers are testing new, low-cost engineered materials as supplements to enhance the contaminant removal efficiency of conventional materials. Composite materials can be produced to take advantage of surface functional groups or chemical properties of a substrate to coat, dope, or decorate with a material of different properties to enhance or add utility to the substrate. Typically, the goal of composite fabrication is to expand the range of contaminants removed in urban stormwater (and other water treatment applications). This section will identify the synthesis, properties, contaminant removal mechanisms, and opportunities for field deployment of different engineered media evaluated for urban stormwater treatment.

E3.1. Metal (Oxide) Composite Engineered Media

As outlined in *Section E2*, conventional inorganic media such as metal oxides, clays, and sand exhibit some affinity for urban stormwater contaminant removal. However, currently there are several limitations to incorporating these media in urban stormwater low-impact developments. For example, metal oxides and clays typically occur as amorphous flocs or powder, which may clog infiltration systems during storm events, or transport adsorbed or complexed contaminants downstream to receiving waters. Although sand can offer benefits of metal sorption and high hydraulic conductivity in infiltration applications,[242] its reactivity is

limited to inorganic species in urban stormwater. Development of engineered media can help overcome the moderate to low reactivity of conventional media while enhancing reactivity during urban stormwater treatment.

E3.1.1. Iron (hydr)oxide-coated sand

In addition to trace metal removal, naturally occurring iron (hydr)oxides can also aid in the attenuation and immobilization of fecal indicator bacteria, which is one of the main classes of contaminants in urban stormwater (**Table E1**). Fe(III) mineral phases adhere to bacteria cell walls, creating bacteria iron oxide flocs[296] and enabling subsequent redox reactions to inactivate the immobilized bacteria.[297] In urban stormwater infiltration applications, cell adhesion to iron (hydr)oxides and adsorption of trace metals could be an effective pollutant removal strategy. However, because iron oxides typically occur as powders or flocs in soils, it is impractical to employ them as filtration media for runoff treatment.

To facilitate their use as a reactive media in existing urban stormwater management practices, researchers have investigated coating iron (hydr)oxides on conventional media to augment low-impact urban stormwater developments.[270] Amorphous iron(III) oxyhydroxides synthesized by slowly increasing the pH of a ferric solution (e.g., ferric chloride) can be easily coated onto granular media substrates like sand.[298, 299] Coating iron (hydr)oxides on sand increases its ability for trace contaminant removal without sacrificing hydraulic conductivity, which is critical for stormwater infiltration applications. For example, Mohanty et al. designed bioinfiltration cells (i.e., columns) amended with iron (hydr)oxide-coated sand to sequester fecal indicator bacteria from simulated stormwater.[260] Even at a 50 wt% sand to iron (hydr)oxide-coated sand loading, 99% of *E. coli* and 97% of *Enterococcus faecalis* (initial concentration of both bacteria: 0.8-1.8×10^6 CFU/mL) were removed from the simulated stormwater compared to

70% and 58% removal with just sand-amended bioinfiltration systems. Furthermore, when flow of bacteria-laden simulated stormwater was halted and resumed to mimic intermittent flow, less than 0.25% of attached bacteria were mobilized from the iron (hydr)oxide-coated sand columns, compared to up to 13.2% mobilization of bacteria attached to uncoated sand. In a column filtration study, Zhang et al. observed no breakthrough of *E. coli* in synthetic stormwater from lab-scale columns packed with iron (hydr)oxide-coated sand for over 6 h of filtration, while breakthrough was observed in only 0.75 h in sand-amended columns.[270] Columns in this study were operated at hydraulic conditions comparable to a typical storm event with no evidence of clogging. While iron (hydr)oxide-coated sand contributed to greater bacterial removal (87% compared to 69%), columns packed with conventional bioretention media (i.e., sand) resulted in a faster bacterial death rate (i.e., 0.90 d^{-1}) compared to the reactive engineered media columns (0.04 d^{-1}). This effect was attributed to the lack of native microorganisms competing for nutrients on the iron oxide coated sands compared to the conventional media, which was inoculated with a native culture.

Iron (hydr)oxide-coated sand has also been investigated for trace metal adsorption. Sansalone prepared iron (hydr)oxide-coated sand for passive removal of Cu, Zn, Cd and Pb trace metals in an exfiltration trench capturing urban stormwater.[271] Test columns amended with sand and coated sand were used to determine trace metal removal in deionized water and real stormwater containing suspended solids, which can complex trace metals.[300] Virgin sand column breakthrough (i.e., $c/c_0 = 0.90$) of metals in deionized water (pH 6.5) occurred 10 times as fast for Zn and Cd, and 25 times as fast for Cu and Pb compared to iron (hydr)oxide-coated sand. This effect was exaggerated when the solution pH was increased above the point of zero charge for the iron oxide coating (pH 7.0–8.0), promoting favorable electrostatic interactions between

the divalent cations and negatively charged coated sand. The lifetime of the iron (hydr)oxide-coated sand tested under the conditions in the Sansalone study was approximated at 15 years.

To provide city planners, civil and structural engineers, and urban landscape architects with adequate information to deploy engineered media like iron (hydr)oxide-coated sand, additional research is needed. For example, even though the studies were conducted with the intended application of employing iron (hydr)oxide-coated sand in infiltration systems, none of the studies report hydraulic conductivity or a comparable relevant parameter. Though, because the engineered media substrate (i.e., sand) has a high hydraulic conductivity, it is reasonable to assume that introducing iron (hydr)oxide-coated sand into existing infiltration systems would not reduce stormwater permeability. To determine the expected lifetime and reactivity of iron (hydr)oxide-coated sands, more information is needed on trace metal adsorption capacity and bacterial removal or inactivation under a wider range of stormwater conditions. This includes information about the iron (hydr)oxide coating stability because trace metals adsorbed onto iron (hydr)oxide coatings may be transported downstream if the coating leaches from sand surfaces over time.

Table E3: Media properties and column performance for trace metal removal in synthetic stormwater.[272]

					Influent concentration (mg/L)				**Exhaustion capacity (mg/g media at $c/c_0 = 0.9$)**			
Media	**SSA (m^2/g)**	**D_{50} (mm)**	**Column porosity**	**EBCT (min)**	**Zn**	**Cu**	**Cd**	**Pb**	**Zn**	**Cu**	**Cd**	**Pb**
GAC	1021.8	0.65	0.37	8.1	5	5	5	5	<0.001	0.0016	<0.001	0.0015
silica sand	0.22	0.50	0.35	4.4	5	5	5	5	1.63	4.10	1.11	3.33
IOCS	15.4	0.50	0.73	4.5	5	5	5	5	0.019	0.122	0.017	0.36
MOCS	1.51	1.19	0.34	0.4	1	1	1	1	<0.001	0.15	<0.001	0.11

GAC = granular activated carbon; IOCS = iron oxide coated sand; MOCS = manganese oxide coated sand; SSA = specific surface area; D_{50} = average particle size; EBCT = empty bed contact time.

E3.1.2. Manganese oxide-coated sand

Similar to iron (hydr)oxides, manganese oxides are abundant, naturally occurring, and can undergo similar surface complexation with trace metals (e.g., Pb, Cu, Cd) via hydroxide functional groups at their microporous surface.[292, 301, 302] In addition to interactions with trace metals, manganese oxides can undergo redox reactions with organic compounds in aquatic environments. For example, humic and fulvic acids as well as simple phenols can reduce Mn(IV) oxides in natural waters to Mn(II) phases.[303, 304] This inherent property of manganese oxides has been exploited through its use as a substrate for trace organic compound oxidation. Mn(III)/Mn(IV) oxide catalysts have been investigated in the oxidation of organic compounds such as toluene,[305] anilines, hydroquinones,[306] and antibiotics[307] in water.

Like their iron (hydr)oxide counterparts, powdered amorphous manganese oxide mineral phases can be precipitated onto sand support media using a reductive synthesis to facilitate employment in infiltration systems. In fact, dissolved Mn^{2+} in raw feed water can be oxidized to Mn^{4+} and coated on sand grains in trickling filters during wastewater treatment.[308] The subsequent $Mn(IV)O_2$ coating catalyzes additional oxidation of nearby Mn^{2+}, facilitating manganese removal.[309] To expedite $Mn(IV)O_2$ coatings on sand grains, a solution of potassium permanganate is added to sand and reduced by addition of an acid (e.g., hydrochloric acid)[310-312] to achieve a birnessite (i.e., a mixed Mn(III)/Mn(IV)) phase manganese oxide-coated sand.[275] Manganese oxide-coated sand has been investigated as both an adsorbent media for trace metal removal[274, 310, 313] and as a heterogeneous oxidation media for trace organic compound degradation in urban stormwater.[273, 275] Liu et al. compared the sorptive removal of Pb, Cu, Cd,

and Zn in synthetic runoff by sand, iron-oxide coated sand, and manganese oxide-coated sand.[272] Both the engineered sand media had higher exhaustion capacities (i.e., metal loading on geomedia at $c/c_0 = 0.9$) than uncoated sand for all trace metals under the same experimental conditions. Exhaustion capacities for Pb, Cd, and Zn were at least twice as high on iron (hydr)oxide-coated sands than on manganese-oxide coated sand due to differences in metal affinities during surface complexation (**Table E3**). In comparison to both coated sands, commercial GAC underperformed with respect to trace metal removal.

Tiwari et al. similarly reported a combined effect of adsorption and co-precipitation of Cu and Pb species on manganese oxide-coated sand surfaces at neutral pH.[311] Grebel et al. demonstrated the range of oxidation rates of representative runoff trace organic compounds by birnessite manganese oxide-coated sand geomedia in column filtration studies.[275] For example, reaction rate constants ranged from 1.8×10^{-3} L/g·s (for bisphenol A) to 66.7×10^{-9} L/g·s (for diuron). Further investigation of this particular manganese oxide-coated sand in synthetic stormwater free of DOC corroborated previous findings, demonstrating high removal efficiency of Cu and Pb (i.e., $c/c_0 = 0$ for over 2000 pore volumes) and very low removal efficiency of Zn and Cd (i.e., $c/c_0 = 1$ in < 1000 pore volumes).[274] Observed decreases in metal removal by manganese oxide-coated sand due to DOC addition were attributed to complexation of DOC with trace metals and not to loss of adsorption sites on sand surfaces.

Charbonnet et al. have also provided important information regarding the stability of the manganese oxide.[273] The coating density of manganese-oxide coated sand decreased from 2 mg Mn/g media (for native media) to 1.7 mg Mn/g (for spent media) after treating 1300 pore volumes of bisphenol A in a synthetic stormwater matrix. This reduction in coating density indicated that approximately 6.4 mg Mn was released, exceeding the 0.91 µM EPA secondary

drinking water standard.[314] Because manganese oxide- and iron (hydr)oxide-coated sands remove trace metals using similar mechanisms, it is possible that leached Mn (and by extension Fe) may act as mobile carriers transporting adsorbed trace metals downstream.

E3.1.3. Phoslock®

High nutrient loads originating from stormwater runoff to receiving waters is a growing concern in the increasingly urban landscapes across the United States.[315] In particular, a study in St. Paul, Minnesota revealed that urban watersheds exhibit high phosphorus retention due to high street density and transport via stormwater runoff.[316] Recent studies have found that controlling and reducing phosphorus loads (rather than nitrogen) is key to mitigating harmful algal blooms and eutrophication in surface waters.[317] To mitigate phosphorus loads to receiving waters from urban runoff, Phoslock® (a commercially available phosphorus adsorbent) could be considered as an engineered media amendment in existing urban stormwater management practices. Phoslock® is a bentonite clay complexed with lanthanum, a rare earth metal.[318] The La^{3+} forms stable complexes with phosphate in water,[319] which can effectively reduce phosphate concentrations in surface waters prone to eutrophication (**Figure E4**). When applied to surface waters, Phoslock® complexes free phosphate ions as it travels through the water column to the sediment bed surface, regulating phosphorus release from the lake bed and limiting excess growth of phytoplankton.[320]

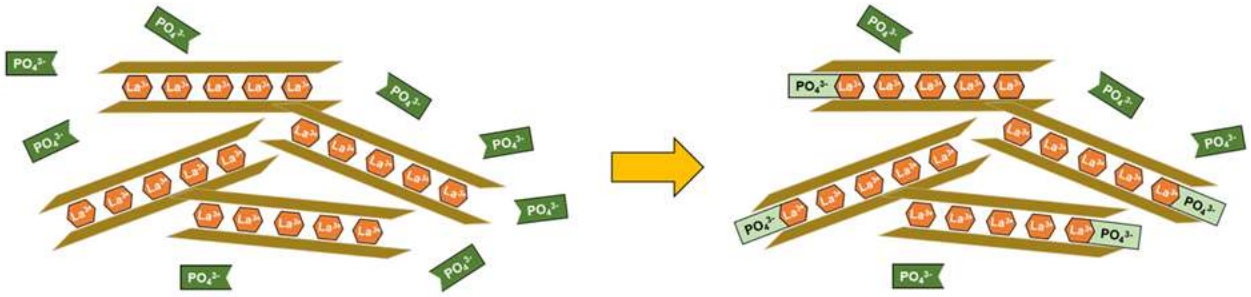

Figure E4. Schematic illustrating how Phoslock, a lanthanum (La3+)-modified bentonite clay can complex free phosphate (PO_4^{3-}) in solution

Because Phoslock® was designed for surface water applications, there are limited studies investigating its use as a filtration media for urban stormwater treatment. Randall et al. examined Phoslock® amendments in vegetated bioretention cell mesocosms to treat synthetic stormwater.[276] The hydraulic conductivity of Phoslock®-amended mesocosms was significantly lower than mesocosms amended with sand, alum, and a commercial oxide-coated media during down-flow operation. Interestingly, sand-Phoslock® mesocosms had much higher removal efficiencies for orthophosphate (85%) than for total phosphorus (34%), which was better removed by sand-only mesocosms (76%). The poor removal efficiency of total phosphorus by sand-Phoslock® mesocosms was attributed to the formation of Fe-PO_4 complexes, which reduced the amount of free phosphate in urban stormwater but promoted phosphorus release from organic carbon decomposition in the bioretention soil. However, Phoslock®-amended mesocosms had the highest nitrate removal efficiencies (i.e., 98%) due to increased denitrification under the anoxic conditions generated in the bioretention columns. To our knowledge, the 2013 Randal and Bradford study is the only peer-reviewed article employing Phoslock® as an engineered urban stormwater media.[276] Other reports examining Phoslock® application to surface waters identify potential negative ecological consequences associated with deployment of Phoslock® in natural systems. For example, there have been several documented studies identifying negative toxicological effects to Daphnia magna (a representative zooplankton controlling phytoplankton growth in surface waters)[321] when La^{3+} is leached during Phoslock® treatment of phosphorus-rich water.[322] Further investigation of safety and other environmental concerns is needed before Phoslock® amendments are considered for urban stormwater treatment.

E3.2. Organic-coated Composite Engineered Media

Many studies have proposed the creation of layered treatment zones[323-325] using combinations of conventional media, engineered materials or hybrid composite materials for water treatment applications.[326-328] However, due to limitations associated with certain media (e.g., hydraulic conductivity), in this section we only describe a few viable candidates for stormwater treatment applications.

E3.2.1 (Modified) Graphene oxide-coated sand

Graphene oxides are single-layer trigonal planar (sp^2) carbon nanosheets decorated with epoxy and hydroxyl groups on the basal planes and carboxylic acid groups along the edges.[329] Produced from chemical exfoliation of oxidized graphite minerals, graphene oxides have high reactive surface area, increased hydrophilicity,[330] and are conducive to additional functionalization.[331] As a result, graphene oxides are used in a wide variety of applications including biosensors,[332] enhanced electron transport in electrochemical systems,[333, 334] drug delivery,[335, 336] and water treatment.[337, 338] Additionally, the recent demonstrated success of the well-established (modified) Hummers method[339] for high throughput synthesis of graphene oxide nanosheets has greatly expanded the practical feasibility of using nanoscale graphene oxide in real, engineered applications.

Similar to iron and manganese oxides, graphene oxide nanosheets are difficult to employ during water treatment unless a support is used (e.g., semipermeable membranes.[340-342] There are several studies investigating (modified) graphene oxide-coated sand for water treatment applications, including for urban stormwater treatment. Coating graphene oxide onto sand can mimic the performance of granular activated carbon used in water treatment by creating a carbonaceous media with high adsorptive capacity for removing (trace) organic compounds[343-345]

and inorganic contaminants.[346, 347] To generate graphene oxide-coated sands, additional modification of graphene oxide is needed. The increased number of oxygen-containing functional groups on graphene oxide compared to graphene impart some hydrophilicity; however, the large domains of remaining hydrophobic aromatic groups[348] can decrease its suitability for coating substrates like sand which require acidic functional group linkages. To facilitate a stable coating of graphene oxide onto sand for stormwater treatment, researchers have modified graphene oxide with hydrophilic species to increase attachment efficiency.[349-351] For example, Gao et al. modified graphene oxide nanosheets with thiol groups by taking advantage of diazonium grafting chemistry[352] to allow self-assembly of graphene oxide onto sand surfaces.[353] The resulting graphene oxide coated sand exhibited five times higher adsorption of mercury and Rhodamine B compared to unmodified sand during column filtration studies. Similarly, there are studies investigating coating sand surfaces with Al^{2+}- and Mg^{2+}-graphene oxide nanosheets which demonstrate higher complexation efficiencies of phosphate and metals (i.e., Zn and Cu), and adsorption of organic compounds (i.e., diclofenac and caffeine) compared to (reduced) graphene oxides.[277, 278]

Gao et al. and Vu et al. have also included important information regarding the stability of the modified graphene oxide-coated sand for stormwater infiltration applications. During a 2-h column filtration study treating mercury and Rhodamine B in water, no leaching of graphene oxide from the sand surface was observed.[353] The Vu et al. study examined removal of phosphate, zinc, caffeine, and *E. coli* model stormwater contaminants in synthetic and real filtered surface runoff during single and multi-contaminant column experiments. In the multiple contaminant experiments using Al–Mg/graphene oxide-coated sand, *E. coli* removal was 93.8% in synthetic runoff and 93.0% in real surface runoff, with minimal remobilization in either

scenario.[277] Furthermore, complete breakthrough of caffeine, zinc and phosphate (0.5 mg/L each) occurred nearly 5,000 pore volumes sooner in real surface runoff than in cleaner synthetic stormwater conditions, which was attributed to sorption site competition with dissolved organic matter present in the real water. The estimated lifetime of the Al–Mg/graphene oxide-coated sand in the Vu et al. study was determined to be at least 15 years given the study conditions.

E3.2.2. Polymer-Clay Composites

Polymer-clay composites are promising stormwater treatment media typically synthesized by mixing (cationic) polymer solutions with a clay solution at ratios corresponding to the clay cation exchange capacity and the desired degree of hydrophobicity.[354] Following mixing, the modified clay slurry is removed, washed and dried. The simple fabrication of these low-cost adsorbents leverages the high reactive surface area and cation exchange capacity of clays[355] with the functionality of organic polymers. Because of their added utility to remove organic and inorganic species, polymer-clay nanocomposites have been proposed since the 90s[356] as effective adsorbents and flocculants for water treatment.[357] Compared to polymers or virgin clays used independently, polymer-clay nanocomposites have higher adsorption capacities and faster kinetic.[358] The hydrophilicity and negative charge of clays[359] allows positively charged polymers (i.e., polycations) to adsorb to the outside of the clay particle as well as exchange with the inner layer cations in swelling clays, resulting in charge reversal.[360] The polymers add hydrophobic domains on the clay surface, which can enhance trace organic compound removal[360] via partitioning to the hydrophobic polymer-clay composite surface (**Figure E5**, left schematic).[361] The polycation coating (which typically possess positively-charged moieties like quaternary amines) can also facilitate removal of negatively charged pathogens[362] and free and complexed dissolved organic carbon species.[362-364] To account for the possibility of polymer

desorption from the composite surface during stormwater treatment, the choice of polymers must weigh functionality with potential toxicity.

The majority of studies investigating polymer-clay composites have been for treatment of trace organics in drinking water sources[365-367] and in wastewater.[368, 369] Of these, only a few studies have performed column experiments to gauge the performance of polymer-clay composites under more field-relevant treatment conditions. Ray et al. synthesized polydiallyldimethylammonium chloride and poly(4-vinylpyridine-co-styrene) montmorillonite clay composite media for urban stormwater treatment during continuous flow of synthetic stormwater in lab-scale columns.[242] At 3 wt% loading (with sand), the clay composites exhibited greater removal of hydrophobic trace organics (e.g., fipronil and perfluorooctanesulfonic acid) compared to more hydrophilic compounds (e.g., 2,4-dichlorophenoxyacetic acid and atrazine). The dual functionality of the modified polymer-clay composites was demonstrated by their simultaneous and complete removal of all divalent trace metals (e.g., Cd^{2+}, Cu^{2+}, Zn^{2+} and Ni^{2+}) and 40–60% removal oxyanions (i.e., As(V) and Cr(VI)) over 150 pore volumes. Interestingly, the hydraulic conductivity of the polymer clay composite-amended columns) was equal to or higher than the hydraulic conductivity of sand. Additionally, over 98% of the polymer coating remained on the clay after 48-h of constant wetting. This finding suggests that it may be feasible to employ polymer-coated clays as urban stormwater media in infiltration applications.

E3.2.3. (Surfactant-)Modified Zeolites (SMZs)

Like clays, zeolites are naturally abundant and negatively charged aluminosilicate minerals with high surface area and cation exchange capacity.[370] Because of these properties, zeolites are similarly easy to modify with positively charged polymers and materials. Zeolites have been employed as adsorbents[287] in wastewater treatment for trace metal removal[290, 371] and

have more recently been investigated for ammonia and phosphate recovery applications.[372] In fact, there are several studies investigating metal-modified zeolites as antimicrobial media for urban stormwater biofilters.[373-375] Cu, Ag, and Zn among other metals possess inherent antimicrobial properties. Li et al. examined Cu^{2+}- and $Cu(OH)_2$- zeolite filter media for inactivation of *E. coli* during stormwater filtration and discovered that over 2-log *E. coli* removal was consistently achieved during five months of treating natural stormwater under typical conditions.[373]

In addition to metal-modified zeolites, there have also been studies investigating surfactant-modified zeolites for enhanced adsorption of other types of micropollutants. A popular candidate for clay and zeolite modification is cetrimonium bromide (also known as cetyltrimethylammonium bromide (CTAB) or hexadecyltrimethylammonium bromide (HDTMA)), which is a quaternary ammonium positively charged surfactant. Similar to clays, the quaternary ammonium cation provides an anchor for the surfactant to attach to the negatively charged zeolite surface via electrostatic attraction. The methylene surfactant tail $(–CH_2)_x$ provides a hydrophobic anchor for adsorption of organic compounds. If the surfactant concentration is increased past the critical micelle concentration, it is possible to reverse the charge of zeolites and generate a positively-charged adsorbent (**Figure E5**, right schematic).[376] This is often done to adsorb negatively-charged contaminants (e.g., arsenate,[376] perchlorate,[377] and chromate,[378] selenate[378] and sulfate.[378] While surfactant-modified zeolites have not been employed for urban stormwater treatment, their ability to remove a broad suite of contaminants is a promising quality for urban stormwater media. As for the longevity of this engineered media, Li et al. probed the biochemical stability of HDTMA-modified zeolites and observed that the HDTMA coating was stable at high ionic strength and over a wide pH range of 3–10.[379]

Furthermore, over 90% of the initial HDTMA remained bound to zeolites after 100 pore volume washes and over 98% remained on the surface after a 12–17 week incubation with activated sludge under aerobic and anaerobic conditions. These observations suggest that surfactant-modified zeolites may be viable as engineered urban stormwater treatment media.

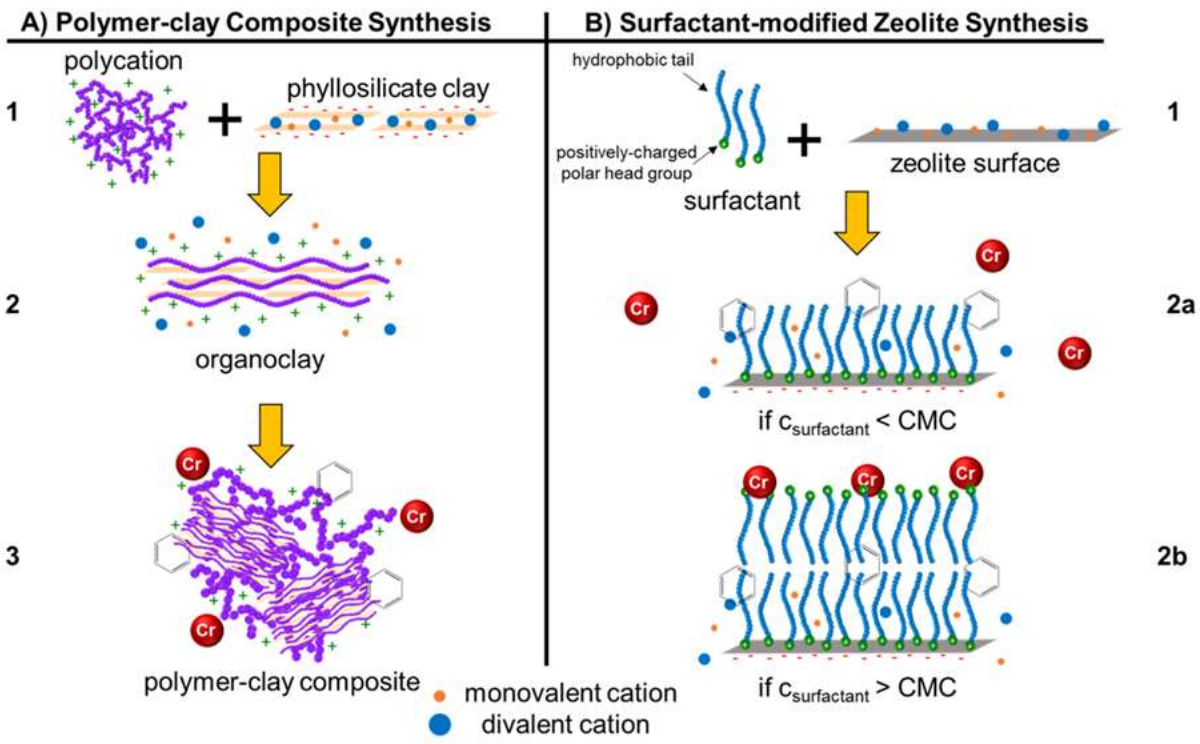

Figure E5. Schematic describing the synthesis of (A) polymer-clay composites and (B) surfactant modified zeolites. Polymer-clay composites are typically synthesized by (A1) mixing polycations and negatively charged phyllosilicate clays. Mono- and di-valent cations within the clay layers are exchanged with the positively charged monomers to create an (A2) organoclay, reversing the negative surface charge of the clay. Further addition of polycation will generate a (A3) composite of positively charged organoclays functionalized with hydrophobic domains to adsorb negatively charged species (e.g., CrO_4^{2-}) as well as organic compounds (e.g., benzene). (B1) Surfactant-modified zeolite synthesis undergoes a similar exchange of mono- and di-valent cations with a positively charged surfactant, such as hexadecyltrimethylammonium bromide. (B2a) The positively charged polar head groups will adsorb to the negatively charged zeolite surface exposing the hydrophobic surfactant tail, which can bind organic compounds. (B2b) If enough surfactant is added to induce micelle formation (e.g., critical micelle concentration (CMC) is reached), additional adsorption of negatively charged species can occur on the modified zeolite composite.

E4. Factors affecting media performance for contaminant removal

Many researchers characterizing novel media for stormwater remediation conduct lab-scale studies using synthetic stormwater to measure contaminant removal under ideal, consistent, and replicable conditions. However, prior to scaling up and implementing novel media in urban stormwater management systems, the following factors influencing contaminant removal must be considered: media characteristics, stormwater composition, and stormwater hydrology.

E4.1. Media Characteristics

In this review, we discuss various conventional and emerging materials designed to target the removal of inorganic and organic stormwater contaminants. The long-term durability and field efficacy of materials incorporated into existing urban stormwater BMPs depends on their chemical characteristics, structural integrity, and susceptibility to clogging and fouling. Here, we present current knowledge regarding the impact of these factors on stormwater treatment based on experimental data. In Section 5, we present several remaining factors requiring additional research to gain a deeper understanding of how stormwater media can be employed in existing treatment systems to improve urban stormwater quality.

E4.1.1 Porosity, Surface Area, Structural Integrity

Porous materials such as biochar and activated carbon are often used to sequester contaminants through intraparticle diffusion of pollutants within pores. Depending on the biomass feedstock and pyrolysis temperature used to produce biochar, the product porosity and bulk density can vary significantly.[380] The low bulk density and mechanical strength of some biochars may impact soil properties and make it difficult to incorporate biochar amendments into existing treatment systems. In particular, structural weaknesses in biochar[381] can cause it to break apart and lead to rapid and frequent clogging.[242] Additionally, biochar's porosity leads to higher water retention, which could also reduce urban stormwater permeability during infiltration. Low

hydraulic conductivity of biochar due to water retention may be overcome if the correct particle size, mass loading, and porosity are selected, particularly during stormwater infiltration applications. Extreme storm events such as floods can physically shear biochar (and similarly structured media), causing transport of contaminants to receiving waters. To mitigate this outcome and ensure that smaller particles are trapped more effectively, it is important to choose support media (e.g., gravel, sand, etc.) with the appropriate particle size, porosity, and density.

In addition to media porosity, other properties (e.g., particle size, surface area, hydration, etc.) can also impact urban stormwater contaminant removal in BMPs. Some media, like clays, can undergo structural changes when introduced to water. In particular, the characteristic layered structure of certain clays (e.g., montmorillonite and other smectites) allows water to become absorbed within the structure and the clay to swell, resulting in strong electrostatic repulsive forces between the negatively-charged layers and expansion.[382] Zeolites also exist in layered structures and can undergo swelling when introduced to water.[383] In fact, it is the expansion characteristic of these materials that contributes easy functionalization with polymers and surfactants. Once modified, as in the case of clays, swelling may occur despite the intercalation of polymers within the layers.[384] If the loading of functionalized clay and zeolite mineral amendments in urban stormwater infrastructure is too high, structural expansion and water absorption could reduce urban stormwater permeability and clog infiltration systems.[385] Considering that the frequency and intensity of stormwater events depend upon regional and seasonal weather patterns, it is often difficult to predict or control the structural changes that media can undergo.

E4.2. Stormwater Composition

In addition to media characteristics, the chemical properties (e.g., pH, redox potential) and composition of urban stormwater (e.g., suspended solids, cationic salts, dissolved organic matter, microbes) can dramatically impact media performance.

E4.2.1 Co-Occurring Inorganic Salts: Cationic Bridging, Nutrients, and Redox Potential

In addition to the target metal contaminants, other inorganic salts and species present in urban stormwater can impact media performance. For example, particularly in subsurface systems, the redox conditions are governed by inorganic species (e.g., Fe, S) and biological processes (e.g., denitrification and respiration). Stormwater media incorporated into subsurface treatment systems could therefore potentially interact with these species and processes that typically contribute to low dissolved oxygen levels and anoxic conditions. Aqueous redox conditions can also impact the solubility of certain metals (e.g., iron oxides can dissolve in anoxic conditions) and the transformation and degradation of certain contaminants (e.g., oxidation of trace organics and reduction of microorganisms/metals).[221]

Negatively-charged adsorbent media used in stormwater remediation (e.g., aluminosilicate clays, activated carbon, biochar) can undergo interactions with divalent cations (e.g., Ca^{2+}, Mg^{2+}) present in urban stormwater, which often serve as bridges between anionic contaminants and the media. Divalent cation bridging was introduced by McKinney[386] and Tezuka[387] as a mechanism for biological floc formation -- divalent cations bridge negatively-charged functional groups within extracellular polymeric substances to aggregate and stabilize microbes. A similar mechanism occurs between negatively-charged surface functional groups on stormwater media -- divalent cations and anionic contaminants in stormwater promote adsorption of compounds such as phosphate,[388] polysaccharides[389] and oils.[390] For example, per- and polyfluoroalkyl substances have been demonstrated to form complexes with biochar and

activated carbon through cationic bridging.[391] Divalent cations in urban stormwater infiltration systems where media is employed may also contribute to metals desorption (e.g., during snow deicing).[392]

E4.2.2 Co-Occurring Organics: DOC and Microbes

High molecular weight, negatively charged, colloidal, and hydrophobic organic species with numerous functional groups such as DOC[393] can also impact media contaminant removal efficacy during urban stormwater treatment in BMPs. DOC, a component of natural organic matter, is one of the most ubiquitous organic constituents in natural and engineered aquatic systems. DOC is notorious for adsorbing to media surfaces and competing with contaminants for adsorption sites.[394, 395] Passivation of media surfaces by DOC could also reduce the lifetime of stormwater media and treatment efficacy. The acidic functional groups of DOC behave similarly to those of metal oxides by participating in complexation of trace metals,[396] which may lead to enhanced contaminant removal if the metal-complexed DOC adsorbs to stormwater media surfaces.[242] During oxidative treatments (e.g., scenarios involving application of manganese oxide-coated sand media), the presence of DOC and its many aromatic and electron-rich moieties can act as an electron shuttle to promote redox reactions.[397]

Another important process impacting media performance is biological fouling, particularly for carbonaceous stormwater media like activated carbon and biochar. Microbes, like DOC, are ubiquitous in aquatic environments. Activated carbon and biochar are essentially carbon-rich substrates that can act as a food source to promote biological growth and fouling of media surfaces.[398] Biofouling of media surfaces will result in similar surface site passivation of stormwater media and reduce the long-term removal of trace contaminants during treatment. Over time, however, the biofilm formation on media surfaces may contribute to media-supported

biodegradation of organic contaminants in urban stormwater. In fact, with thoughtful design, known stormwater composition and redox conditions could be used to stimulate microbial growth using media like biochar.

E4.3. Media Quality Assessments for Field Applicability

The information in the preceding sections provide insight into the multitude of factors and attributes of stormwater and media associated with maximizing contaminant removal during urban stormwater treatment. There is potential for media amendment in existing stormwater BMPs to greatly increase contaminant removal during urban stormwater management. Trends of increasing annual precipitation in the United States[399] combined with the negative impacts of anthropogenic activity and frequency of extreme weather events (e.g., floods)[400] will result in more overflow events and will drive the need for improved urban runoff management. In regions prone to water scarcity, proper stormwater management can be leveraged to augment the urban water supply. Major cities are beginning to recognize the untapped potential of using urban runoff as a water resource investing millions of dollars to convert urban landscapes into stormwater capture basins and providing utility rebates to residences and commercial properties to financially incentivize urban stormwater capture.[401] For example, the City of Los Angeles and local stakeholders have partnered to transform an existing landfill in Sun Valley into the Rory M. Shaw Wetlands Park Project (cost: $22.5 million) to address local flooding issues and to increase water conservation efforts.[402] The City of Seattle Public Utilities offers a Residential RainWise rebate program to single family residences to install cisterns for stormwater capture and other green infrastructure such as rain gardens, porous pavement, and grass-centered driveways to help reduce the damage caused by combined sewer overflow events.[223] To help city planners and

researchers determine if a media is suitable for (de)centralized urban stormwater treatment, the authors recommend the following considerations and tests:

E4.3.1. Characterization of Media Physicochemical Properties

The discussions of conventional and engineered media have included information regarding specific properties linked to contaminant removal. If a new media is under consideration for a particular field application, it is necessary to understand the physical and chemical properties of the media to predict interactions with water, common stormwater matrix constituents, and contaminants of interest. Recommended analytical methods for characterizing stormwater media are provided in **Table E4**. It is important to note that the information of recommended analyses in this section is a limited view of many techniques available to characterize solid materials.

If the media is organic in nature (e.g., compost, activated carbon and biochar), the carbon content and corresponding porosity will be key predictors of aqueous interactions (including contaminants). As discussed previously, the media feedstock has significant implications on the type of contaminants removed and the affinity of those contaminants to the media. This is due in large part to the carbon content of the feed and the resulting aromaticity and porosity associated with the method of thermochemical (i.e., pyrolysis) processing. For example, a study by Singh et al. suggests that biochars produced from feedstocks with low carbon content (e.g., manure) and at low pyrolysis temperatures have 20 times less stability compared to biochars of high carbon content feeds and pyrolysis temperatures.[403] Proximate analysis and elemental composition provide important information regarding the composition of organic (particularly carbonaceous) media which is facilitated by TGA weight loss measurements upon heating (**Table E4**). The available surface area and porosity can be obtained via Brunauer-Emmett-Teller (BET) theory

and analysis. Following elemental analysis, if more information is desired regarding media aromaticity, ^{13}C nuclear magnetic resonance analysis can be performed.

For primarily inorganic media, several techniques can be employed to characterize mineral phases and structural and chemical bonding environments, which can provide insight into the potential for cation exchange capacity and complexation via acid-base functional groups. X-ray techniques (e.g., XRD and XRF, **Table E4**) provide structural and elemental composition information for inorganic materials with an atomic lattice structure.

Table 4: Techniques recommended for characterization of organic and inorganic media

Type of media	Instrument	Measured parameters	References
organic (carbonaceous)	Thermogravimetric Analyzer (TGA)	moisture, volatile matter, ash and fixed carbon	Mayoral et al.[404] Grønli et al.[405]
	CHNSO Elemental Analyzer	elemental composition	Kuwata et al.[406]
	BET Surface Analyzer	specific surface area, porosity	Dollimore et al.[407]
	Nuclear Magnetic Resonance (NMR)	^{13}C spectra, degree of aromaticity	Hammes et al.[408]
inorganic	X-ray Diffractometer (XRD)	phase identification and prediction, structure verification	Nayak and Singh[409]
	X-ray Fluorescence Spectrometer (XRF)	elemental composition	Elaiopoulos et al.[410]
organic and inorganic	X-ray Photoelectron Spectrometer (XPS)	surface analyses of atomic bonding, oxidation states, atomic properties	Smart et al.[411]
	Fourier-transform Infrared Spectrometer (FTIR): Attenuated Total Reflection (ATR) or Diffuse Reflectance Infrared Spectroscopy (DRIFTS)	bulk and surface chemical fingerprint	Yoon and Ratner[412]
	Zetasizer or Electrophoretic Light Scattering (ELS) Instrument	zeta potential (surface charge); electrophoretic	Jiang et al.[413]

	moieties	
Texture Analyzer	elastic modulus, hardness, fracture toughness	Jones et al.[414]
Column* Constant or Falling Head Tests	saturated hydraulic conductivity, water permeability	ASTM[415]

*Column refers to a filter column; this technique does not require analytical instrumentation

There are several analytical techniques that are suitable for both organic and inorganic media, making them particularly appropriate to characterize hybrid inorganic-organic composite media. XPS and FTIR provide surface chemistry and atomic bonding information, which can help identify available functional groups for stormwater contaminant removal. Media surface charge is another useful physicochemical quality that can facilitate contaminant removal and other electrostatic interactions with common ions in stormwater. Media hydraulic conductivity and water permeability are other important properties which can help assess the suitability of media for contaminant removal during urban stormwater treatment, particularly during stormwater infiltration applications. For example, a 30-month field study where biochar was amended in a sandy loam soil revealed that biochar resulted in increased local hydraulic conductivity and lower bulk density.[416] If the media has low hydraulic conductivity then augmented stormwater BMPs may become clogged during stormwater infiltration. Finally, it may be desirable to determine the media's mechanical strength if stress and shear are a concern for the structural stability in certain BMPs.

E4.3.2. Recommended Lab-scale Media Studies

Lab-scale studies provide practical and useful information of media behavior and performance, particularly when field-scale or pilot studies are too costly, difficult, or time consuming to execute. Many reports investigating media for stormwater treatment and water

treatment generally perform laboratory-scale batch experiments to gauge media contaminant affinity, kinetics, and removal capacity (e.g., isotherm experiments). Media behavior from batch studies can be informative to predict field performance; however, additional experiments may be required to more accurately assess media longevity and reactivity under field conditions. One important lab-scale experiment that should be considered for stormwater media is column infiltration. In contrast to batch studies, column studies allow media to continuously interact with a constant concentration of contaminants in the influent source. This distinction is critical to determining the lifetime of a stormwater media. Continuous operation and contaminant treatment will be applicable regardless of whether the media is implemented in (de)centralized BMPs for passive remediation or in designated treatment facilities near urban stormwater BMPs. Column studies can mimic field conditions of stormwater infiltration to allow for analysis of media behavior during intermittent storm events,[238, 260] after long periods of drying and rehydration, and media regeneration during backwashing.

E4.3.3. Leaching and Desorption

For long-term media stability in stormwater BMPs, it is important to determine the potential for leaching and desorption. There are limited studies (described in previous sections) that examine contaminant desorption during stormwater treatment. Desorption is particularly troublesome for adsorption-based media where contaminants may be loosely adsorbed via weak interactions such as electrostatic attraction or van der Waals and hydrophobic interactions. Furthermore, changes in stormwater composition can weaken contaminant chemisorption (e.g., hydrogen bonding, complexation) and lead to contaminant desorption from media in stormwater BMPs, which will neutralize any benefits of media amendment to reduce contaminant loads to receiving waters.

In addition to contaminant desorption, tests need to be conducted to determine if modifications to media surfaces will leach during stormwater infiltration. For example, a study on manganese oxide-coated sand suggests that the coating can leach from the sand surface during infiltration, releasing levels of dissolved manganese exceeding the EPA recommended level.[273] Both analyses of leaching and desorption are easily performed by taking advantage of column studies. Measuring contaminant concentrations in column effluent and detecting the presence of media modifiers (e.g., polymers) after complete breakthrough has been achieved will indicate if desorption and/or leaching has occurred. To mitigate the potential for additional environmental and human risks, it is important to consider the toxicities of media modification materials.

Table E5 (not shown). Summary of studies on conventional media performance to remove various stormwater pollutants. This table is contained in the associated Microsoft Excel® spreadsheet.

E5. Future Research Directions

This review presents an overview of physicochemical characteristics, reactivities, and interfacial properties of current and emerging media available to enhance contaminant removal of existing stormwater best management practices. The international stormwater database reveals that the most commonly used and monitored BMPs are grass swales, retention ponds, detention basins, and wetland basins. While these systems offer the potential to reduce runoff volume, our data synthesis indicates that they exhibit low removal efficiencies for many contaminants (e.g., < 40% for Total N, Total P, and COD). Furthermore, the lack of information on organic contaminant occurrence and removal as well as the variability in the type and number of reporting sites pose a challenge in fully assessing the performance of BMPs.

A variety of low-cost materials have been tested for stormwater pollutant removal. Organic materials such as compost, activated carbon, and biochar possess surface functional

groups favorable to adsorption of metals and trace organics. Although sand can maintain high hydraulic conductivity and effectively remove solids, it displays low affinity for dissolved contaminants such as nutrients and organic contaminants. Clays and zeolites are often employed to remove metals in stormwater. Nutrients such as ammonium can be removed through ion exchange processes by zeolites. Novel engineered media that modify or combine these conventional media (e.g., surfactant modified zeolites, polymer clay composites, metal oxide-coated sands) offer the benefit of enhancing stormwater pollutant removal without sacrificing hydraulic performance.

Studies on conventional and emerging media discussed in this review showed promising results for stormwater treatment. However, additional physicochemical characteristics impacting media performance and longevity must also be considered. For example, media with a high water retention capacity could be more prone to flooding and clogging during high volume storm events, ultimately resulting in a shorter lifetime. Additionally, stormwater composition can impact pollutant removal by altering stormwater pollutants or the surface of the media.

E6. Conclusions

In order to develop smarter designs of engineered systems for stormwater treatment, it is first crucial to improve our understanding of the relationship between media performance and hydrological factors such as intermittency of flow, length of wet and dry periods, and contaminant remobilization. For example, during extreme storm events, levels of contaminants will be high and treatment efficiency in BMPs will be reduced due to overwhelmed capacity. In the paper “Modelling Urban Stormwater Treatment—A Unified Approach”, Wong et al. present an algorithmic model to predict the hydrodynamic behavior of storage facilities (wetlands and ponds), vegetated swales, and infiltration systems (sediments basins and biofilters) operating

under variable conditions.[417] The authors conclude that the fundamental physical processes occurring in these systems during storm events include: (i) initial perception of contaminants through sedimentation and filtration and (ii) continuing flow attenuation and detention.[417] Future research is necessary to build stormwater treatment systems that can be operated at different spatial and temporal scales of hydraulic loading.

The majority of the current studies on conventional media for stormwater treatment have been conducted in synthetic water matrices (**Table E2**). There is a need for additional studies to be conducted using real stormwater matrices because, despite the high concentration and occurrence of certain common constituents (e.g., fats, oils, and greases rank third in **Table E1**), there is little research on the removal or impact of these constituents. For instance, only a few publications address the mechanisms employed by emerging engineered media to remove nutrients and nitrogenous compounds. Our synthesis of stormwater BMP data (**Figure E1**) showed low nutrient removal across all BMP categories, yet few studies evaluate the addition of engineered media to BMPs for the purpose of nutrient removal. Nitrogenous compound removal is impacted by nitrogen speciation and microbiological nitrification, processes that transform the nitrogen species but do not remove it.[226] Certain BMPs designed to have high infiltration rates give rise to aerobic conditions favoring nitrification,[226] which could lead to increased nitrate concentrations in stormwater treatment systems. Additionally, inputs of nitrogen in stormwater runoff are primarily in the form of dissolved nitrogen, which is soluble and difficult to capture. Engineered media can promote the removal of nitrogenous compounds and nutrients through ion exchange processes and co-precipitation with trace metals. However, depending on the corresponding solubility product, the pollutant concentration may not decrease to levels that conform to water quality standards. Thus, to gain a more comprehensive view of media

performance in contaminant removal, additional research on more realistic stormwater matrices containing representative pollutants (e.g., nutrients, fats, oils, greases) is necessary.

Few studies have focused on the durability and longevity of media intended for stormwater remediation or currently incorporated in existing stormwater BMP systems. Although some researchers have explored the impacts of regeneration and backwashing on increasing the lifetime of filtration media (e.g., manganese oxide-coated sand,[273] Al-Mg/graphene oxide composites,[278] base-treated juniper media,[418] there is a lack of published data from field studies to demonstrate the feasibility of these processes in real-world applications. Further research on waste management and media reuse is necessary to compare the levelized cost and labor implications of incorporating stormwater media into existing BMPs or replacing other remediation technologies.

Factors such as media characteristics (e.g., porosity, surface area, structural integrity) and stormwater composition (e.g., inorganic salts, nutrients, redox potential, microbes and DOC) can influence media performance and longevity. In order to fully assess the suitability and applicability of media, characterization analyses (e.g.) and column studies employing real stormwater matrices are needed.

Few studies examine stormwater treatment by media in BMPs in the United States at the pilot scale;[230, 231, 268, 419] however, it is this critical knowledge gap that limits deployment of media (particularly engineered media) in existing or new urban stormwater BMPs. For example, until the media are scrutinized under more realistic field-level conditions, it is difficult to assess economic viability, primary advantages and disadvantages with respect to contaminant sequestration and stormwater permeability, and opportunities for reuse and regeneration of

exhausted media. More pilot studies are imperative before media can be utilized regularly in urban stormwater treatment.

References

(1) Qasem, N. A. A.; Mohammed, R. H.; Lawal, D. U. Removal of heavy metal ions from wastewater: a comprehensive and critical review (vol 4, 36, 2021). *Npj Clean Water* **2021**, *4* (1). DOI: 10.1038/s41545-021-00144-z.

(2) Margot, J.; Rossi, L.; Barry, D. A.; Holliger, C. A review of the fate of micropollutants in wastewater treatment plants. *WIREs Water* **2015**, *2* (5), 457-487. DOI: 10.1002/wat2.1090.
(3) Bakare, B. F.; Adeyinka, G. C. Evaluating the Potential Health Risks of Selected Heavy Metals across Four Wastewater Treatment Water Works in Durban, South Africa. *Toxics* **2022**, *10* (6). DOI: 10.3390/toxics10060340.
(4) Kolpin, D. W.; Furlong, E. T.; Meyer, M. T.; Thurman, E. M.; Zaugg, S. D.; Barber, L. B.; Buxton, H. T. Pharmaceuticals, Hormones, and Other Organic Wastewater Contaminants in U.S. Streams, 1999−2000: A National Reconnaissance. *Environ. Sci. Technol.* **2002**, *36* (6), 1202-1211. DOI: 10.1021/es011055j.
(5) Miklos, D. B.; Remy, C.; Jekel, M.; Linden, K. G.; Drewes, J. E.; Hubner, U. Evaluation of advanced oxidation processes for water and wastewater treatment - A critical review. *Water Res.* **2018**, *139*, 118-131. DOI: 10.1016/j.watres.2018.03.042.
(6) Schwarzenbach, R. P.; Escher, B. I.; Fenner, K.; Hofstetter, T. B.; Johnson, C. A.; von Gunten, U.; Wehrli, B. The challenge of micropollutants in aquatic systems. *Science* **2006**, *313* (5790), 1072-1077. DOI: 10.1126/science.1127291.
(7) Asano, T. *Water reuse : issues, technologies, and applications*; McGraw-Hill, 2007.
(8) Eggen, R. I. L.; Hollender, J.; Joss, A.; Scharer, M.; Stamm, C. Reducing the Discharge of Micropollutants in the Aquatic Environment: The Benefits of Upgrading Wastewater Treatment Plants. *Environ. Sci. Tehnol.* **2014**, *48*, 7683-7689.
(9) Khan, J.; Lin, S.; Nizeyimana, J. C.; Wu, Y.; Wang, Q.; Liu, X. Removal of copper ions from wastewater via adsorption on modified hematite (α-Fe2O3) iron oxide coated sand. *J. Cleaner Prod.* **2021**, *319* (128687). DOI: https://doi.org/10.1016/j.jclepro.2021.128687.
(10) Lindqvist, N.; Tuhkanen, T.; Kronberg, L. Occurrence of acidic pharmaceuticals in raw and treated sewages and in receiving waters. *Water Res.* **2005**, *39*, 2219-2228. DOI: 10.1016/j.watres.2005.04.003.
(11) Rout, P. R.; Zhang, T. C.; Bhunia, P.; Surampalli, R. Y. Treatment technologies for emerging contaminants in wastewater treatment plants: A review. *Sci. Total Environ.* **2021**, *753*. DOI: 10.1016/j.scitotenv.2020.141990.

(12) Dodd, M. C.; Huang, C.-H. Transformation of the Antibacterial Agent Sulfamethoxazole in Reactions with Chlorine: Kinetics, Mechanisms, and Pathways. *Environ. Sci. Tehnol.* **2004**, *38*, 5607-5615. DOI: 10.1021/es035225z.
(13) Karaolia, P.; Michael, I.; Garcia-Fernandez, I.; Aguera, A.; Malato, S.; Fernandez-Ibanez, P.; Fatta-Kassinos, D. Reduction of clarithromycin and sulfamethoxazole-resistant Enterococcus by pilot-scale solar-driven Fenton oxidation. *Sci. Total Environ.* **2014**, *468-469*, 19-27. DOI: 10.1016/j.scitotenv.2013.08.027
(14) Tetreault, G. R.; Bennett, C. J.; Cheng, C.; Servos, M. R.; McMaster, M. E. Reproductive and histopathological effects in wild fish inhabiting an effluent-dominated stream, Wascana Creek, SK, Canada. *Aquat. Toxicol.* **2012**, *110*, 149-161. DOI: 10.1016/j.aquatox.2012.01.004.

(15) Vajda, A. M.; Barber, L. B.; Gray, J. L.; Lopez, E. M.; Woodling, J. D.; Norris, D. O. Reproductive disruption in fish downstream from an Estrogenic wastewater effluent. *Environ. Sci. Technol.* **2008**, *42* (9), 3407-3414. DOI: 10.1021/es0720661.
(16) Kidd, K. A.; Blanchfield, P. J.; Mills, K. H.; Palace, V. P.; Evans, R. E.; Lazorchak, J. M.; Flick, R. W. Collapse of a fish population after exposure to a synthetic estrogen. *Proceedings of the National Academy of Sciences* **2007**, *104* (21), 8897-8901. DOI: 10.1073/pnas.0609568104.
(17) Lee, Y.; Kovalova, L.; McArdell, C. S.; von Gunten, U. Prediction of micropollutant elimination during ozonation of a hospital wastewater effluent. *Water Res.* **2014**, *64*, 134-148. DOI: 10.1016/j.watres.2014.06.027.
(18) Von Gunten, U. Ozonation of drinking water: Part II. Disinfection and by-product formation in presence of bromide, iodide or chlorine. *Water Res.* **2003**, *37* (7), 1469-1487. DOI: 10.1016/s0043-1354(02)00458-x.
(19) Richardson, S.; Plewa, M.; Wagner, E.; Schoeny, R.; Demarini, D. Occurrence, genotoxicity, and carcinogenicity of regulated and emerging disinfection by-products in drinking water: A review and roadmap for research. *Mutat. Res. Rev. Mutat. Res.* **2007**, *636* (1-3), 178-242. DOI: 10.1016/j.mrrev.2007.09.001.
(20) Hua, G.; Reckhow, D. A. Comparison of disinfection byproduct formation from chlorine and alternative disinfectants. *Water Res.* **2007**, *41* (8), 1667-1678. DOI: 10.1016/j.watres.2007.01.032.
(21) Von Gunten, U. Oxidation Processes in Water: Are We on Track? *Environ. Sci. Technol.* **2018**, *52*, 5062-5075. DOI: https://doi.org/10.1021/acs.est.8b00586.
(22) Kosaka, K.; Asami, M.; Konno, Y.; Oya, M.; Kunikane, S. Identification of Antiyellowing Agents as Precursors of N-Nitrosodimethylamine Production on Ozonation from Sewage Treatment Plant Influent. *Environ. Sci. Tehnol.* **2009**, *43*, 5236-5241. DOI: https://doi.org/10.1021/es900227g.
(23) Watts, M. J.; Linden, K. G. Chlorine photolysis and subsequent OH radical production during UV treatment of chlorinated water. *Water Res. (Oxford)* **2007**, *41* (13), 2871-2878. DOI: 10.1016/j.watres.2007.03.032.
(24) Watts, M. J.; Rosenfeldt, E. J.; Linden, K. G. Comparative OH radical oxidation using UV-Cl2 and UV-H2O2 processes. *Aqua (London)* **2007**, *56* (8), 469-477. DOI: 10.2166/aqua.2007.028.
(25) Wols, B. A.; Hofman-Caris, C. H. M.; Harmsen, D. J. H.; Beerendonk, E. F. Degradation of 40 selected pharmaceuticals by UV/H2O2. *Water Res.* **2013**, *47* (15), 5876-5888. DOI: 10.1016/j.watres.2013.07.008.
(26) Chaplin, B. P. Critical review of electrochemical advanced oxidation processes for water treatment applications. *Environ. Sci. Process. Impacts.* **2014**, *16* (6), 1182-1123. DOI: 10.1039/c3em00679d.
(27) Wadley, S.; Waite, T. D. I. Fenton Process. In *Advanced Oxidation Processes for Water and Wastewater Treatment*, IWA Publishing, 2004; pp 111-136.
(28) Zhang, M. H.; Dong, H.; Zhao, L.; Wang, D. X.; Meng, D. A review on Fenton process for organic wastewater treatment based on optimization perspective. *Sci. Total Environ.* **2019**, *670*, 110-121. DOI: 10.1016/j.scitotenv.2019.03.180.
(29) Garrido-Cardenas, J. A.; Esteban-García, B.; Agüera, A.; Sánchez-Pérez, J. A.; Manzano-Agugliaro, F. Wastewater Treatment by Advanced Oxidation Process and Their Worldwide Research Trends. *Int. J. Env. Res. Pub. He.* **2020**, *17* (1). DOI: 10.3390/ijerph17010170.

(30) Scruggs, C. E.; Thomson, B. M. Opportunities and Challenges for Direct Potable Water Reuse in Arid Inland Communities. *J. Water. Res. Plan. Man.* **2017**, *143* (10). DOI: 10.1061/(Asce)Wr.1943-5452.0000822.

(31) Sharma, V. K.; Chen, L.; Zboril, R. Review on High Valent FeVI (Ferrate): A Sustainable Green Oxidant in Organic Chemistry and Transformation of Pharmaceuticals. *ACS Sustain. Chem. Eng.* **2016**, *4* (1), 18-34. DOI: 10.1021/acssuschemeng.5b01202.
(32) Sharma, V. K.; Zboril, R.; Varma, R. S. Ferrates: greener oxidants with multimodal action in water treatment technologies. *Acc. Chem. Res.* **2015**, *48* (2), 182-191. DOI: 10.1021/ar5004219.
(33) Licht, S.; Naschitz, V.; Liu, B.; Ghosh, S.; Halperin, N.; Halperin, L.; Rozen, D. Chemical synthesis of battery grade super-iron barium and potassium Fe(VI) ferrate compounds. *J. Power Sources* **2001**, *99* (1-2), 7-14. DOI: Doi 10.1016/S0378-7753(00)00658-3.
(34) Wang, S. Q.; Yang, Z. H.; Liu, D. R.; Wang, S. W. Ultrasonic-assisted convenient chemical synthesis of battery grade potassium ferrate(VI). *Electrochim. Acta* **2010**, *55* (6), 1985-1989. DOI: 10.1016/j.electacta.2009.11.019.
(35) Norcross, B. E.; Lewis, W. C.; Gai, H. F.; Noureldin, N. A.; Lee, D. G. The oxidation of secondary alcohols by potassium tetraoxoferrate(VI). *Canadian Journal of Chemistry-Revue Canadienne De Chimie* **1997**, *75* (2), 129-139. DOI: DOI 10.1139/v97-017.
(36) Li, C.; Li, X. Z.; Graham, N.; Gao, N. Y. The aqueous degradation of bisphenol A and steroid estrogens by ferrate. *Water Res.* **2008**, *42* (1-2), 109-120. DOI: 10.1016/j.watres.2007.07.023.
(37) Sharma, V. K.; Mishra, S. K.; Nesnas, N. Oxidation of Sulfonamide Antimicrobials by Ferrate(VI) [$Fe^{VI}O_4^{2-}$]. *Environ. Sci. Tehnol.* **2006**, *40*, 7222-7227. DOI: https://doi.org/10.1021/es060351z.

(38) Anquandah, G. A. K.; Sharma, V. K.; Knight, D. A.; Batchu, S. R.; Gardinali, P. R. Oxidation of Trimethoprim by Ferrate(VI): Kinetics, Products, and Antibacterial Activity. *Environ. Sci. Technol.* **2011**, *45* (24), 10575-10581. DOI: 10.1021/es202237g.
(39) Feng, M.; Wang, X.; Chen, J.; Qu, R.; Sui, Y.; Cizmas, L.; Wang, Z.; Sharma, V. K. Degradation of fluoroquinolone antibiotics by ferrate(VI): Effects of water constituents and oxidized products. *Water Res.* **2016**, *103*, 48-57. DOI: 10.1016/j.watres.2016.07.014.
(40) Sharma, V. K.; Mishra, S. K.; Ray, A. K. Kinetic assessment of the potassium ferrate(VI) oxidation of antibacterial drug sulfamethoxazole. *Chemosphere* **2006**, *62* (1), 128-134. DOI: 10.1016/j.chemosphere.2005.03.095.
(41) Yang, B.; Ying, G.-G.; Zhang, L.-J.; Zhou, L.-J.; Liu, S.; Fang, Y.-X. Kinetics modeling and reaction mechanism of ferrate(VI) oxidation of benzotriazoles. *Water Res.* **2011**, *45*, 2261-2269. DOI: https://doi.org/10.1016/j.watres.2011.01.022.
(42) Yang, B.; Ying, G.-G.; Zhao, J.-L.; Liu, S.; Zhou, L.-J.; Chen, F. Removal of selected endocrine disrupting chemicals (EDCs) and pharmaceuticals and personal care products (PPCPs) during ferrate(VI) treatment of secondary wastewater effluents. *Water Res.* **2012**, *46* (7), 2194-2204. DOI: 10.1016/j.watres.2012.01.047.
(43) Zajíček, P.; Kolář, M.; Prucek, R.; Ranc, V.; Bednář, P.; Varma, R. S.; Sharma, V. K.; Zbořil, R. Oxidative degradation of triazine- and sulfonylurea-based herbicides using Fe(VI): The case study of atrazine and iodosulfuron with kinetics and degradation products. *Sep. Purif. Technol.* **2015**, *156*, 1041-1046. DOI: 10.1016/j.seppur.2015.08.024.

(44) Wang, S.; Shao, B.; Qiao, J.; Guan, X. Application of Fe(VI) in abating contaminants in water: State of art and knowledge gaps. *Front. Environ. Sci. Eng.* **2021**, *15* (5). DOI: 10.1007/s11783-020-1373-3.
(45) Lee, Y.; Zimmermann, S. G.; Kieu, A. T.; Von Gunten, U. Ferrate (Fe(VI)) Application for Municipal Wastewater Treatment: A Novel Process for Simultaneous Micropollutant Oxidation and Phosphate Removal. *Environ. Sci. Technol.* **2009**, *43* (10), 3831-3838. DOI: 10.1021/es803588k.
(46) Prucek, R.; Tucek, J.; Kolarik, J.; Huskova, I.; Filip, J.; Varma, R. S.; Sharma, V. K.; Zboril, R. Ferrate(VI)-prompted removal of metals in aqueous media: mechanistic delineation of enhanced efficiency via metal entrenchment in magnetic oxides. *Environ. Sci. Technol.* **2015**, *49* (4), 2319-2327. DOI: 10.1021/es5048683.
(47) Lim, M.; Kim, M.-J. Effectiveness of Potassium Ferrate (K2FeO4) for Simultaneous Removal of Heavy Metals and Natural Organic Matters from River Water. *Water, Air, Soil Pollut.* **2010**, *211* (1-4), 313-322. DOI: 10.1007/s11270-009-0302-7.
(48) Cui, J.; Zheng, L.; Deng, Y. Emergency water treatment with ferrate(vi) in response to natural disasters. *Environ. Sci. Water Res. Technol.* **2018**, *4* (3), 359-368. DOI: 10.1039/c7ew00467b.
(49) Prucek, R.; Tuček, J.; Kolařík, J.; Filip, J.; Marušák, Z.; Sharma, V. K.; Zbořil, R. Ferrate(VI)-Induced Arsenite and Arsenate Removal by In Situ Structural Incorporation into Magnetic Iron(III) Oxide Nanoparticles. *Environ. Sci. Technol.* **2013**, *47* (7), 3283-3292. DOI: 10.1021/es3042719.
(50) Wang, N.; Wang, N.; Tan, L.; Zhang, R.; Zhao, Q.; Wang, H. Removal of aqueous As(III) Sb(III) by potassium ferrate (K_2FeO_4): The function of oxidation and flocculation. *Sci. Total Environ.* **2020**, *726*, 138541. DOI: 10.1016/j.scitotenv.2020.138541.
(51) Goodwill, J. E.; Mai, X.; Jiang, Y.; Reckhow, D. A.; Tobiason, J. E. Oxidation of manganese(II) with ferrate: Stoichiometry, kinetics, products and impact of organic carbon. *Chemosphere* **2016**, *159*, 457-464. DOI: 10.1016/j.chemosphere.2016.06.014.
(52) Sharma, V. K. Disinfection performance of Fe(VI) in water and wastewater: a review. *Water Sci. Technol.* **2007**, *55* (1-2), 225-232. DOI: 10.2166/wst.2007.019.
(53) Fan, J.; Lin, B.-H.; Chang, C.-W.; Zhang, Y.; Lin, T.-F. Evaluation of potassium ferrate as an alternative disinfectant on cyanobacteria inactivation and associated toxin fate in various waters. *Water Res.* **2018**, *129*, 199-207. DOI: 10.1016/j.watres.2017.11.026.
(54) Jiang, J.-Q.; Wang, S.; Panagoulopoulos, A. The role of potassium ferrate(VI) in the inactivation of Escherichia coli and in the reduction of COD for water remediation. *Desalination* **2007**, *210* (1-3), 266-273. DOI: 10.1016/j.desal.2006.05.051.
(55) Jiang, J.-Q.; Lloyd, B. Progress in the Development and Use of Ferrate(VI) Salts as an Oxidant and Coagulant for Water and Wastewater Treatment. *Water Res.* **2002**, *36*, 1397-1408.
(56) Jiang, J.-Q.; Wang, S.; Panagoulopoulos, A. The exploration of potassium ferrate(VI) as a disinfectant/coagulant in water and wastewater treatment. *Chemosphere* **2006**, *63* (2), 212-219. DOI: 10.1016/j.chemosphere.2005.08.020.
(57) Hao, L.; Liu, M.; Wang, N.; Li, G. A critical review on arsenic removal from water using iron-based adsorbents. *RSC Advances* **2018**, *8* (69), 39545-39560. DOI: 10.1039/c8ra08512a.
(58) Sharma, V. K. Oxidation of inorganic contaminants by ferrates (VI, V, and IV)--kinetics and mechanisms: a review. *J. Environ. Manage.* **2011**, *92* (4), 1051-1073. DOI: 10.1016/j.jenvman.2010.11.026.

(59) Jiang, Y.; Goodwill, J. E.; Tobiason, J. E.; Reckhow, D. A. Bromide oxidation by ferrate(VI): The formation of active bromine and bromate. *Water Res.* **2016**, *96*, 188-197. DOI: 10.1016/j.watres.2016.03.065.
(60) Han, Q.; Wang, H.; Dong, W.; Liu, T.; Yin, Y. Formation and inhibition of bromate during ferrate(VI) – Ozone oxidation process. *Sep. Purif. Technol.* **2013**, *118*, 653-658. DOI: 10.1016/j.seppur.2013.07.042.
(61) Liu, J.; Lujan, H.; Dhungana, B.; Hockaday, W. C.; Sayes, C. M.; Cobb, G. P.; Sharma, V. K. Ferrate(VI) pretreatment before disinfection: An effective approach to controlling unsaturated and aromatic halo-disinfection byproducts in chlorinated and chloraminated drinking waters. *Environ. Inter.* **2020**, *138*, 105641. DOI: 10.1016/j.envint.2020.105641.
(62) Han, Q.; Wang, H.; Dong, W.; Liu, T.; Yin, Y. Formation and inhibition of bromate during ferrate(VI) – Ozone oxidation process. *Sep. Purif. Technol.* **2013**, *118*, 653-658. DOI: 10.1016/j.seppur.2013.07.042.
(63) Gombos, E.; Barkács, K.; Felföldi, T.; Vértes, C.; Makó, M.; Palkó, G.; Záray, G. Removal of organic matters in wastewater treatment by ferrate (VI)-technology. *Microchem. J.* **2013**, *107*, 115-120. DOI: 10.1016/j.microc.2012.05.019.
(64) Sharma, V. K. Ferrate(VI) and ferrate(V) oxidation of organic compounds: Kinetics and mechanism. *Coord. Chem. Rev.* **2013**, *257* (2), 495-510. DOI: 10.1016/j.ccr.2012.04.014.
(65) Karlesa, A.; De Vera, G. A. D.; Dodd, M. C.; Park, J.; Espino, M. P. B.; Lee, Y. Ferrate(VI) Oxidation of β-Lactam Antibiotics: Reaction Kinetics, Antibacterial Activity Changes, and Transformation Products. *Environ. Sci. Technol.* **2014**, *48* (17), 10380-10389. DOI: 10.1021/es5028426.
(66) Hu, L.; Martin, H. M.; Arcs-Bulted, O.; Sugihara, M. N.; Keatlng, K. A.; Strathmann, T. J. Oxidation of Carbamazepine by Mn(VII) and Fe(VI): Reaction Kinetics and Mechanism. *Environ. Sci. Technol.* **2009**, *43* (2), 509-515. DOI: 10.1021/es8023513.
(67) Ma, Y.; Gao, N.; Li, C. Degradation and Pathway of Tetracycline Hydrochloride in Aqueous Solution by Potassium Ferrate. *Environ. Eng. Sci.* **2012**, *29* (5), 357-362. DOI: 10.1089/ees.2010.0475.
(68) Manoli, K.; Nakhla, G.; Feng, M.; Sharma, V. K.; Ray, A. K. Silica gel-enhanced oxidation of caffeine by ferrate(VI). *Chem. Eng. J.* **2017**, *330*, 987-994. DOI: 10.1016/j.cej.2017.08.036.
(69) Sharma, V. K.; Burnett, C. R.; O'Connor, D. B.; Cabelli, D. Iron(VI) and iron(V) oxidation of thiocyanate. *Environ. Sci. Technol.* **2002**, *36* (19), 4182-4186. DOI: 10.1021/es020570u.
(70) Sharma, V. K.; Burnett, C. R.; Yngard, R. A.; Cabelli, D. E. Iron(VI) and Iron(V) Oxidation of Copper(I) Cyanide. *Environ. Sci. Technol.* **2005**, *39* (10), 3849-3854. DOI: 10.1021/es048196g.
(71) Sharma, V. K.; Feng, M. B.; Dionysiou, D. D.; Zhou, H. C.; Jinadatha, C.; Manoli, K.; Smith, M. F.; Luque, R.; Ma, X. M.; Huang, C. H. Reactive High-Valent Iron Intermediates in Enhancing Treatment of Water by Ferrate. *Environ. Sci. Technol.* **2022**, *56* (1), 30-47. DOI: 10.1021/acs.est.1c04616.
(72) Yates, B. J.; Darlington, R.; Zboril, R.; Sharma, V. K. High-valent iron-based oxidants to treat perfluorooctanesulfonate and perfluorooctanoic acid in water. *Environ. Chem. Lett.* **2014**, *12* (3), 413-417. DOI: 10.1007/s10311-014-0463-5.
(73) Kralchevska, R. P.; Prucek, R.; Kolarík, J.; Tucek, J.; Machala, L.; Filip, J.; Sharma, V. K.; Zboril, R. Remarkable efficiency of phosphate removal: Ferrate(VI)-induced in situ sorption on core-shell nanoparticles. *Water Res.* **2016**, *103*, 83-91. DOI: 10.1016/j.watres.2016.07.021.

(74) Dong, S.; Mu, Y.; Sun, X. Removal of toxic metals using ferrate(VI): a review. *Water Sci. Technol.* **2019**, *80* (7), 1213-1225. DOI: 10.2166/wst.2019.376.
(75) Xie, X.; Cheng, H. A simple treatment method for phenylarsenic compounds: Oxidation by ferrate (VI) and simultaneous removal of the arsenate released with in situ formed Fe(III) oxide-hydroxide. *Environ Int* **2019**, *127*, 730-741. DOI: 10.1016/j.envint.2019.03.059.
(76) Sailo, L.; Pachuau, L.; Yang, J. K.; Lee, S. M.; Tiwari, D. Efficient use of ferrate(VI) for the remediation of wastewater contaminated with metal complexes. *Environ. Eng. Res.* **2015**, *20* (1), 89-97. DOI: 10.4491/eer.2014.079.
(77) Tiwari, D.; Sailo, L.; Pachuau, L. Remediation of aquatic environment contaminated with the iminodiacetic acid metal complexes using ferrate(VI). *Sep. Purif. Technol.* **2014**, *132*, 77-83. DOI: 10.1016/j.seppur.2014.05.010.
(78) Chen, G.; Lam, W. W. Y.; Lo, P. K.; Man, W. L.; Chen, L.; Lau, K. C.; Lau, T. C. Mechanism of Water Oxidation by Ferrate(VI) at pH 7–9. *Chemistry – A European Journal* **2018**, *24* (70), 18735-18742. DOI: 10.1002/chem.201803757.
(79) Cheung, P. C. W.; Williams, D. R.; Barrett, J.; Barker, J.; Kirk, D. W. On the Origins of Some Spectroscopic Properties of "Purple Iron" (the Tetraoxoferrate(VI) Ion) and Its Pourbaix Safe-Space. *Molecules* **2021**, *26* (17), 5266. DOI: 10.3390/molecules26175266.
(80) Lee, Y.; Um, I. H.; Yoon, J. Arsenic(III) oxidation by iron(VI) (ferrate) and subsequent removal of arsenic(V) by iron(III) coagulation. *Environ. Sci. Technol.* **2003**, *37* (24), 5750-5756. DOI: 10.1021/es034203+.
(81) SCHREYER, J. M.; OCKERMAN, L. T. Stability of the Ferrate(VI) Ion in Aqueous Solution. *Anal. Chem.* **1951**, *23*, 1312−1314.
(82) Ma, L.; Lam, W. W. Y.; Lo, P. K.; Lau, K. C.; Lau, T. C. Ca-Induced Oxygen Generation by FeO at pH 9-10. *Angew Chem Int Edit* **2016**, *55* (9), 3012-3016. DOI: DOI 10.1002/anie.201510156.

(83) Jiang, Y.; Goodwill, J. E.; Tobiason, J. E.; Reckhow, D. A. Effect of Different Solutes, Natural Organic Matter, and Particulate Fe(III) on Ferrate(VI) Decomposition in Aqueous Solutions. *Environ. Sci. Technol.* **2015**, *49* (5), 2841-2848. DOI: 10.1021/es505516w.
(84) Kolář, M.; Novák, P.; Šišková, K. M.; Machala, L.; Malina, O.; Tuček, J.; Sharma, V. K.; Zbořil, R. Impact of inorganic buffering ions on the stability of Fe(vi) in aqueous solution: role of the carbonate ion. *Phys. Chem. Chem. Phys.* **2016**, *18* (6), 4415-4422. DOI: 10.1039/c5cp07543b.
(85) Wang, B.; Lan, C. Q. Biomass production and nitrogen and phosphorus removal by the green alga Neochloris oleoabundans in simulated wastewater and secondary municipal wastewater effluent. *Bioresour. Technol.* **2011**, *102* (10), 5639-5644. DOI: 10.1016/j.biortech.2011.02.054.
(86) Burton, F. L.; Tchobanoglous, G.; Tsuchihashi, R.; Stensel, H. D.; Metcalf; Eddy, I. *Wastewater Engineering: Treatment and Resource Recovery*; McGraw-Hill Education, 2013.
(87) Azoulay, A.; Garzon, P.; Eisenberg, M. J. Comparison of the mineral content of tap water and bottled waters. *J. Gen. Intern. Med.* **2001**, *16* (3), 168-175. DOI: 10.1111/j.1525-1497.2001.04189.x.
(88) Xu, J. L.; Kralles, Z. T.; Dai, N. Effects of Sunlight on the Trichloronitromethane Formation Potential of Wastewater Effluents: Dependence on Nitrite Concentration. *Environ. Sci. Technol.* **2019**, *53* (8), 4285-4294. DOI: 10.1021/acs.est.9b00447.
(89) Pinter, J.; Jones, B. S.; Vriens, B. Loads and elimination of trace elements in wastewater in the Great Lakes basin. *Water Res.* **2022**, *209*, 117949. DOI: 10.1016/j.watres.2021.117949.

(90) Maizel, A. C.; Remucal, C. K. The effect of advanced secondary municipal wastewater treatment on the molecular composition of dissolved organic matter. *Water Res.* **2017**, *122*, 42-52. DOI: 10.1016/j.watres.2017.05.055.
(91) Griffith, D. R.; Barnes, R. T.; Raymond, P. A. Inputs of Fossil Carbon from Wastewater Treatment Plants to U.S. Rivers and Oceans. *Environ. Sci. Technol.* **2009**, *43* (15), 5647-5651. DOI: 10.1021/es9004043.
(92) Manoli, K.; Nakhla, G.; Ray, A. K.; Sharma, V. K. Oxidation of caffeine by acid-activated ferrate(VI): Effect of ions and natural organic matter. *AIChE J.* **2017**, *63* (11), 4998-5006. DOI: 10.1002/aic.15878.
(93) Wang, H. Y.; Liu, Y. B.; Jiang, J. Q. Reaction kinetics and oxidation product formation in the degradation of acetaminophen by ferrate (VI). *Chemosphere* **2016**, *155*, 583-590. DOI: 10.1016/j.chemosphere.2016.04.088.
(94) Deng, Y.; Jung, C.; Liang, Y. M.; Goodey, N.; Waite, T. D. Ferrate(VI) decomposition in water in the absence and presence of natural organic matter (NOM). *Chem. Eng. J.* **2018**, *334*, 2335-2342. DOI: 10.1016/j.cej.2017.12.006.
(95) Feng, M.; Wang, X.; Chen, J.; Qu, R.; Sui, Y.; Cizmas, L.; Wang, Z.; Sharma, V. K. Degradation of fluoroquinolone antibiotics by ferrate(VI): Effects of water constituents and oxidized products. *Water Res* **2016**, *103*, 48-57. DOI: 10.1016/j.watres.2016.07.014.
(96) Manoli, K.; Nakhla, G.; Ray, A. K.; Sharma, V. K. Oxidation of caffeine by acid-activated ferrate(VI): Effect of ions and natural organic matter. *Aiche J.* **2017**, *63* (11), 4998-5006. DOI: 10.1002/aic.15878.
(97) Feng, M.; Cizmas, L.; Wang, Z.; Sharma, V. K. Activation of ferrate(VI) by ammonia in oxidation of flumequine: Kinetics, transformation products, and antibacterial activity assessment. *Chem. Eng. J.* **2017**, *323*, 584-591. DOI: http://dx.doi.org/10.1016/j.cej.2017.04.123.
(98) Delaude, L.; Laszlo, P. A novel oxidizing reagent based on potassium ferrate(VI). *J. Org. Chem.* **1996**, *61* (18), 6360-6370. DOI: DOI 10.1021/jo960633p.
(99) Manoli, K.; Nakhla, G.; Feng, M.; Sharma, V. K.; Ray, A. K. Silica gel-enhanced oxidation of caffeine by ferrate(VI). *Chem. Eng. J.* **2017**, *330*, 987-994. DOI: 10.1016/j.cej.2017.08.036.
(100) Al-Abduly, A.; Sharma, V. K. Oxidation of benzothiophene, dibenzothiophene, and methyl-dibenzothiophene by ferrate(VI). *J Hazard Mater* **2014**, *279*, 296-301. DOI: 10.1016/j.jhazmat.2014.06.083.
(101) Kinsela, A. S.; Jones, A. M.; Bligh, M. W.; Pham, A. N.; Collins, R. N.; Harrison, J. J.; Wilsher, K. L.; Payne, T. E.; Waite, T. D. Influence of Dissolved Silicate on Rates of Fe(II) Oxidation. *Environ. Sci. Technol.* **2016**, *50* (21), 11663-11671. DOI: 10.1021/acs.est.6b03015.
(102) Schaller, J.; Cramer, A.; Carminati, A.; Zarebanadkouki, M. Biogenic amorphous silica as main driver for plant available water in soils. *Sci Rep-Uk* **2020**, *10* (1). DOI: 10.1038/s41598-020-59437-x.
(103) Jiang, J. Q.; Wang, S.; Panagoulopoulos, A. The exploration of potassium ferrate(VI) as a disinfectant/coagulant in water and wastewater treatment. *Chemosphere* **2006**, *63* (2), 212-219. DOI: 10.1016/j.chemosphere.2005.08.020.
(104) Manger, G. E. A Mineral Analysis of Some Common Sands and Their Silica Content. *J. Sediment. Petrol.* **1934**, *4* (3), 141-151.
(105) Von Gunten, U. Ozonation of drinking water: Part I. Oxidation kinetics and product formation. *Water Res.* **2003**, *37* (7), 1443-1467. DOI: 10.1016/s0043-1354(02)00457-8.
(106) Wenk, J.; Aeschbacher, M.; Salhi, E.; Canonica, S.; Von Gunten, U.; Sander, M. Chemical Oxidation of Dissolved Organic Matter by Chlorine Dioxide, Chlorine, And Ozone: Effects on

Its Optical and Antioxidant Properties. *Environ. Sci. Technol.* **2013**, *47* (19), 11147-11156. DOI: 10.1021/es402516b.
(107) Pan, Y.; Zhang, X. Four Groups of New Aromatic Halogenated Disinfection Byproducts: Effect of Bromide Concentration on Their Formation and Speciation in Chlorinated Drinking Water. *Environ. Sci. Technol.* **2013**, *47* (3), 1265-1273. DOI: 10.1021/es303729n.
(108) Rodríguez, E.; Onstad, G. D.; Kull, T. P. J.; Metcalf, J. S.; Acero, J. L.; Von Gunten, U. Oxidative elimination of cyanotoxins: Comparison of ozone, chlorine, chlorine dioxide and permanganate. *Water Res.* **2007**, *41* (15), 3381-3393. DOI: 10.1016/j.watres.2007.03.033.
(109) Hu, J.-Y.; Aizawa, T.; Ookubo, S. Products of Aqueous Chlorination of Bisphenol A and Their Estrogenic Activity. *Environ. Sci. Technol.* **2002**, *36* (9), 1980-1987. DOI: 10.1021/es011177b.
(110) Alum, A.; Yoon, Y.; Westerhoff, P.; Abbaszadegan, M. Oxidation of bisphenol A, 17?-estradiol, and 17?-ethynyl estradiol and byproduct estrogenicity. *Environ. Toxicol.* **2004**, *19* (3), 257-264. DOI: 10.1002/tox.20018.
(111) Gomes, J. F.; Frasson, D.; Pereira, J. L.; Goncalves, F. J. M.; Castro, L. M.; Quinta-Ferreira, R. M.; Martins, R. C. Ecotoxicity variation through parabens degradation by single and catalytic ozonation using volcanic rock. *Chem. Eng. J.* **2019**, *360*, 30-37. DOI: 10.1016/j.cej.2018.11.194.
(112) Jiang, Y.; Goodwill, J. E.; Tobiason, J. E.; Reckhow, D. A. Bromide oxidation by ferrate(VI): The formation of active bromine and bromate. *Water Res.* **2016**, *96*, 188-197. DOI: 10.1016/j.watres.2016.03.065.
(113) Wood, R. H. The Heat, Free Energy and Entropy of the Ferrate(VI) Ion. *J. Am. Chem. Soc.* **1958**, *80* (9), 2038-2041. DOI: 10.1021/ja01542a002.
(114) Sharma, V. K. Potassium ferrate(VI): an environmentally friendly oxidant. *Adv. Environ. Res.* **2002**, *6* (2), 143-156. DOI: 10.1016/s1093-0191(01)00119-8.
(115) Sharma, V. K.; Mishra, S. K.; Nesnas, N. Oxidation of Sulfonamide Antimicrobials by Ferrate(VI) [$Fe^{VI}O4^{2-}$]. *Environ. Sci. Technol.* **2006**, *40* (23), 7222-7227. DOI: 10.1021/es060351z.
(116) Rush, J. D.; Zhao, Z.; Bielski, B. H. J. Reaction of Ferrate(VI)/Ferrate(V) with Hydrogen Peroxide and Superoxide Anion - a Stopped-Flow and Premix Pulse Radiolysis Study. *Free Radical Res.* **1996**, *24* (3), 187-198.
(117) Sarma, R.; Angeles-Boza, A. M.; Brinkley, D. W.; Roth, J. P. Studies of the Di-iron(VI) Intermediate in Ferrate-Dependent Oxygen Evolution from Water. *J. Am. Chem. Soc.* **2012**, *134* (37), 15371-15386. DOI: 10.1021/ja304786s.
(118) Luo, C.; Feng, M.; Sharma, V. K.; Huang, C.-H. Revelation of ferrate(VI) unimoleular decay under alkaline conditions: Investigation of involvement of Fe(IV) and Fe(V) species. *Chem. Eng. J.* **2020**, *388* (124134). DOI: https://doi.org/10.1016/j.cej.2020.124134.
(119) Feng, M.; Cizmas, L.; Wang, Z.; Sharma, V. K. Activation of ferrate(VI) by ammonia in oxidation of flumequine: Kinetics, transformation products, and antibacterial activity assessment. *Chem. Eng. J.* **2017**, *323*, 584-591. DOI: http://dx.doi.org/10.1016/j.cej.2017.04.123.
(120) Feng, M. B.; Cizmas, L.; Wang, Z. Y.; Sharma, V. K. Synergistic effect of aqueous removal of fluoroquinolones by a combined use of peroxymonosulfate and ferrate(VI). *Chemosphere* **2017**, *177*, 144-148. DOI: 10.1016/j.chemosphere.2017.03.008.
(121) Manoli, K.; Li, R.; Kim, J.; Feng, M.; Huang, C.-H.; Sharma, V. K. Ferrate(VI)-peracetic acid oxidation process: Rapid degradation of pharmaceuticals in water. *Chem. Eng. J.* **2022**, *429*, 132384. DOI: 10.1016/j.cej.2021.132384.

(122) Manoli, K.; Nakhla, G.; Ray, A. K.; Sharma, V. K. Enhanced oxidative transformation of organic contaminants by activation of ferrate(VI): Possible involvement of Fe(V)/Fe(IV) species. *Chem. Eng. J.* **2017**, *307*, 513-517. DOI: 10.1016/j.cej.2016.08.109.
(123) Tian, S.-Q.; Wang, L.; Liu, Y.-L.; Ma, J. Degradation of organic pollutants by ferrate/biochar: Enhanced formation of strong intermediate oxidative iron species. *Water Res.* **2020**, *183*, 116054. DOI: 10.1016/j.watres.2020.116054.
(124) Wu, S. H.; Li, H. R.; Li, X.; He, H. J.; Yang, C. P. Performances and mechanisms of efficient degradation of atrazine using peroxymonosulfate and ferrate as oxidants. *Chem. Eng. J.* **2018**, *353*, 533-541. DOI: 10.1016/j.cej.2018.06.133.
(125) Sharma, V. K.; O'Connor, D. B.; Cabelli, D. E. Sequential One-Electron Reduction of Fe(V) to Fe(III) by Cyanide in Alkaline Medium. *J. Phys. Chem. B* **2001**, *105* (46), 11529-11532. DOI: 10.1021/jp012223x.
(126) Lee, Y.; Kissner, R.; Von Gunten, U. Reaction of Ferrate(VI) with ABTS and Self-Decay of Ferrate(VI): Kinetics and Mechanisms. *Environ. Sci. Technol.* **2014**, *48* (9), 5154-5162. DOI: 10.1021/es500804g.
(127) Shao, B. B.; Dong, H. Y.; Sun, B.; Guan, X. H. Role of Ferrate(IV) and Ferrate(V) in Activating Ferrate(VI) by Calcium Sulfite for Enhanced Oxidation of Organic Contaminants. *Environ. Sci. Technol.* **2019**, *53* (2), 894-902. DOI: 10.1021/acs.est.8b04990.
(128) Feng, M. B.; Sharma, V. K. Enhanced oxidation of antibiotics by ferrate(VI)-sulfur(IV) system: Elucidating multi-oxidant mechanism. *Chem. Eng. J.* **2018**, *341*, 137-145. DOI: 10.1016/j.cej.2018.01.112.
(129) Zhang, J.; Zhu, L.; Shi, Z. Y.; Gao, Y. Rapid removal of organic pollutants by activation sulfite with ferrate. *Chemosphere* **2017**, *186*, 576-579. DOI: 10.1016/j.chemosphere.2017.07.102.
(130) Sun, S. F.; Pang, S. Y.; Jiang, J.; Ma, J.; Huang, Z. S.; Zhang, J. M.; Liu, Y. L.; Xu, C. B.; Liu, Q. L.; Yuan, Y. X. The combination of ferrate(VI) and sulfite as a novel advanced oxidation process for enhanced degradation of organic contaminants. *Chem. Eng. J.* **2018**, *333*, 11-19. DOI: 10.1016/j.cej.2017.09.082.
(131) Al-Abduly, A.; Sharma, V. K. Oxidation of benzothiophene, dibenzothiophene, and methyl-dibenzothiophene by ferrate(VI). *J. Hazard. Mater.* **2014**, *279*, 296-301. DOI: 10.1016/j.jhazmat.2014.06.083.
(132) Kinsela, A. S.; Jones, A. M.; Bligh, M. W.; Pham, A. N.; Collins, R. N.; Harrison, J. J.; Wilsher, K. L.; Payne, T. E.; Waite, T. D. Influence of Dissolved Silicate on Rates of Fe(II) Oxidation. *Environ. Sci. Technol.* **2016**, *50* (21), 11663-11671. DOI: 10.1021/acs.est.6b03015.
(133) Manger, G. E. A Mineral Analysis of Some Common Sands and Their Silica Content. *J. Sediment. Petrol.* **1934**, *4* (3), 141-151.
(134) Esperanza, M.; Suidan, M. T.; Nishimura, F.; Wang, Z.-M.; Sorial, G. A.; Zaffiro, A.; McCauley, P.; Brenner, R.; Sayles, G. Determination of Sex Hormones and Nonylphenol Ethoxylates in the Aqueous Matrixes of Two Pilot-Scale Municipal Wastewater Treatment Plants. *Environ. Sci. Technol.* **2004**, *38* (11), 3028-3035. DOI: 10.1021/es0350886.
(135) Kuch, H. M.; Ballschmiter, K. Determination of Endocrine-Disrupting Phenolic Compounds and Estrogens in Surface and Drinking Water by HRGC−(NCI)−MS in the Picogram per Liter Range. *Environ. Sci. Technol.* **2001**, *35* (15), 3201-3206. DOI: 10.1021/es010034m.
(136) Ying, G.-G.; Kookana, R. S.; Kumar, A.; Mortimer, M. Occurrence and implications of estrogens and xenoestrogens in sewage effluents and receiving waters from South East

Queensland. *Sci. Total Environ.* **2009**, *407* (18), 5147-5155. DOI: 10.1016/j.scitotenv.2009.06.002.
(137) Guan, W.; Xie, Z.; Zhang, J. Preparation and Aromatic Hydrocarbon Removal Performance of Potassium Ferrate. *J Spectrosc* **2014**, *2014*, 1-8. DOI: 10.1155/2014/171484.
(138) Luo, Z.; Strouse, M.; Jiang, J.-Q.; Sharma, V. K. Methodologies for the analytical determination of ferrate(VI): A Review. *J. Environ. Sci. Health A.* **2011**, *46* (5), 453-460. DOI: 10.1080/10934529.2011.551723.
(139) Lee, Y.; Yoon, J.; Von Gunten, U. Spectrophotometric determination of ferrate (Fe(VI)) in water by ABTS. *Water Res.* **2005**, *39* (10), 1946-1953. DOI: 10.1016/j.watres.2005.03.005.
(140) Wang, Z.; Jiang, J.; Pang, S.; Zhou, Y.; Guan, C.; Gao, Y.; Li, J.; Yang, Y.; Qiu, W.; Jiang, C. Is Sulfate Radical Really Generated from Peroxydisulfate Activated by Iron(II) for Environmental Decontamination? *Environ. Sci. Technol.* **2018**, *52* (19), 11276-11284. DOI: 10.1021/acs.est.8b02266.
(141) Delaude, L.; Laszlo, P. A Novel Oxidizing Reagent Based on Potassium Ferrate(VI)1. *J. Org. Chem.* **1996**, *61* (18), 6360-6370. DOI: 10.1021/jo960633p.
(142) Kaur, H.; Chaudhary, S.; Kaur, H.; Chaudhary, M.; Jena, K. C. Hydrolysis and Condensation of Tetraethyl Orthosilicate at the Air–Aqueous Interface: Implications for Silica Nanoparticle Formation. *ACS Applied Nano Mater.* **2022**, *5* (1), 411-422. DOI: 10.1021/acsanm.1c03250.
(143) Liu, S.; Sun, Y.; Wang, R.; Mishra, S. B.; Duan, H.; Qu, H. Modification of sand with iron and copper derived from electroplating wastewater for efficient adsorption of phosphorus from aqueous solutions: A combinatorial approach for an effective waste minimization. *J. Cleaner Prod.* **2020**, *200*, 471-477. DOI: 10.1016/J.JCLEPRO.2018.07.254.
(144) Dayana, I.; Sembiring, T.; Tetuko, A. P.; Sembiring, K.; Maulida, N.; Cahyarani, Z.; Setiadi, E. A.; Asri, N. S.; Ginting, M.; Sebayang, P. The effect of tetraethyl orthosilicate (TEOS) additions as silica precursors on the magnetite nano-particles (Fe3O4) properties for the application of ferro-lubricant. *J. Mol. Liq.* **2019**, *294*, 111557. DOI: 10.1016/j.molliq.2019.111557.
(145) Chen, B. Y.; Kuo, H. W.; Sharma, V. K.; Den, W. Chitosan Encapsulation of Ferrate(VI) for Controlled Release to Water:Mechanistic Insights and Degradation of Organic Contaminant. *Sci Rep-Uk* **2019**, *9*. DOI: 10.1038/s41598-019-54798-4.

(146) Wang, H. L.; Liu, S. Q.; Zhang, X. Y. Preparation and application of sustained release microcapsules of potassium ferrate(VI) for dinitro butyl phenol (DNBP) wastewater treatment. *J. Hazard. Mater.* **2009**, *169* (1-3), 448-453. DOI: 10.1016/j.jhazmat.2009.03.130.
(147) Yuan, B. L.; Ye, M. R.; Lan, H. C. Preparation and properties of encapsulated potassium ferrate for oxidative remediation of trichloroethylene contaminated groundwater. *Abstr Pap Am Chem S* **2006**, *232*, 611-611.
(148) Yan, X. F.; Sun, J.; Kenjiahan, A.; Dai, X. H.; Ni, B. J.; Yuan, Z. G. Rapid and strong biocidal effect of ferrate on sulfidogenic and methanogenic sewer biofilms. *Water Res.* **2020**, *169*. DOI: 10.1016/j.watres.2019.115208.

(149) Li, C.; Li, X. Z.; Graham, N. A study of the preparation and reactivity of potassium ferrate. *Chemosphere* **2005**, *61* (4), 537-543. DOI: 10.1016/j.chemosphere.2005.02.027.
(150) Yu, J.; Jiao, R.; Sun, H.; Xu, H.; He, Y.; Wang, D. Removal of microorganic pollutants in aquatic environment: The utilization of Fe(VI). *J. Environ. Manage.* **2022**, *316*. DOI: 10.1016/j.jenvman.2022.115328.

(151) Kamachi, T.; Kouno, T.; Yoshizawa, K. Participation of multioxidants in the pH dependence of the reactivity of ferrate(VI). *J. Org. Chem.* **2005**, *70* (11), 4380-4388. DOI: 10.1021/jo050091o.
(152) Benjamin, M. M.; Lawler, D. F. *Water Quality Engineering: Physical/Chemical Treatment Processes*; John Wiley & Sons, 2013.
(153) Zhang, X.; Feng, M.; Luo, C.; Nesnas, N.; Huang, C.-H.; Sharma, V. K. Effect of Metal Ions on Oxidation of Micropollutants by Ferrate(VI): Enhancing Role of Fe^{IV} Species. *Environ. Sci. Tehnol.* **2021**, *55* (1), 623-633. DOI: 10.1021/acs.est.0c04674.
(154) Goodwill, J. E.; Jiang, Y.; Reckhow, D. A.; Gikonyo, J.; Tobiason, J. E. Characterization of Particles from Ferrate Preoxidation. *Environ. Sci. Technol.* **2015**, *49* (8), 4955-4962. DOI: 10.1021/acs.est.5b00225.
(155) Huang, Z.-S.; Wang, L.; Liu, Y.-L.; Jiang, J.; Xue, M.; Xu, C.-B.; Zhen, Y.-F.; Wang, Y.-C.; Ma, J. Impact of Phosphate on Ferrate Oxidation of Organic Compounds: An Underestimated Oxidant. *Environ. Sci. Technol.* **2018**, *52* (23), 13897-13907. DOI: 10.1021/acs.est.8b04655.
(156) Lee, Y.; Yoon, J.; von Gunten, U. Kinetics of the oxidation of phenols and phenolic endocrine disruptors during water treatment with ferrate (Fe(VI)). *Environ. Sci. Technol.* **2005**, *39* (22), 8978-8984. DOI: 10.1021/es051198w.
(157) Huang, H.; Sommerfeld, D.; Dunn, B. C.; Eyring, E. M.; Lloyd, C. R. Ferrate(VI) Oxidation of Aqueous Phenol: Kinetics and Mechanism. *J. Phys. Chem. A* **2001**, *105* (14), 3536-3541. DOI: 10.1021/jp0039621.
(158) Chen, J.; Qi, Y.; Pan, X.; Wu, N.; Zuo, J.; Li, C.; Qu, R.; Wang, Z.; Chen, Z. Mechanistic insights into the reactivity of Ferrate(VI) with phenolic compounds and the formation of coupling products. *Water Res.* **2019**, *158*, 338-349. DOI: 10.1016/j.watres.2019.04.045.
(159) Rashid, M. A. M.; Rahman, M.; Mahmud, A. O.; Morshed, A. S. M.; Haque, M. M.; Hossain, M. M. UV-Vis Spectrophotometer as an Alternative Technique for the Determination of Hydroquinone in Vinyl Acetate Monomer. *Photochem.* **2022**, *2* (2), 435-447. DOI: 10.3390/photochem2020030.
(160) Moldovan, Z.; Popa, D. E.; David, I. G.; Buleandra, M.; Badea, I. A. A Derivative Spectrometric Method for Hydroquinone Determination in the Presence of Kojic Acid, Glycolic Acid, and Ascorbic Acid. *J. Spectrosc.* **2017**, *2017*. DOI: 10.1155/2017/6929520.

(161) Zhu, J.; Yu, F.; Meng, J.; Shao, B.; Dong, H.; Chu, W.; Cao, T.; Wei, G.; Wang, H.; Guan, X. Overlooked Role of Fe(IV) and Fe(V) in Organic Contaminant Oxidation by Fe(VI). *Environ. Sci. Tehnol.* **2020**, *54* (15), 9702-9710. DOI: 10.1021/acs.est.0c03212.
(162) Sun, S. F.; Jiang, J.; Qiu, L. P.; Pang, S. Y.; Li, J.; Liu, C. H.; Wang, L. H.; Xue, M.; Ma, J. Activation of ferrate by carbon nanotube for enhanced degradation of bromophenols: Kinetics, products, and involvement of Fe(V)/Fe(IV). *Water Res.* **2019**, *156*, 1-8. DOI: 10.1016/j.watres.2019.02.057.
(163) Luo, M.; Zhang, H.; Zhou, P.; Xiong, Z.; Huang, B.; Peng, J.; Liu, R.; Liu, W.; Lai, B. Efficient activation of ferrate(VI) by colloid manganese dioxide: Comprehensive elucidation of the surface-promoted mechanism. *Water Res.* **2022**, *215*, 118243. DOI: 10.1016/j.watres.2022.118243.
(164) Luo, Y.; Guo, W.; Ngo, H. H.; Nghiem, L. D.; Hai, F. I.; Zhang, J.; Liang, S.; Wang, X. C. A review on the occurrence of micropollutants in the aquatic environment and their fate and removal during wastewater treatment. *Sci. Total Environ.* **2014**, *473-474*, 619-641. DOI: 10.1016/j.scitotenv.2013.12.065.

(165) Das, T. K.; Poater, A. Review on the Use of Heavy Metal Deposits from Water Treatment Waste towards Catalytic Chemical Syntheses. *Int. J. Mol. Sci.* **2021**, *22* (24). DOI: 10.3390/ijms222413383 .
(166) Baquero, F.; Martinez, J. L.; Canton, R. Antibiotics and antibiotic resistance in water environments. *Curr. Opin. Biotechnol.* **2008**, *19* (3), 260-265. DOI: 10.1016/j.copbio.2008.05.006 From NLM Medline.
(167) Kummerer, K. Antibiotics in the aquatic environment – A review – Part I. *Chemosphere* **2009**, *75*, 417-434. DOI: 10.1016/j.chemosphere.2008.11.086.
(168) Ferrari, B.; Paxéus, N.; Lo Giudice, R.; Pollio, A.; Garric, J. Ecotoxicological impact of pharmaceuticals found in treated wastewaters:: study of carbamazepine, clofibric acid, and diclofenac (vol 55, pg 359, 2003). *Ecotox. Environ. Safe.* **2003**, *56* (3), 450-450. DOI: 10.1016/S0147-6513(03)00111-8.
(169) Okaikue-Woodi, F. E. K.; Ray, J. R. Synthesis of ferrate (Fe(vi))-coated sand for stabilized reactivity and enhanced treatment of phenol. *J. Mater. Chem. A* **2023**, 11, 13552-13563. DOI: 10.1039/D3TA01950K.
(170) Harada, H.; Kurauchi, M.; Hayashi, R.; Eki, T. Shortened lifespan of nematode Caenorhabditis elegans after prolonged exposure to heavy metals and detergents. *Ecotoxicol. Environ. Saf.* **2007**, *66* (3), 378-383. DOI: 10.1016/j.ecoenv.2006.02.017 From NLM Medline.
(171) Li, Y.; Song, W.; Fu, W.; Tsang, D. C. W.; Yang, X. The roles of halides in the acetaminophen degradation by UV/H2O2 treatment: Kinetics, mechanisms, and products analysis. *Chem. Eng. J.* **2015**, *271*, 214-222. DOI: https://doi.org/10.1016/j.cej.2015.02.090.
(172) Yang, X.; Flowers, R. C.; Weinberg, H. S.; Singer, P. C. Occurrence and removal of pharmaceuticals and personal care products (PPCPs) in an advanced wastewater reclamation plant. *Water Res.* **2011**, *45*, 5218-5228. DOI: https://doi.org/10.1016/j.watres.2011.07.026.
(173) Miao, X.-S.; Bishay, F.; Chen, M.; Metcalfe, C. D. Occurrence of Antimicrobials in the Final Effluents of Wastewater Treatment Plants in Canada. *Environ. Sci. Tehnol.* **2004**, *38*, 3533-3541. DOI: https://doi.org/10.1021/es030653q.
(174) Mawhinney, D. B.; Vanderford, B. J.; Snyder, S. A. Transformation of 1H-benzotriazole by ozone in aqueous solution. *Environ. Sci. Technol.* **2012**, *46* (13), 7102-7111. DOI: 10.1021/es300338e.
(175) Steigerwald, J. M.; Peng, S. W.; Ray, J. R. Novel Perfluorooctanesulfonate-Imprinted Polymer Immobilized on Spent Coffee Grounds Biochar for Selective Removal of Perfluoroalkyl Acids in Synthetic Wastewater. *Acs Est Eng* **2023**. DOI: 10.1021/acsestengg.2c00336.
(176) Ling, Y.; Alzate-Sanchez, D. M.; Klemes, M. J.; Dichtel, W. R.; Helbling, D. E. Evaluating the effects of water matrix constituents on micropollutant removal by activated carbon and b-cyclodextrin polymer adsorbents. *Water Res.* **2020**, *173* (115551). DOI: https://doi.org/10.1016/j.watres.2020.115551.
(177) Rodríguez-Chueca, J.; Polo-López, M. I.; Mosteo, R.; Ormad, M. P.; Fernández-Ibáñez, P. Disinfection of real and simulated urban wastewater effluents using a mild solar photo-Fenton. *Appl Catal B-Environ* **2014**, *150*, 619-629. DOI: 10.1016/j.apcatb.2013.12.027.
(178) Masue, Y.; Loeppert, R. H.; Kramer, T. A. Arsenate and arsenite adsorption and desorption behavior on coprecipitated aluminum:iron hydroxides. *Environ. Sci. Technol.* **2007**, *41* (3), 837-842. DOI: 10.1021/es061160z .
(179) Zhang, Y. T.; Liu, C.; Xu, B. B.; Qi, F.; Chu, W. Degradation of benzotriazole by a novel Fenton-like reaction with mesoporous Cu/MnO: Combination of adsorption and catalysis oxidation. *Appl Catal B-Environ* **2016**, *199*, 447-457. DOI: 10.1016/j.apcatb.2016.06.003.

(180) Miao, Y. X.; Wang, S. L.; Wang, C. W.; Liu, Y. L.; Sun, M. B.; Chen, Y. Effect of chelating agent on benzotriazole removal during post copper chemical mechanical polishing cleaning. *Microelectron. Eng.* **2014**, *130*, 18-23. DOI: 10.1016/j.mee.2014.08.012.
(181) Finsgar, M.; Milosev, I. Inhibition of copper corrosion by 1,2,3-benzotriazole: A review. *Corros. Sci.* **2010**, *52* (9), 2737-2749. DOI: 10.1016/j.corsci.2010.05.002.
(182) Kim, H. C.; Kim, M. J.; Lim, T.; Park, K. J.; Kim, K. H.; Choe, S.; Kim, S. K.; Kim, J. J. Effects of nitrogen atoms of benzotriazole and its derivatives on the properties of electrodeposited Cu films. *Thin Solid Films* **2014**, *550*, 421-427. DOI: 10.1016/j.tsf.2013.10.124.
(183) Costarramone, N.; Kneip, A.; Castetbon, A. Ferrate(VI) oxidation of cyanide in water. *Environ. Technol.* **2004**, *25* (8), 945-955. DOI: 10.1080/09593330.2004.9619388.
(184) Yngard, R.; Damrongsiri, S.; Osathaphan, K.; Sharma, V. K. Ferrate(VI) oxidation of zinc-cyanide complex. *Chemosphere* **2007**, *69* (5), 729-735. DOI: 10.1016/j.chemosphere.2007.05.017.
(185) Zhang, S.; Gitungo, S.; Dyksen, J. E.; Raczko, R. F.; Axe, L. Indicator Compounds Representative of Contaminants of Emerging Concern (CECs) Found in the Water Cycle in the United States. *Int. J. Environ. Res. Public Health* **2021**, *18* (3), 1288. DOI: 10.3390/ijerph18031288.
(186) Snyder, S. A.; Westerhoff, P.; Yoon, Y.; Sedlak, D. L. Pharmaceuticals, personal care products, and endocrine disruptors in water: Implications for the water industry. *Environ Eng Sci* **2003**, *20* (5), 449-469. DOI: 10.1089/109287503768335931.
(187) Xu, B. B.; Wu, F. C.; Zhao, X. L.; Liao, H. Q. Benzotriazole removal from water by Zn-Al-O binary metal oxide adsorbent: Behavior, kinetics and mechanism. *J. Hazard. Mater.* **2010**, *184* (1-3), 147-155. DOI: 10.1016/j.jhazmat.2010.08.017.
(188) Hart, D. S.; Davis, L. C.; Erickson, L. E.; Callender, T. M. Sorption and partitioning parameters of benzotriazole compounds. *Microchem. J.* **2004**, *77* (1), 9-17. DOI: 10.1016/j.microc.2003.08.005.
(189) Chowdhury, I. R.; Chowdhury, S.; Mazumder, M. A. J.; Al-Ahmed, A. Removal of lead ions (Pb(2+)) from water and wastewater: a review on the low-cost adsorbents. *Appl Water Sci* **2022**, *12* (8), 185. DOI: 10.1007/s13201-022-01703-6 .
(190) Qutob, M.; Hussein, M. A.; Alamry, K. A.; Rafatullah, M. A review on the degradation of acetaminophen by advanced oxidation process: pathway, by-products, biotoxicity, and density functional theory calculation. *RSC Advances* **2022**, *12* (29), 18373-18396. DOI: 10.1039/d2ra02469a.
(191) Jelbabarezi, B.; Dehghanzadeh, R.; Sheikhi, S.; Shahmahdi, N.; Aslani, H.; Maryamabadi, A. Oxidative degradation of sulfamethoxazole from secondary treated effluent by ferrate(VI): kinetics, by-products, degradation pathway and toxicity assessment. *J. Environ. Health Sci. Eng.* **2022**, *20*. DOI: https://doi.org/10.1007/s40201-021-00769-9.
(192) Jandi, M.; Mishra, S. B.; Nxumalo, E. N.; Mhlanga, S. D.; Mishra, A. K. Smart pathways for the photocatalytic degradation of sulfamethoxazole drug using F-Pd co-doped TiO nanocomposites. *Appl Catal B-Environ* **2020**, *267*. DOI: 10.1016/j.apcatb.2020.118716.

(193) Michael-Kordatou, I.; Michael, C.; Duan, X.; He, X.; Dionysiou, D. D.; Mills, M. A.; Fatta-Kassinos, D. Dissolved effluent organic matter: Characteristics and potential implications in wastewater treatment and reuse applications. *Water Res.* **2015**, *77*, 213-248. DOI: 10.1016/j.watres.2015.03.011.
(194) Vasquez, M. I.; Fatta-Kassinos, D. Is the evaluation of "traditional" physicochemical parameters sufficient to explain the potential toxicity of the treated wastewater at sewage

treatment plants? *Environ. Sci. Pollut. Res.* **2013**, *20* (6), 3516-3528. DOI: 10.1007/s11356-013-1637-6.
(195) Krasner, S. W.; Westerhoff, P.; Chen, B.; Rittmann, B. E.; Nam, S.-n.; Amy, G. Impact of Wastewater Treatment Processes on Organic Carbon, Organic Nitrogen, and DBP Precursors in Effluent Organic Matter. *Environ. Sci. Tehnol.* **2009**, *43*, 2911-2918. DOI: 10.1021/es802443t.
(196) Worms, I. A. M.; Traber, J.; Kistler, D.; Sigg, L.; Slaveykova, V. I. Uptake of Cd(II) and Pb(II) by microalgae in presence of colloidal organic matter from wastewater treatment plant effluents. *Environ. Pollut.* **2010**, *158* (2), 369-374. DOI: 10.1016/j.envpol.2009.09.007.
(197) Louis, Y.; Pernet-Coudrier, B.; Varrault, G. Implications of effluent organic matter and its hydrophilic fraction on zinc (II) complexation in rivers under strong urban pressure: Aromaticity as an inaccurate indicator of DOM-metal binding. *Sci. Total Environ.* **2014**, *490*, 830-837. DOI: 10.1016/j.scitotenv.2014.04.123.
(198) Sarathy, V.; Allen, H. E. Copper complexation by dissolved organic matter from surface water and wastewater effluent. *Ecotox Environ Safe* **2005**, *61* (3), 337-344. DOI: 10.1016/j.ecoenv.2005.01.006.
(199) Wang, D. X.; He, J. H.; Ma, J.; Zhang, J.; Strathmann, T. J. Understanding molecular-level reactions between permanganate/ferrate and dissolved effluent organic matter from municipal secondary effluent. *Water Res.* **2023**, *247*. DOI: 10.1016/j.watres.2023.120768.

(200) Steigerwald, J. M.; Ray, J. R. Adsorption behavior of perfluorooctanesulfonate (PFOS) onto activated spent coffee grounds biochar in synthetic wastewater effluent. *J. Hazard. Mater. Lett.* **2021**, *2*. DOI: 10.1016/j.hazl.2021.100025.
(201) Yu, J.; Lv, L.; Lan, P.; Zhang, S. J.; Pan, B. C.; Zhang, W. M. Effect of effluent organic matter on the adsorption of perfluorinated compounds onto activated carbon. *J. Hazard. Mater.* **2012**, *225*, 99-106. DOI: 10.1016/j.jhazmat.2012.04.073.
(202) Shi, Z. Y.; Wang, D. X.; Gao, Z. Q.; Ji, X.; Zhang, J.; Jin, C. Enhanced ferrate oxidation of organic pollutants in the presence of Cu (II) Ion. *J. Hazard. Mater.* **2022**, *433*. DOI: 10.1016/j.jhazmat.2022.128772.

(203) Motsa, M. M.; Mamba, B. B.; Verliefde, A. R. D. Forward osmosis membrane performance during simulated wastewater reclamation: Fouling mechanisms and fouling layer properties. *J. Water Proc. Eng.* **2018**, *23*, 109-118. DOI: 10.1016/j.jwpe.2018.03.007.
(204) Guo, B. L.; Wang, J. Y.; Sathiyan, K.; Ma, X. M.; Lichtfouse, E.; Huang, C. H.; Sharma, V. K. Enhanced Oxidation of Antibiotics by Ferrate Mediated with Natural Organic Matter: Role of Phenolic Moieties. *Environ. Sci. Technol.* **2023**, *57* (47), 19033-19042. DOI: 10.1021/acs.est.3c03165.
(205) Deng, Y.; Guan, X. H. Unlocking the potential of ferrate(VI) in water treatment: Toward one-step multifunctional solutions. *J. Hazard. Mater.* **2024**, *464*. DOI: 10.1016/j.jhazmat.2023.132920.

(206) Zheng, L.; Cui, J. K.; Deng, Y. Emergency water treatment with combined ferrate(vi) and ferric salts for disasters and disease outbreaks. *Environ. Sci.:Water Res. Technol.* **2020**, *6* (10), 2816-2831. DOI: 10.1039/d0ew00483a.
(207) Viollier, E.; Inglett, P. W.; Hunter, K.; Roychoudhury, A. N.; Van Cappellen, P. The ferrozine method revisited: Fe(II)/Fe(III) determination in natural waters. *Appl. Geochem.* **2000**, *15* (6), 785-790. DOI: 10.1016/s0883-2927(99)00097-9.

(208) Giokas, D. L.; Paleologos, E. K.; Karayannis, M. I. Speciation of Fe(II) and Fe(III) by the modified ferrozine method, FIA-spectrophotometry, and flame AAS after cloud-point extraction. *Anal Bioanal Chem* **2002**, *373* (4-5), 237-243. DOI: 10.1007/s00216-002-1326-7.
(209) Pogliani, L.; Ameta, S. C.; Haghi, A. K. *Chemistry and industrial techniques for chemical engineers*; Apple Academic Press, 2021.
(210) Wulfsberg, G. *Inorganic chemistry*; University Science Books, 2000.
(211) Hogan, D. M.; Walbridge, M. R. Best Management Practices for Nutrient and Sediment Retention in Urban Stormwater Runoff. *J. Environ. Qual.* **2007**, *36* (2), 386-395. DOI: 10.2134/jeq2006.0142.
(212) Czemiel Berndtsson, J. Green roof performance towards management of runoff water quantity and quality: A review. *Ecol. Eng.* **2010**, *36* (4), 351-360. DOI: 10.1016/j.ecoleng.2009.12.014.
(213) DeBell, K. M. U.S. EPA's report to congress on the impacts and control of combined sewer overflows and sanitary sewer overflows. EPA, U. S., Ed.; 2004.
(214) Göbel, P.; Dierkes, C.; Coldewey, W. G. Storm water runoff concentration matrix for urban areas. *J. Contam. Hydrol.* **2007**, *91* (1-2), 26-42. DOI: 10.1016/j.jconhyd.2006.08.008.
(215) Spahr, S.; Teixido, M.; Sedlak, D. L.; Luthy, R. G. Hydrophilic trace organic contaminants in urban stormwater: occurrence, toxicological relevance, and the need to enhance green stormwater infrastructure. *Environ. Sci. Water Res. Technol.* **2020**, *6* (1), 15-44. DOI: 10.1039/c9ew00674e.
(216) Houtz, E. F.; Sedlak, D. L. Oxidative Conversion as a Means of Detecting Precursors to Perfluoroalkyl Acids in Urban Runoff. *Environ. Sci. Tehnol.* **2012**, *46*, 9342-9349. DOI: dx.doi.org/10.1021/es302274g.
(217) Zgheib, S.; Moilleron, R.; Chebbo, G. Priority pollutants in urban stormwater: Part 1 -- Case of separate storm sewers. *Water Res.* **2012**, *46*, 6683-6692. DOI: doi:10.1016/j.watres.2011.12.012.
(218) Shammaa, Y.; Zhu, D. Z. Techniques for Controlling Total Suspended Solids in Stormwater Runoff. *Can. Water Resour. J.* **2001**, *26* (3), 359-375. DOI: 10.4296/cwrj2603359.
(219) Paerl, H. W.; Scott, J. T.; McCarthy, M. J.; Newel, S. E.; Gardner, W. S.; Havens, K. E.; Hoffman, D. K.; Wilhelm, S. W.; Wurtsbaugh, W. A. It Takes Two to Tango: When and Where Dual Nutrient (N & P) Reductions Are Needed to Protect Lakes and Downstream Ecosystems. *Environ. Sci. Tehnol.* **2016**, *50*, 10805-10813. DOI: 10.1021/acs.est.6b02575.
(220) EPA, U. *Water quality assessment and TMDL information*; United States Environmental Protection Agency, Washington, D.C., 2016.
(221) Grebel, J. E.; Mohanty, S. K.; Torkelson, A. A.; Boehm, A. B.; Higgins, C. P.; Maxwell, R. M.; Nelson, K. L.; Sedlak, D. L. Engineered infiltration systems for urban stormwater reclamation. *Environ. Eng. Sci.* **2013**, *30* (8), 437-454. DOI: 10.1089/ees.2012.0312
(222) The national stormwater quality database (NSQD), version 4.02. *The national stormwater quality database (NSQD)*. https://bmpdatabase.org/home
(223) Tackett, T.; Jacobs, D.; Carlstad, C.; Scheller, J.; Zhen, J.; Riverson, J. Evaluating and Implementing Seattle's Green Stormwater Infrastructure Approaches at a Creek Watershed Scale. In *Proceedings of the Water Environment Federation*, 2013; pp 6017-6041.
(224) Deletic, A.; Fletcher, A. F. Performance of grass filters used for stormwater treatment—a field and modelling study. *J. Hydrol.* **2005**, *317*, 261-275. DOI: 10.1016/j.jhydrol.2005.05.021.
(225) Elliott, A. H.; Trowsdale, S. A. A review of models for low impact urban stormwater drainage. *Environ. Modell. Softw.* **2007**, *22* (3), 394-405. DOI: 10.1016/j.envsoft.2005.12.005.

(226) Collins, K. A.; Lawrence, T. J.; Stander, E. K.; Jontos, R. J.; Kaushal, S. S.; Newcomer, T. A.; Grimm, N. B.; Ekberg, M. L. C. Opportunities and challenges for managing nitrogen in urban stormwater: A review and synthesis. *Ecol. Eng.* **2010**, *36* (11), 1507-1519. DOI: 10.1016/j.ecoleng.2010.03.015.
(227) Chong, M. N.; Sidhu, J.; Aryal, R.; Tang, J.; Gernjak, W.; Escher, B.; Toze, S. Urban stormwater harvesting and reuse: a probe into the chemical, toxicology and microbiological contaminants in water quality. *Environ. Monit. Assess.* **2013**, *185* (8), 6645-6652. DOI: 10.1007/s10661-012-3053-7.
(228) Nnadi, E. O.; Newman, A. P.; Coupe, S. J.; Mbanaso, F. U. Stormwater harvesting for irrigation purposes: An investigation of chemical quality of water recycled in pervious pavement system. *J. Environ. Manage.* **2015**, *147*, 246-256. DOI: 10.1016/j.jenvman.2014.08.020.
(229) Database, B. *International Stormwater BMP Database*. https://bmpdatabase.org
(230) Ashoori, N.; Teixido, M.; Spahr, S.; Lefevre, G. H.; Sedlak, D. L.; Luthy, R. G. Evaluation of pilot-scale biochar-amended woodchip bioreactors to remove nitrate, metals, and trace organic contaminants from urban stormwater runoff. *Water Res.* **2019**, *154*, 1-11. DOI: 10.1016/j.watres.2019.01.040.
(231) Boving, T. B.; Neary, K. Attenuation of polycyclic aromatic hydrocarbons from urban stormwater runoff by wood filters. *J. Contam. Hydrol.* **2007**, *91* (1-2), 43-57. DOI: 10.1016/j.jconhyd.2006.08.009.
(232) Boving, T. B.; Zhang, W. Removal of aqueous-phase polynuclear aromatic hydrocarbons using aspen wood fibers. *Chemosphere* **2004**, *54* (7), 831-839. DOI: 10.1016/j.chemosphere.2003.07.007.
(233) Clark, S. E. Urban Stormwater Filtration: Optimization of Design Parameters and a Pilot-Scale Evaluation. University of Alabama, 2000.
(234) Erickson, A. J.; Gulliver, J. S.; Arnold, W. A.; Brekke, C.; Bredal, M. Abiotic Capture of Stormwater Nitrates with Granular Activated Carbon. *Environ. Eng. Sci.* **2016**, *33* (5), 354-363. DOI: 10.1089/ees.2015.0469.
(235) Faucette, B.; Cardoso, F.; Mulbry, W.; Millner, P. Performance of Compost Filtration Practice for Green Infrastructure Stormwater Applications. *Water Environ. Res* **2013**, *85* (9), 806-814. DOI: 10.2175/106143013x13736496908915.
(236) Jang, A.; Seo, Y.; Bishop, P. L. The removal of heavy metals in urban runoff by sorption on mulch. *Environ. Pollut.* **2005**, *133* (1), 117-127. DOI: 10.1016/j.envpol.2004.05.020.
(237) Johnson, P. A.; Clark, S.; Pitt, R.; Durrans, S. R.; Urrutia, M.; Gill, S.; Kirby, J. METALS REMOVAL TECHNOLOGIES FOR STORMWATER. In Industrial Waster Conference, San Antonio, TX, USA; 2003.
(238) Mohanty, S. K.; Cantrell, K. B.; Nelson, K. L.; Boehm, A. B. Efficacy of biochar to remove Escherichia coli from stormwater under steady and intermittent flow. *Water Res.* **2014**, *61*, 288-296. DOI: 10.1016/j.watres.2014.05.026.
(239) Reddy, K. R.; Xie, T.; Dastgheibi, S. Evaluation of Biochar as a Potential Filter Media for the Removal of Mixed Contaminants from Urban Storm Water Runoff. *J. Environ. Eng.* **2014**, *140* (12), 04014043. DOI: 10.1061/(asce)ee.1943-7870.0000872.
(240) Ray, A. B.; Selvakumar, A.; Tafuri, A. N. Removal of selected pollutants from aqueous media by hardwood mulch. *J. Hazard. Mater.* **2006**, *136* (2), 213-218. DOI: 10.1016/j.jhazmat.2005.11.094.
(241) Ray, A. B.; Wojtenko, I.; Field, R. Treatment of Urban Stormwater for Dissolved Pollutants: A Comparative Study of Natural Organic Filter Media. *Remediation* **2005**, *15*.

(242) Ray, J. R.; Shabtai, I. A.; Teixido, M.; Mishael, Y. G.; Sedlak, D. L. Polymer-clay composite geomedia for sorptive removal of trace organic compounds and metals in urban stormwater. *Water Res.* **2019**, *157*, 454-462. DOI: 10.1016/j.watres.2019.03.097 From NLM Medline.
(243) Shimabuku, K. K.; Kearns, J. P.; Martinez, J. E.; Mahoney, R. B.; Moreno-Vasquez, L.; Summers, R. S. Biochar sorbents for sulfamethoxazole removal from surface water, stormwater, and wastewater effluent. *Water Res.* **2016**, *96*, 236-245. DOI: 10.1016/j.watres.2016.03.049.
(244) Silvertooth, J. R.; Huang, H.-W.; Provolt, J. J.; Nason, J. A. *ASSESSMENT OF COPPER REMOVAL FROM HIGHWAY STORMWATER RUNOFF USING APATITE II™ AND COMPOST: LABORATORY AND FIELD TESTING*; Oregon State University, 2015.
(245) Syring, S. M.; Krishnamurthy, R.; MacKay, A. A. Attenuation of Roadway-Derived Heavy Metals by Wood Chips. *J. Environ. Eng.* **2009**, *135* (9), 747-757. DOI: 10.1061/(Asce)Ee.1943-7870.0000034.
(246) Tobiason, S. A.; Logan, L. R. J.; Nickerson, C. STORMWATER METALS REMOVAL TESTING AT SEATTLE-TACOMA INTERNATIONAL AIRPORT. In *Conference of the Water Environment Federation*, Ft Lauderdale, FL, 2002.
(247) Ulrich, B. A.; Im, E. A.; Werner, D.; Higgins, C. P. Biochar and Activated Carbon for Enhanced Trace Organic Contaminant Retention in Stormwater Infiltration Systems. *Environ. Sci. Technol.* **2015**, *49* (10), 6222-6230. DOI: 10.1021/acs.est.5b00376.
(248) Ulrich, B. A.; Loehnert, M.; Higgins, C. P. Improved contaminant removal in vegetated stormwater biofilters amended with biochar. *Environ. Sci.: Water Res. Technol.* **2017**, *3* (4), 726-734. DOI: 10.1039/c7ew00070g.
(249) van Lienden, C.; Shan, L.; Rao, S.; Ranieri, E.; Young, T. M. Metals Removal from Stormwater by Commercial and Non-Commercial Granular Activated Carbons. *Water Environ. Res* **2010**, *82* (4), 351-356. DOI: 10.2175/106143009x12487095236874.
(250) Zhou, W. F.; Beck, B. F.; Green, T. S. Evaluation of a peat filtration system for treating highway runoff in a karst setting. *Environ. Geol.* **2003**, *44* (2), 187-202. DOI: 10.1007/s00254-002-0745-2.
(251) Mohanty, S. K.; Valenca, R.; Berger, A. W.; Yu, I. K. M.; Xiong, X. N.; Saunders, T. M.; Tsang, D. C. W. Plenty of room for carbon on the ground: Potential applications of biochar for stormwater treatment. *Sci. Total Environ.* **2018**, *625*, 1644-1658. DOI: 10.1016/j.scitotenv.2018.01.037.
(252) Wu, M.; Pan, B.; Zhang, D.; Xiao, D.; Li, H.; Wang, C.; Ning, P. The sorption of organic contaminants on biochars derived from sediments with high organic carbon content. *Chemosphere* **2013**, *90* (2), 782-788. DOI: 10.1016/j.chemosphere.2012.09.075.
(253) Inyang, M.; Dickenson, E. The potential role of biochar in the removal of organic and microbial contaminants from potable and reuse water: A review. *Chemosphere* **2015**, *134*, 232-240. DOI: 10.1016/j.chemosphere.2015.03.072.
(254) Uchimiya, M.; Lima, I. M.; Klasson, K. T.; Chang, S. C.; Wartelle, L. H.; Rodgers, J. E. Immobilization of Heavy Metal Ions (Cu, Cd, Ni, and Pb) by Broiler Litter-Derived Biochars in Water and Soil. *J. Agric. Food. Chem.* **2010**, *58* (9), 5538-5544. DOI: 10.1021/jf9044217.

(255) Ahmad, M.; Rajapaksha, A. U.; Lim, J. E.; Zhang, M.; Bolan, N.; Mohan, D.; Vithanage, M.; Lee, S. S.; Ok, Y. S. Biochar as a sorbent for contaminant management in soil and water: A review. *Chemosphere* **2014**, *99*, 19-33. DOI: 10.1016/j.chemosphere.2013.10.071.
(256) Afrooz, A. R. M. N.; Boehm, A. B. Effects of submerged zone, media aging, and antecedent dry period on the performance of biochar-amended biofilters in removing fecal

indicators and nutrients from natural stormwater. *Ecol. Eng.* **2017**, *102*, 320-330. DOI: 10.1016/j.ecoleng.2017.02.053.
(257) Barrett, M. E. Performance, cost, and maintenance requirements of Austin sand filters. *J Water Res Pl-Asce* **2003**, *129* (3), 234-242. DOI: 10.1061/(Asce)0733-9496(2003)129:3(234).
(258) Barrett, M. E. *Evaluation of Sand Filter Performance*; The University of Texas at Austin, 2010.
(259) Erickson, A. J.; Gulliver, J. S.; Weiss, P. T. Enhanced sand filtration for storm water phosphorus removal. *J. Environ. Eng.* **2007**, *133* (5), 485-497. DOI: 10.1061/(Asce)0733-9372(2007)133:5(485).
(260) Mohanty, S. K.; Torkelson, A. A.; Dodd, H.; Nelson, K. L.; Boehm, A. B. Engineering Solutions to Improve the Removal of Fecal Indicator Bacteria by Bioinfiltration Systems during Intermittent Flow of Stormwater. *Environ. Sci. Technol.* **2013**, *47* (19), 10791-10798. DOI: 10.1021/es305136b.
(261) Prabhukumar, G.; Bhupal, G. S.; Pagilla, K. R. Laboratory Evaluation of Sorptive Filtration Media Mixtures for Targeted Pollutant Removals from Simulated Stormwater. *Water Environ. Res* **2015**, *87* (9), 789-795. DOI: 10.2175/106143015X14362865226239.
(262) Reddy, K. R.; Xie, T.; Dastgheibi, S. Nutrients Removal from Urban Stormwater by Different Filter Materials. *Water Air Soil Poll* **2014**, *225* (1). DOI: ARTN 1778

10.1007/s11270-013-1778-8.
(263) Reddy, K. R.; Xie, T.; Dstgheibi, S. Removal of heavy metals from urban stormwater runoff using different filter materials. *J. Environ. Chem. Eng.* **2014**, *2* (1). DOI: doi.org/10.1016/j.jece.2013.12.020.
(264) Reddy, K. R.; Xie, T.; Dastgheibi, S. PAHs Removal from Urban Storm Water Runoff by Different Filter Materials. *J. Hazard. Toxic Radioact Waste* **2014**, *18* (2), 04014008. DOI: 10.1061/(asce)hz.2153-5515.0000222.
(265) Reddy, K. R.; Xie, T.; Dastgheibi, S. Adsorption of mixtures of nutrients and heavy metals in simulated urban stormwater by different filter materials. *J. Environ. Sci. Health A* **2014**, *49* (5), 524-539. DOI: 10.1080/10934529.2014.859030.
(266) Smith, D. P. Chabazite Biofilter for Enhanced Stormwater Nitrogen Removal. *Water Environ. Res* **2011**, *83* (4), 373-384. DOI: 10.2175/106143010x12851009156123.
(267) Zarezadeh, V.; Lung, T.; Dorman, T.; Shipley, H. J.; Giacomoni, M. Assessing the performance of sand filter basins in treating urban stormwater runoff. *Environ. Monit. Assess.* **2018**, *190* (12). DOI: 10.1007/s10661-018-7069-5.

(268) Erickson, A. J.; Gulliver, J. S.; Weiss, P. T. Capturing phosphates with iron enhanced sand filtration. *Water Res.* **2012**, *46* (9), 3032-3042. DOI: 10.1016/j.watres.2012.03.009.
(269) Ernst, C.; Katz, L.; Barrett, M. Removal of Dissolved Copper and Zinc from Highway Runoff via Adsorption. *J. Sustain. Water Built Environ.* **2016**, *2* (1). DOI: 10.1061/jswbay.0000803.
(270) Zhang, L.; Seagren, E. A.; Davis, A. P.; Karns, J. S. The Capture and Destruction of

from Simulated Urban Runoff Using Conventional Bioretention Media and Iron Oxide-coated Sand. *Water Environ. Res.* **2010**, *82* (8), 701-714. DOI: 10.2175/106143010x12609736966441.
(271) Sansalone, J. J. Adsorptive infiltration of metals in urban drainage - media characteristics. *Sci. Total Environ.* **1999**, *235* (1-3), 179-188. DOI: Doi 10.1016/S0048-9697(99)00211-9.

(272) Liu, D. F.; Sansalone, J. J.; Cartledge, F. K. Comparison of sorptive filter media for treatment of metals in runoff. *J. Environ. Eng.* **2005**, *131* (8), 1178-1186. DOI: 10.1061/(Asce)0733-9372(2005)131:8(1178).
(273) Charbonnet, J. A.; Duan, Y.; Van Genuchten, C. M.; Sedlak, D. L. Chemical Regeneration of Manganese Oxide-Coated Sand for Oxidation of Organic Stormwater Contaminants. *Environ. Sci. Technol.* **2018**, *52* (18), 10728-10736. DOI: 10.1021/acs.est.8b03304.
(274) Charbonnet, J. A.; Duan, Y.; Sedlak, D. L. The use of manganese oxide-coated sand for the removal of trace metal ions from stormwater. *Environ. Sci.: Water Res. Technol.* **2020**, *6* (3), 593-603. DOI: 10.1039/c9ew00781d.
(275) Grebel, J. E.; Charbonnet, J. A.; Sedlak, D. L. Oxidation of organic contaminants by manganese oxide geomedia for passive urban stormwater treatment systems. *Water Res.* **2016**, *88*, 481-491. DOI: 10.1016/j.watres.2015.10.019.
(276) Randall, M. T.; Bradford, A. Bioretention gardens for improved nutrient removal. *Water Qual Res J Can* **2013**, *48* (4), 372-386. DOI: 10.2166/wqrjc.2013.016.
(277) Vu, C. T.; Wu, T. T. Engineered multifunctional sand for enhanced removal of stormwater runoff contaminants in fixed-bed column systems. *Chemosphere* **2019**, *224*, 852-861. DOI: 10.1016/j.chemosphere.2019.02.145.
(278) Ahmadi, A.; Yang, W. W.; Jones, S.; Wu, T. T. Separation-free Al-Mg/graphene oxide composites for enhancement of urban stormwater runoff quality. *Adv Compos Hybrid Ma* **2018**, *1* (3), 591-601. DOI: 10.1007/s42114-018-0042-5.
(279) Reinsch, C. T.; Admiraal, D. M.; Dvorak, B.; Cecrle, C. A.; Franti, T. G.; Stansbury, J. S. Yard waste compost as a stormwater protection treatment for construction sites. *Water Environ. Res* **2007**, *79* (8), 868-876. DOI: 10.2175/106143007x220545.
(280) Halaburka, B. J.; LeFevre, G. H.; Luthy, R. G. Evaluation of Mechanistic Models for Nitrate Removal in Woodchip Bioreactors. *Environ. Sci. Technol.* **2017**, *51* (9), 5156-5164. DOI: 10.1021/acs.est.7b01025.
(281) Peterson, I. J.; Igielski, S.; Davis, A. P. Enhanced Denitrification in Bioretention Using Woodchips as an Organic Carbon Source. *J. Sustain. Water Built Environ.* **2015**, *1* (4). DOI: 10.1061/JSWBAY.0000800.
(282) Urbonas, B. Assessment of Stormwater Bmps and Their Technology. *Water Sci. Technol.* **1994**, *29* (1-2), 347-353. DOI: DOI 10.2166/wst.1994.0682.
(283) Clark, S. E.; Pitt, R. Targeting treatment technologies to address specific stormwater pollutants and numeric discharge limits. *Water Res.* **2012**, *46* (20), 6715-6730. DOI: 10.1016/j.watres.2012.07.009.
(284) Prabhukumar, G.; Bhupal, G. S.; Pagilla, K. R. Laboratory Evaluation of Sorptive Filtration Media Mixtures for Targeted Pollutant Removals from Simulated Stormwater. *Water Environ. Res* **2015**, *87* (9), 789-795. DOI: 10.2175/106143015x14362865226239.
(285) Masoner, J. R.; Kolpin, D. W.; Cozzarelli, I. M.; Barber, L. B.; Burden, D. S.; Foreman, W. T.; Forshay, K. J.; Furlong, E. T.; Groves, J. F.; Hladik, M. L.; et al. Urban Stormwater: An Overlooked Pathway of Extensive Mixed Contaminants to Surface and Groundwaters in the United States. *Environ. Sci. Technol.* **2019**, *53* (17), 10070-10081. DOI: 10.1021/acs.est.9b02867 .
(286) Xie, J.; Wang, Z.; Wu, D. Y.; Zhang, Z. J.; Kong, H. N. Synthesis of Zeolite/Aluminum Oxide Hydrate from Coal Fly Ash: A New Type of Adsorbent for Simultaneous Removal of Cationic and Anionic Pollutants. *Ind. Eng. Chem. Res.* **2013**, *52* (42), 14890-14897. DOI: 10.1021/ie4021396.

(287) Jiang, N.; Shang, R.; Heijman, S. G. J.; Rietveld, L. C. High-silica zeolites for adsorption of organic micro-pollutants in water treatment: A review. *Water Res.* **2018**, *144*, 145-161. DOI: 10.1016/j.watres.2018.07.017.
(288) Jiang, N.; Erdos, M.; Moultos, O. A.; Shang, R.; Vlugt, T. J. H.; Heijman, S. G. J.; Rietveld, L. C. The adsorption mechanisms of organic micropollutants on high-silica zeolites causing S-shaped adsorption isotherms: An experimental and Monte Carlo simulation study. *Chem. Eng. J.* **2020**, *389*. DOI: 10.1016/j.cej.2019.123968.

(289) Uddin, M. K. A review on the adsorption of heavy metals by clay minerals, with special focus on the past decade. *Chem. Eng. J.* **2017**, *308*, 438-462. DOI: 10.1016/j.cej.2016.09.029.
(290) Wang, S.; Peng, Y. Natural zeolites as effective adsorbents in water and wastewater treatment. *Chem. Eng. J.* **2010**, *156* (1), 11-24. DOI: 10.1016/j.cej.2009.10.029.
(291) He, S. B.; Xue, G.; Kong, H. N. The performance of BAF using natural zeolite as filter media under conditions of low temperature and ammonium shock load. *J. Hazard. Mater.* **2007**, *143* (1-2), 291-295. DOI: 10.1016/j.jhazmat.2006.09.024.
(292) Farley, K. J.; Dzombak, D. A.; Morel, F. M. M. A Surface Precipitation Model for the Sorption of Cations on Metal-Oxides. *J. Colloid Interface Sci.* **1985**, *106* (1), 226-242. DOI: Doi 10.1016/0021-9797(85)90400-X.
(293) Raogadde, R.; Laitinen, H. A. Studies of Heavy-Metal Adsorption by Hydrous Iron and Manganese Oxides. *Anal. Chem.* **1974**, *46* (13), 2022-2026.
(294) Ugwu, I. M.; Igbokwe, O. A. Heavy metal adsorption by hydrous iron and manganese oxides. In *Advanced Sorption Process Applications*, Edebali, S. Ed.; Intech Open, 2019.
(295) Hsieh, C.-h.; Deavis, A. P. Evaluation and Optimization of Bioretention Media for Treatment of Urban Storm Water Runoff. *J. Environ. Eng.* **2005**, *131* (11).
(296) Delaire, C.; van Genuchten, C. M.; Amrose, S. E.; Gadgil, A. J. Bacteria attenuation by iron electrocoagulation governed by interactions between bacterial phosphate groups and Fe(III) precipitates. *Water Res.* **2016**, *103*, 74-82. DOI: 10.1016/j.watres.2016.07.020.
(297) Giannakis, S.; Voumard, M.; Rtimi, S.; Pulgarin, C. Bacterial disinfection by the photo-Fenton process: Extracellular oxidation or intracellular photo-catalysis? *Appl Catal B-Environ* **2018**, *227*, 285-295. DOI: 10.1016/j.apcatb.2018.01.044.
(298) Knapp, E. P.; Herman, J. S.; Hornberger, G. M.; Mills, A. L. The effect of distribution of iron-oxyhydroxide grain coatings on the transport of bacterial cells in porous media. *Environ. Geol.* **1998**, *33* (4), 243-248. DOI: DOI 10.1007/s002540050243.
(299) Mills, A. L.; Herman, J. S.; Hornberger, G. M.; Dejesus, T. H. Effect of Solution Ionic-Strength and Iron Coatings on Mineral Grains on the Sorption of Bacterial-Cells to Quartz Sand. *Appl Environ Microb* **1994**, *60* (9), 3300-3306. DOI: Doi 10.1128/Aem.60.9.3300-3306.1994.
(300) Herngren, L.; Goonetilleke, A.; Ayoko, G. A. Understanding heavy metal and suspended solids relationships in urban stormwater using simulated rainfall. *J. Environ. Manage.* **2005**, *76* (2), 149-158. DOI: 10.1016/j.jenvman.2005.01.013.
(301) Al-Degs, Y. S.; Tutunju, M. F.; Shawabkeh, R. A. The feasibility of using diatomite and Mn-diatomite for remediation of Pb, Cu, and Cd from water. *Sep. Sci. Technol.* **2000**, *35* (14), 2299-2310. DOI: 10.1081/Ss-100102103.

(302) Wang, Y.; Feng, X. H.; Villalobos, M.; Tan, W. F.; Liu, F. Sorption behavior of heavy metals on birnessite: Relationship with its Mn average oxidation state and implications for types of sorption sites. *Chem. Geol.* **2012**, *292*, 25-34. DOI: 10.1016/j.chemgeo.2011.11.001.

(303) Stone, A. T.; Morgan, J. J. Reduction and Dissolution of Manganese(Iii) and Manganese(Iv) Oxides by Organics .1. Reaction with Hydroquinone. *Environ. Sci. Technol.* **1984**, *18* (6), 450-456. DOI: 10.1021/es00124a011.
(304) Sunda, W. G.; Kieber, D. J. Oxidation of Humic Substances by Manganese Oxides Yields Low-Molecular-Weight Organic Substrates. *Nature* **1994**, *367* (6458), 62-64. DOI: DOI 10.1038/367062a0.
(305) Santos, V. P.; Pereira, M. F. R.; Orfao, J. J. M.; Figueiredo, J. L. The role of lattice oxygen on the activity of manganese oxides towards the oxidation of volatile organic compounds. *Appl Catal B-Environ* **2010**, *99* (1-2), 353-363. DOI: 10.1016/j.apcatb.2010.07.007.
(306) Laha, S.; Luthy, R. G. Oxidation of Aniline and Other Primary Aromatic-Amines by Manganese-Dioxide. *Environ. Sci. Technol.* **1990**, *24* (3), 363-373. DOI: DOI 10.1021/es00073a012.
(307) Song, Y.; Jiang, J.; Ma, J.; Zhou, Y.; von Gunten, U. Enhanced transformation of sulfonamide antibiotics by manganese(IV) oxide in the presence of model humic constituents. *Water Res.* **2019**, *153*, 200-207. DOI: 10.1016/j.watres.2019.01.011.
(308) Gouzinis, A.; Kosmidis, N.; Vayenas, D. V.; Lyberatos, G. Removal of Mn and simultaneous removal of NH_3, Fe and Mn from potable water using a trickling filter. *Water Res.* **1998**, *32* (8), 2442-2450. DOI: Doi 10.1016/S0043-1354(97)00471-5.

(309) Morgan, J. Chemical equilibria and kinetic properties of manganese in natural water. In *Principles and Applications of Water Chemistry*, Wiley Ed.; 1967; pp 561-623.
(310) Han, R. P.; Zou, W. H.; Zhang, Z. P.; Shi, J.; Yang, J. J. Removal of copper(II) and lead(II) from aqueous solution by manganese oxide coated sand - I. Characterization and kinetic study. *J. Hazard. Mater.* **2006**, *137* (1), 384-395. DOI: 10.1016/j.jhazmat.2006.02.021.
(311) Tiwari, D.; Laldanwngliana, C.; Choi, C. H.; Lee, S. M. Manganese-modified natural sand in the remediation of aquatic environment contaminated with heavy metal toxic ions. *Chem. Eng. J.* **2011**, *171* (3), 958-966. DOI: 10.1016/j.cej.2011.04.046.
(312) Foroughi, M.; Khiadani, M.; Amin, M.; Pourzamani, H.; Dastjerdi, M. Treatment of synthetic urban runoff using manganese oxide-coated sand in the presence of magnetic field. *Int. J. Environ. Health Eng.* **2013**, *2* (1), 31-31. DOI: 10.4103/2277-9183.115794.
(313) Guha, H.; Saiers, J. E.; Brooks, S.; Jardine, P.; Jayachandran, K. Chromium transport, oxidation, and adsorption in manganese-coated sand. *J. Contam. Hydrol.* **2001**, *49* (3-4), 311-334. DOI: Doi 10.1016/S0169-7722(00)00199-6.
(314) EPA, U. S. *National Recommended Water Quality Criteria - Human Health Criteria Table*; United States Environmental Protection Agency, Washington, DC, 2019.
(315) Adyel, T. M.; Oldham, C. E.; Hipsey, M. R. Stormwater nutrient attenuation in a constructed wetland with alternating surface and subsurface flow pathways: Event to annual dynamics. *Water Res.* **2016**, *107*, 66-82. DOI: 10.1016/j.watres.2016.10.005.
(316) Hobbie, S. E.; Finlay, J. C.; Janke, B. D.; Nidzgorski, D. A.; Millet, D. B.; Baker, L. A. Contrasting nitrogen and phosphorus budgets in urban watersheds and implications for managing urban water pollution (vol 114, pg 4177, 2017). *P Natl Acad Sci USA* **2017**, *114* (20), E4116-E4116. DOI: 10.1073/pnas.1706049114.
(317) Schindler, D. W.; Carpenter, S. R.; Chapra, S. C.; Hecky, R. E.; Orihel, D. M. Reducing Phosphorus to Curb Lake Eutrophication is a Success. *Environ. Sci. Technol.* **2016**, *50* (17), 8923-8929. DOI: 10.1021/acs.est.6b02204.

(318) Haghseresht, F.; Wang, S.; Do, D. D. A novel lanthanum-modified bentonite, Phoslock, for phosphate removal from wastewaters. *Applied Clay Science* **2009**, *46*, 369-375. DOI: :10.1016/j.clay.2009.09.009.
(319) Xie, J.; Wang, Z.; Lu, S. Y.; Wu, D. Y.; Zhang, Z. J.; Kong, H. N. Removal and recovery of phosphate from water by lanthanum hydroxide materials. *Chem. Eng. J.* **2014**, *254*, 163-170. DOI: 10.1016/j.cej.2014.05.113.
(320) Spears, B. M.; Lürling, M.; Yasseri, S.; Castro-Castellon, A. T.; Gibbs, M.; Meis, S.; McDonald, C.; McIntosh, J.; Sleep, D.; Van Oosterhout, F. Lake responses following lanthanum-modified bentonite clay (Phoslock®) application: An analysis of water column lanthanum data from 16 case study lakes. *Water Res.* **2013**, *47* (15), 5930-5942. DOI: 10.1016/j.watres.2013.07.016.
(321) Slijkerman, D. M. E.; Baird, D. J.; Conrad, A.; Jak, R. G.; van Straalen, N. M. Assessing structural and functional plankton responses to carbendazim toxicity. *Environ. Toxicol. Chem.* **2004**, *23* (2), 455-462. DOI: Doi 10.1897/03-12.
(322) Lürling, M.; Tolman, Y. Effects of lanthanum and lanthanum-modified clay on growth, survival and reproduction of. *Water Res.* **2010**, *44* (1), 309-319. DOI: 10.1016/j.watres.2009.09.034.
(323) Sun, Y. Q.; Chen, S. S.; Lau, A. Y. T.; Tsang, D. C. W.; Mohanty, S. K.; Bhatnagar, A.; Rinklebe, J.; Lin, K. Y. A.; Ok, Y. S. Waste-derived compost and biochar amendments for stormwater treatment in bioretention column: Co-transport of metals and colloids. *J. Hazard. Mater.* **2020**, *383*. DOI: 10.1016/j.jhazmat.2019.121243.

(324) Xiong, J. Q.; Ren, S. H.; He, Y. F.; Wang, X. C. C.; Bai, X. C.; Wang, J. X.; Dzakpasu, M. Bioretention cell incorporating Fe-biochar and saturated zones for enhanced stormwater runoff treatment. *Chemosphere* **2019**, *237*. DOI: 10.1016/j.chemosphere.2019.124424.

(325) Kim, H. J.; Choi, J.-W.; Kim, T.-H.; Park, J.-S.; An, B. Effect of TSS Removal from Stormwater by Mixed Media Column on T-N, T-P, and Organic Material Removal. *Water (Basel)* **2018**, *10* (8), 1069. DOI: 10.3390/w10081069.
(326) Jing, G. H.; Wang, L.; Yu, H. J.; Amer, W. A.; Zhang, L. Recent progress on study of hybrid hydrogels for water treatment. *Colloid Surface A* **2013**, *416*, 86-94. DOI: 10.1016/j.colsurfa.2012.09.043.
(327) Su, C. M. Environmental implications and applications of engineered nanoscale magnetite and its hybrid nanocomposites: A review of recent literature. *J. Hazard. Mater.* **2017**, *322*, 48-84. DOI: 10.1016/j.jhazmat.2016.06.060.
(328) Upadhyay, R. K.; Soin, N.; Roy, S. S. Role of graphene/metal oxide composites as photocatalysts, adsorbents and disinfectants in water treatment: a review. *Rsc Advances* **2014**, *4* (8), 3823-3851. DOI: 10.1039/c3ra45013a.
(329) Marcano, D. C.; Kosynkin, D. V.; Berlin, J. M.; Sinitskii, A.; Sun, Z. Z.; Slesarev, A.; Alemany, L. B.; Lu, W.; Tour, J. M. Improved Synthesis of Graphene Oxide. *Acs Nano* **2010**, *4* (8), 4806-4814. DOI: 10.1021/nn1006368.
(330) Li, D.; Müller, M. B.; Gilje, S.; Kaner, R. B.; Wallace, G. G. Processable aqueous dispersions of graphene nanosheets. *Nat Nanotechnol* **2008**, *3* (2), 101-105. DOI: 10.1038/nnano.2007.451.
(331) Dreyer, D. R.; Park, S.; Bielawski, C. W.; Ruoff, R. S. The chemistry of graphene oxide. *Chem. Soc. Rev.* **2010**, *39* (1), 228-240. DOI: 10.1039/b917103g.

(332) Chung, C.; Kim, Y. K.; Shin, D.; Ryoo, S. R.; Hong, B. H.; Min, D. H. Biomedical Applications of Graphene and Graphene Oxide. *Acc. Chem. Res.* **2013**, *46* (10), 2211-2224. DOI: 10.1021/ar300159f.
(333) Chen, D.; Feng, H. B.; Li, J. H. Graphene Oxide: Preparation, Functionalization, and Electrochemical Applications. *Chem. Rev.* **2012**, *112* (11), 6027-6053. DOI: 10.1021/cr300115g.
(334) Zhou, M.; Zhai, Y. M.; Dong, S. J. Electrochemical Sensing and Biosensing Platform Based on Chemically Reduced Graphene Oxide. *Anal. Chem.* **2009**, *81* (14), 5603-5613. DOI: 10.1021/ac900136z.
(335) Liu, J. Q.; Cui, L.; Losic, D. Graphene and graphene oxide as new nanocarriers for drug delivery applications. *Acta Biomater* **2013**, *9* (12), 9243-9257. DOI: 10.1016/j.actbio.2013.08.016.
(336) Sun, X. M.; Liu, Z.; Welsher, K.; Robinson, J. T.; Goodwin, A.; Zaric, S.; Dai, H. J. Nano-Graphene Oxide for Cellular Imaging and Drug Delivery. *Nano Res* **2008**, *1* (3), 203-212. DOI: 10.1007/s12274-008-8021-8.
(337) Ray, J. R.; Tadepalli, S.; Nergiz, S. Z.; Liu, K. K.; You, L.; Tang, Y. J.; Singamaneni, S.; Jun, Y. S. Hydrophilic, Bactericidal Nanoheater-Enabled Reverse Osmosis Membranes to Improve Fouling Resistance. *Acs Appl Mater Inter* **2015**, *7* (21), 11117-11126. DOI: 10.1021/am509174j.
(338) Wang, J. Q.; Zhang, P.; Liang, B.; Liu, Y. X.; Xu, T.; Wang, L. F.; Cao, B.; Pan, K. Graphene Oxide as an Effective Barrier on a Porous Nanofibrous Membrane for Water Treatment. *Acs Appl Mater Inter* **2016**, *8* (9), 6211-6218. DOI: 10.1021/acsami.5b12723.
(339) Chen, J.; Yao, B. W.; Li, C.; Shi, G. Q. An improved Hummers method for eco-friendly synthesis of graphene oxide. *Carbon* **2013**, *64*, 225-229. DOI: 10.1016/j.carbon.2013.07.055.
(340) Hu, M.; Mi, B. X. Enabling Graphene Oxide Nanosheets as Water Separation Membranes. *Environ. Sci. Technol.* **2013**, *47* (8), 3715-3723. DOI: 10.1021/es400571g.
(341) Lee, J.; Chae, H. R.; Won, Y. J.; Lee, K.; Lee, C. H.; Lee, H. H.; Kim, I. C.; Lee, J. M. Graphene oxide nanoplatelets composite membrane with hydrophilic and antifouling properties for wastewater treatment. *J. Membr. Sci.* **2013**, *448*, 223-230. DOI: 10.1016/j.memsci.2013.08.017.
(342) Goh, K. L.; Setiawan, L.; Wei, L.; Si, R. M.; Fane, A. G.; Wang, R.; Chen, Y. Graphene oxide as effective selective barriers on a hollow fiber membrane for water treatment process. *J. Membr. Sci.* **2015**, *474*, 244-253, Article. DOI: 10.1016/j.memsci.2014.09.057.
(343) Ray, S. K.; Majumder, C.; Saha, P. Functionalized reduced graphene oxide (fRGO) for removal of fulvic acid contaminant. *Rsc Advances* **2017**, *7* (35), 21768-21779. DOI: 10.1039/c7ra01069a.
(344) Yang, K. J.; Chen, B. L.; Zhu, L. Z. Graphene-coated materials using silica particles as a framework for highly efficient removal of aromatic pollutants in water. *Sci Rep-Uk* **2015**, *5*. DOI: 10.1038/srep11641.

(345) Prasad, N. B. S.; Govindaraju, K.; Kumar, G. V.; Suganya, U. K. S.; Anand, V. K. Graphene from sugarcane extract and its application on organic dyes adsorption. *Pollut. Res.* **2015**, *34* (4), 803-808.
(346) Hou, W. J.; Zhang, Y. M.; Liu, T.; Lu, H. W.; He, L. Graphene oxide coated quartz sand as a high performance adsorption material in the application of water treatment. *Rsc Advances* **2015**, *5* (11), 8037-8043. DOI: 10.1039/c4ra11430b.

(347) Yang, Y.; Zhao, Y. Q.; Babatunde, A. Q.; Wang, L.; Ren, Y. X.; Han, Y. Characteristics and mechanisms of phosphate adsorption on dewatered alum sludge. *Sep. Purif. Technol.* **2006**, *51* (2), 193-200. DOI: 10.1016/j.seppur.2006.01.013.
(348) Kim, J.; Cote, L. J.; Kim, F.; Yuan, W.; Shull, K. R.; Huang, J. X. Graphene Oxide Sheets at Interfaces. *J. Am. Chem. Soc.* **2010**, *132* (23), 8180-8186. DOI: 10.1021/ja102777p.
(349) Huang, Y.; Wang, M. X.; Gong, Y. Y.; Zeng, E. Y. Efficient removal of mercury from simulated groundwater using thiol-modified graphene oxide/Fe-Mn composite in fixed-bed columns: Experimental performance and mathematical modeling. *Sci. Total Environ.* **2020**, *714*. DOI: 10.1016/j.scitotenv.2020.136636.

(350) Li, X. F.; Sun, J. Z.; Che, Y. L.; Lv, Y.; Liu, F. Antibacterial properties of chitosan chloride-graphene oxide composites modified quartz sand filter media in water treatment. *Int. J. Biol. Macromol.* **2019**, *121*, 760-773. DOI: 10.1016/j.ijbiomac.2018.10.123.
(351) Wen, T.; Wu, X. L.; Tan, X. L.; Wang, X. K.; Xu, A. W. One-Pot Synthesis of Water-Swellable Mg-Al Layered Double Hydroxides and Graphene Oxide Nanocomposites for Efficient Removal of As(V) from Aqueous Solutions. *Acs Appl Mater Inter* **2013**, *5* (8), 3304-3311. DOI: 10.1021/am4003556.
(352) Lomeda, J. R.; Doyle, C. D.; Kosynkin, D. V.; Hwang, W. F.; Tour, J. M. Diazonium Functionalization of Surfactant-Wrapped Chemically Converted Graphene Sheets. *J. Am. Chem. Soc.* **2008**, *130* (48), 16201-16206. DOI: 10.1021/ja806499w.
(353) Gao, W.; Majumder, M.; Alemany, L. B.; Narayanan, T. N.; Ibarra, M. A.; Pradhan, B. K.; Ajayan, P. M. Engineered Graphite Oxide Materials for Application in Water Purification. *Acs Appl Mater Inter* **2011**, *3* (6), 1821-1826. DOI: 10.1021/am200300u.
(354) Radian, A.; Mishael, Y. G. Characterizing and designing polycation - Clay nanocomposites as a basis for imazapyr controlled release formulations. *Environ. Sci. Technol.* **2008**, *42* (5), 1511-1516, Article. DOI: 10.1021/es7023753.
(355) Lin, S. Heavy metal removal from water by sorption using surfactant-modified montmorillonite. *J. Hazard. Mater.* **2002**, *92* (3), 315-326. DOI: 10.1016/S0304-3894(02)00026-2.
(356) Usuki, A.; Hasegawa, N.; Kato, M. Polymer-clay nanocomposites. In *Inorganic Polymeric Nanocomposites and Membranes*, Advances in Polymer Science, Vol. 179; Springer-Verlag Berlin, 2005; pp 135-195.
(357) Wu, Y. P.; Wang, Y. Q.; Zhang, H. F.; Wang, Y. Z.; Yu, D. S.; Zhang, L. Q.; Yang, J. Rubber-pristine clay nanocomposites prepared by co-coagulating rubber latex and clay aqueous suspension. *Compos. Sci. Technol.* **2005**, *65* (7-8), 1195-1202, Article. DOI: 10.1016/j.compscitech.2004.11.016.
(358) Unuabonah, E. I.; Taubert, A. Clay-polymer nanocomposites (CPNs): Adsorbents of the future for water treatment. *Applied Clay Science* **2014**, *99*, 83-92, Review. DOI: 10.1016/j.clay.2014.06.016.
(359) Okada, A.; Usuki, A. The chemistry of polymer-clay hybrids. *Mater. Sci. Eng. C-Biomimetic Mater. Sens. Syst.* **1995**, *3* (2), 109-115, Article; Proceedings Paper. DOI: 10.1016/0928-4931(95)00110-7.
(360) Yang, L. Y.; Zhou, Z.; Xiao, L.; Wang, X. R. Chemical and biological regeneration of HDTMA-modified montmorillonite after sorption with phenol. *Environ. Sci. Technol.* **2003**, *37* (21), 5057-5061, Article. DOI: 10.1021/es0342493.

(361) Park, Y.; Ayoko, G. A.; Frost, R. L. Application of organoclays for the adsorption of recalcitrant organic molecules from aqueous media. *J. Colloid Interface Sci.* **2011**, *354* (1), 292-305, Article. DOI: 10.1016/j.jcis.2010.09.068.
(362) Undabeytia, T.; Posada, R.; Nir, S.; Galindo, I.; Laiz, L.; Saiz-Jimenez, C.; Morillo, E. Removal of waterborne microorganisms by filtration using clay-polymer complexes. *J. Hazard. Mater.* **2014**, *279*, 190-196, Article. DOI: 10.1016/j.jhazmat.2014.07.006.
(363) Anirudhan, T. S.; Suchithra, P. S. Heavy metals uptake from aqueous solutions and industrial wastewaters by humic acid-immobilized polymer/bentonite composite: Kinetics and equilibrium modeling. *Chem. Eng. J.* **2010**, *156* (1), 146-156, Article. DOI: 10.1016/j.cej.2009.10.011.
(364) Chang, M. Y.; Juang, R. S. Adsorption of tannic acid, humic acid, and dyes from water using the composite of chitosan and activated clay. *J. Colloid Interface Sci.* **2004**, *278* (1), 18-25, Article. DOI: 10.1016/j.jcis.2004.05.029.
(365) Ganigar, R.; Rytwo, G.; Gonen, Y.; Radian, A.; Mishael, Y. G. Polymer-clay nanocomposites for the removal of trichlorophenol and trinitrophenol from water. *Applied Clay Science* **2010**, *49* (3), 311-316, Article. DOI: 10.1016/j.clay.2010.06.015.
(366) Kohay, H.; Izbitski, A.; Mishael, Y. G. Developing Polycation-Clay Sorbents for Efficient Filtration of Diclofenac: Effect of Dissolved Organic Matter and Comparison to Activated Carbon. *Environ. Sci. Technol.* **2015**, *49* (15), 9280-9288, Article. DOI: 10.1021/acs.est.5b01530.
(367) Radian, A.; Mishael, Y. Effect of Humic Acid on Pyrene Removal from Water by Polycation-Clay Mineral Composites and Activated Carbon. *Environ. Sci. Technol.* **2012**, *46* (11), 6228-6235, Article. DOI: 10.1021/es300964d.
(368) El-Zahhar, A. A.; Awwad, N. S.; El-Katori, E. E. Removal of bromophenol blue dye from industrial waste water by synthesizing polymer-clay composite. *J. Mol. Liq.* **2014**, *199*, 454-461, Review. DOI: 10.1016/j.molliq.2014.07.034.
(369) Unuabonah, E. I.; Olu-Owolabi, B. I.; Fasuyi, E. I.; Adebowale, K. O. Modeling of fixed-bed column studies for the adsorption of cadmium onto novel polymer-clay composite adsorbent. *J. Hazard. Mater.* **2010**, *179* (1-3), 415-423, Article. DOI: 10.1016/j.jhazmat.2010.03.020.
(370) Elshorbagy, W.; Chowdhury, R. Water Treat. 2013.
(371) Hui, K. S.; Chao, C. Y. H.; Kot, S. C. Removal of mixed heavy metal ions in wastewater by zeolite 4A and residual products from recycled coal fly ash. *J. Hazard. Mater.* **2005**, *127* (1-3), 89-101, Article. DOI: 10.1016/j.jhazmat.2005.06.027.
(372) Karapinar, N. Application of natural zeolite for phosphorus and ammonium removal from aqueous solutions. *J. Hazard. Mater.* **2009**, *170* (2-3), 1186-1191, Article. DOI: 10.1016/j.jhazmat.2009.05.094.
(373) Li, Y. L.; Deletic, A.; McCarthy, D. T. Removal of E.coli from urban stormwater using antimicrobial-modified filter media. *J. Hazard. Mater.* **2014**, *271*, 73-81, Article. DOI: 10.1016/j.jhazmat.2014.01.057.
(374) Li, Y. L.; McCarthy, D. T.; Deletic, A. Stable copper-zeolite filter media for bacteria removal in stormwater. *J. Hazard. Mater.* **2014**, *273*, 222-230, Article. DOI: 10.1016/j.jhazmat.2014.03.036.
(375) Li, Y. L.; McCarthy, D. T.; Deletic, A. *Escherichia coli* removal in copper-zeolite-integrated stormwater biofilters: Effect of vegetation, operational time, intermittent drying weather. *Ecol. Eng.* **2016**, *90*, 234-243, Article. DOI: 10.1016/j.ecoleng.2016.01.066.

(376) Chutia, P.; Kato, S.; Kojima, T.; Satokawa, S. Adsorption of As(V) on surfactant-modified natural zeolites. *J. Hazard. Mater.* **2009**, *162* (1), 204-211, Article. DOI: 10.1016/j.jhazmat.2008.05.024.
(377) Zhang, P. F.; Avudzega, D. M.; Bowman, R. S. Removal of perchlorate from contaminated waters using surfactant-modified zeolite. *J. Environ. Qual.* **2007**, *36* (4), 1069-1075, Article. DOI: 10.2134/jeq2006.0432.
(378) Haggerty, G. M.; Bowman, R. S. SORPTION OF CHROMATE AND OTHER INORGANIC ANIONS BY ORGANO-ZEOLITE. *Environ. Sci. Technol.* **1994**, *28* (3), 452-458, Article. DOI: 10.1021/es00052a017.
(379) Li, Z. H.; Roy, S. J.; Zou, Y. Q.; Bowman, R. S. Long-term chemical and biological stability of surfactant modified zeolite. *Environ. Sci. Technol.* **1998**, *32* (17), 2628-2632, Article. DOI: 10.1021/es970841e.
(380) Brewer, C. E.; Chuang, V. J.; Masiello, C. A.; Gonnermann, H.; Gao, X. D.; Dugan, B.; Driver, L. E.; Panzacchi, P.; Zygourakis, K.; Davies, C. A. New approaches to measuring biochar density and porosity. *Biomass Bioenerg.* **2014**, *66*, 176-185, Article. DOI: 10.1016/j.biombioe.2014.03.059.
(381) Lehmann, J.; Joseph, S. *Biochar for Environmental Management: Science, Technology and Implementation*; Routledge, 2015.
(382) Karaborni, S.; Smit, B.; Heidug, W.; Urai, J.; vanOort, E. The swelling of clays: Molecular simulations of the hydration of montmorillonite. *Science* **1996**, *271* (5252), 1102-1104, Article. DOI: 10.1126/science.271.5252.1102.
(383) Roth, W. J.; Cejka, J.; Millini, R.; Montanari, E.; Gil, B.; Kubu, M. Swelling and Interlayer Chemistry of Layered MWW Zeolites MCM-22 and MCM-56 with High Al Content. *Chem. Mater.* **2015**, *27* (13), 4620-4629, Article. DOI: 10.1021/acs.chemmater.5b01030.
(384) Zhang, J. P.; Wang, A. Q. Study on superabsorbent composites. IX: Synthesis, characterization and swelling behaviors of polyacrylamide/clay composites based on various clays. *Reactive & Functional Polymers* **2007**, *67* (8), 737-745, Article. DOI: 10.1016/j.reactfunctpolym.2007.05.001.
(385) Richards, T.; Neretnieks, I. Filtering of Clay Colloids in Bentonite Detritus Material. *Chem. Eng. Technol.* **2010**, *33* (8), 1303-1310, Article. DOI: 10.1002/ceat.201000108.
(386) McKinney, R. E.; Edwards, G. P. A Fundamental Approach to the Activated Sludge Process: II. A Proposed Theory of Floc Formation [with Discussion]. *Sewage and industrial wastes* **1952**, *24* (3), 280-287.
(387) Tezuka, Y. CATION-DEPENDENT FLOCCULATION IN A FLAVOBACTERIUM SPECIES PREDOMINANT IN ACTIVATED SLUDGE. *Appl. Microbiol.* **1969**, *17* (2), 222-&, Article. DOI: 10.1128/aem.17.2.222-226.1969.
(388) Qian, T. T.; Zhang, X. S.; Hu, J. Y.; Jiang, H. Effects of environmental conditions on the release of phosphorus from biochar. *Chemosphere* **2013**, *93* (9), 2069-2075, Article. DOI: 10.1016/j.chemosphere.2013.07.041.
(389) Dontsova, K. M.; Bigham, J. M. Anionic polysaccharide sorption by clay minerals. *Soil Sci. Soc. Am. J.* **2005**, *69* (4), 1026-1035, Article. DOI: 10.2136/sssaj2004.0203.
(390) Kobayashi, K.; Liang, Y. F.; Murata, S.; Matsuoka, T.; Takahashi, S.; Amano, K.; Nishi, N.; Sakka, T. Stability Evaluation of Cation Bridging on Muscovite Surface for Improved Description of Ion-Specific Wettability Alteration. *J. Phys. Chem. C* **2017**, *121* (17), 9273-9281, Article. DOI: 10.1021/acs.jpcc.6b12116.

(391) Arvaniti, O. S.; Stasinakis, A. S. Review on the occurrence, fate and removal of perfluorinated compounds during wastewater treatment. *Sci. Total Environ.* **2015**, *524*, 81-92, Review. DOI: 10.1016/j.scitotenv.2015.04.023.
(392) Huber, M.; Hilbig, H.; Badenberg, S. C.; Fassnacht, J.; Drewes, J. E.; Helmreich, B. Heavy metal removal mechanisms of sorptive filter materials for road runoff treatment and remobilization under de-icing salt applications. *Water Res.* **2016**, *102*, 453-463, Article. DOI: 10.1016/j.watres.2016.06.063.
(393) Leenheer, J. A.; Croue, J.-P. Peer Reviewed: Characterizing Aquatic Dissolved Organic Matter. *Environ. Sci. Tehnol.* **2003**, *37* (1), 18A-26A.
(394) Davis, J. A. ADSORPTION OF NATURAL DISSOLVED ORGANIC-MATTER AT THE OXIDE WATER INTERFACE. *Geochim. Cosmochim. Acta* **1982**, *46* (11), 2381-2393, Article. DOI: 10.1016/0016-7037(82)90209-5.
(395) Newcombe, G.; Morrison, J.; Hepplewhite, C. Simultaneous adsorption of MIB and NOM onto activated carbon. I. Characterisation of the system and NOM adsorption. *Carbon* **2002**, *40* (12), 2135-2146, Article. DOI: 10.1016/s0008-6223(02)00097-0.
(396) Reuter, J. H.; Perdue, E. M. IMPORTANCE OF HEAVY METAL-ORGANIC MATTER INTERACTIONS IN NATURAL-WATERS. *Geochim. Cosmochim. Acta* **1977**, *41* (2), 325-334, Article. DOI: 10.1016/0016-7037(77)90240-x.
(397) Kang, S. H.; Choi, W. Oxidative Degradation of Organic Compounds Using Zero-Valent Iron in the Presence of Natural Organic Matter Serving as an Electron Shuttle. *Environ. Sci. Technol.* **2009**, *43* (3), 878-883, Article. DOI: 10.1021/es801705f.
(398) Weber, W. J.; Pirbazari, M.; Melson, G. L. BIOLOGICAL GROWTH ON ACTIVATED CARBON - INVESTIGATION BY SCANNING ELECTRON-MICROSCOPY. *Environ. Sci. Technol.* **1978**, *12* (7), 817-819, Article.
(399) Sinha, E.; Michalak, A. M.; Balaji, V. Eutrophication will increase during the 21st century as a result of precipitation changes. *Science* **2017**, *357* (6349), 405-408, Article. DOI: 10.1126/science.aan2409.
(400) Schoof, J. T. High-resolution projections of 21st century daily precipitation for the contiguous US. *J. Geophys. Res.-Atmos.* **2015**, *120* (8), 3029-3042, Article. DOI: 10.1002/2014jd022376.
(401) BenDor, T. K.; Shandas, V.; Miles, B.; Belt, K.; Olander, L. Ecosystem services and U.S. stormwater planning: An approach for improving urban stormwater decisions. *Environ. Sci. Policy* **2018**, *88*, 92-103. DOI: 10.1016/j.envsci.2018.06.006.
(402) Hagekhalil, A.; Kharaghani, S.; Tam, W.; Haimann, R.; Susilo, K. City of Los Angeles-The Green Blue City One Water Program, Part 3 of 5: Pollutant Load Reduction-Public Green Infrastructure. 2014, American Society of Civil Engineers. DOI: 10.1061/9780784478745.045.
(403) Singh, B. P.; Cowie, A. L.; Smernik, R. J. Biochar Carbon Stability in a Clayey Soil As a Function of Feedstock and Pyrolysis Temperature. *Environ. Sci. Technol.* **2012**, *46* (21), 11770-11778, Article. DOI: 10.1021/es302545b.
(404) Mayoral, M. C.; Izquierdo, M. T.; Andrés, J. M.; Rubio, B. Different approaches to proximate analysis by thermogravimetry analysis. *Thermochim. Acta* **2001**, *370* (1-2), 91-97, Article. DOI: 10.1016/s0040-6031(00)00789-9.
(405) Gronli, M. G.; Várhegyi, G.; Di Blasi, C. Thermogravimetric analysis and devolatilization kinetics of wood. *Ind. Eng. Chem. Res.* **2002**, *41* (17), 4201-4208, Article. DOI: 10.1021/ie0201157.

(406) Kuwata, M.; Zorn, S. R.; Martin, S. T. Using Elemental Ratios to Predict the Density of Organic Material Composed of Carbon, Hydrogen, and Oxygen. *Environ. Sci. Technol.* **2012**, *46* (2), 787-794, Article. DOI: 10.1021/es202525q.
(407) Dollimore, D.; Spooner, P.; Turner, A. The bet method of analysis of gas adsorption data and its relevance to the calculation of surface areas. *Surface technology* **1976**, *4* (2), 121-160. DOI: 10.1016/0376-4583(76)90024-8.
(408) Hammes, K.; Smernik, R. J.; Skjemstad, J. O.; Schmidt, M. W. I. Characterisation and evaluation of reference materials for black carbon analysis using elemental composition, colour, BET surface area and ^{13}C NMR spectroscopy. *Appl. Geochem.* **2008**, *23* (8), 2113-2122, Article. DOI: 10.1016/j.apgeochem.2008.04.023.
(409) Nayak, P. S.; Singh, B. K. Instrumental characterization of clay by XRF, XRD and FTIR. *Bull. Mater. Sci.* **2007**, *30* (3), 235-238, Article. DOI: 10.1007/s12034-007-0042-5.
(410) Elaiopoulos, K.; Perraki, T.; Grigoropoulou, E. Monitoring the effect of hydrothermal treatments on the structure of a natural zeolite through a combined XRD, FTIR, XRF, SEM and N₂-porosimetry analysis. *Microporous Mesoporous Mater.* **2010**, *134* (1-3), 29-43, Article. DOI: 10.1016/j.micromeso.2010.05.004.
(411) Smart, R. S.; Skinner, W. M.; Gerson, A. R. XPS of sulphide mineral surfaces: Metal-deficient, polysulphides, defects and elemental sulphur. *Surf. Interface Anal.* **1999**, *28* (1), 101-105, Article; Proceedings Paper.
(412) Yoon, S. C.; Ratner, B. D. SURFACE AND BULK STRUCTURE OF SEGMENTED POLY(ETHER URETHANES) WITH PERFLUORO CHAIN EXTENDERS .2. FTIR, DSC, AND X-RAY PHOTOELECTRON SPECTROSCOPIC STUDIES. *Macromolecules* **1988**, *21* (8), 2392-2400, Article. DOI: 10.1021/ma00186a016.
(413) Jiang, J. K.; Oberdörster, G.; Biswas, P. Characterization of size, surface charge, and agglomeration state of nanoparticle dispersions for toxicological studies. *J. Nanopart. Res.* **2009**, *11* (1), 77-89, Article. DOI: 10.1007/s11051-008-9446-4.
(414) Jones, D. S.; Woolfson, A. D.; Djokic, J. Texture profile analysis of bioadhesive polymeric semisolids: Mechanical characterization and investigation of interactions between formulation components. *J. Appl. Polym. Sci.* **1996**, *61* (12), 2229-2234.
(415) ASTM. *ASTM D2434 standard test method for permeability of granular soils (constant head)*; 2000.
(416) Hardie, M.; Clothier, B.; Bound, S.; Oliver, G.; Close, D. Does biochar influence soil physical properties and soil water availability? *Plant Soil* **2014**, *376* (1-2), 347-361, Article. DOI: 10.1007/s11104-013-1980-x.
(417) Wong, T. H. F.; Fletcher, T. D.; Duncan, H. P.; Jenkins, G. A. Modelling urban stormwater treatment - A unified approach. *Ecol. Eng.* **2006**, *27* (1), 58-70, Article. DOI: 10.1016/j.ecoleng.2005.10.014.
(418) Min, S. H.; Eberhardt, T. L.; Jang, M. Base-treated juniper fiber media for removing heavy metals in stormwater runoff. *Pol. J. Environ. Stud.* **2007**, *16* (5), 731-738, Article.
(419) Tian, J.; Jin, J.; Chiu, P. C.; Cha, D. K.; Guo, M. X.; Imhoff, P. T. A pilot-scale, bi-layer bioretention system with biochar and zero-valent iron for enhanced nitrate removal from stormwater. *Water Res.* **2019**, *148*, 378-387, Article. DOI: 10.1016/j.watres.2018.10.030.